Improved Statistical Approach for Climate Projection over Bangladesh using Downscaling of Global Climate Model Outputs

A dissertation submitted to the Institute of Statistical Research and Training (ISRT), University of Dhaka in fulfillment of the requirements for the degree of Doctor of Philosophy in Applied Statistics

Md. Bazlur Rashid
PhD Researcher
Registration Number: 24
Session: 2016-2017
Institute of Statistical Research and Training (ISRT)
University of Dhaka
Dhaka-1000, Bangladesh

Institute of Statistical Research and Training (ISRT)
University of Dhaka
Dhaka-1000, Bangladesh

January 2023

Improved Statistical Approach for Climate Projection over Bangladesh using Downscaling of Global Climate Model Outputs

A dissertation submitted to the Institute of Statistical Research and Training (ISRT), University of Dhaka in fulfillment of the requirements for the degree of Doctor of Philosophy in Applied Statistics

Md. Bazlur Rashid
PhD Researcher
Registration Number: 24
Session: 2016-2017
Institute of Statistical Research and Training (ISRT)
University of Dhaka
Dhaka-1000, Bangladesh

Institute of Statistical Research and Training (ISRT)
University of Dhaka
Dhaka-1000, Bangladesh

January 2023

D E C L A R A T I O N

It is hereby declared that the research work presented in the thesis entitled "**Improved Statistical Approach for Climate Projection over Bangladesh using Downscaling of Global Climate Model Outputs**" or any part of it has not been submitted elsewhere for any other degree or diploma.

Md. Bazlur Rashid

Registration Number: 24

Session: 2016-2017

Institute of Statistical Research and Training (ISRT)

University of Dhaka

Dhaka-1000

Bangladesh

C E R T I F I C A T E

This is to certify that Md. Bazlur Rashid, a Ph D student of the Institute of Statistical Research and Training (ISRT), University of Dhaka has carried out his research work entitled "**Improved Statistical Approach for Climate Projection over Bangladesh using Downscaling of Global Climate Model Outputs**" under my supervision.

Prof. Dr. Syed Shahadat Hossain

(Supervisor)

Institute of Statistical Research and Training (ISRT)

University of Dhaka

Dhaka-1000

Bangladesh

ACKNOWLEDGEMENT

All great enormous thanks to the Glorious Almighty Allah, the Omniscient and the sole nourish the sustainer of the universe, who taught me and guided my step to this humble effort and also for the blessing, protection and help in all aspects of my life.

At the foremost, I wish to express my profound gratitude to my supervisor Professor Dr. Syed Shahadat Hossain, Institute of Statistical Research and Training (ISRT), University of Dhaka, for his overall guidance throughout my research and for spending many hours discussing and reviewing the draft manuscript of this thesis. The preparation of this thesis would never have been possible without his constructive suggestions, continual encouragement, and guidance.

I am thankful to the Hon'ble Vice-Chancellor, University of Dhaka and Dr. Md. Abdus Samad, Professor, Department of Applied Mathematics, Dean, Faculty of Science, University of Dhaka for their cordial administrative support and encouragement with helpful suggestions.

I like to thank to the respected Senior Secretary, Ministry of Defence for giving me permission for to enroll in this Ph D course and Director, Mr. Md. Azizur Rahman, Bangladesh Meteorological Department (BMD), for providing necessary data, moral support and encouragement.

I am personally grateful to Dr. Md. Abdul Mannan, Meteorologist, Bangladesh Meteorological Department (BMD), for his constant encouragement and cordial help.

I would also like to thank Dr. Samarendra Karmakar, Former Director of SMRC and Bangladesh Meteorological Department; Dr. Anisul Haque, Professor, Institute of Water and Flood Management (IWFM), BUET and Dr. Md. Munsur Rahman, Professor, Institute of Water and Flood Management (IWFM), BUET for their inspiration and moral support.

I am sincerely thankful to my respected colleagues Dr. Md. Shadekul Alam, Assistant Director, BMD, S. M. Quamrul Hassan, Md. Abdur Rahman Khan, Kh. Hafizur Rahman, Md. Monowar Hossain, Dr. Muhammad Abul Kalam Mallik, Md. Arif Hossein, Md. Omar Faruq, AKM Nazmul Haque, Md. Shaheenul Islam, Razia Sultana, Afruza Sultana and others for their helpful co-operation and suggestions.

Finally, I am grateful to my wife, Mist. Kawsari Kumkum, my dearest daughters Kawsari Nadia and Adila Kumkum, who have taken all of their sufferings to provide me adequate time for study.

–The Author

January, 2023

D E D I C A T I O N

This Thesis is Dedicated

To My Beloved Parents

TABLE OF CONTENTS

List of Figures

List of Tables

A B S T R A C T

Climate of Bangladesh is expected to be changed under the influence of Global Warming conditions. However, it is essential to quantify it irrespective of time and space. Empirical Statistical Downscaling (ESD) is an approach through which the magnitudes of the projected variable at the local level with time can be estimated based on the projected output of Global Climate Models (GCMs). In this study, two main climate variables of mean temperature and rainfall are considered for projection as well as to calculate their projected magnitudes at different future lengths. In this way, 10 most suitable GCMs are considered for temperature projection. But for rainfall projection 5 most appropriate GCMs are selected for the pre-monsoon season (March-May); 3 most appropriate GCMs for monsoon (June-September) and post-monsoon seasons (October-November) separately. The mean of the selected models for each group is also calculated to determine the ensemble prediction. To understand the current climate and its behaviour and to justify the model performance on historical records, daily mean temperature (average of the maximum and minimum temperature records) and rainfall of 34 stations (which are widely distributed over Bangladesh) are collected from the archive of Bangladesh Meteorological Department (BMD) during the period of 1981-2010. There is a missing value within daily records, which is essential to extract, and the missing value of temperature and rainfall are calculated using the R-package of multiple regression, and consequently, an updated climate record has been prepared for this study. To proceed for the study three emission scenarios of RCP2.6, RCP4.5 and RCP8.5 under CMIP5 are selected and the relevant GCM model outputs are commonly selected from all of these scenarios. Then the GCM outputs are downscaled through ESD Package (an R-package specially developed for statistical downscaling), adopting the Principal Component Analysis (PCA) method to produce the projected magnitudes of mean temperature and rainfall at each of the selected locations on month basis for the period of 2021-2100. The simulated results are evaluated with observation at station location basis as well as at the national average (considering the average of all BMD stations location). The evaluation of the projection result has been conducted using the technique of the five-fold cross-validation method. To evaluate how well the downscaled GCM ensembles represent the past trends and interannual variability for each station, the observed seasonal data in the period 1981–2010 is compared with the statistical characteristics of the downscaled ensembles. The trend in the period of 1981–2010 is calculated for the observed value and each downscaled ensemble member at all stations. Then the result has been analyzed. Analysis reveals that the seasonal and annual mean

temperatures are projected to increase in the near future and far future for each emission scenario. The increment rates during pre-monsoon season are +0.62, +0.5 and +0.54°C in the near future and 0.78, 1.19 and 2.04°C in the far future, respectively for RCP2.6, RCP4.5 and RCP8.5. In the monsoon season, the projected rates are +0.25, +0.13 and +0.37°C in the near future and +0.33, +0.45 and +1.27°C in the far future, respectively. The projection of post-monsoon season is higher than other seasons; in the near future, the magnitudes are +0.6, +0.72 and +0.94°C and are +0.76, +1.42 and +2.81°C in the far future. Winter season is also projected to be warming at high rate, and the projection rates are +0.45, +0.44 and +0.86°C for the near future and are +0.65, +1.06 and +2.23°C in the far future. The annual mean temperature is likely to be higher with the projection rate of +0.48, +0.45 and +0.68°C in the near future and it is of +0.71, +1.16 and +2.83°C in far future, respectively for RCP2.6, RCP4.5 and RCP8.5. Analysis also depicts that the frequency of the wet-day (with rainfall ≥ 1mm/day) is projected to increase in all seasons in the near and far future for RCP2.6. It is projected to increase in pre-monsoon and post-monsoon seasons as well as annually both in the near and far future, but it is likely to decrease in both of the time slabs of monsoon season for RCP4.5. For the case of a very high emission scenario of RCP8.5, wet-day frequency is projected to increase in pre-monsoon but decrease in monsoon season both in the near and far future. As a whole, the annual wet day frequency indicates an increasing trend.

A B B R E V I A T I O N

A	ACI	Akaike Information Criterion
	AMIP	Atmospheric Model Inter-comparison Project
	AOGCM	Atmosphere-Ocean General Circulation Model
	AR4	Fourth Assessment Report
B	BESK	Binary Electronic Sequence Calculator
	BMD	Bangladesh Meteorological Department
C	CC	Correlation Coefficient
	CDF	Cumulative Distribution Function
	CMIP	Coupled Model Intercomparison Project
	COP21	Twenty-first Conference of Parties
	CI	Confidence Interval
E	ESD	Empirical Statistical Downscaling
	EMS	Earth system model
	ENIAC	Electronic Numerical Integrator and Computer
	EOF	Empirical Orthogonal Function
F	FAR	First Assessment Report
G	GCM	Global Climate Model
	GFDL	Geophysical Fluid Dynamics Laboratory
	GHG	Green House Gas
	GPCP	Global Precipitation Climatology Project
I	IAV	Interannual Variability
	IPCC	Intergovernmental Panel on Climate Change
	IPO	Inter-decadal Pacific Oscillation
J	JNWPU	Joint Numerical Weather Prediction Unit
M	MB	Multiplicative Bias
	MMD	Multi-Model Data

	MOS	Model Output Statistics
N	NCAR	National Center for Atmospheric Research
	NAS	National Academy of Science
	NWP	Numerical Weather Prediction
P	PDF	Probability Density Function
	PC	Principal Component
	PCA	Principal Component Analysis
	PCMDI	Program for Climate Model Diagnosis and Intercomparison
	PDO	Pacific Decadal Oscillation
R	RCM	Regional Climate Model
	RCP	Representative concentration pathways
S	SAR	Second Assessment Report
	SDG	Sustainable Development Goal
	SDSM	Statistical Downscaling Model
	SRES	Special Report on Emissions Scenarios
	SVD	Singular Value Decomposition
	SVM	Support Vector Machine
T	TAR	Third Assessment Report
U	UNEP	United Nations Environment Programme
W	WCRP	World Climate Research Programme
	WMO	World Meteorological Organization
	WGCM	Working Group on Coupled Modelling

CHAPTER ONE: INTRODUCTION

1.1 Preamble

Climate projections define the simulations of Earth's climate for the future decades (typically until 2100) based on assumed 'scenarios' for the concentrations of greenhouse gases, aerosols, and other atmospheric constituents that affect the Earth's radiative balance. Climate projections are obtained by running numerical models of Earth's climate, covering the whole globe or a selected region. These models are named Global Climate Models (GCMs), General Circulation Models, or Regional Climate Models (RCMs).

Climate Models are fundamental tools for understanding the possible impacts of climate change, including changes in temperature, precipitation and sea level. The climate model is the mathematical model to simulate and analyzes the interactions between the atmosphere and underlying surfaces like ocean, land and ice. A GCM comprises a series of models of the Earth's atmosphere, oceans and land surface. GCMs split the globe into several layers and produce three-dimensional gridded spaces for a better understanding of the climate. GCMs are sufficiently skilled to determine the past and current climate.

GCMs are also valuable predictive tools but cannot determine the fine-scale heterogeneity of climate variability and change due to their coarse resolution. Various topographic features like mountains, water bodies, infrastructure, land-cover characteristics and components of the climate system are much finer than GCM's resolution. However, these heterogeneities are essential to the decision-makers who require information on potential impacts on crop production, hydrology, species distribution etc., at a scale of 10-50 kilometres. Several methods have also been developed to reduce the gap between GCM's deliberation and society's requirements for decision-making.

The derivation of fine-scale climate information is based on the assumption that the local climate is determined by the interactions between large-scale atmospheric characteristics (circulation, temperature, moisture, etc.) and local conditions (water bodies, mountain ranges, land surface properties, etc.). It is possible to simulate these interactions and establish relationships between present-day local climate and atmospheric conditions utilizing the downscaling process.

Downscaling can be done based on spatial and temporal aspects of climate projections. Spatial downscaling indicates the methods used to derive finer-resolution spatial climate information from coarser-resolution GCM output to a finer resolution or even a specific location. Temporal downscaling denotes the derivation of fine-scale temporal information from a longer-scale temporal GCM output. The dynamical downscaling process refers to the use of an RCM with high resolution.

RCMs intake the large-scale atmospheric information from GCM output at the lateral boundaries and include more complex topography, land-sea contrast, surface heterogeneities, and detailed physical processes to generate a piece of more realistic climate information at a spatial resolution

of about 20-50 kilometers. As RCM is nested in a GCM, the overall quality of dynamically downscaled RCM output depends on the accuracy of the large-scale forcing of the GCM and its biases (Seaby *et al*., 2013). Though RCM contains a regional scale feature, it is subject to systematic errors and therefore requires bias corrections and further downscaling to a higher resolution.

Statistical downscaling establishes empirical relationships between historical and current large-scale atmospheric and local climate variables. Once a relationship has been defined and validated, future atmospheric variables projected by GCMs are used to predict future local climate variables. Statistical downscaling can be able to produce location-specific climate projections, which RCMs cannot be detected. However, this approach depends on the critical assumption that the relationship between present large-scale circulation and local climate remains effective under different forcing conditions of possible future climates (Zorita and von Storch, 1999).

Dynamical and statistical approaches are utilized jointly. Dynamical-statistical downscaling involves the utilization of an RCM to downscale GCM products before using statistical equations for further downscale RCM output to a finer resolution. Dynamical downscaling helps to improve specific aspects of regional climate modelling and provides better predictors for further statistical downscaling to a higher-resolution output (Guyennon *et al*., 2013). Statistical-dynamical downscaling is a more complex approach but less computationally demanding than dynamical downscaling. This method statistically pre-filters the GCM outputs into a few characteristic states that are further used in RCM simulations (Fuentes and Heimann, 2000).

Earth's climate is changing, initially as a result of human interventions. People are adding different chemical elements like greenhouse gases to the atmosphere, which is driving the climate to a warmer place. The warming is apparent in long-term data from the top of the earth to the depths of the oceans. When climate change is global, climate changes are not estimated to be uniform across the world. Climate change represents rising challenges to man and other animals' health, safety and quality of life on earth.

The future climate in Bangladesh will be overstated by both global and regional change. For a global change, the global climate is getting warmer due to the summation of greenhouse gases (GHGs) in the air resulting in more heat gain due to the greenhouse effect. However, temperature warming is not the only factor responsible for climate change in Bangladesh. Regional change such as development and soil use conversion has affected the temperature and precipitation trend in Bangladesh since the last century (Fahad *et al*., 2017). This thesis goal to conduct research on future climate change in Bangladesh based on the projections of future climate by the Intergovernmental Panel on Climate Change (IPCC) made using Global Climate Models (GCMs).

1.2 The history of climate modelling

The development of the climate model has been initiated for a long. In 1922, weather prediction by the numerical process was initiated first. Following this, a research article was presented and published by Guy Callendar in 1938. In 1946, John Von Neumann proposed to use new computers, such as the Electronic Numerical Integrator and Computer (ENIAC) at the University of Pennsylvania, for forecasting weather. The new meteorology group was formed at Princeton by Von Neumann and headed by Jule G Charney, who later on became a key figure in Climate Science. The group used ENIAC to run the first computerized regional weather forecast in 1950. On July 01, 1954, the US Weather Bureau and the military decided to create the Joint Numerical Weather Prediction Unit (JNWPU). A Swedish-Norwegian collaboration defeated the JNWPU team by a few months to deliver the World's first real-time numerical weather forecast in December 1954. The forecasts, which focused on the North Atlantic, are performed using a Swedish Computer called the Binary Electronic Sequence Calculator (BESK).

In 1956, Russian climatologist Mikhail Budyko published a book entitled "The Heat Balance of the Earth's Surface". Using a simple energy-balance model, he calculated the Earth's average global temperature by balancing incoming solar energy with outgoing thermal energy. In 1956, Manabe wrote a vital chapter in the history of climate modelling. Smagorinsky and Manabe worked together to understand the complexity of models, such as the evaporation of rainfall and exchange of heat across ocean, land and ice. At the same time, Norman Phillips developed General Circulation Model first in April of 1956. Akio Arakawa and Yale Mintz also worked on developing a model that could stay computationally stable over a long period and not "blow up" after a few days, which was a problem with the Phillips model. Their ongoing work is known as the "Mintz-Arakawa Model" with the first iteration running by 1963. In July of 1963, Fritz Moller, a meteorologist at the University of Munich, was visiting Manabe at Geophysical Fluid Dynamics Laboratory (GFDL) and published a paper entitled, "On the impact of changes in the CO2 emission in the air on the radiation balance of the earth's surface and on the climate" in the Paper of Geophysical Research. Warren Washington and Akira Kasahara established a climate modelling group at the National Center for Atmospheric Research (NCAR) in Boulder, Colorado, in 1964. The Kasahara-Washington model offers finer resolution, but its main legacy is that it established NCAR as a leading climate modelling centre from the 1960s onwards. On January 07, 1966, the Committee on Atmospheric Sciences at the National Academy of Science (NAS) published a report called Weather and Climate Modification: Problems and Prospects. The report concluded the committee's two-year investigation into the "Recent advances in mathematical modelling of atmospheric processes". Following these, Kirk Bryan first developed a model with the provision of a 3D ocean circulation in February 1967.

On May 01 1967, the most influential climate modelling paper entitled "Thermal Equilibrium of the atmosphere with a given distribution of relative humidity", the most influential climate modelling paper of all time was published by Manabe along with his co-author Richard Wetherald on May 01 of 1967. They produced the first credible prediction using a 1D radiative-convective model to determine atmospheric temperature with the changes in CO2 concentration levels. NASA's Nimbus III satellite was launched on April 14, 1969. This satellite had the specific task

of taking measurements of the Earth, which would help to test and validate climate models. In October of 1972, the UK Met Office scientists described their first GCM in a journal paper, which had been developing since 1963 when the Met Office first created its "Dynamical Climatology Branch". They expressed in the abstract that the model incorporated the hydrological cycle, topography, a simple scheme for the radiative exchanges and arrangements for the simulation of deep free convection (subgrid-scale) and for the representing exchanges of momentum, sensible and latent heat with the underlying surface. In continuation to this, Manabe published a paper with Kirk Bryan (1969) in which they presented the results from the first coupled atmosphere-ocean GCM (AOGCM) on January 01, 1975.

Then in February of 1977, a journal called Methods in Computational Physics: Advances in Research and Applications published an influential special volume on the "General Circulation Models of the Atmosphere". Various climate modelling groups, including UCLA, NCAR and the UK Met Office, submitted papers describing how their current models work. These papers, particularly the UCLA paper by Akio Arakawa and Vivian Lamb, formed the backbone of most climate models' "computational domain" for years afterwards. The International Council of Scientific Unions and the World Meteorological Organization united to sponsor the World Climate Research Programme (WCRP) launch in 1980. The main goal of this programme is to regulate the predictability of climate and to control the effect of human-indues on climate. In 1983, the Community Climate Model (CCM) was created by the US National Center for Atmospheric Research (NCAR) in Colorado. It aims to be a "freely available global atmosphere model for use by the wider climate research community". The United Nations Environment Programme (UNEP) and the World Meteorological Organization (WMO) established the Intergovernmental Panel on Climate Change (IPCC) in November 1988. The Atmospheric Model Inter-comparison Project (AMIP) was launched to establish a protocol that can be used to undertake the "systematic validation, diagnosis, and inter-comparison" of all atmospheric GCMs 1989.

On 27-30 August 1990 first IPCC report was published. On September 20, 1990, the Journal of Geophysical Research published a vital paper confirming that the clouds are the main reason for the significant differences- a "roughly threefold variation" in the way the various models respond to changes in CO2 concentrations. A book called "Climate System Modeling", edited by NCAR's Kevin Trenberth in January 1992 and published by Cambridge University Press. The book contained the end result of a series of workshops where scientists from a range of backgrounds came together to set down the current knowledge on climate models. World Climate Research Programme (WCRP) introduced the CMIP in 1995. In November of 2000 carbon cycle was included in climate models. The report "National Strategy for Advancing Climate Modeling" was published by the National Research Council of the US on September 07 2012. The report recognized the evolutionary changes to computing hardware and software present a challenge to climate modeler’s. It indicated that future, an increasing trend in computing power would be achieved the desired goal of climate modelling.

To determine the real climate scenario climate model needs to include more and more climate features. Accordingly, the GCMs are incorporating more and more forcings. As a result, GCMs are simulating many more aspects of the climate system, including atmospheric chemistry and aerosols, land surface interactions, land and sea ice, and biogeochemical cycles. Models that

include interactive biogeochemical cycles is referred to as Earth system models (ESMs; Hayhoe *et al*., 2017). The result of ESMs is often utilized in the applied field as the coarser ESM output can be translated or downscaled frequently to address the local climate process for the interest (Hostetler *et al*., 2018).

Over the decades, scientists have been using mathematical models to help us to learn more about the Earth's climate. Over time these models have increased in complexity as separate components have been merged to form coupled systems. Figure 1.1 shows the evolution of such systems as designed by NASA, and figure 1.2 illustrates the development of the complexity of the climate model over the period (IPCC, 2007).

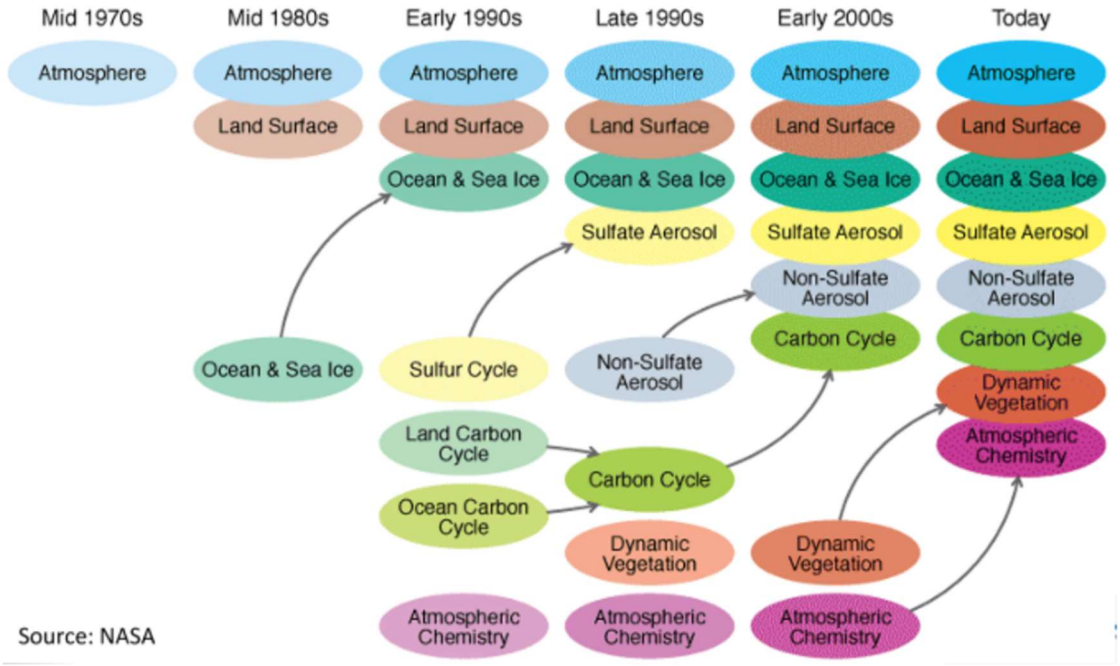

Fig.1.1: The development of climate models since 1970s

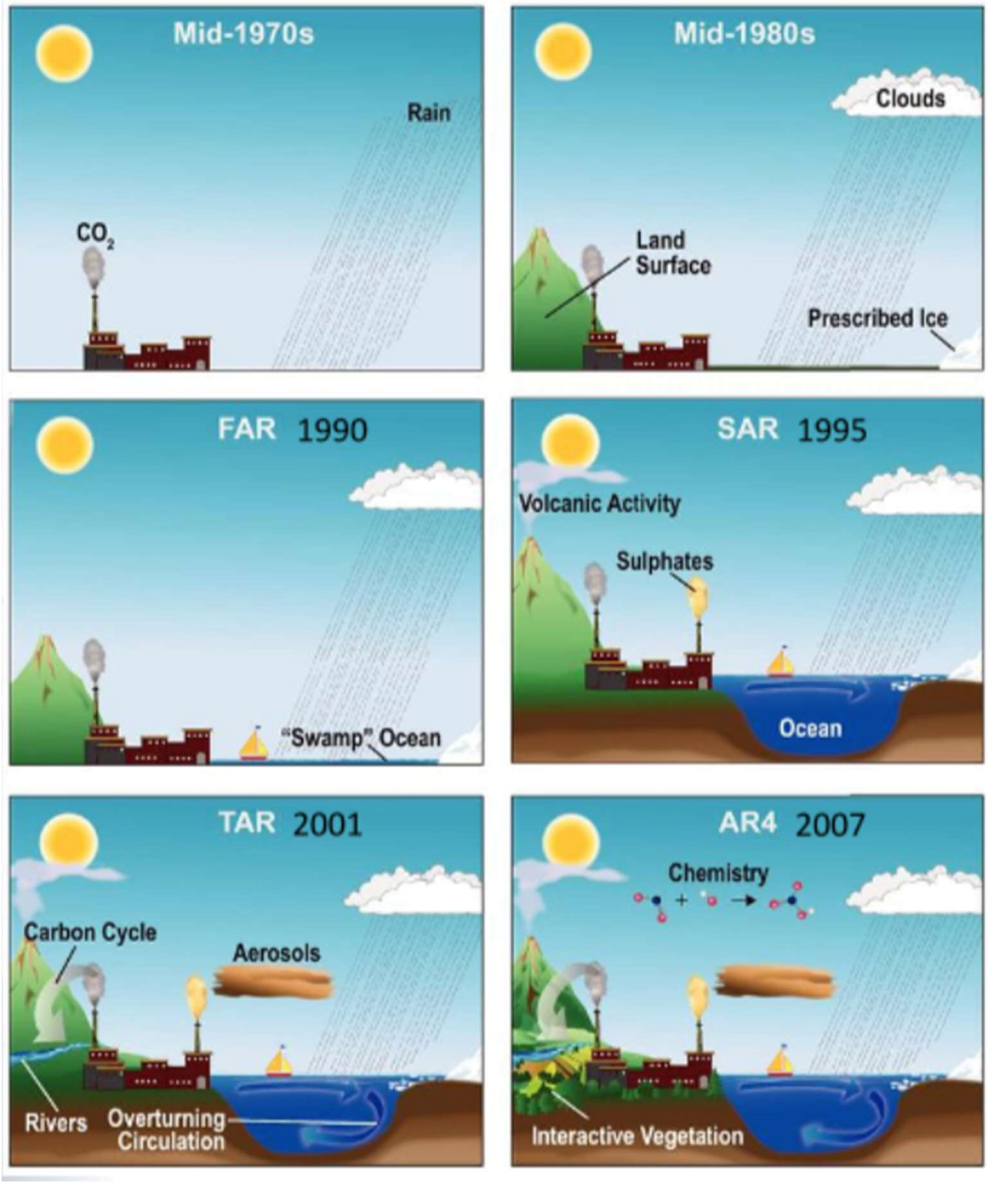

Fig.1.2: Development of the complexity of climate model over the period (Source: IPCC, 2007)

Over the period, the spatial resolution of the climate model increased in addition to the complexity. The spatial resolution of the climate model starts from 500 km. It has evolved through the first four IPCC assessment reports- (i) First Assessment Report ("FAR") published in 1990, (ii) Second Assessment Report ("SAR") in 1995, (iii) Third Assessment Report ("TAR") in 2001 and (iv) Fourth Assessment Report ("AR4") in 2007. In the fifth report from 2014, the resolution of several global models considered was about 50 km (IPCC, 2013). The increased spatial resulted from increased computing power by considering the better representation of all climate effects, including extreme climate events.

1.3 Climate Model Intercomparison Project (CMIP)

Many institutions are involved in the development and running of climate models. Though all of these models are largely based on the same existing knowledge of climate systems, there are differences among them. In 1995, the CMIP started a framework for coordinated climate model experiments. Through this platform, scientists are allowed to simulate, analyze, validate and consistently improve GCMs. The GCMs provide the forcings from the interaction of the atmosphere and ocean. In continuation to this, the data generated through the fifth CMIP project were used extensively in the IPCCs 5th Assessment Report (IPCC, 2013, 2014) for improved understanding of (i) climate and assessing the mechanisms responsible for model differences, (ii) making future projections for the policymakers and adaptation process and (iii) evaluating how realistic the models are in simulating the recent past.

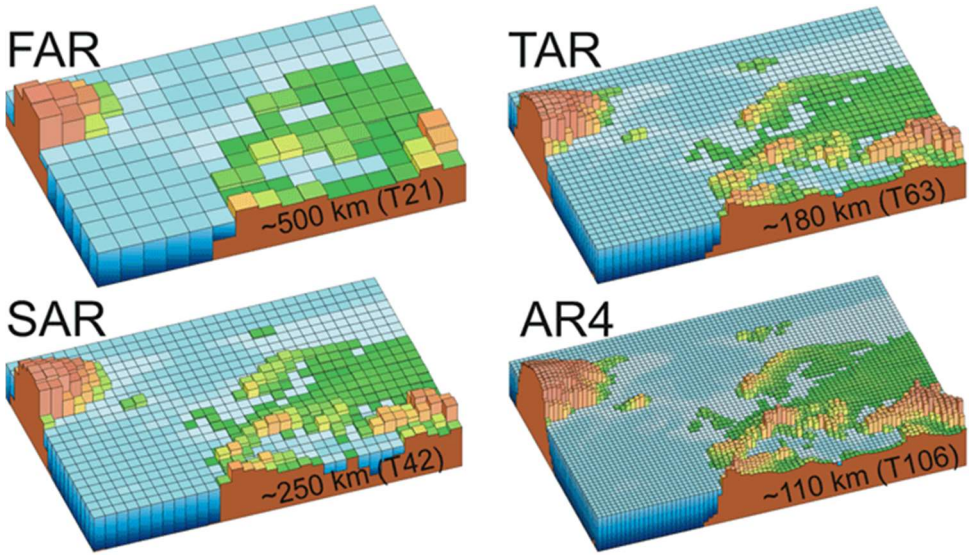

Fig.1.3: Advancement of Climate Model resolution through updated assessment reports of IPCC (Source: IPCC, 2007)

1.4 Evolution of GCMs

General Circulation Models (GCMs) conduct the projection of future climate, mathematical models that simulate complex atmospheric motions using supercomputers (McGuffie, 2007). GCMs were first developed in the 1950s for weather and climate forecasting after the detection of an increasing trend of carbon dioxide in the atmosphere by Keeling (1993). The climate modelling society shifted its attention to examining how greenhouse gases (GHGs) affect the climate system and the cause or causes of global warming. Manabe and Wetherald were the first scientists to simulate the effect of doubling carbon dioxide concentration in the atmosphere (Manabe & Wetherald, 1967a, 1975b). The GCMs revised by the IPCC in the First Assessment Report (FAR), published in 1990, were based on the Manabe and Wetherald (1975b) model integrated with a straightforward ocean system. Since then, GCMs have developed significantly in terms of incorporating more features and accuracy. GCMs are now combined with an ocean dynamics

system and incorporate several atmospheric feedback systems to simulate the complex ocean and atmospheric processes.

Nowadays, physical principles of climate models are well-established and have been verified to reproduce observed features of recent and past climate changes. The Atmosphere-Ocean General Circulation Models (AOGCMs) are considerably dependable models that deliver reliable quantitative estimates of future climate scenarios, especially at continental and large scales. These estimates are higher for some climate variables (e.g., temperature) than others (e.g., precipitation) based on confidence. Since the IPCC Third Assessment Report (TAR), many modelling advances have occurred. Model enhancements can, however, be classified into three categories. First, the dynamical cores have been improved, and many models' horizontal and vertical resolutions have been improved. Secondly, more processes have been merged into the models, particularly in modelling aerosols and land surface and sea ice systems. Thirdly, the parameterizations of physical procedures have been developed.

Finally, development in models comes from their physical background and skill in demonstrating present and past climate changes. Models have been shown to be essential tools for simulating and understanding climate. At the same time, there is considerable confidence that they can provide credible quantitative estimates of future climate change. Climate models remain to have significant limitations, such as in their demonstration of clouds, which lead to uncertainties in the magnitude and regional details of predicted climate change. Nevertheless, over the last several decades of model improvement, they have consistently provided a robust and unambiguous picture of significant climate warming in response to increasing greenhouse gases.

The Working Group on Coupled Modelling (WGCM) under the World Climate Research Programme (WCRP) built up the Coupled Model Intercomparison Project (CMIP) as a standard trial protocol for studying the output of coupled atmosphere-ocean general circulation models (AOGCMs). CMIP delivers a community-based configuration supporting climate model analysis, justification, inter-comparison, documentation and data access. This outline permits a different community of scientists to analyze GCMs systematically, a process that works to help model enhancement. Almost the whole international climate modeller has joined this project since its beginning in 1995. The Program for Climate Model Diagnosis and Intercomparison (PCMDI) stores much of the CMIP information and affords another backing for CMIP. Coupled atmosphere-ocean general circulation models permit the simulated climate to modify to changes in climate forcing, such as increasing carbon dioxide and other gases. CMIP was created in 1995 by assembling output from different models based on which climate forcing is detained constant. Advanced versions of CMIP have collected output from a perfect scenario of global warming, with atmospheric CO2 increasing at the rate of 1% per year till it doubles at about year seventy. CMIP data are accessible for study by permitted diagnostic sub-projects. The project of CMIP3 included realistic scenarios for both past and present climate forcing. The research based on this dataset provided much of the new physics underlying the Intergovernmental Panel on Climate Change

(IPCC) Fourth Assessment Report (AR4). The scenarios of the CMIP5 experiment design have been finalized with the following sets of trials:

- Decadal hindcasts and predictions simulations,
- Long-term simulations and
- Atmospheric simulations for especially computationally-demanding models.

The climate model outputs from simulations of the past, present and future climate were collected by the Program for Climate Model Diagnosis and Intercomparison (PCMDI) during the years 2013 and 2014 in order to conduct CMIP5, the outcome of which has mostly contributed to the Fourth Assessment Report (AR5) of the IPCC in 2014. Although the next generation of GCMs and associated simulations (the 6th Coupled Model Intercomparison Project, CMIP6) have become limited available very recently, CMIP5 "s GCMs are still in use in many research projects worldwide.

1.5 Emission scenarios

Since exact Green House Gas (GHG) emissions for the future are unknown, the IPCC has developed several emission scenarios based on demographic, social, economic, technological and environmental developments that diverge in the future, which are known as the Special Report on Emissions Scenarios (SRES) (Nakicenovic *et al*., 2000). Each scenario represents a potential future based on the storyline, which describes the critical driving force that will alter future emissions, such as population change and economic development. On the other hand, a scenario family can have several different outcomes due to the selection of energy sources (IPCC-TGICA, 2007). The coupled model intercomparison project (CMIP) has become one of the foundational elements of climate science at present based on climate simulations.

The objective of CMIP is to realize well past, present, and future climate change due to natural or unforced variability to changes in radiative forcing in a multi-model attitude. Its significance and opportunity are increasing significantly. CMIP has synchronized six past large model intercomparison schemes. Examination of extensive simulation data from various CMIP trials has been widely used in many intergovernmental panels on climate change (IPCC) assessment reports. However, CMIP5 works to deliver a framework for harmonized climate change trials for the next five years and thus contains mockups for assessment in the AR5 and the same times others that spread in favour of the AR5. CMIP5 is meant to be not only comprehensive but also possibly include all the different model intercomparison activities.

CMIP5 stimulates a standard set of model simulations in order to (a) estimate how actual the models are in simulating the recent past, (b) afford prognoses of future climate change on two time periods, near future (out to about 2035) and far future (out to 2100 and beyond and (c) realize some of the aspects responsible for differences in model projections, those involving the carbon monitoring. In AR5, the IPCC has introduced a new set of emission scenarios called the Representative Concentration Pathways (RCPs) (Van Vuuren *et al*., 2011). There are 4 RCPs:

RCP2.6, RCP4.5, RCP6 and RCP8.5 and the names are based on the total radiative forcing, i.e. the total human emissions of GHG expressed in W/m2.

1.6 Representative concentration pathways (RCPs)

RCPs are the pathways of concentration which are used in the IPCC AR5. They are recommended pathways for greenhouse gas and aerosol concentrations and land use change. RCPs are consistent with a set of extensive climate outcomes used by climate modelling experts, and the pathways are considered by the radiative forcing produced by the end of the 21st century. Radiative forcing is the additional heat the lower troposphere will retain due to extra greenhouse gases, measured in Watts per square metre (W/m^2). The complication of humanity's possible future emissions has been reduced to just four RCPs. These take into account the impact of atmospheric concentrations of carbon dioxide and other greenhouse gases and aerosols (such as sulfate and soot). Each of the RCPs maintains the period of 1850–2100. Each of the pathways represents a larger set of scenarios in the scientific works. The complete set of emissions scenarios, with and without climate policy, is included within the range of the RCPs. These have one mitigation scenario leading to a very low forcing level called RCP2.6, two medium stabilization scenarios (RCP4.5 and RCP6) and one severe emission scenario (RCP8.5).

The 8.5 RCP rises from little effort to reduce emissions and represents a failure to control warming by 2100. It is comparable to the highest-emission scenario in the IPCC Fourth Assessment Report (AR4). The RCP of 6.0 stabilizes total radiative forcing shortly after 2100 by reducing greenhouse gases. RCP4.5 is similar to the lowest-emission scenario evaluated in the IPCC AR4. 2.6 pathway is the most motivated pathway. It sees emissions peak early, then fall due to the active elimination of carbon dioxide gases. This RCP is also denoted as RCP3PD (representing the mid-century peak radiative forcing of $3W/ m^2$ monitored by a decline). 2.6 pathway needs initial contribution from all the main emitters, including those in developing countries. It has no equivalent in IPCC AR4.

These RCPs are significant progress in the climate research community and deliver a source for emissions mitigation and impact analysis and pathways that will help exchange information among physical, biological and social experts. Scientists working on impacts, adaptation and mitigation will obtain the outputs model sooner and have more time to finish their part of the AR5, and they can also be settled without constraining future work on combined assessments. As climate models improve, the latest techniques can employ the same pathways and permit modellers to isolate the effects of changes in the climate models themselves. Improvement of the pathways also brings together a diverse range of research scientists that will help create fully unified Earth-system models that contain a demonstration of the global interest and civilization, impacts and vulnerabilities.

1.7 GCMs Work in Bangladesh and Its Research Gap

Global Climate Models (GCM) are geophysical models (Lupo, A. *et al*., 2013) that project the climate characteristics (rainfall, temperature, moisture level, etc.) for the whole World. The models consider data from multiple geographic grids to make this projection. Country-specific climate profiles are generated by simulation from the GCM using parameters estimated from local station-based observations over the different seasons. However, for small geographic regions like Bangladesh, the number of grids under consideration in GCM is too small to establish a strong justification for the local projection (Cheung, C. C., 2014). For example, only four points within Bangladesh are used for GCM. Usually, such a small number of geographic points do not represent the region well. That is why statistical techniques are required to be used to revise these GCM projections into a more justifiable local projection. This revision process is known as statistical downscaling (Maraun *et al*., 2010).

Primarily, a mean ensemble of several GCM models (Khan *et al*.,2020) is generated, and many statistical approaches are used for these downscaling. In the first step, the mean ensemble of GCMs is validated to see whether it reflects the observed climate pattern. Different statistical techniques are also in use for this validation. Despite the availability of many statistical methods for both of these steps (validation and downscaling), their use in Bangladesh, using local data, have not been noticed earlier. A few researchers (Rahman and Mcbean, 2011; Mukherjee *et al*., 2011; Nury *et al*., 2013; Rahaman *et al*., 2015, Pour *et al*., 2018 etc.), so far, have used only linear regression to determine some climate parameters from GCM projections such as the maximum temperature, minimum temperature, precipitation trend and the number of heavy rainy days.

Most works are limited to a particular season, a single variable, or very few mean ensemble GCM models. However, none of these studies has taken seasonal climate change into account. At the same time, a small number of GCM does not give an accurate representation of future climate scenarios (Mezghani *et al*., 2019); these studies considered a mean ensemble of only a few GCM data. Consideration of mean ensemble of more GCM models and other improved statistical techniques for validation of GCM data (quantile-based mapping, bias corrections model etc.) and for statistical downscaling (for example, spatial, temporal models, PCA etc.), including seasonal adjustments are available and underuse (Maraun 2013, Rashid, *et al*., 2018, 2019, 2020 & 2021a) in a few other countries.

The objective of this research, therefore, is to apply these improved statistical techniques for the Bangladesh scenario to find and suggest an appropriate model for statistical downscaling of rainfall and temperature and extreme weather events projections generated by GCM for Bangladesh.

1.8 Research questions and statement of the problem

In Bangladesh, some researchers have studied using statistical downscaling to project the future climate in Bangladesh, and these studies included temperature and precipitation projections only. These studies used regression techniques to determine some climate parameters from GCM projections, such as the maximum temperature, minimum temperature, precipitation trend and the number of heavy rain days. However, no PCA based downscaling for Bangladesh has been undertaken. In addition, current studies for Bangladesh do not look at seasonal climate change clearly. Moreover, this study will attempt to find and/or develop efficient statistical methods/tools for climate projection.

The specific objectives are –

i. To rescue the missing data with the aim of generating a robust climate for Bangladesh;
ii. To select a suitable model for Bangladesh region using the Empirical Statistical Downscaling (ESD) Method for realizing and understanding climate parameters of rainfall, temperature and extreme weather events;
iii. To assess the uncertainties of the model involved in future climate predictions;
iv. To identify a suitable downscaling approach for climate model estimating the projection of climate parameters;
v. To measure the magnitude of the projection of temperature and rainfall and relevant other parameters.

1.9 Socio-economic Benefit of the Research

These projections of future climatic conditions in Bangladesh have many benefits. This research will tell us how climate may change in the near future (2021-2050) and far future (2071-2100), which is essential when assessing potential impacts. For example, infrastructure in Bangladesh may be at risk of future floods under 1.5°C, 2°C, and 4°C Global Warming Scenarios (Mohammed *et al*., 2018). Human health condition is also vulnerable; for example, a warmer climate can cause heat stress or heat stock, and it can result in more severe air pollution problems in city areas. Moreover, the transmission of diseases are also probable to escalate in a warmer climate (Confalonieri *et al*., 2007). For example, Dengue fever could become more challenging over Dhaka city due to warming temperatures as noted by Sultana *et al*. (2020).

Temperature warming may also impact many different sectors; for example, agriculture and fisheries are highly sensitive due to climate change. The power sector may also be affected due to

higher energy consumption by air conditioning equipment; the accessibility of groundwater is another issue because consumption is influenced by extreme heat conditions. Climate change effects will influence broadly across the country dependent on a local level, such as environments (such as sea, plain land or hills) and climate (such as dry or wet), among others. Regional-scale climate change risk calculations would help improve area and sector-specific mitigation and adaptation measures to diminish vulnerability to climate change. Finally, this study will provide valuable evidence to those exploring these impacts in various segments and for policymakers to take a positive attitude to adaptation and mitigation actions to climate change. Moreover, this research can supplement projections of future climate undertaken by BMD or any others research organization, especially from a third party and an academic point of view.

1.10 Outline of the thesis

This thesis paper has ten (10) chapters. The first chapter describes a summary of the fundamental issues of climate projections, such as the history of climate modelling. The development of climate models is explained, including the Climate Model Intercomparison Project, Evolutions of GCMs, emission scenarios and representative concentration pathways (RCPs). In this chapter is also presented GCMs work in Bangladesh and its research gap, research questions and social and economic benefit of the research.

Chapter 2 is a literature review focused on the current and previous research on future climate projection using Global Circulation Models (GCMs) and evaluating GCM performance. This chapter explained different model evaluation methods and also detailed presented GCMs projections, including spatial resolution in GCMs, dynamical downscaling, statistical downscaling and selection of statistical downscaling method.

Chapter 3 is about the climate of Bangladesh and the data used in this study: 1) the general description of the climate of Bangladesh, 2) historical disaster statistics of Bangladesh, and 3) the seasons of Bangladesh. This chapter also discusses GCMs data and, finally, the criteria for selecting GCMs in this study.

Chapter 4 explains the methodology used by missing data, missing data mechanisms and empirical statistical downscaling. In this chapter also detailed discusses the model setup using empirical-statistical downscaling method and working flow diagram.

Chapter 5 presents missing value calculations in the different observed stations in Bangladesh. Missing value calculations are based on the standard statistical method.

Chapter 6 presents the results of statistical downscaling of mean temperature in different seasons in Bangladesh, such as pre-monsoon, monsoon, post-monsoon and winter seasons.

Chapter 7 presents the results of statistical downscaling of wet-day frequency in different seasons in Bangladesh, such as pre-monsoon, monsoon and post-monsoon seasons.

Chapter 8 presents the results of future climate projections for Bangladesh, including a comparison of simulated projection with IPCC and other sources.

Chapter 9 summarizes of research findings, implications of this study, limitations of this study and recommendations for future work.

Finally, the chapter 10 reference part is added at the end of the thesis.

CHAPTER TWO: LITERATURE REVIEW

2.1 Preamble

GCMs can afford future projections of climate variables (Stocker *et al.*, 2013) but generally at a low resolution that is of inefficient use in impact studies assessing the local response to global climate change. These prognoses can nevertheless deliver some vital evidence about large-scale climate change. A general way of forthcoming the question of local climate change is through so-called downscaling, where the material about large-scale climate change is combined with information about how the local climate depends on the large-scale situation and, at the same time, local geographical factors (Rashid *et al*. 2020, 2021a, 2021b & Benestad, 2016). One implicit assumption of downscaling is that the climate models have a minimum skilful scale that is different from the spatial resolution (Takayabu *et al.*, 2015) and that local climates have a predictable dependence on the large-scale structures that the model is capable of reproducing. Some descriptions for the climate models' have small accuracy scales include simplicity and idealistic depiction of the earth, the use of distinct numbers and imperfect mathematical processes for solving numerical operations, a lack of small-scale surface details, the presence of unsettled small-scale procedures, and an imperfect model design due to our partial thoughtful of the climate system.

2.2 Evaluating GCM performance

Due to non-linear properties, the climate system's response to perturbations is governed to some extent by its actual state (Spelman and Manabe, 1984). Therefore, for models to calculate future climatic states consistently, they must simulate the current climatic conditions with some yet unknown degree of reliability. Poor model performance in simulating the present climate could show that specific physical or dynamic processes have not been represented. The better a model simulates the composite spatial patterns and seasonal and diurnal deviations of present climate, the more skill there is that all the essential processes have been effectively represented. So, when new models are created, considerable effort is dedicated to evaluating their ability to simulate the present climate (e.g., Collins *et al.*, 2006; Delworth *et al.*, 2006). Some of the valuations of model skill presented here are based on the 20th-century simulations that constitute a part of the Multi-Model Data (MMD) archived at the Program for Climate Model Diagnosis and Intercomparison (PCMDI). In these simulations, model developers have initiated the models from pre-industrial 'control' simulations and then executed the natural and anthropogenic forcing thought to be significant for simulating the climate of the last 140 years.

2.2.1 Model evaluation methods

A forecast based on a model can often be considered correct or incorrect, but the model itself should always be shown critically. This is a fact for both weather and climate prediction. Weather forecasts are on a regular basis and can be fast verified against what happened. Over time, statistics can be collected that give data on the skill of a particular model or forecast. Skill scores in a model

can be gained through simulations of the historical record or of palaeoclimate, but such opportunities are much more limited than those available through weather forecasts. In climate change experiments, at the same time, models are used to make predictions of possible future changes over time scales of many eras and for which there are no precise past analogues.

Generally, a climate model is a hybrid system with many components. The model must be verified at the system level, that is, by running the complete model and matching the results with observations. Such checks can expose problems, but the model's complication often hides their source. For this reason, it is also significant to test the model at the component level, that is, by separating specific components and examining them independently of the complete model. Component-level monitoring of climate models is standard. Physical parameterizations used in climate models are being verified through many case studies (some based on observations and some idealized) organized through programs. These activities have been ongoing for a decade or more, and many results have been available (e.g., Randall *et al.*, 2003). System-level assessment is concentrated on the outputs of the full model (i.e., model simulations of specific observed climate variables), and particular methods are discussed in more detail below.

Model Inter-comparisons and Ensembles: The global climate model inter-comparison arrangements that launched in the late 1980s (e.g., Cess *et al.*, 1989), and it continued with the Atmospheric Model Inter-comparison Project (AMIP) which have now expanded to add many models' inter-comparison projects covering virtually all climate model components and several coupled model. The most prestigious organized effort to collect and investigates Atmosphere-Ocean General Circulation Model (AOGCM) output from standardized trials have been undertaken in the last few years. It differs from previous model inter-comparisons in that a complete set of experiments includes unforced control simulations, simulations trying to yield observed climate change over the industrial period and simulations of future climate change. It is also varied in that, for each trial, multiple simulations are performed by some individual models to do it more accessible to distinguish climate change indicators from internal variability within the climate classification. Perhaps the most significant change from previous efforts is collecting a more inclusive model output, introduced centrally at the Program for Climate Model Diagnosis and Inter-comparison (PCMDI). This documentation, denoted here as 'The Multi-Model Data set (MMD) at PCMDI', has allowed hundreds of researchers from outside the modelling groups to analyze the models from various viewpoints. The improvement in diagnostic analysis of climate model results represents a vital step forward since the Third Assessment Report (TAR). Overall, the vigorous, continuing inter-comparison actions have augmented statements among modelling groups, permitted rapid documentation and rectification of modelling errors and encouraged the creation of standardized benchmark calculations, as well as a more complete and efficient record of modelling improvement.

Metrics of Model Reliability: For any given metric, it is vital to judging how good a trial it is of model outcomes for making projections of future climate change. This cannot be verified directly since no observed periods force changes similar to those estimated over the 21st century. Though, relationships between observable metrics and the predicted quantity of phenomena can be explored across model ensembles. Shukla *et al.* (2006) related a measure of the reliability of the simulated surface temperature in the 20th century with simulated 21st-century temperature change in a multi-model ensemble, and they established that the models with the lowest 20th-century error produced a relatively large amount of surface temperature rises in the 21st century. Knutti *et al.* (2006) analyzed different physical ensembles and showed that models with a strong seasonal cycle in surface temperature tended to have more considerable climate sensitivity. More composite metrics have also been made based on multiple observables in present-day climate and have been illustrated to have the potential to narrow the uncertainty in climate sensitivity tests across a particular model ensemble (Murphy *et al.*, 2004; Piani *et al.*, 2005). The above studies demonstrate that potential and quantitative metrics for the likelihood of model forecasts may be developed, but because the expansion of robust metrics is still at an early phase, the model assessments presented in this chapter are based mostly on experience and physical thought, as has been the norm in the past.

Testing Models against Past and Present Climate: Testing models' skills to simulate the present climate is integral to model evaluation. In doing this, confident, practical choices are needed, for example, between a long-time sequence or mean from a control run with fixed radiative forcing (often pre-industrial relatively than present day), or a shorter, short time series from a 20th-century simulation including historical variations in forcing. Such conclusions are made by individual investigators, dependent on the particular problem being analyzed. Variations between model and observations should be considered unimportant if they are within: (a). unpredictable internal variability, (b). expected differences in forcing and (c) uncertainties in the observed fields.

Other Methods of Evaluation: Simulations of climate conditions from the more distant past allow models to be evaluated in areas that are meaningfully dissimilar from the present. Such examinations complement the present and 'industrial period climate evaluations since 20th-century climate differences have been minor compared with the anticipated future changes under forcing scenarios derived from the IPCC Special Report on Emission Scenarios (SRES). The drawbacks of palaeoclimate trials are that uncertainty in both forcing and actual climate variables tends to be greater than in the instrumental period and that the number of climate variables for which there are well palaeo-proxies is limited. Additionally, climate conditions may have been so that processes determining quantities such as climate sensitivity differed from those likely to operate in the 21st century. Finally, the time scales of change were so long that there were complications in trial design, at least for General Circulation Models (GCMs).

2.3 GCM projections

Although nowadays GCMs are much more potent than when first developed in the 1950s, they still have limitations, and it remains impossible to apply their projections directly to a small spatial scale regional impact study. This is because the spatial resolution needs to be more coarse compared to the size of a city or small region. Furthermore, GCMs cannot simulate local landscapes or topography, such as rivers and mountains, limiting their representation of a small region or area (Wilby & Wigley, 1997). Giorgi *et al.* (2001) have summarized the techniques available for deriving local or regional scale climate information from GCM-based simulations of future climate scenarios. They fall into three categories: i) increase spatial resolution and use variable resolution in the GCM; ii) dynamical downscaling by using a regional climate model (RCM) and iii) empirical or statistical downscaling. These methods are concisely reviewed in the following sections.

2.3.1 Spatial resolution in GCMs

Alternatively, there has been the suggestion of using variable resolution in GCMs, which is to simplify variables such as sea ice, trace gas and aerosol forcing because high resolution of these variables can be obtained without performing the whole transient simulation (Giorgi *et al.*, 2001). The use of higher spatial resolution can improve the projection quality in terms of regional details. However, this method demands a massive amount of computational power. Therefore, the computational power can be concentrated on simulating other variables. The weakness of this approach is that a finer spatial scale GCM will require a different set of model formulations to optimize its performance. Furthermore, a sufficient minimal resolution must be retained outside the high resolutions area of interest to prevent the model's degradation.

2.3.2 Dynamical downscaling

A regional climate model (RCM) can produce high-resolution climatic variables for a region. The basic strategy is to use GCMs to simulate the response of global circulation to large-scale forcing. If the initial condition of the RCM is derived from GCMs, it can produce a high resolutions climate change scenario for a region. Then the RCM will account for the sub-grid scale force, which is highly dependent on regional characteristics. This technique is called nested regional climate modelling or dynamical downscaling.

Climate models are quite coarse resolutions for hydrological and meteorological modelling that impact assessments through mathematical models for which GCM output variables are not suitable to employ. This might hamper many applications of GCM projection-related research activities. To bridge this difficulty, RCMs are constructed based on dynamic downscaling using initial and time-dependent lateral boundary conditions of GCMs where no feedback generates from RCM simulation to the driving of GCM (IPCC, 2001). The RCM techniques have come from numerical weather prediction (NWP), and Dickinson *et al.* (1989) is the primary developer of RCM that has a spatial resolution of up to 10-20 km or less. These RCMs still need to be better to support the

fully spatial-temporal scale necessary for small hydrological-related climate impact studies; in that case, local and location-specific scenarios are demandable.

2.3.3 Statistical downscaling

The statistical downscaling method has been trained to target the GCM or RCM scenarios into other fine spatial and temporal downscaling, applying statistical relations between climate output variables and local variables. The statistical downscaling methods are functionally much easier and cheaper than RCMs. Statistical downscaling is to establish statistical relations between large-scale atmospheric patterns and observed local weather phenomena to solve the discrepancy between climate change scenarios and the resolution for impact assessment at the micro level (Maraun *et al.*, 2010). Future projections of local target variables can be made with established relations and future atmospheric patterns of a climate model. Statistical downscaling methods are generally divided into three parts-

i. Regression downscaling or transfer function model;
ii. Weather generator and
iii. Weather type

The Regression downscaling or transfer function methods work statistically linear or nonlinear relationships between observed local variables and GCM output variables. A reanalysis dataset in which observations and GCM are combined to synthesize the system's state is required to fit the relationships instead of GCM outputs. The future projections of scenarios from GCMs do not count for the actual past weather states. The Regression downscaling models are generally applied when a specific site needs to assess the impact of climate change scenarios. The weak central part of this method is the need for more statistical relationships for some variables.

Weather generators work stochastic simulation techniques that organize the statistical characteristics of observations. Here, the parameters are arranged according to the changes derived by climate models for future conditions. Within a short computation time, many climate scenarios can be produced, including natural variables for climate-related variables of interest at a specific site or multiple sites. The weak point of weather generators is that an infinite number of series can be simulated, which makes it challenging to select a representative scenario among them.

Weather-type methods employ global circulation patterns into several types and match the patterns to local weather variables (generally rainfall). Local climate projection is simulated using a classified pattern similar to the atmospheric circulation pattern from GCM scenarios (Bardossy *et al.*, 1992). The local variables are closely linked to global circulation at weather-type methods (Bardossy *et al.*, 1992). Here, the main drawbacks are- (i) No strong relation can frequently be found between global circulation patterns and local variables and (ii) Future patterns may significantly deviate from observations not remained in the past observations.

2.2.4 Selection of statistical downscaling method

The selection of the statistical downscaling method of any given scheme depends on the characteristics of the local variables (Wilby *et al.*, 2004). Generally, normally distributed variables such as temperate are suitable for regression methods. On the other hand, another downscaling method, such as a weather generator, could be adopted when the local variables are highly heterogeneous such as precipitation. Because this formula can identify or generate different possibilities of climate events. If the future change of hydrological or meteorological variables according to climate projection is needed for assessing climate change influence at a specific location. The bias correction in chapter five is sometimes suitable to apply.

When the future projection of a local variable (like temperature) is affected by downscale climate methods in chapter six. A regression model is settled with climate variables of the reanalysis data and local variables (explained in chapters 6 & 7). The future scenarios of variables of local phenomena are predicted by the climate variables of GCM. Coarse and spatial resolutions of GCM data with observed gridded data are employed to establish a spatial downscaling model, and the bias-corrected coarse GCM grid data is downscaled to better GCM grid data (illustrated in Chapter 5)

CHAPTER THREE: THE CLIMATE OF BANGLADESH AND DATA USED IN THIS STUDY

3.1 The climate of Bangladesh

Bangladesh is one of the most significant deltaic countries in the world. It has flat, low-lying plain land made up of alluvial soil, having only a small hilly area in the northeast and southeast regions. The most extensive Himalayan Range is to the north. At the same time, the vast Bay of Bengal is in the south. Bangladesh is approximately positioned between 20.57°N to 26.63°N and 88.02°E to 92.68°E. It is confined to the west, north and east by India. In the southeast, there is a common border with Myanmar. There are 230 rivers in Bangladesh. However, 57 originate from outside the country, and most of the rivers flow to the Bay of Bengal from north to south. The Ganges (Padma), the Brahmaputra and the Meghna are the main rivers in Bangladesh. The shoreline of Bangladesh is about 720 km long along the continental shelf, which has shallow bathymetry. The total area of Bangladesh is about 1, 44,735 sq. km. About 160 million, of which about 80% live in rural areas.

Bangladesh is located in a sub-tropical region. Here, the climate is a very significant influence of the Himalayas and north-east hilly regions. These mountain and hilly areas block the frigid katabolic winds flowing down from central Asia and retain the bulk of the Indian subcontinent warmer than most locations at related latitudes. Consequently, land regions in Bangladesh have a climate with severe summer environments that are alternative to cold winters where temperature plunges to below ten-degree centigrade. In contrast to the country's coastal regions, warmth is uniform, and the rains are frequent.

Southwest monsoon is the main feature that monitors the climate of Bangladesh; more than 71% of the annual rainfall is received during a short span of four months (June-September). The onset and withdrawal of southwest monsoon are crucial factors of monsoon rainfall. It profoundly impacts Bangladesh's water resources, power generation, agriculture, economics, ecosystems and fisheries. Oppositely, in the winter season, it abruptly falls down the temperature in the north and north-western parts of Bangladesh. It also impacts different segments in Bangladesh, especially agriculture.

3.1.1 Historical disaster statistics of Bangladesh

Bangladesh is a disaster-prone country worldwide, and every year many disasters face in Bangladesh. The country has been visible to many meteorological, hydrological and seismic hazards in the records. A few of the extreme meteorological and hydrological events are the Great Backerganj Cyclone (1876), the Worst killer cyclone of November 1970, the Urichar cyclone May 1985, the killer cyclone of April 1991, cyclone Sidr 2007, cyclone Aila 2009, 21 May 2016 Cyclonic Storm ‘ROANU’, floods of 1954, 1987, 1988, the historic flood of 1998, flood of 2007,

Demra Tornado of 1969, Manikganj Tornado of 1974, Madaripur Tornado of 1977, Saturia Tornado of 1989, and Tangail Tornado 1996 (Khatun et. al., 2016).

3.1.2 Meteorological Seasons of Bangladesh

Winter or Northeast Monsoon (December – February)

This season is characterized by very light northerly winds, mild temperatures and dry weather and clear to occasionally cloudy skies with fog over the country. This season, the average temperature range is (18-22)ºC (Khatun *et al*., 2016). During this period, when the ridge of sub-continental high pressure extends up to the north-western part of Bangladesh, temperatures begin to fall, and sometimes temperature goes below 10°C, then a cold wave situation occurs over the country. Bangladesh Meteorological Department uses different categories of cold waves, such as mild cold waves (8-10)°C, moderate cold waves (6-8)°C and severe cold waves (less than 6°C), respectively. Only 2 % of the total annual rainfall occurs in this season. During this season, rainfall occurs in the country only when a westerly low (western disturbance- which originates over the Mediterranean Sea) conjugates with the Easterly trough over Bangladesh.

Summer or Pre-Monsoon (March - May)

The mean temperature during the summer months remains within (23-30)°C. April and May are the hottest months. The highest maximum temperature ranging from (36-40)°C is reached in the north-western and south-western regions of the country. When the maximum temperature exceeds 36°C, a heat wave occurs over Bangladesh. BMD uses different criteria for heat waves such as mild heat wave (36-38)°C, moderate heat wave (38-40)°C and severe heat wave (greater than 40°C). Due to intense heating of the land, surface heat low develops over Bihar, West Bengal of India and the north-western part of Bangladesh; as a result, in the afternoon, moisture incursion occurs from the Bay of Bengal. For that low-pressure system develops and is favourable for the formation of thunder cloud and severe thunderstorms in these regions. These severe thunderstorms, known as Nor'westers ('Kalbaishakhi' in Bengali) often accompanied by fierce squalls, thunder and heavy rainfall with hails.

During the pre-monsoon season, Nor'westers occur in many places over Bangladesh frequently. Due to very severe thunderstorm activity in the upper catchment hilly regions, sometimes flash flood occurs in the northeastern part of Bangladesh.Only19% of the total annual rainfall occurs in this season. This season is also favourable for cyclogenesis in the Bay of Bengal. Some depressions may develop into cyclonic storms, which initially move northwestwards and then recurve to the northeast, moving towards Bangladesh and Myanmar coasts. Some cyclonic storms may attain very severe intensity with associated storm surges and landfall over the Bangladesh coast. The cyclone that hit the country's east coast on 29 April 1991 reportedly resulted in nearly 1, 38,882 deaths.

Southwest Monsoon (June - September)

This season, the surface wind changes to a south-westerly/southerly direction over the southern and central districts and to south-easterly over the country's northern districts. Wind speed is light to moderate. The onset and withdrawal of monsoons vary from place to place and annually. The expected date of onset of the Southwest monsoon in the southeastern districts of the country is the first week of June, and it will engulf the whole country through the first half of June. Monsoon begins withdrawal from the north-western part of Bangladesh, and the expected date of withdrawal from that part is 30 September (Ahmed and Karmakar, 1993). Generally, rain with widespread cloud cover and high humidity are the characteristics of this season. Due to heavy to very heavy rainfall over the southeastern part of the country, sometimes landslides occur in hilly regions. More than 71 % of the total annual rainfall occurs in this season. In the Southwest monsoon season, almost every year, a flood occurs in Bangladesh. During this season, monsoon depressions form over the Bay of Bengal, generally moving north-westwards, crossing the Indian coast and sometimes towards Bangladesh coasts. Depressions seldom attain Cyclone intensity in this season. With the progress of the monsoon, the summer's extremely hot temperatures fall visibly throughout the country.

Autumn or Post-Monsoon (October - November)

This is the intermediate season, from the summer monsoon to the winter. Precipitation declines considerably in October and November, and the dry period starts over the country. Only 8 % of the total annual rainfall occurs in this season. The lowest minimum does not fall below 10.0oC throughout the country. Tropical cyclones form over the Bay of Bengal this season and move initially towards the west and then northwest and sometimes re-curved towards the northeast affecting in Bangladesh coast. Some of these tropical storms in this season may attain very severe intensity with associated storm surges.

3.2 Observation locations in Bangladesh

Currently, 43 synoptic stations are in operation in Bangladesh Meteorological Department (BMD). BMD also has 10 Pilot Balloon stations and 3 Rawinsonde stations. According to Blue Books (WMO/UNDP/BGD/79/031 TECH. NOTE No.8), in 1947, there were 15 stations for primary Meteorological data; also, there were some parts time stations during that time. The number of stations increased to 41, but a few were closed subsequently, and by gradually adding/deleting, the total number of stations was 33 in 1981. Later on, some observatories were established, and at present, the total number is 43. In this study, data from 35 observatories were considered only (Table: 3.1). The processed monthly surface synoptic data for 22 observatories from 1948-1960 and 38 observatories from 1961-1980 was published in WMO/UNDP/BGD/79/031 TECH. NOTE No.8 and WMO/UNDP/BGD/79/031 TECH. NOTE No.9 respectively. The raw data were archived or stored on tape and hard disk. However, the data before 1948 were not available at BMD.

Table: 3.1: Observational stations descriptions of BMD.

No.	Division	Station	Latitude (° N)	Longitude (° E)	Elavation(m)	Establish (Year)	Local_ID
1	Dhaka	Dhaka	23.783	90.38333	8.45	1949	11111
2	Dhaka	Tangail	24.25	89.93333	10.2	1983	41909
3	Dhaka	Mymensingh	24.733	90.4166	18	1883	10609
4	Dhaka	Faridpur	23.6	89.85	8.1	1883	11505
5	Dhaka	Madaripur	23.16667	90.18333	7	1976	11513
6	Chattogram	Ambagan	22.35	91.8166	33.2	1937	41977
7	Chattogram	Ctg_Patenga	22.216	91.8	5.5	1937	11921
8	Chattogram	Cox'Bazar	21.45	91.96667	2.1	1908	11927
9	Chattogram	Chandpur	23.2333	90.7	4.88	1964	11316
10	Chattogram	Cumilla	23.43333	91.18333	7.5	1883	11313
11	Chattogram	Feni	23.0333	91.41667	6.4	1973	11805
12	Chattogram	Hatiya	22.45	91.1	2.44	1965	11814
13	Chattogram	Kutubdia	21.81667	91.85	2.74	1977	11925
14	Chattogram	M_Court	22.86667	91.1	4.87	1883	11809
15	Chattogram	Rangamati	22.6333	92.15	68.89	1957	12007
16	Chattogram	Sandwip	22.48333	91.43333	2.1	1966	11916
17	Chattogram	Sitakunda	22.6333	91.7	7.3	1977	11912
18	Chattogram	Teknaf	20.86667	92.3	5	1976	11929
19	khulna	Khulna	22.78333	89.5333	2.1	1921	11604
20	khulna	Jashore	23.2	89.3333	6.1	1867	11407
21	khulna	Satkhira	22.7166	89.08333	3.96	1877	11610
22	khulna	Chuadanga	23.65	88.81667	11.58	1986	41926
23	khulna	Mongla	22.46667	89.6	1.8	1988	41958
24	Barisal	Barisal	22.7166	90.36667	2.1	1883	11704
25	Barisal	Patuakhali	22.33333	90.33333	1.5	1973	12103
26	Barisal	Bhola	22.68333	90.65	4.3	1965	11706
27	Barisal	khepupara	21.98333	90.23333	1.83	1973	12110
28	Rajshahi	Rajshahi	24.36667	88.7	19.5	1883	10320
29	Rajshahi	Bogura	24.85	89.36667	17.9	1884	10408
30	Rajshahi	Ishurdi	24.15	89.0333	12.9	1963	10910
31	Rangpur	Rangpur	25.73333	89.2666	32.61	1883	10208
32	Rangpur	Dinajpur	25.65	88.68333	37.58	1883	10120
33	Rangpur	Sayedpur	25.75	88.91667	39.6	1980	41858
34	Sylhet	Sylhet	24.9	91.88333	33.53	1952	10705
35	Sylhet	Srimangal	24.3	91.73333	21.95	1905	10724

3.3 Descriptions GCMs data

This analysis is based on data from GCMs developed for the IPCC AR5 (CMIP5 Archive) run across three emission scenarios (RCPs 2.6, 4.5 and 8.5). The GCM data have been downloaded from the KNMI Climate Explorer (https://climexp.knmi.nl/start.cgi) and gridded to a 2.5-degree resolution grid from 1900 to 2100.

3.3.1 Criteria for selecting GCMs in this study

The model simulations are ranked based on the user-defined weights for the focus regions, variables, seasons, and skill scores (Kajsa M. P. *et al*., 2020). They are ranking of GCM model based on the following criteria:

a. A grade of the model simulations is made for the distinct skill scores for each region, variable and season.
b. The rankings are then multiplied by the corresponding weights, and the sum is calculated for each model simulation.
c. A new ranking of the model simulations is made based on the sum of the weighted rankings.

To derive this ranking, the Global Precipitation Climatology Project (GPCP) data was used as a reference for precipitation. The European Centre for Medium-Range Weather Forecasts, ERA5 data for temperature also found the better performance of GCM for different regions in the earth. For South Asia, a performance score and model ranking is calculated for the model ensembles, and the ten best-performing simulations GCM in south Asia are shown in Fig. 3.1. But Bangladesh is a small part of south Asia, and these ten GCMS cannot actually represent in Bangladeshi climate. So, Bangladesh needs a more accurate GCMs model.

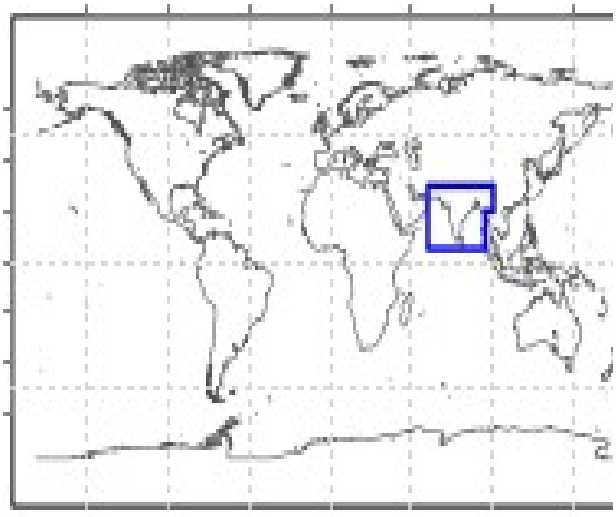

#	Model name	Rank
1	ACCESS1-0.r1i1p1	7
4	BNU-ESM.r1i1p1	9
49	HadGEM2-AO.r1i1p1	10
62	MIROC5.r1i1p1	4
63	MIROC5.r2i1p1	3
64	MIROC5.r3i1p1	6
67	MPI-ESM-LR.r1i1p1	1
68	MPI-ESM-LR.r2i1p1	2
69	MPI-ESM-LR.r3i1p1	5
70	MPI-ESM-MR.r1i1p1	8

Fig. 3.1: Model Skill Evaluation over South Asia. (source: https://gcmeval.met.no/)

My analysis is carried out within the R-environment using the Empirical Statistical Downscaling (esd) package (Benestad *et al*., 2015) to analyze and visualize the data and perform the statistical downscaling for location specific climate projection in Bangladesh. The 'esd' package has a wide range of functionalities, including methods for reading and processing data, generating various infographics, and performing statistical analysis (e.g., calculating empirical orthogonal functions, principal component analysis, and empirical-statistical downscaling) and is suitable for processing results from global climate models.

CHAPTER FOUR: METHODOLOGY

4.1 Preamble

Downscaling of climate change models is the process of using large-scale climate models to create climate predictions at finer temporal and spatial scales to fit the local level's purpose. This involves using GCMs representing physical processes in the atmosphere, sea, cryosphere and land surface. There are mainly two approaches to downscaling:

i. Dynamical downscaling: In this process, GCM's outputs are used to drive higher resolution RCMs for better representation of local terrain and other conditions;

ii. Statistical downscaling: It aims to establish a link between large-scale climate phenomena and observed.

Statistical downscaling is used when RCM data are unavailable in the region, and the resolution is low if it is there. Statistical downscaling is better with higher quality and longer duration of historically observed weather data.

4.2 Missing Data

In statistics, missing data occur when no data value is stored for the variable on an observation. In longitudinal studies, researchers often face missing data problems.

i. Subjects can be missed at particular time points;

ii. Subjects may provide responses to a subset of the study variables;

iii. Subjects might drop out of the study or be lost to follow-up after specific time points.

In statistics, missing data refers to a data set that was not recorded at a particular time.

4.2.1 Extraction of Missing Data

The missing data mechanisms address the fundamental question of "Why is the data missing?" Let R_{ij} be a pointer variable where-

$$R_{ij} = \begin{cases} 1, & if\ subject\ i\ observed\ at\ time\ j. \\ 0, & if\ the\ subject\ was\ not\ observed\ at\ time\ j. \end{cases}$$

If a study calls for measurement at n timepoint, then the $n \times 1$ complete dependent variable vector is -

$$y_i^{'} = (y_{i1}, y_{i2}, \dots\dots, y_{in}) \qquad (1)$$

Here, y_i is the potential dependent variable vector for subject i which can be partitioned in two part: y_i^o as the observed dependent variable and y_i^M as the unobserved dependent variable.

Again, $n \times 1$ missing data indicator vector for a subject is then-

$$R_i^{'} = (R_{i1}, R_{i2}, \dots\dots, R_{in}) \qquad (2)$$

where,

$$R_{ij} = \begin{cases} 1\,, & y_{ij}\ is\ observed\ at\ time\ j. \\ 0\,, & y_{ij}\ is\ not\ observed\ at\ time\ j. \end{cases}$$

For dropout subject in longitudinal studies, we consider a dropout variable D_i,

where $D_i = \begin{cases} j^{'}, if\ subject\ i\ dropout\ between\ the\ (j^{'}-1)^{th}\ and\ j^{'}\ timepoint \\ where, y_{i1}, \dots\dots, y_{i,j^{'}-1}\ are\ observed\ and\ y_{ij^{'}}, \dots\dots, y_{in}. \\ n, if\ subject\ was\ missing\ at\ the\ last\ timepoint \\ 0, if\ subject\ with\ complete\ data\ across\ time. \end{cases}$

Missing Completely at Random (MCAR): If missing data indicators R_i are independent of both y_i^o and y_i^M that's mean they do not depend on the dependents variables values that were observed or those that were not observed.

Missing at Random (MAR):

MAR describe that the missing data are related to the observed data (both x_i and y_i^o) but the missingness is not additionally related to the unobserved data y_i^M. MAR describe that the missing data where R_i is independent of y_i^M.

Missing not at Random (MNAR):

MNAR is the situation where the missingness is related to the unobserved dependent variable vector y_i^M after taking observed variables (x_i and y_i^o) into account.

Suppose that all subjects have data at time 1, but not in time 2. Because some are missing at time 2. Then, the regression is –

$$y_{ij} = \beta_0 + \beta_1 D_1 + \beta_2 x_i + \epsilon_i \qquad (3)$$

Where $D_i = \begin{cases} 1\,, & for\ the\ subjects\ that\ only\ have\ data\ at\ teh\ first\ timepoint. \\ 0\,, & for\ the\ subjects\ with\ data\ at\ both\ timepoint. \end{cases}$

β_2 is the vector of regression coefficients for the set of covariates include in x_i.

We can also interact the dropout variable with covariate to yield –

$$y_{ij} = \beta_0 + \beta_1 D_1 + \beta_2 x_i + \beta_3 (D_i \times x_i) + \epsilon_i \qquad (4)$$

Where β_3 is the vector of regression coefficients for the interaction of dropout with covariates. Now test hypothesis-

$$\mathrm{H}_o: \beta_1 = \beta_3 = 0$$

$$\mathrm{H}_1: Atleast\ one\ of\ them\ not\ equal\ zero.$$

$Devaiance = -2[lnL(model2) - lnL(model1)]$ which follows χ^2_σ at α% level of significance. IF P-value (Deviance)$< \alpha$, H_o can be rejected, otherwise accepted where null hypothesis is that there is no interaction effect.

4.3 Empirical-statistical downscaling

The empirical-statistical downscaling approach used in this study involved in deriving statistical relationships between the observed data over the different seasons from station-based observations in the period of 1981-2010 and the large-scale climate patterns represented by the common EOFs of the observed data or ERA5 reanalysis and GCM simulations. PCA is applied to the seasonally averaged observational data, which disintegrated the data into a set of spatial patterns, associated Principal Components (PC) describing their discrepancy in time, and eigenvalues explaining the relative weight of the several patterns.

The first two leading PCs, which are accounted for approximately large of the variability of the observed variables, are used as predictands. A common Empirical Orthogonal Function (EOF) analysis, as proposed by Benestad (2001), has been applied to the reanalysis or observed data and GCM data for the domain 85 to 105°E/-5 to 30°N to denote the large-scale predictors (Benestad *et al*., 2016). The global model data (one simulation at a time, using the entire length of available data 1850-2100) are combined with observed data for the period 1981-2010 along the time axis before performing the EOF analysis on both. This procedure decomposes the data into a set of common spatial patterns and eigenvalues and two principal components for each pattern representing the variations in time associated with the reanalysis and GCM data, respectively. The PCs associated with the observed/reanalysis data are then used to calibrate a statistical model defined as follows:

$$Y_1 = \beta_0 + \beta_1(x_1) + \beta_2(x_2) + \beta_3(x_3) + \cdots \quad (5)$$

Wherever, Y_1 is the initial leading PC of the predictand, x_1, x_2, x_3 .... are the leading PCs of the predictor, and $\beta_0, \beta_1, \beta_2$, ... are coefficients obtained through multiple regression. Similar models are fitted for the second PC of the predictand. The number of predictor patterns is chosen in such a way that the ensemble members can capture almost all of the variances. In this regard, ten-leading common EOF patterns can explain almost all (90-100 %) of the variances of the GCM simulation and observed data. A stepwise multiple regression is used to estimate model parameters, using predictand and predictor data from the calibration period 1981-2010. Only the part of the predictor PCs that represent the reanalysis are included in the regression. The number of predictors is reduced using the Akaike Information Criterion (AIC), a measure of model performance which takes both model quality and difficulty into assume in order to avoid overfitting (Akaike, 1974). In practice, this means that one or several of the coefficients $\beta_0, \beta_1, \beta_2$, ... can be established to zero during model calibration. The statistical model is then applied to the predictor PCs associated with the GCM data to obtain future projections of the predictand PCs. Future estimation of the local data could then be constructed from the prognoses of the predictand PCs joint with the

corresponding spatial magnitude and eigenvalues. The procedure of common EOF analysis and stepwise multiple regression is repeated for each GCM simulation, but because the calculations are rather efficient, they could nevertheless be applied to a large number of simulations.

To evaluate the skill of the empirical-statistical models, five-fold cross-validation is applied in which the fitting process is repeated five times (Maraun *et al*., 2018), each time left one-fifth of the predictor and predictand data out of the multiple regression (Wilks, 2011). In this process, chosen period of 1981-2010 is divided into five non-overlapping blocks, and a statistical model is calibrated against 4 of these blocks and used to predict the remaining blocks. The calibration period is covered the simulated present climate, whereas the validation period is covered the simulated future climate. Predictions are then made for the left-out period, and a cross-validation score is calculated as the correlation between these independent variables (prediction) and the original principal components. In total, this yields one model prediction. Cross-validation is performed for every regression model and each PC and GCM simulation.

To evaluate how well the downscaled GCM ensembles represent the past trends and interannual variability for each station, the observed seasonal data in the period 1981–2010 is compared with the statistical characteristics of the downscaled ensembles. The trend in the period of 1981–2010 is calculated for the observed value and each downscaled ensemble member at all stations.

To estimate the probability of seeing a trend of the observed strength given that the downscaled multi-model ensemble is a true representation of the distribution, the observed trend in the calibration period is compared with the probability density function (pdf) of a normal distribution with statistical characteristics (mean and standard deviation) given by trends of the downscaled ensemble members in the same period.

To assess the representation of the interannual variability, the number of observed values outside of the 90 percent confidence interval (CI) of the downscaled ensemble is counted, and the probability of the outcome is calculated using a binomial pdf.

4.4 Model Setup using Empirical Statistical Downscaling (ESD) Method

Let us assume that we have measurements of some variables at locations $x_1, x_2, \ldots x_p$ taken at times $t_1, t_2, \ldots t_n$. For each time t_j $(j = 1, \ldots, n)$ we can think of the measurements x_j $(j = 1, \ldots, n)$ as a map or field. We put these measurements in a matrix A as n fields each being p points long. We arrange each field into a row vector in A so that the size of A becomes n by p. We can then interpret each of the p columns in A as a time series for a given location. The EOF analysis is performed using A as the data matrix. In the below procedure of ESD, the variable in F can be observed in data of 34 BMD weather stations (O_1, $O_2, \ldots O_{34}$). Now, we examine the coupling between observed data and GCM model data measured at locations G_1, $G_2, \ldots G_{34}$ taken at times $t_1, t_2, \ldots x_n$ by using the bilinear interpolation method. For each eigenvalue λ_i chosen we find the corresponding eigenvector. Each of these eigenvectors can be regarded as a field. These eigenvectors are the EOFs which we are looking for. It is assumed that the eigenvectors are ordered to the size of the eigenvalues. Thus, EOF1 is the eigenvector associated with the biggest eigenvalue and the associated second biggest eigenvalue is EOF2, etc. Each eigenvalue λ_i, gives a measure of the fraction of the total variance explained by Singular Value Decomposition (SVD). A data matrix is constructed from this time sequence,and the EOF analysis is performed. The first twenty EOFs explain all the variance in the data, which implies that the data can be completely reconstructed using twenty patterns and twenty-time series. For example (Fig.4.1), twenty leading PCs which are captured 99.8% (81.56% for the 1st PC and 7.45% for 2nd PC) of variability of the observed ERA5 temperature data set, are used as predictands. This shows that the EOF method correctly finds the right number of independent patterns that make up the variability in the field. Finally, we develop twenty-one models for different RCPs, especially twelve for temperature and nine for rainfall data.

The full procedure of ESD is given below:

Step 1: Creation of Covariance matrix:

$$A = \begin{bmatrix} x_{11} & x_{12} & \ldots & x_{1p} \\ x_{21} & x_{22} & \ldots & x_{2p} \\ \vdots & \vdots & \ldots & \vdots \\ x_{n1} & x_{n2} & \ldots & x_{np} \end{bmatrix}$$

$$cov\,(A) = A'A$$

Step 2: Calculation of Eigen values

$$|cov(A) - \lambda I| = 0, \lambda = \lambda_1\,,\ \lambda_2,\ \ldots$$

Step 3: Calculation of EOF for each λ:

$$EOF(1) = \lambda_1 \begin{bmatrix} a_{11}x_{11} \\ a_{21}x_{21} \\ \vdots \end{bmatrix}$$

$$EOF(2) = \lambda_1 \begin{bmatrix} a_{12}x_{12} \\ a_{22}x_{22} \\ \vdots \end{bmatrix}$$

and so on.

Step 4: Arrangement of observed data for calculation:

$$F = \begin{bmatrix} O_{11} & O_{12} & \dots & O_{1,34} \\ O_{21} & O_{22} & \dots & O_{1,34} \\ \vdots & \vdots & \dots & \vdots \\ O_{n1} & O_{n2} & \dots & O_{n,34} \end{bmatrix}$$

$$PC(1) = \lambda_1, PC(2) = \lambda_2, \cdots$$

Step 5: Process of EOF analysis for GCM output:

$$GCM = Generate\ [Gridded\ F, Orginal\ GCM]_{Bilinear\ Interpolation}$$

$$G = \begin{bmatrix} G_{11} & G_{12} & \dots & G_{1,34} \\ G_{21} & G_{22} & \dots & G_{1,34} \\ \vdots & \vdots & \dots & \vdots \\ G_{n1} & G_{n2} & \dots & G_{n,34} \end{bmatrix}$$

$$For\ each\ \lambda_1 = EOF(1), EOF(2), \dots$$

$$\begin{bmatrix} Y & X_1 & X_2 & \dots & X_{20} \\ PC_1 & EOF_1 & EOF_2 & \dots & EOF_{20} \\ PC_2 & EOF_1 & EOF_2 & \dots & EOF_{20} \\ \vdots & \vdots & \vdots & \dots & \vdots \end{bmatrix}$$

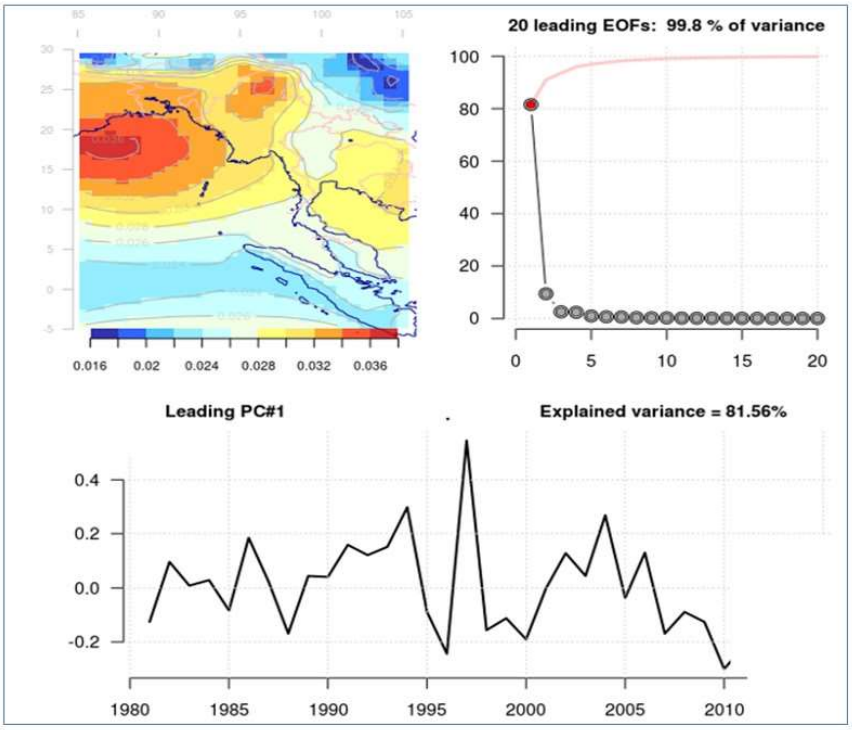

Fig.4.1: 20 Leading EOFs

Step 6: Model:

$$Y_1 = B_0 + B_1(x_1) + B_2(x_2) + B_3(x_3) + \cdots$$

Step 7: Selection of suitable Model:

Variable	RCP	No of Model	Seasons
Temperature	2.6	4	4 seasons
	4.5	4	4 seasons
	8.5	4	4 seasons
Rainfall	2.6	3	3 seasons
	4.5	3	3 seasons
	8.5	3	3 seasons
		Total =21	

4.5 Working Flow Diagram

As per the methodology described above, the flow diagram of the downscaling process has been given in Fig. 4.2. In the first step, the calculation of the first PCA from observed data has been conducted. Calculation of leading EOF based on GCM output has been done in the second stage. In the third stage, multivariate regression was established using ESD. Then a comparison of multivariate regression was conducted with the first PCA. In the final stage, the maximum correlation with the GCM has been selected to proceed for future projection.

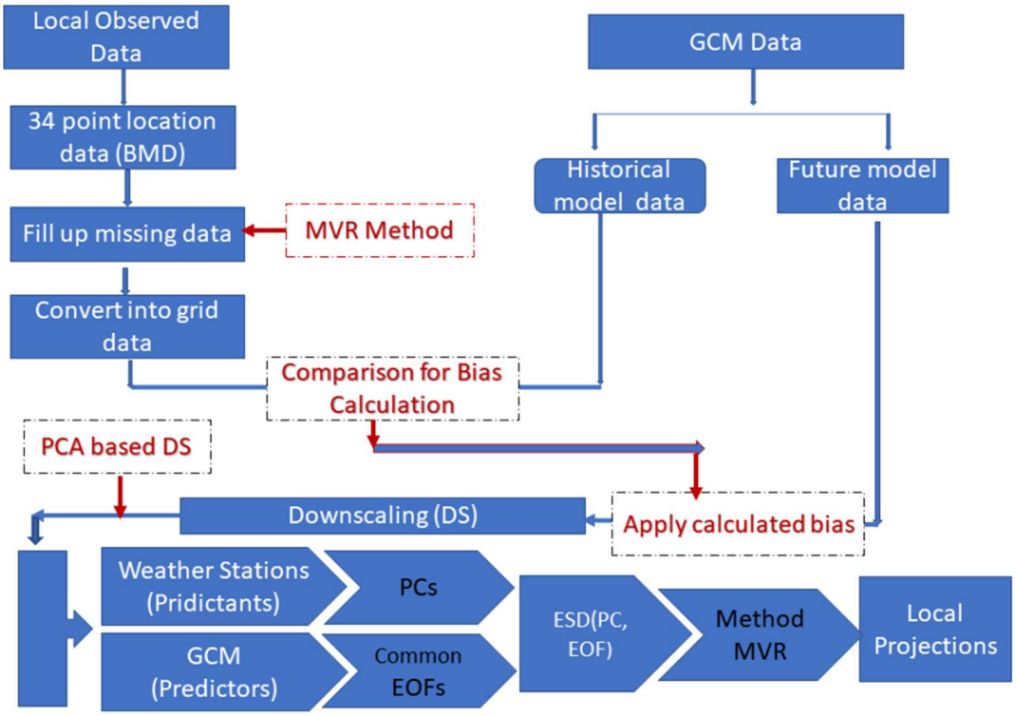

Fig. 4.2: Flow diagram of Downscaling Process

CHAPTER FIVE: OBSERVED MISSING DATA CALCULATION

5.1 Preamble

In the manual observation process, data can be missing due to incomplete data entry, equipment malfunctioning, loss of records, and many other reasons. So, there are usually some missing data in each archive data set. However, these data are very useful, and it requires recovery with the aim of recovering these data as the best way to form a model for the missing data calculation. This could be done through spatial correlation among the available data. The distribution can then be used to compute the missing data via sampling from the conditional distribution. But various other methods are also helpful. Multiple regression method has been adopted here to calculate or generate the missing data under this study.

5.1 Observed Missing data calculation

The GCMs data are usually assessed based on various observations or reference data sets. For validation GCMs, a good set of observation data is very necessary. In this analysis, 34 BMD stations data are used as an observed data set, and their locations are given in Fig. 5.1; in addition, their classified elevation is depicted in Fig. 5.2). As BMD stations are established at different times, but for analysis, same observation length is also required. To overcome this limitation, it is required to check the available and missing data periods. An R-package 'RgoogleMaps' has been utilized on the BMD's maximum temperature data set, and the result has been displayed in Fig. 5.3.

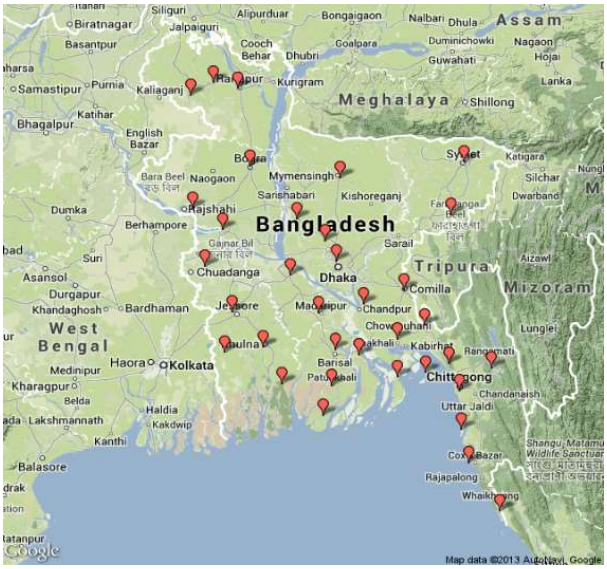

Fig. 5.1: Station location under study in Google maps

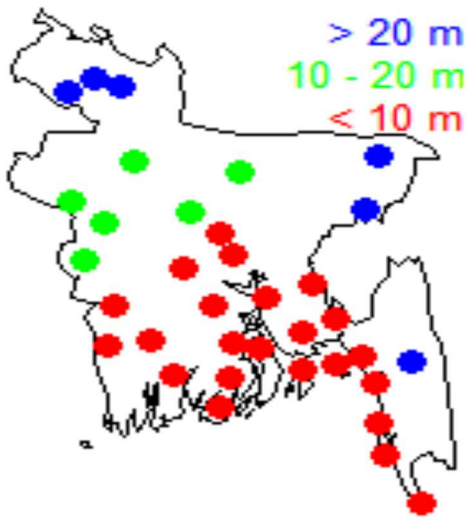

Fig. 5.2: Station elevation map of BMD

(Source: http://www.bmd.gov.bd/p/Climate-Report/)

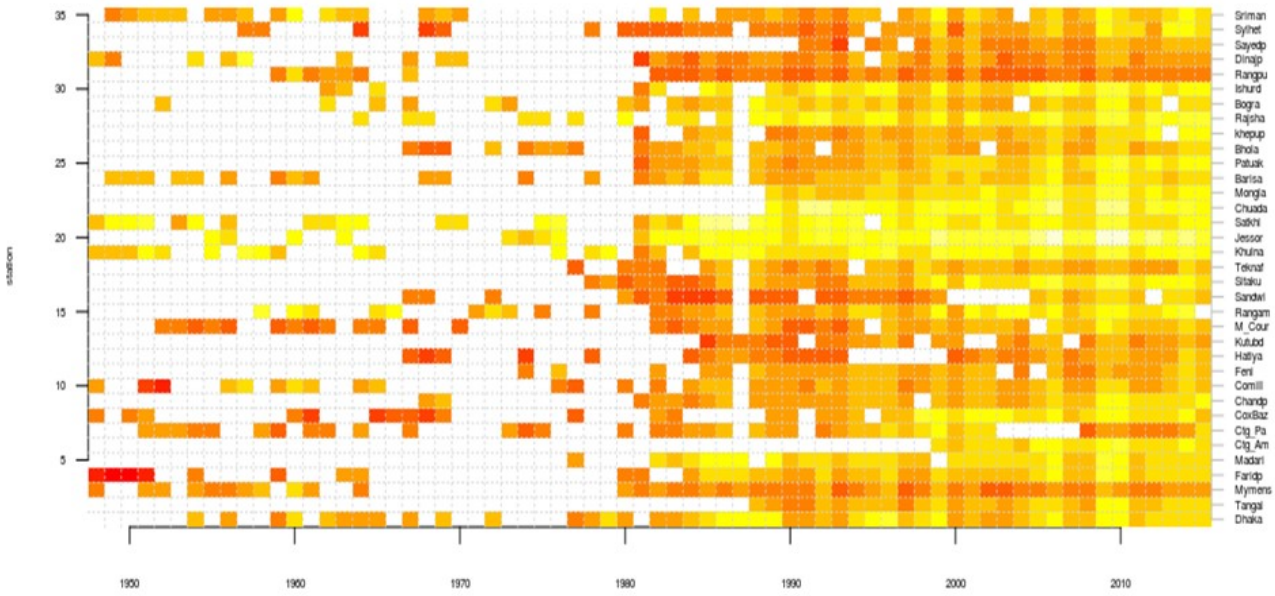

Fig. 5.3: Temperature data availability in my study stations (based on 360 days per year)

Fig. 5.3 shows the maximum temperature data availability at BMD stations from 1948 to 2015. The color box indicates data availability of 360 days or more per year, and the white box indicates that maximum data availability is less than 360 days per year. Fig. 5.3 also indicates that the missing data provision is rigorous in each of the stations before 1980, but the data is almost acceptable in level at all stations after 1981. The details are given in Table 5.1.

Table 5.1: Data gap of BMD's station

Sl	Station Name	Short name of the Station (6 alphabets)	Year of Data Availability	Large Number of Data Missing before 1981	Large Number of Data Missing after 1981
1.	Srimangal	Sriman	1949	Yes	No
2.	Sylhet	Sylhet	1957	Yes	No
3.	Sayedpur	Sayedp	1991	Yes	Yes
4.	Dinajpur	Dinajp	1948	Yes	No
5.	Rangpur	Rangpu	1959	Yes	No
6.	Ishudi	Ishudi	1962	Yes	No
7.	Bogura	Bogra	1952	Yes	No
8.	Rajshahi	Rajsha	1964	Yes	No
9.	Khepupara	Khepup	1981	Yes	No
10.	Bhola	Bhola	1977	Yes	No
11.	Patuakhali	Patuak	1981	Yes	No
12.	Barisal	Barisa	1949	Yes	No
13.	Mongla	Mongla	1988	Yes	Yes
14.	Chaudanga	Chuada	1988	Yes	Yes
15.	Satkhira	Satkhi	1948	Yes	No
16.	Jessore	Jessor	1956	Yes	No
17.	Khulna	Khulna	1948	Yes	No
18.	Teknaf	Teknaf	1977	Yes	No
19.	Sitakunda	Sitaku	1978	Yes	No
20.	Sandip	Sandip	1967	Yes	Yes
21.	Rangamati	Rangama	1957	Yes	No
22.	M_Court	M_Cour	1952	Yes	No
23.	Kutubdia	Kutubd	1985	Yes	No
24.	Hatiya	Hatiya	1957	Yes	Yes
25.	Feni	Feni	1974	Yes	No
26.	Comilla	Comill	1948	Yes	No
27.	Chandpur	Chandp	1968	Yes	No
28.	CoxsBazar	CoxBaz	1948	Yes	No
29.	Patenga (Chottogram)	Ctg_Pa	1951	Yes	Yes
30.	Ambagan (Chottogram)	Ctg_Am	1998	Yes	Yes
31.	Madaripur	Madari	1977	Yes	No
32.	Faridpur	Faridp	1948	Yes	No
33.	Mymensingh	Mymens	1948	Yes	No
34.	Tangail	Tangai	1987	Yes	No
35.	Dhaka	Dhaka	1954	Yes	No

Based on the information in Table 5.1, the data period of 1981-2010 has been considered for the study, which is also a climate period recognized by World Meteorological Organization (WMO).

To fill up the missing gaps of data, pairwise correlations are calculated for each of the target stations with the remaining stations. The magnitudes of the highest three stations correlation coefficients (CCs) are considered. Then a regression equation was fit with these three stations CC to determine the target stations' maximum temperature. Similarly, the missing values of all of the stations are calculated. The details are given in Table 5.5.

Table 5.2 shows the correlation coefficient between Dhaka and Tangail is 0.15; Dhaka and Mymensingh is 0.71; Dhaka and Faridpur is 0.79, and so on. However, the highest correlation coefficient of 0.79 is between Dhaka and Faridpur. The second highest of 0.76 is between Dhaka and Barishal, and the third highest of 0.74 is between Dhaka and Chandpur.

Fig. 5.4 to 5.6 indicate that dark green color belongs to greater than equal 0.9, green greater than equal 0.8, red color greater than equal 0.7, orange greater than equal 0.6, black greater than equal 0.5, dark red greater than equal 0.4 and finally purple means less than 0.4.

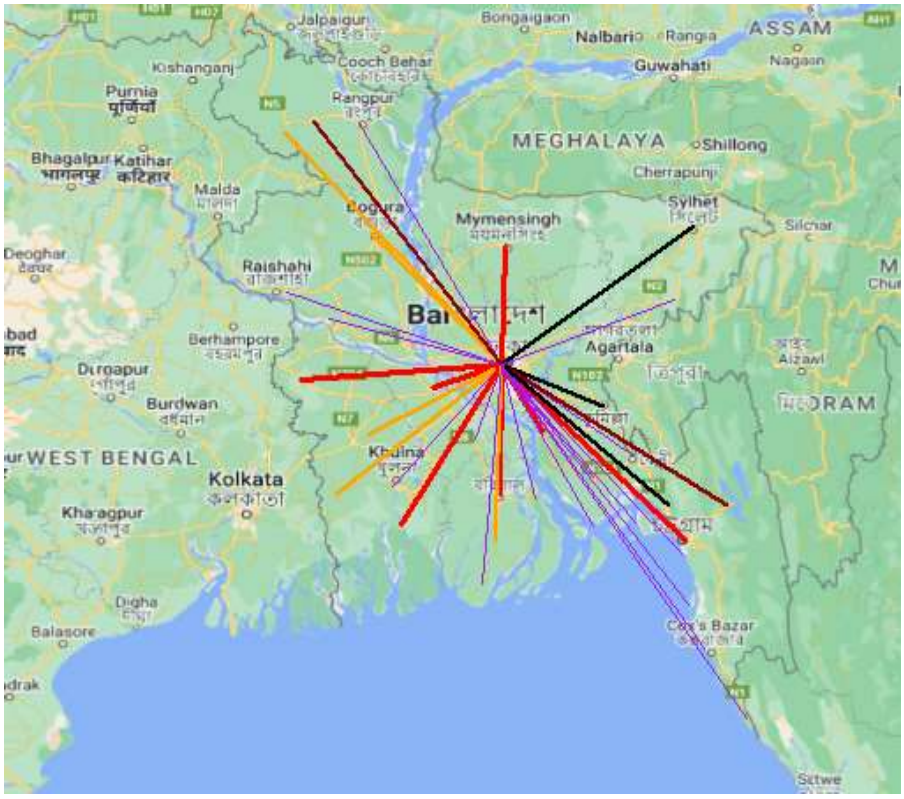

Fig: 5.4: Pairwise correlation: target station (Dhaka) with other stations

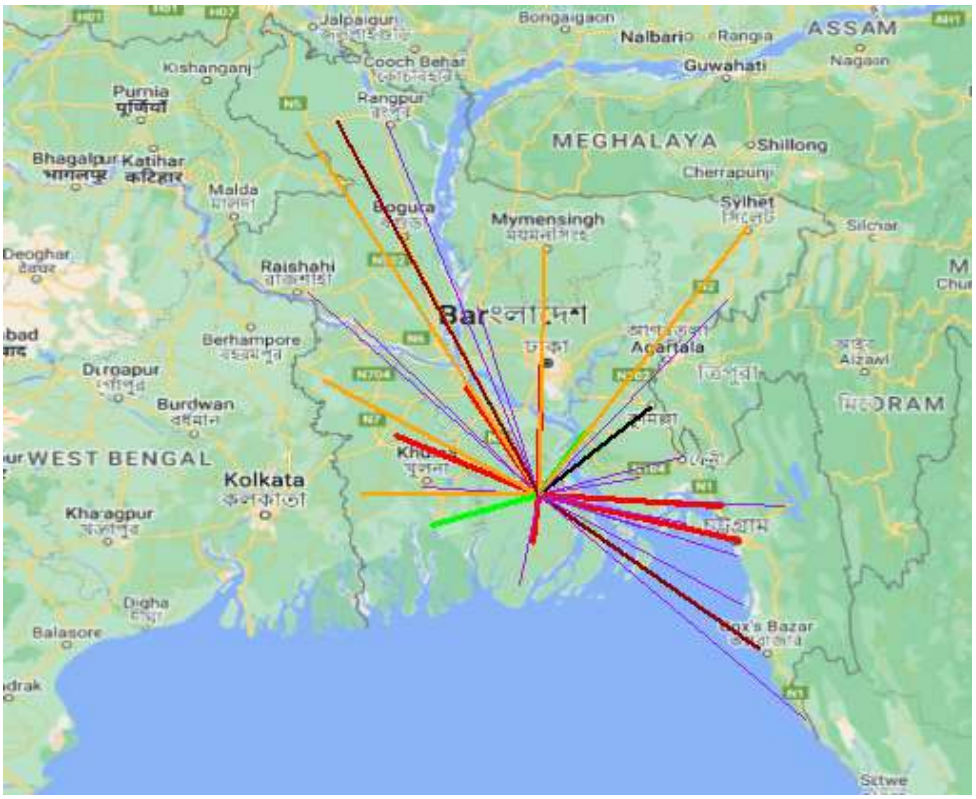

Fig: 5.5: Pairwise correlation: target station (Barishal) with other stations

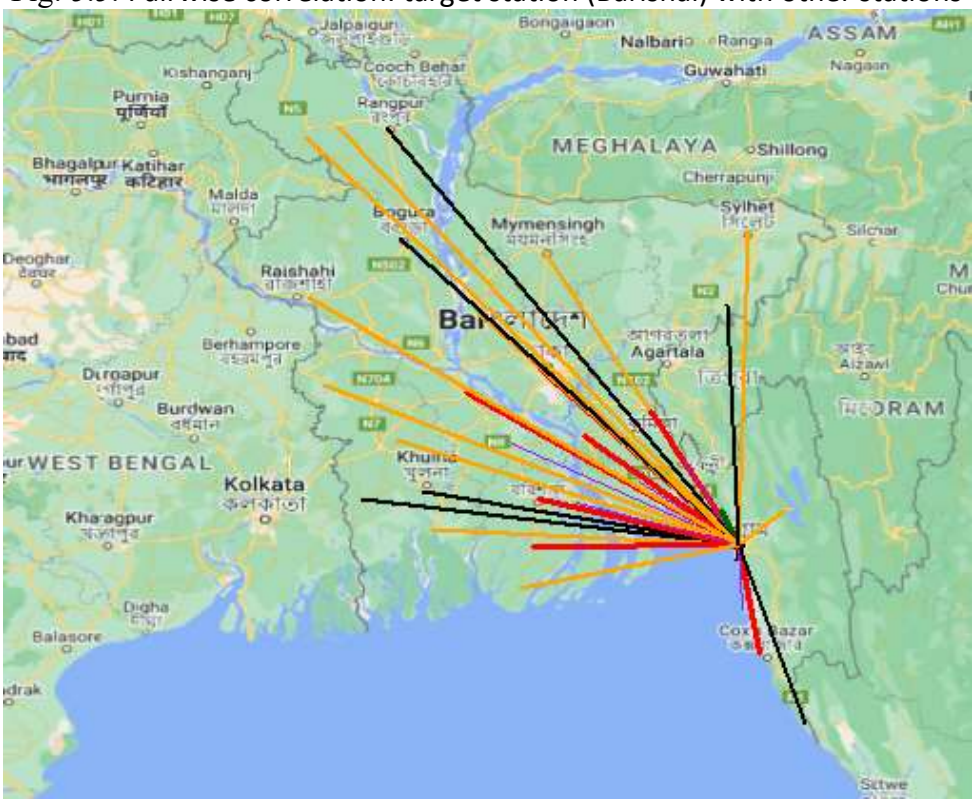

Fig: 5.6: Pairwise correlation: target station (Ambagan_Chattogram) with other stations

Table 5.2: Pairwise correlation of target station (Dhaka) with other stations

Target Station	Rest of Stations	r values	Target Station	Rest of Stations	r values
Dhaka	Tangail	0.15	Dhaka	Khulna	0.35
	Mymensingh	0.71		Jessore	0.68
	Faridpur	0.79		Satkhira	0.67
	Madaripur	0.03		Chuadanga	0.71
	Ctg_Ambagan	0.71		Mongla	0.71
	Ctg_Patenga	0.33		Barishal	0.76
	Cox'Bazar	0.28		Patuakhali	0.65
	Chandpur	0.74		Bhola	0.22
	Comilla	0.50		khepupara	0.24
	Feni	0.19		Rajshahi	0.30
	Hatiya	-0.18		Bogra	0.64
	Kutubdia	0.22		Ishurdi	0.08
	M_Court	0.22		Rangpur	0.30
	Rangamati	0.45		Dinajpur	0.66
	Sandwip	0.15		Sayedpur	0.47
	Sitakunda	0.55		Sylhet	0.58
	Teknaf	0.07		Srimangal	0.25

It can be explained that the correlation coefficient between Barishal and Dhaka is 0.76; between Barishal and Tangail is 0.19; between Barishal and Mymensingh is 0.63, and so on. Among the CCs the highest correlation coefficient of 0.84 is between Barishal and Mongla; the second highest CC of 0.82 is between Barishal and Chandpur; the third highest CC of 0.76 is between Barishal and Dhaka. After consideration of these CC fitting with the multiple regression, the magnitude of the R-squared value increased to 0.927 (Tables 5.3 and 5.5).

Similarly, the correlation coefficient between Ambagan (Chattogram) and the rest of the BMD stations is considered. The highest correlation coefficient of 0.90 is found between Ambagan and Sitakunda, the second highest of 0.78 is between Ambagan and Cumilla and the third highest of 0.78 is seen between Ambagan and Cox's Bazar. After consideration of these CC fitting with the multiple regression, the magnitude of the R-squared value increased to 0.888 (Tables 5.4 and 5.5).

Table 5.3: Pairwise correlation of target station (Barishal) with other stations

Target Station	Rest of Stations	r values	Target Station	Rest of Stations	r values
Barishal	Dhaka	0.76	Barishal	Teknaf	0.17
	Tangail	0.19		Khulna	0.36
	Mymensingh	0.63		Jessore	0.74
	Faridpur	0.75		Satkhira	0.64
	Madaripur	0.08		Chuadanga	0.70
	Ctg_Ambagan	0.77		Mongla	0.84
	Ctg_Patenga	0.33		Patuakhali	0.74
	Cox'Bazar	0.43		Bhola	0.16
	Chandpur	0.82		khepupara	0.33
	Comilla	0.51		Rajshahi	0.23
	Feni	0.18		Bogra	0.63
	Hatiya	0.01		Ishurdi	0.19
	Kutubdia	0.18		Rangpur	0.27
	M_Court	0.28		Dinajpur	0.66
	Rangamati	0.38		Sayedpur	0.45
	Sandwip	0.06		Sylhet	0.62
	Sitakunda	0.75		Srimangal	0.15

Table 5.4: Pairwise correlation of target station (Ambagan) with other stations

Target Station	Rest of Stations	r values	Target Station	Rest of Stations	r values
Ambagan (Chattogram)	Dhaka	0.71	Ambagan (Chattogram)	Khulna	0.60
	Tangail	0.61		Jessore	0.61
	Mymensingh	0.67		Satkhira	0.56
	Faridpur	0.72		Chuadanga	0.60
	Madaripur	0.01		Mongla	0.65
	Ctg_Patenga	0.52		Barisal	0.77
	Cox'Bazar	0.78		Patuakhali	0.74
	Chandpur	0.74		Bhola	0.10
	Cumilla	0.79		khepupara	0.66
	Feni	0.16		Rajshahi	0.61
	Hatiya	0.67		Bogra	0.51
	Kutubdia	0.19		Ishurdi	0.62
	M_Court	0.26		Rangpur	0.50
	Rangamati	0.67		Dinajpur	0.61
	Sandwip	0.21		Sayedpur	0.61
	Sitakunda	0.90		Sylhet	0.65
	Teknaf	0.55		Srimangal	0.59

Table 5.5: Results of study stations

Station	The highest value of CC with station	The second highest value of CC with station	The third highest value CC with station	Multiple R-squared	P Value less than
Dhaka	0.79 (Faridpur)	0.76 (Barishal)	0.74 (Chandpur)	0.932	2.2×10^{-16}
Tangail	0.74 (Chuadanga)	0.72 (Mongla)	0.61 (Ctg_Ambagan)	0.867	do
Mymensingh	0.75(Dinajpur)	0.72 (Faridpur)	0.71 (Dhaka)	0.841	do
Faridpur	0.85(Mongla)	0.83(Chuadanga)	0.79 (Dhaka)	0.957	do
Madaripur	0.37(Rajshahi)	0.34(Rangpur)	0.13 (Satkhira)	0.879	do
Ctg_Ambagan	0.90 (Sitakunda)	0.79 (Cumilla)	0.78 (Cox'sbazar)	0.888	do
Ctg_Patenga	0.52 (Ctg_Ambagan)	0.35 (Sitakunda)	0.33 (Barishal)	0.835	do
Cox'Bazar	0.78 (Ctg_Ambagan)	0.64 (Sitakunda)	0.57 (Mongla)	0.806	do
Chandpur	0.82 (Barishal)	0.75 (Mongla)	0.74 (Dhaka)	0.934	do
Cumilla	0.79 (Ctg_Ambagan)	0.69 (Mongla)	0.64 (Chuadanga)	0.826	do
Feni	0.50 (Khulna)	0.34 (Khepupara)	0.23 (Teknaf)	0.753	do
Hatiya	0.67 (Ctg_Ambagan)	0.16 (Khulna)	0.13 (Mongla)	0.868	do
Kutubdia	0.26 (Ctg_Patenga)	0.22 (Dhaka)	0.22 (Mymensingh)	0.800	do
M_Court	0.28 (Chandpur)	0.28 (Barishal)	0.26 (Ctg_Ambagan)	0.924	do
Rangamati	0.67 (Ctg_Ambagan)	0.64 (Mongla)	0.50 (Chuadanga)	0.812	do
Sandwip	0.49 (Bhola)	0.21 (Ctg_Ambagan)	0.17 (Bogura)	0.815	do
Sitakunda	0.90 (Ctg_Ambagan)	0.75 (Barishal)	0.74 (Sylhet)	0.900	do
Teknaf	0.75 (Sayedpur)	0.55 (Ctg_Ambagan)	0.43 (Khulna)	0.648	do
Khulna	0.81 (Mongla)	0.73 (Chuadanga)	0.63 (Khepupara)	0.942	do
Jessore	0.83 (Mongla)	0.77 (Chuadanga)	0.76 (Faridpur)	0.944	do
Satkhira	0.75 (Mongla)	0.74 (Faridpur)	0.72 (Chuadanga)	0.942	do
Chuadanga	0.83 (Faridpur)	0.82 (Rajshahi)	0.82 (Ishurdi)	0.855	do
Mongla	0.85 (Faridpur)	0.84 (Barishal)	0.84 (Patuakhali)	0.916	do
Barishal	0.84 (Mongla)	082 (Chandpur)	0.76 (Dhaka)	0.927	do
Patuakhali	0.84 (Mongla)	0.74 (Barishal)	0.74 (Ctg_Ambagan)	0.941	do

Station	The highest value of CC with station	The second highest value of CC with station	The third highest value CC with station	Multiple R-squared	P Value less than
Bhola	0.49 (Sandwip)	0.22 (Dhaka)	0.20 (Mymensingh)	0.871	do
khepupara	0.73 (Mongla)	0.66 (Ctg_Ambagan)	0.63 (Khulna)	0.894	do
Rajshahi	0.82 (Chuadanga)	0.71 (Mongla)	0.61 (Rajshahi)	0.931	do
Bogura	0.68 (Dinajpur)	0.64 (Dhaka)	0.61 (Mymensingh)	0.914	do
Ishurdi	0.82 (Chuadanga)	0.76 (Mongla)	0.45 (Sayedpur)	0.940	do
Rangpur	0.56 (Chuadanga)	0.56 (Sayedpur)	0.50 (Mongla)	0.947	do
Dinajpur	0.75 (Mymensingh)	0.68 (Bogura)	0.67 (Chuadanga)	0.868	do
Sayedpur	0.61 (Ctg_Ambagan)	0.56 (Rangpur)	0.55 (Mymensingh)	0.961	do
Sylhet	0.74 (Sitakunda)	0.65 (Ctg_Ambagan)	0.64 (Chandpur)	0.564	do
Srimangal	0.59 (Ctg_Ambagan)	0.40 (Mongla)	0.38 (Chuadanga)	0.685	do

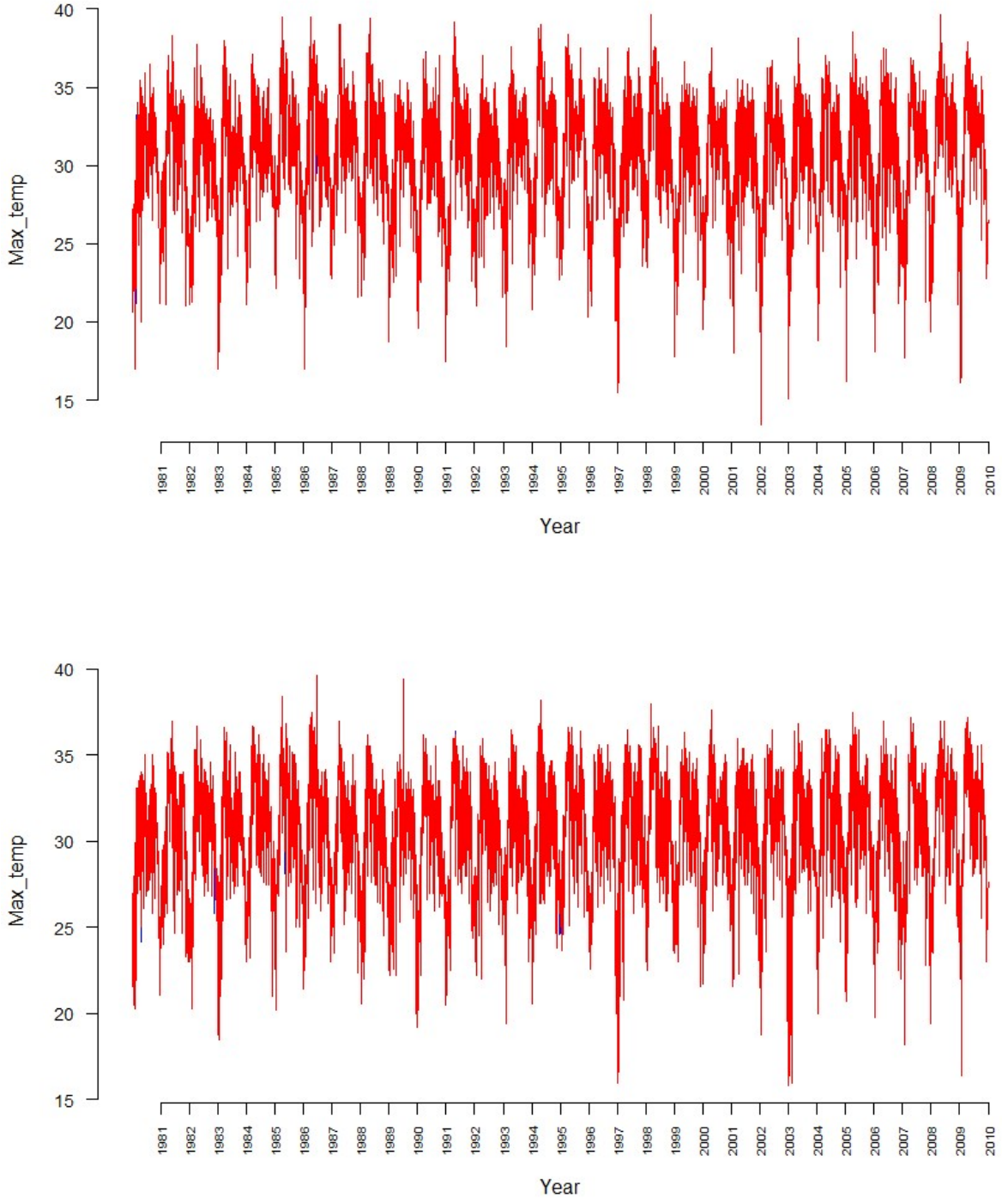

Fig. 5.7: Maximum temperature of original data with filled missing data at Dhaka Station(upper) and Barishal Station (bottom)

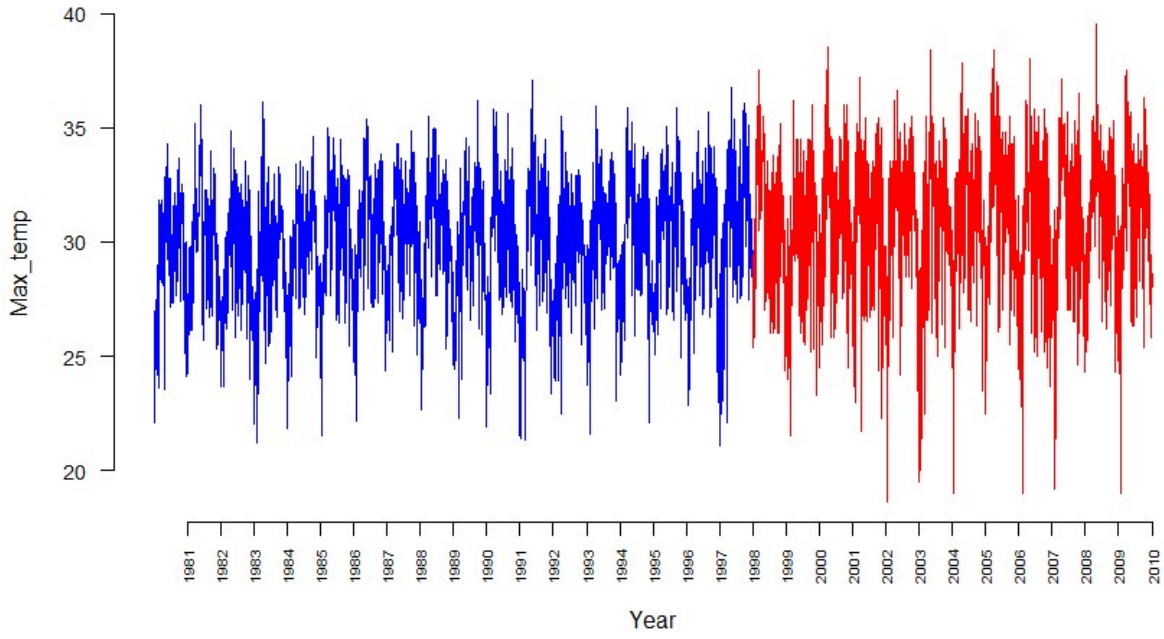

Figure. 5.8: Maximum temperature of original data (red color) and generated missing data (blue color) by multiple regression method based on the best correlated stations for Ambagan (Chattogram) station

After filling up the missing data, the temporal variation of data has been displayed to see the continuity of data and understand the model's performance. Accordingly, the final output of maximum temperature for Dhaka and Barishal station data which are filled up with missing data based on the best fitting regression model as given in Fig. 5.7. Similarly, Fig. 5.8 is the final output of the maximum temperature of Ambagan (Chattogram), which has the highest missing data because here there were no records of data from 1998 (Table 5.1). But this study finds the best correlation of 0.90, 0.79 & 0.77 and then sets up regression models; these stations and model capture R-squared values 0.888 and P values of 2.2×10^{-16}, which declares the best fitting model. Similarly, missing values have filled up for the remaining stations' station-based temperature and rainfall data.

CHAPTER SIX: STATISTICAL DOWNSCALING OF TEMPERATURE

6.1 Preamble

Principal Component Analysis (PCA) is similar to Empirical Orthogonal Function (EOF). PCA is considered for groups of stations rather than gridded fields. PCA can also signify data on an irregular grid, such as rotated fields from regional climate model outputs. It is possible to grid the spatial modes of the PCA onto a regular grid and hence convert the PCA class into an EOF. Though EOFs weights each grid box with its grid box area, PCA does not apply any weighting to the different series (which may indicate that the PCA underlines correlated variability from nearby stations). PCAs are useful for exploring large-scale variability since the leading mode will catch patterns with coherent variations across the stations.

The Empirical Statistical Downscaling (ESD) method is applied in this study to use the large-scale variabilities that the models can produce credibly to say approximately local change. GCMs have at least a minimum skillful value, meaning that their distinct grid-box values are not a good depiction of the region they represent in the real world. Using common EOF analysis makes it possible to recognize common spatial patterns in the local station and GCM data on a scale that climate models represent well. A potential constraint of the downscaling method presented here is that the predictor-predictand association may not be stationary, and the statistical model may not apply in the future. The stationarity hypothesis is vital to empirical-statistical downscaling but challenging to validate, especially without access to long observational records. Here, the local temperature is downscaled from the mean temperature over the area of 80-100°E/15-45°N. Some circumstances could change the predictor-predictand connection in a specific time of climate change activities. So, the local temperature response to large-scale temperature patterns could be influenced by changes in precipitation patterns, cyclonic activity and the timing of the monsoon. One way to report this could be to integrate additional predictor variables that describe other aspects of the climate.

6.2 Temperature of Pre-monsoon Season

Based on the different RCPs, emission scenarios for temperature and observed data of BMD in pre-monsoon season are selected for their relevance with the South Asia domain. An evaluation of the common EOFs from GCM and observed temperatures are performed to measure the goodness of fit of the GCM output in respect of observation (local temperature data). The residuals from the downscaled values are examined against sufficiency. Screening of predictors has been conducted using ten (10) best GCMs. These GCMs are- ACCESS1-0-r1, ACCESS1.3-r1, bcc-csm1-1-r1, bcc-csm1-1-m-r1, BNU-ESM-r1, CanESM2-r1, CanESM2-r2, CanESM2-r4, CanESM2-r5, CCSM4-r1 (where r means model realization). Among various stations' observed temperature data, the best cross-validated correlation predictors and predictand are selected and are shown in Fig.

6.2.1 to Fig. 6.2.3, respectively, for different RCPs. These figures indicate that the correlation between predictors and predictands of temperature are 0.88, 0.84 and 0.88.

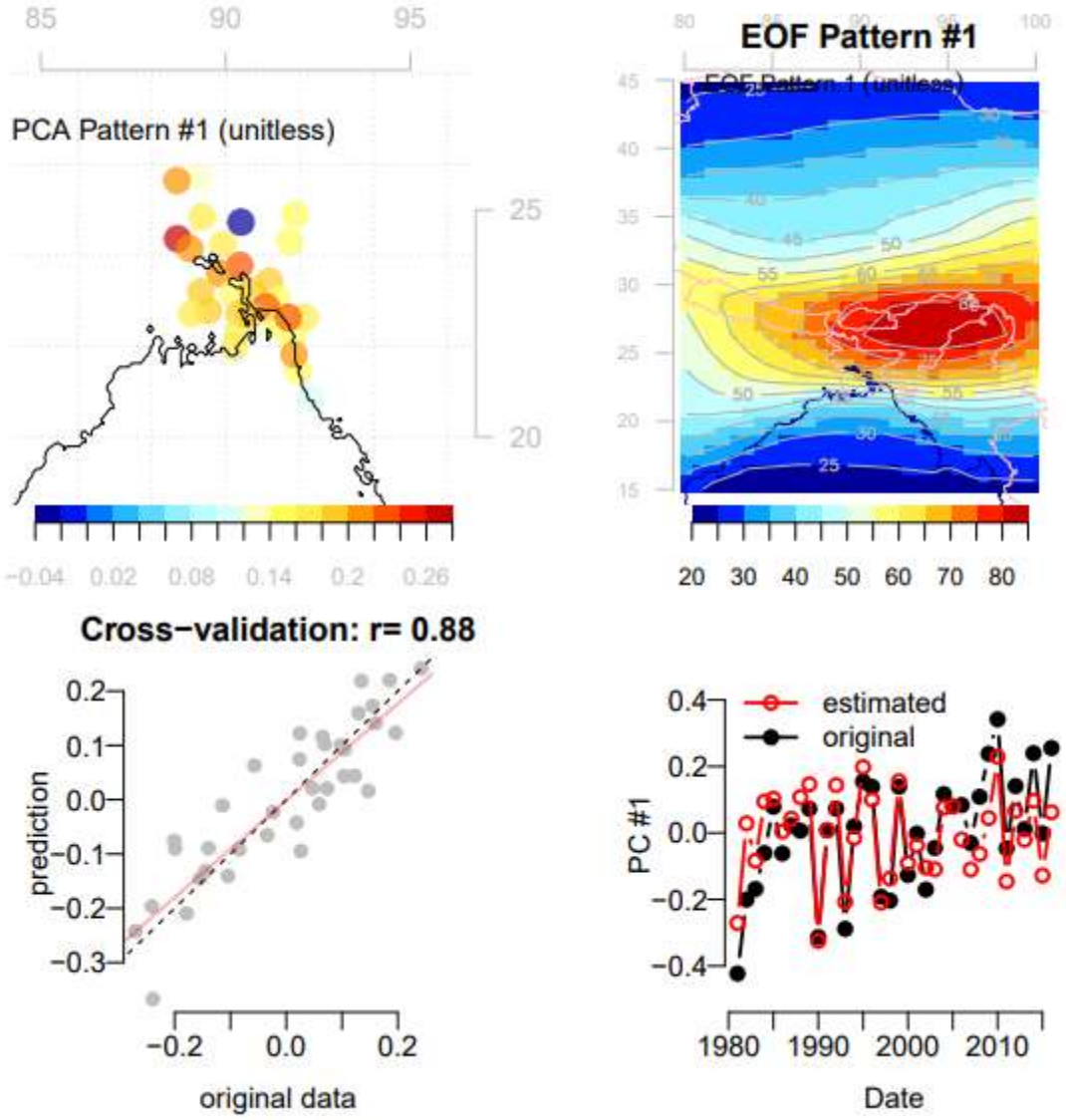

Fig. 6.2.1: Downscaled mean temperature of the pre-monsoon season based on the observed data and using PCA for downscaling a group of stations simultaneously for RCP2.6. The top-left panel illustrates the spatial pattern connected with the leading principal component (PC1) of the predictand. The top-right panel express the leading spatial pattern of the predictor. The lower left panel indicates a cross-validation comparing the original PC1 of the predictand and the corresponding estimated values obtained by ESD. The lower-right panel indicates time series of the estimated and original PC1 of the predictand.

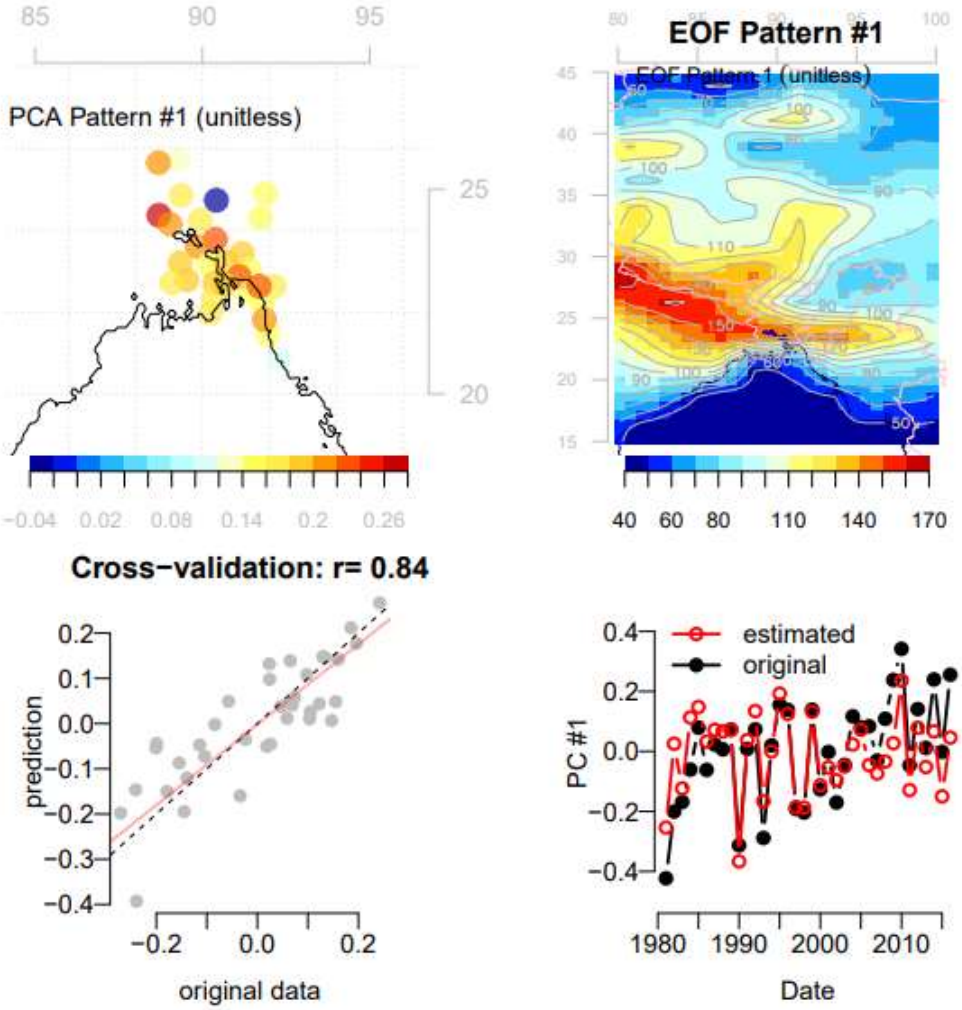

Fig. 6.2.2: Downscaled mean temperature of the pre-monsoon season based on the observed data and using PCA for downscaling a group of stations simultaneously for RCP4.5. The top-left panel illustrates the spatial pattern connected with the leading principal component (PC1) of the predictand. The top-right panel express the leading spatial pattern of the predictor. The lower left panel indicates a cross-validation comparing the original PC1 of the predictand and the corresponding estimated values obtained by ESD. The lower-right panel indicates time series of the estimated and original PC1 of the predictand.

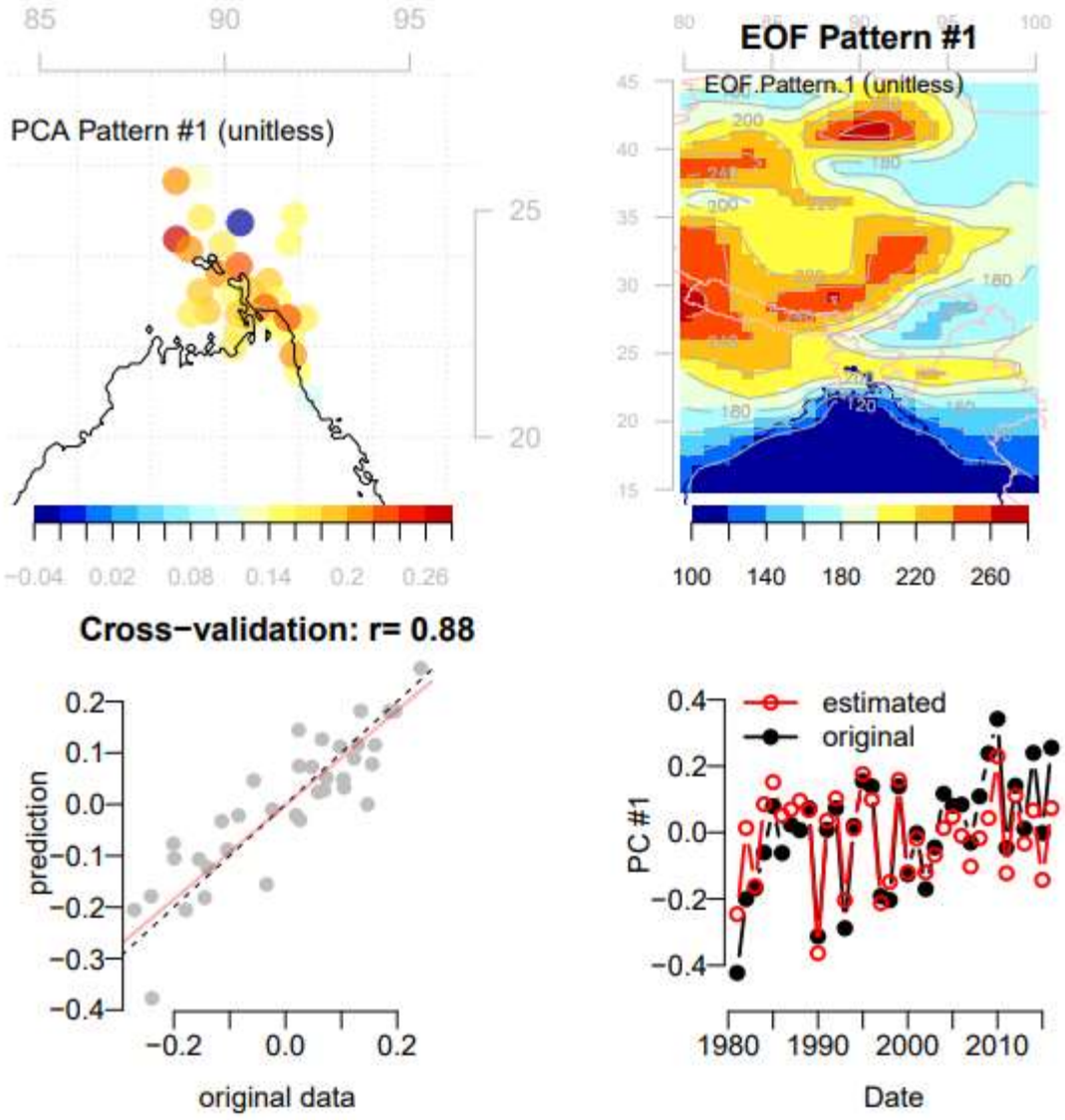

Fig. 6.2.3. Downscaled mean temperature of the pre-monsoon season based on the observed data and using PCA for downscaling a group of stations simultaneously for RCP8.5. The top-left panel illustrates the spatial pattern connected with the leading principal component (PC1) of the predictand. The top-right panel express the leading spatial pattern of the predictor. The lower left panel indicates a cross-validation comparing the original PC1 of the predictand and the corresponding estimated values obtained by ESD. The lower-right panel indicates time series of the estimated and original PC1 of the predictand.

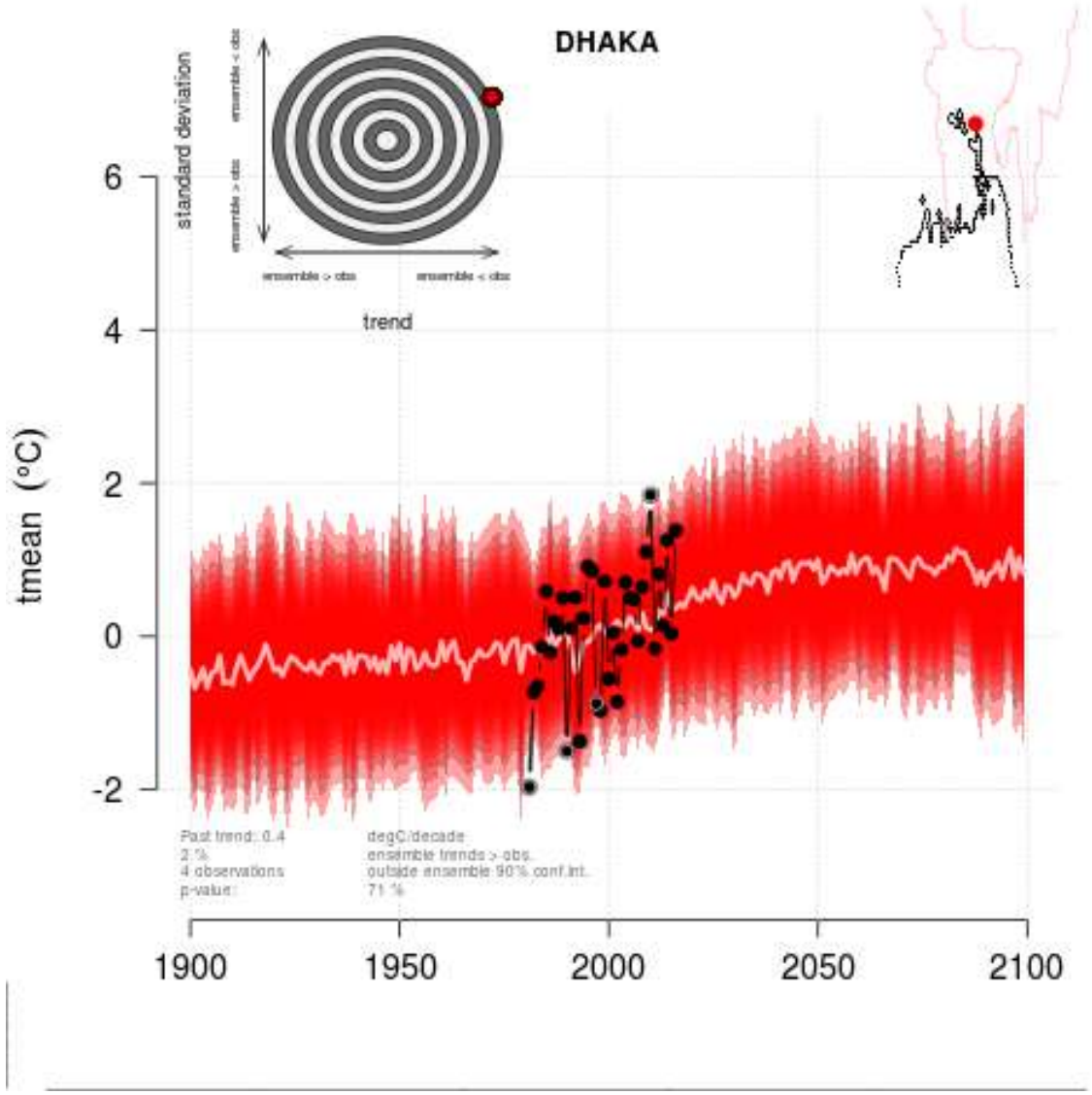

Fig. 6.2.4: Mean temperature of pre-monsoon season over Dhaka for RCP2.6 scenarios run by CMIP5 experiments, respectively, relative to the period 1981-2010. The light central line is one standard deviation from the mean based on the included GCM simulations for each experiment and the gray-dashed lines mark the 90% confidence region. At the same times, wheel graph shows the probability of finding the observed number of values outside of the downscaled ensemble 90% Confidence Interval (CI), which is taken as a degree of how well fit the ensemble denotes the Interannual Variability (IAV). Values towards the top (bottom) recommend that the downscaled ensemble underestimates (overestimates) the IAV.

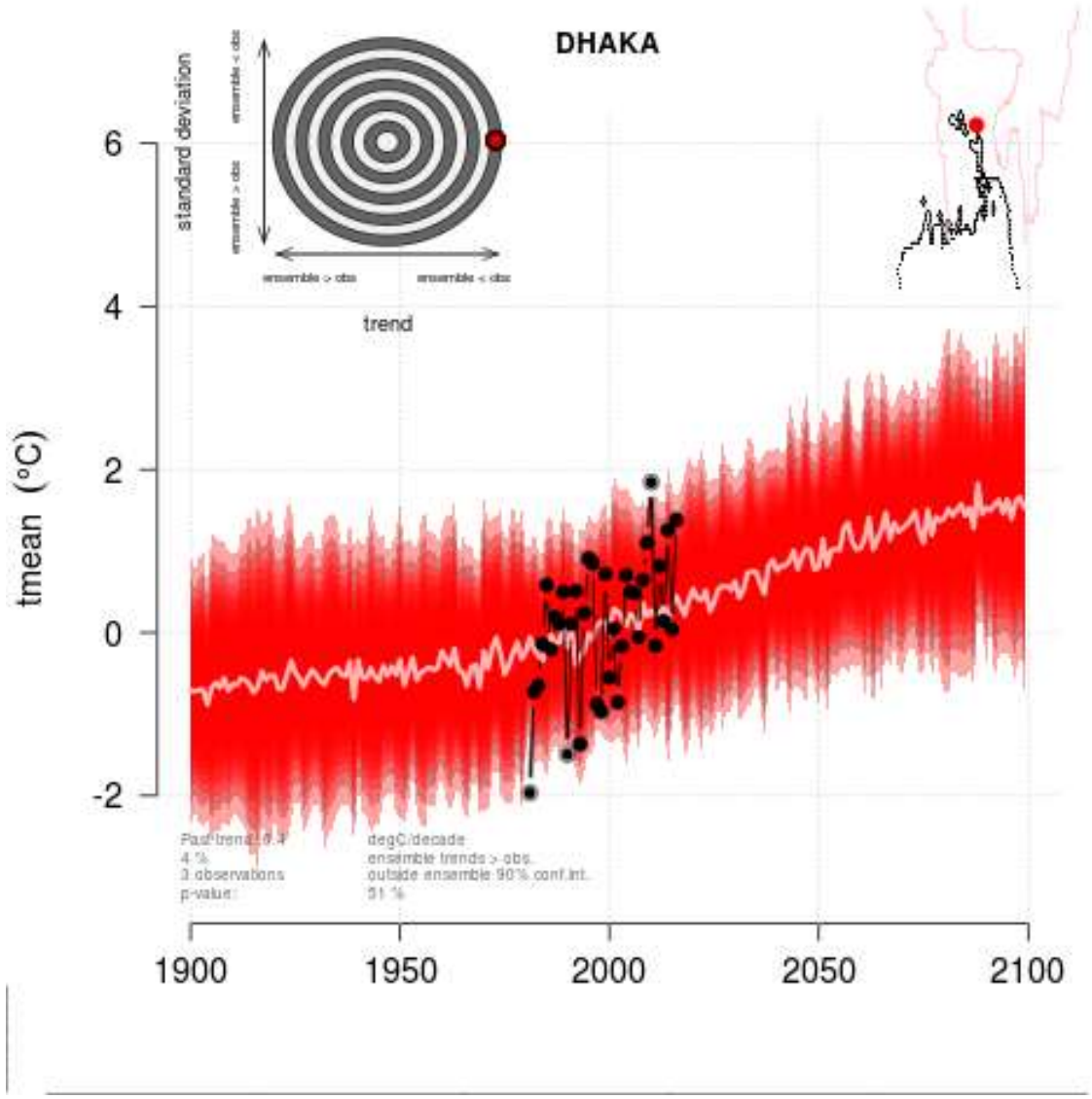

Fig. 6.2.5: Mean temperature of pre-monsoon season over Dhaka for RCP4.5 scenarios run by CMIP5 experiments, respectively, relative to the period 1981-2010. The light central line is one standard deviation from the mean based on the included GCM simulations for each experiment and the gray-dashed lines mark the 90% confidence region. At the same times, wheel graph shows the probability of finding the observed number of values outside of the downscaled ensemble 90% Confidence Interval (CI), which is taken as a degree of how well fit the ensemble denotes the Interannual Variability (IAV). Values towards the top (bottom) recommend that the downscaled ensemble underestimates (overestimates) the IAV.

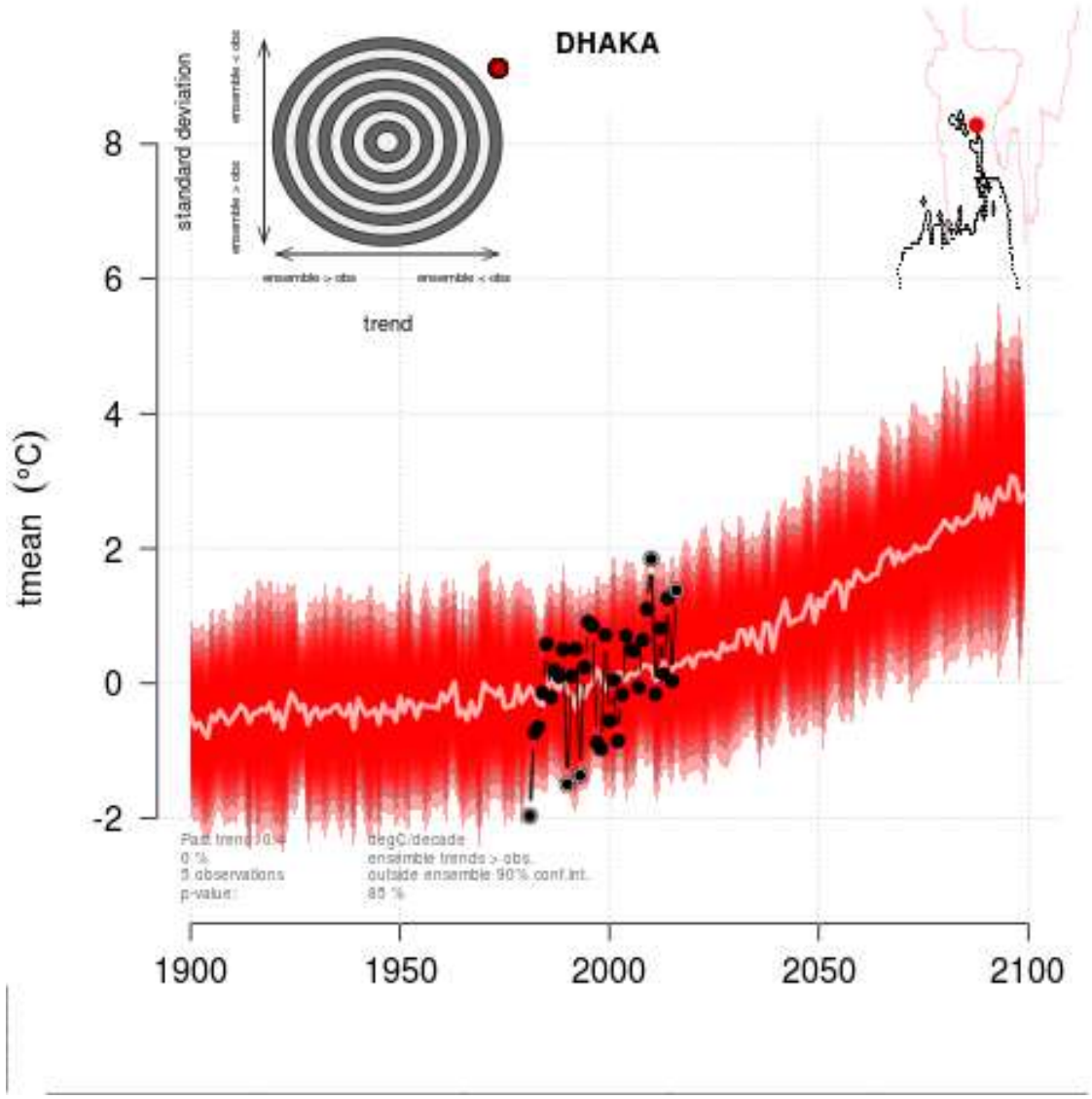

Fig. 6.2.6: Mean temperature of pre-monsoon season over Dhaka for RCP8.5 scenarios run by CMIP5 experiments, respectively, relative to the period 1981-2010. The light central line is one standard deviation from the mean based on the included GCM simulations for each experiment and the gray-dashed lines mark the 90% confidence region. At the same times, wheel graph shows the probability of finding the observed number of values outside of the downscaled ensemble 90% Confidence Interval (CI), which is taken as a degree of how well fit the ensemble denotes the Interannual Variability (IAV). Values towards the top (bottom) recommend that the downscaled ensemble underestimates (overestimates) the IAV.

RCP2.6 **RCP4.5** **RCP8.5**

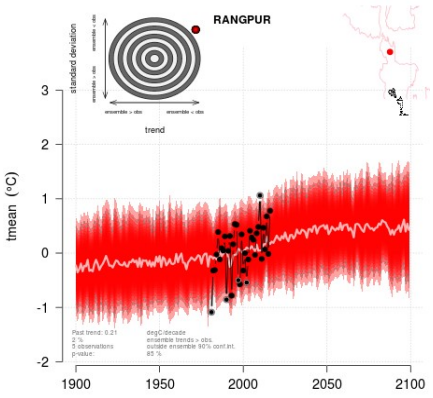

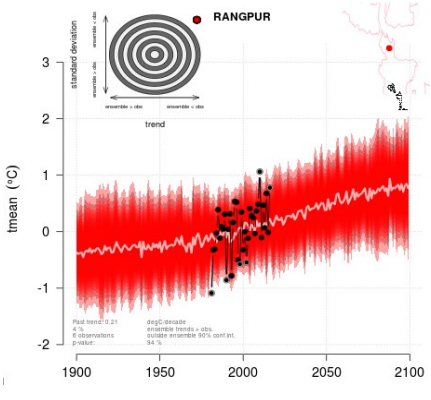

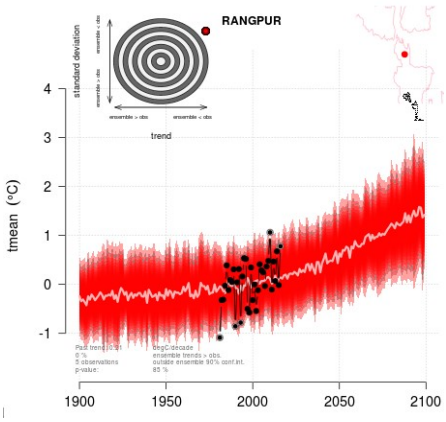

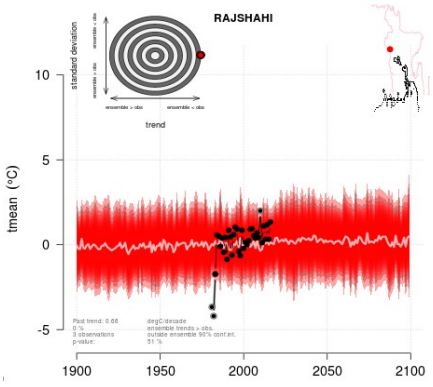

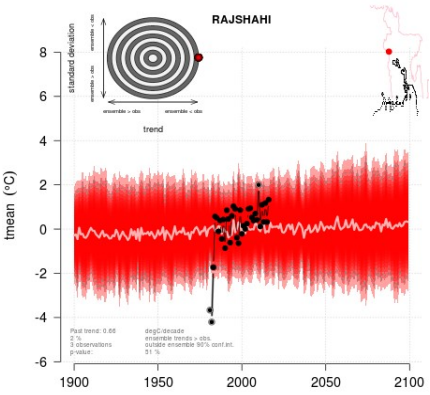

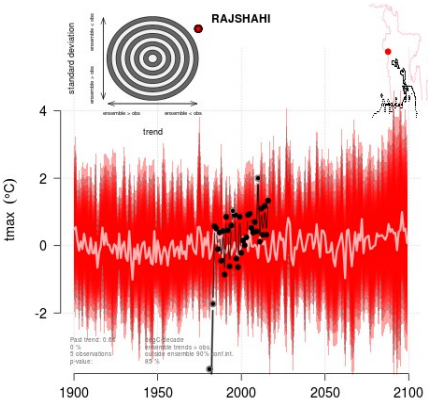

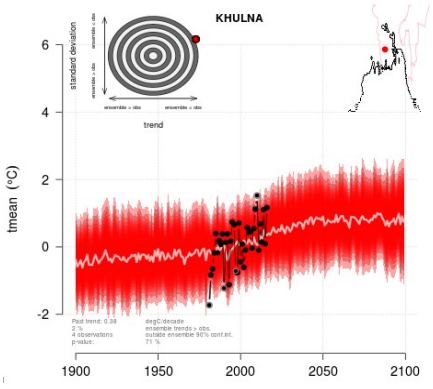

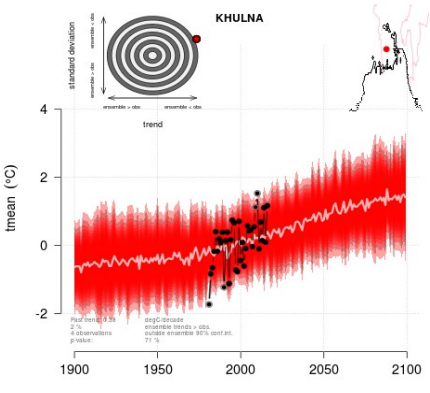

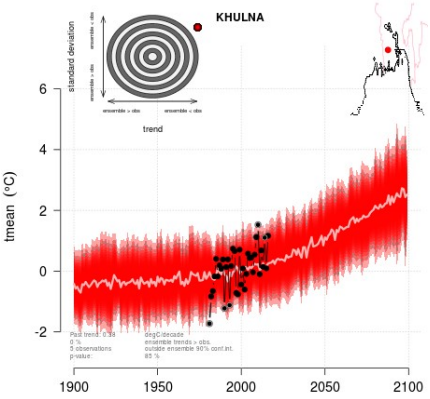

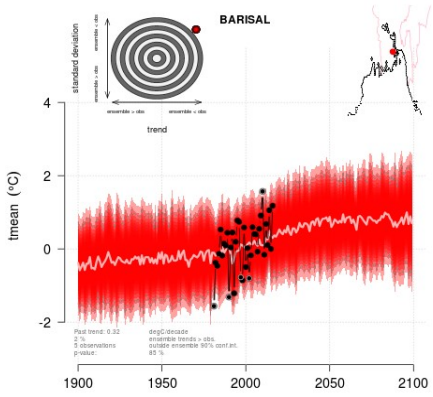
BARISAL
standard deviation
trend
tmean (°C)
1900
1950
2000
2050
2100

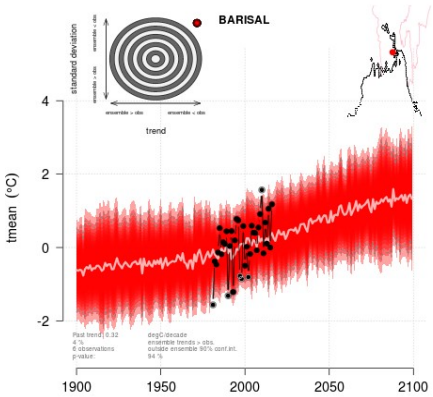
BARISAL
standard deviation
trend
tmean (°C)
1900
1950
2000
2050
2100

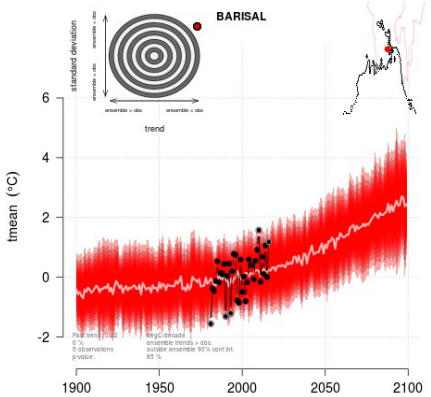
BARISAL
standard deviation
trend
tmean (°C)
1900
1950
2000
2050
2100

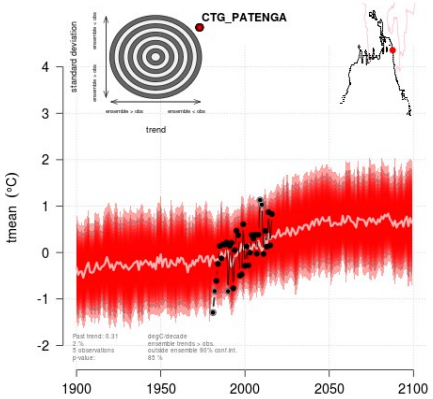
CTG_PATENGA
standard deviation
trend
tmean (°C)
1900
1950
2000
2050
2100

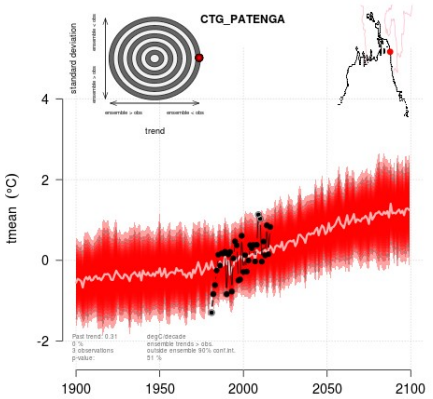
CTG_PATENGA
standard deviation
trend
tmean (°C)
1900
1950
2000
2050
2100

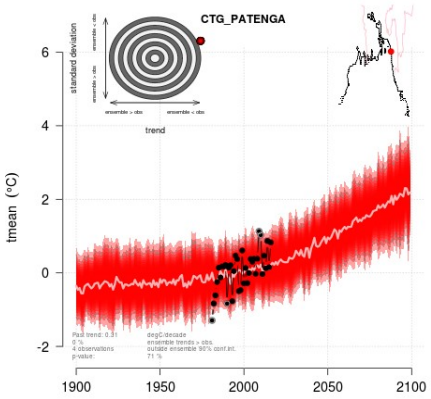
CTG_PATENGA
standard deviation
trend
tmean (°C)
1900
1950
2000
2050
2100

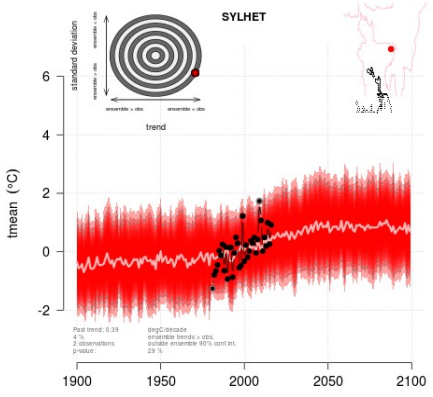
SYLHET
standard deviation
trend
tmean (°C)
1900
1950
2000
2050
2100

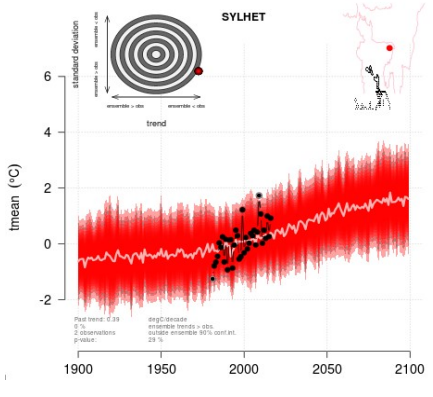
SYLHET
standard deviation
trend
tmean (°C)
1900
1950
2000
2050
2100

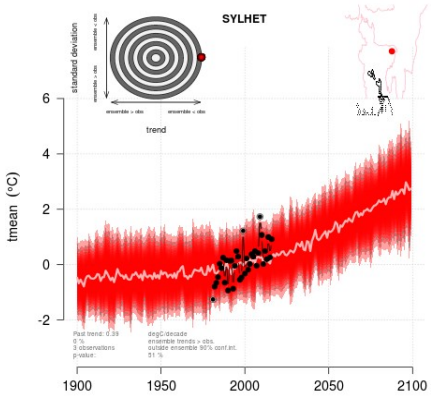
SYLHET
standard deviation
trend
tmean (°C)
1900
1950
2000
2050
2100

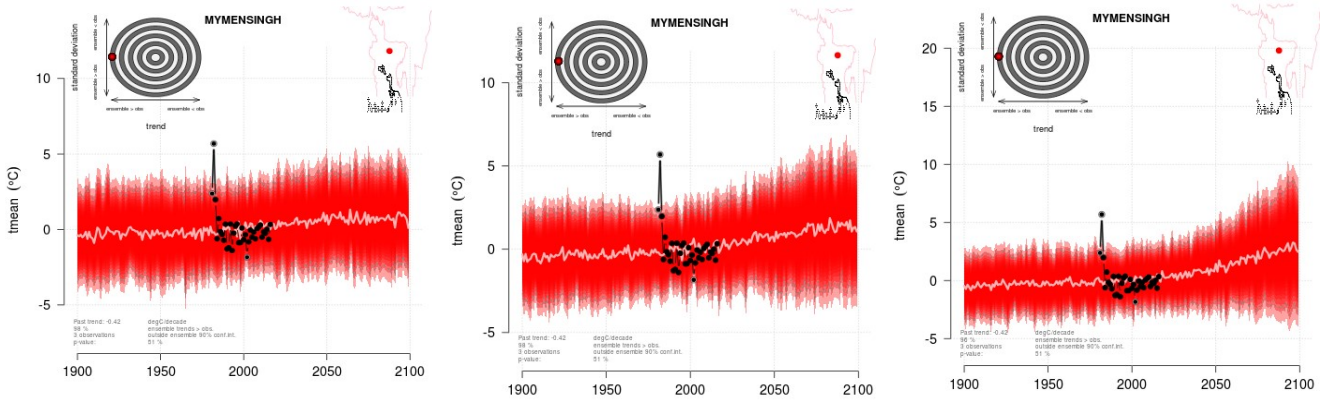

Fig. 6.2.7: Mean temperature of pre-monsoon season over other divisional points change for different RCP scenarios run by CMIP5 experiments, respectively, relative to the period 1981-2010. The light central line is one standard deviation from the mean based on the included GCM simulations for each experiment and the gray-dashed lines mark the 90% confidence region. At the same times, wheel graph shows the probability of finding the observed number of values outside of the downscaled ensemble 90% Confidence Interval (CI), which is taken as a degree of how well fit the ensemble denotes the Interannual Variability (IAV). Values towards the top (bottom) recommend that the downscaled ensemble underestimates (overestimates) the IAV.

Fig. 6.2.4 to Fig. 6.2.7 shows downscaled climate projections of the mean temperature of pre-monsoon season at the divisional place in Bangladesh for different RCPs (RCP2.6, RCP4.5 and RCP8.5) and wheel graph shows the probability of finding the observed number of values outside of the downscaled ensemble at 90% CI, which is taken as a measure of how well the ensemble represents the IAV in each station. The maximum number of stations is well captured as they have high interannual variability. Some stations indicate underestimated interannual variability. These are- Dhaka, Rajshahi and Khulna for RCP8.5, Chattogram for RCP2.6, Barisal for RCP4.5 and RCP8.5 and Rangpur for all RCPs. The results are given in Table 6.2.1, which includes the average change in the mean temperature of the pre-monsoon season relative to 1981-2010 for the two periods of (a) near future (2021-2050) and (b) far future (2071-2100). The projection results indicate an increase of pre-monsoon mean temperature at Dhaka by 0.75°C for the near future and 0.93°C for the far future for RCP2.6. For RCP4.5, the estimated warming near future is 0.57°C; for the far future, it is 1.36°C. The scenario for RCP8.5 suggests an increase of pre-monsoon temperatures by 0.64°C and 2.35°C for the near and far future, respectively. The mean projected change in pre-monsoon temperature for Bangladesh, assuming RCP2.6, is 0.62°C for the near future and 0.78°C for the far future. For RCP4.5, it is 0.50°C for the near future and 1.19°C for the far future. For the high emission scenario of RCP8.5, the near future estimated warming is 0.54°C, but it is considerably higher with the increment magnitude of 2.04°C. The uppermost projected warming for RCP2.6 is 1.62°C at Sitakunda for the near future, and it is 2.03°C at the same place in the far future. Similarly, RCP4.5 captured 1.66°C at Sitakunda in the near future and 3.59°C at

the same place in the far future. For the most severe emission scenario of RCP8.5, the projected warming is 1.41°C at Sitakunda for the near future and 5.74°C at the same place in the far future. The details are given in Table 6.2.1.

Table 6.2.1: Projected mean temperature anomaly in pre-monsoon season compared to 1981-2010

Division	Station Location	Emission scenario					
		RCP2.6		RCP4.5		RCP8.5	
		Near Future	Far Future	Near Future	Far Future	Near Future	Far Future
Dhaka	Dhaka	0.75	0.93	0.57	1.36	0.64	2.35
	Tangail	0.58	0.74	0.46	1.15	0.58	2.11
	Faridpur	0.72	0.89	0.55	1.33	0.62	2.29
	Madaripur	0.32	0.79	0.6	1.08	0.46	2.17
Mymensingh	Mymensingh	0.31	0.54	0.48	1.23	0.67	2.53
Chattogram	Chattogram	0.57	0.7	0.48	1.08	0.46	1.76
	Cox'Bazar	0.7	0.84	0.6	1.34	0.55	2.14
	Chandpur	0.71	0.87	0.57	1.34	0.6	2.25
	Cumilla	0.62	0.76	0.47	1.13	0.52	1.92
	Feni	0.59	0.75	0.51	1.18	0.53	2.02
	Hatiya	0.57	0.73	0.51	1.18	0.52	2.01
	Kutubdia	0.64	0.74	0.43	0.98	0.41	1.51
	M_Court	1.09	1.57	1.24	2.55	1.01	4.28
	Rangamati	0.87	1.11	0.82	1.89	0.83	3.2
	Sandwip	0.63	0.81	0.56	1.29	0.58	2.2
	Sitakunda	1.62	2.03	1.66	3.59	1.41	5.74
	Teknaf	0.65	0.82	0.63	1.39	0.58	2.3
Khulna	Khulna	0.68	0.83	0.52	1.23	0.56	2.09
	Jashore	0.57	0.68	0.37	0.93	0.46	1.63
	Satkhira	0.35	0.45	0.19	0.53	0.31	1.04
Barishal	Barishal	0.64	0.8	0.49	1.19	0.56	2.07
	Patuakhali	0.67	0.83	0.55	1.28	0.57	2.17
	Bhola	0.56	0.74	0.41	1.06	0.56	2.02
	Khepupara	0.62	0.76	0.48	1.12	0.51	1.9
Rajshahi	Rajshahi	0.43	0.38	0.02	0.14	0.1	0.1
	Bogura	0.45	0.54	0.27	0.72	0.39	1.33

Division	Station Location	Emission scenario					
		RCP2.6		RCP4.5		RCP8.5	
		Near Future	Far Future	Near Future	Far Future	Near Future	Far Future
	Ishurdi	0.39	0.12	-0.27	-0.08	0.17	-0.12
Rangpur	Rangpur	0.39	0.48	0.28	0.69	0.34	1.22
	Dinajpur	0.47	0.56	0.24	0.65	0.36	1.2
Sylhet	Sylhet	0.75	0.87	0.62	1.42	0.59	2.25
	Srimangal	0.46	0.55	0.29	0.78	0.41	1.43
Country		0.62	0.78	0.5	1.19	0.54	2.04

[Projection range indication: (i) Light green color: -0.5 to 0.49°C; (ii) Red text: 0.5 to 1.0°C; (iii) Light Red fill: 1.1 to 2.0°C and (iv) Light red fill with red text: ≥ 2.1°C]

6.3 Temperature of Monsoon Season

An evaluation of the common EOFs from GCM and observed temperature are performed to measure the goodness of fit of the GCM output in respect of observation based on local temperature and model ERAINT reanalysis data. The residuals from the downscaled value are verified against sufficiency. Screening of predictors has been conducted using the best ten (10) GCMs. These GCMs are ACCESS1.0.r1, BNU.ESM.r1, CanESM2.r2, CCSM4.r3, CMCC.CM.r1, CNRM.CM5.r1, EC.EARTH.r9, EC.EARTH.r12, FIO.ESM.r1, FIO.ESM.r2 (where r means model realization). Among various stations' temperature, the best cross-validated correlation predictors and predictand are selected and shown in Figures 6.3.1 to Figure 6.3.3 for different RCPs. These figures indicate that the correlation between predictors and predictands of temperature are 0.44, 0.56 and 0.59.

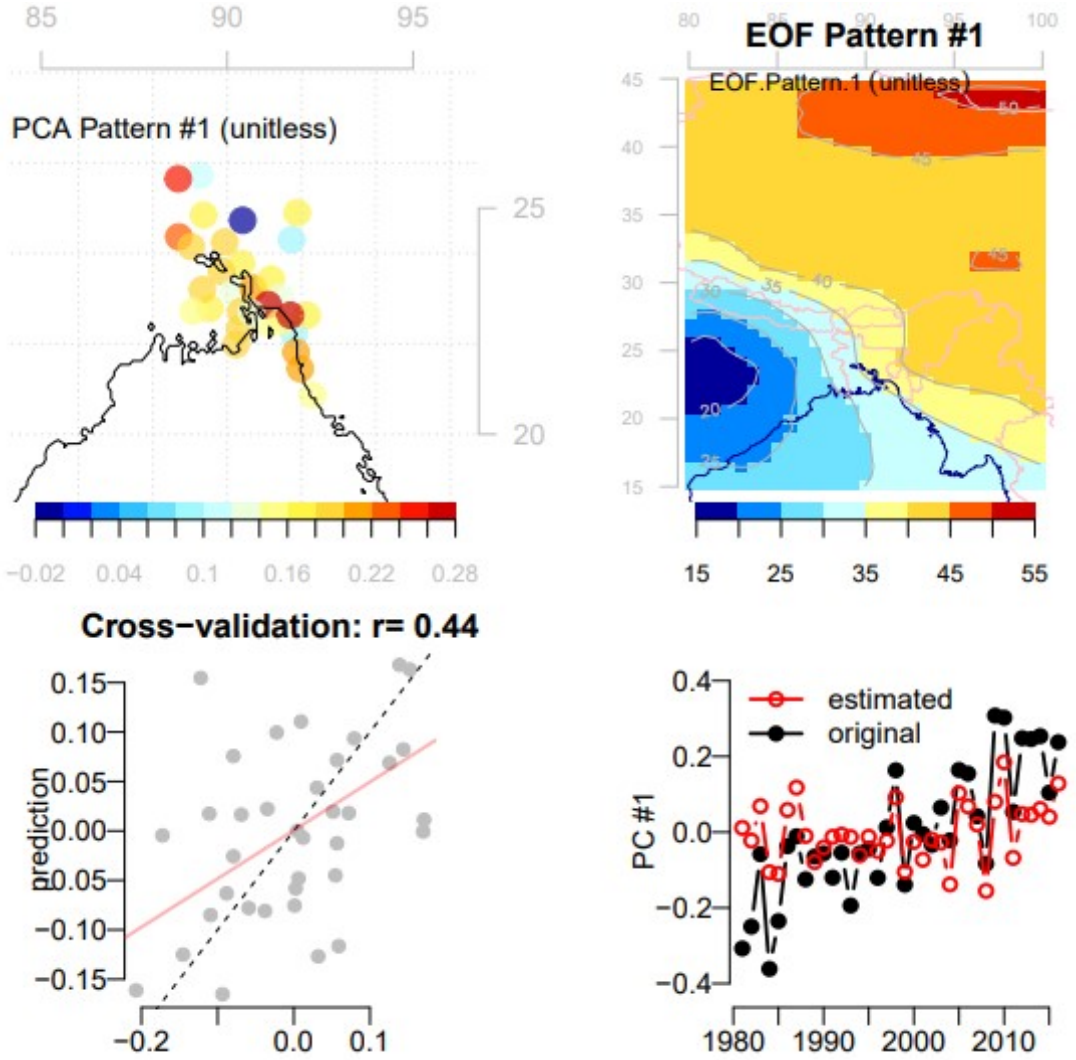

Fig. 6.3.1: Cross validation of temperature of monsoon season based on the observed data and using PCA for downscaling a group of stations simultaneously for rcp26

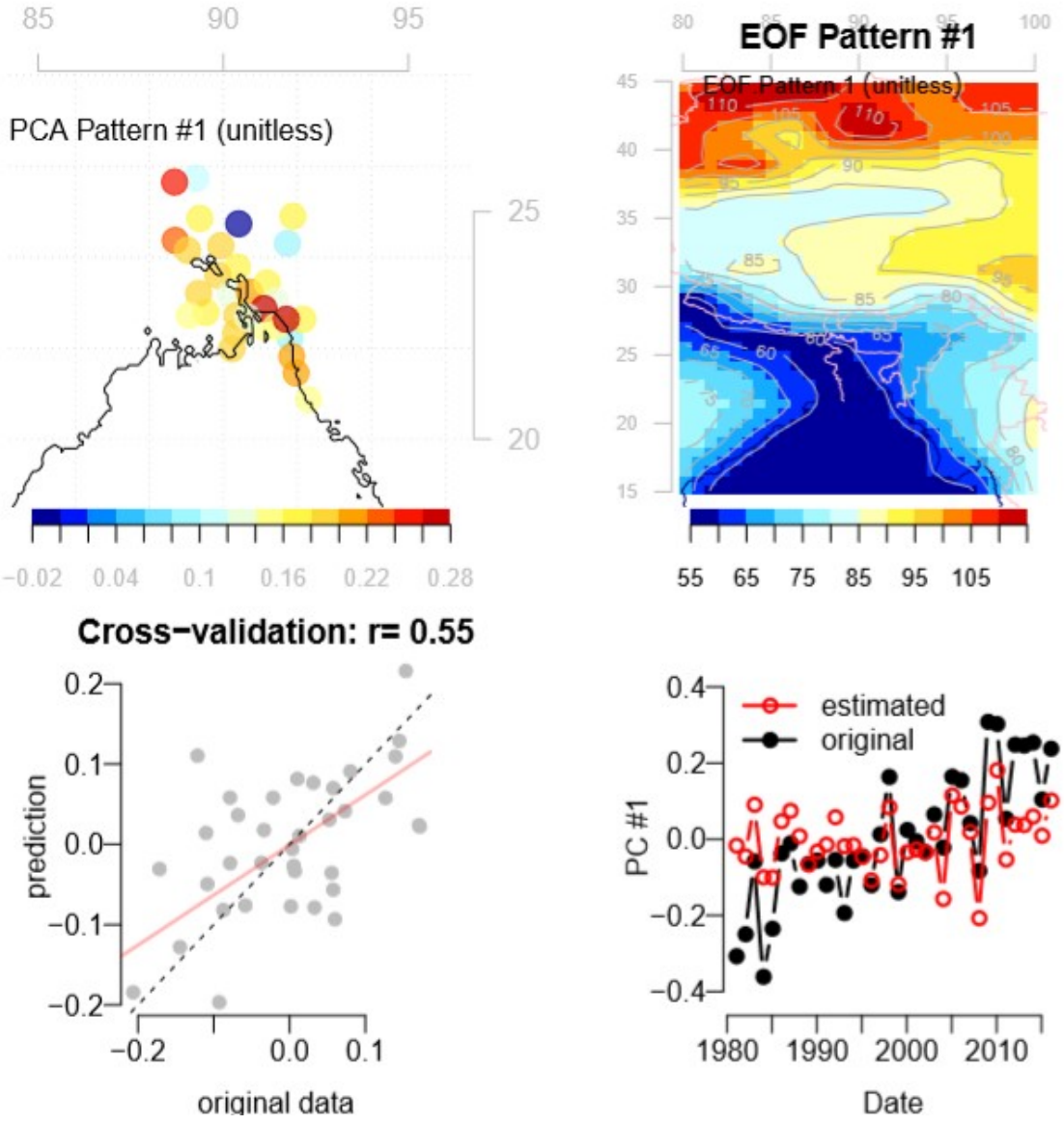

Fig. 6.3.2: Cross validation of temperature of monsoon season based on the observed data and using PCA for downscaling a group of stations simultaneously for rcp45

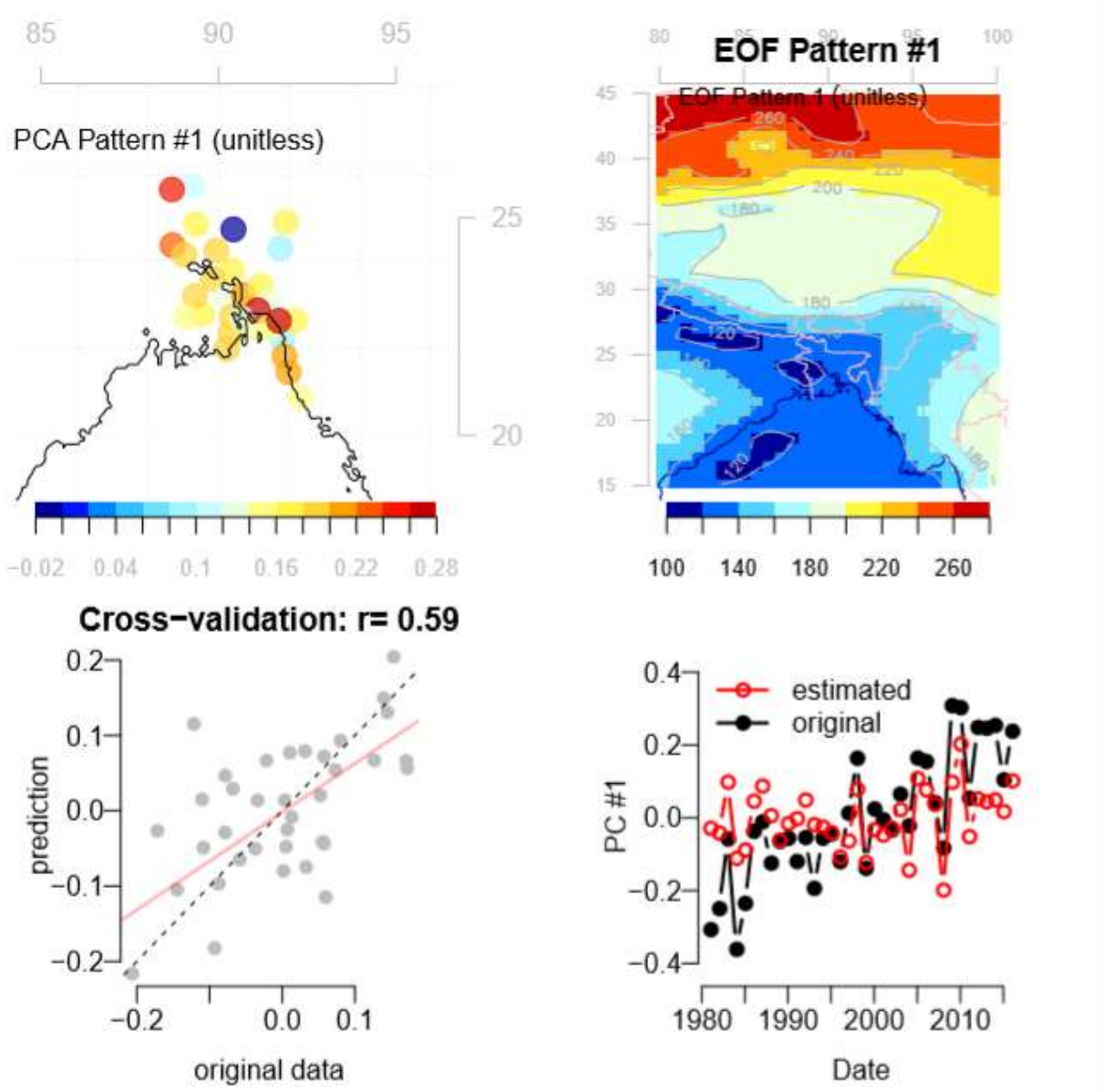

Fig. 6.3.3: Cross validation of temperature of monsoon season based on the observed data and using PCA for downscaling a group of stations simultaneously for rcp85

RCP2.6 **RCP4.5** **RCP8.5**

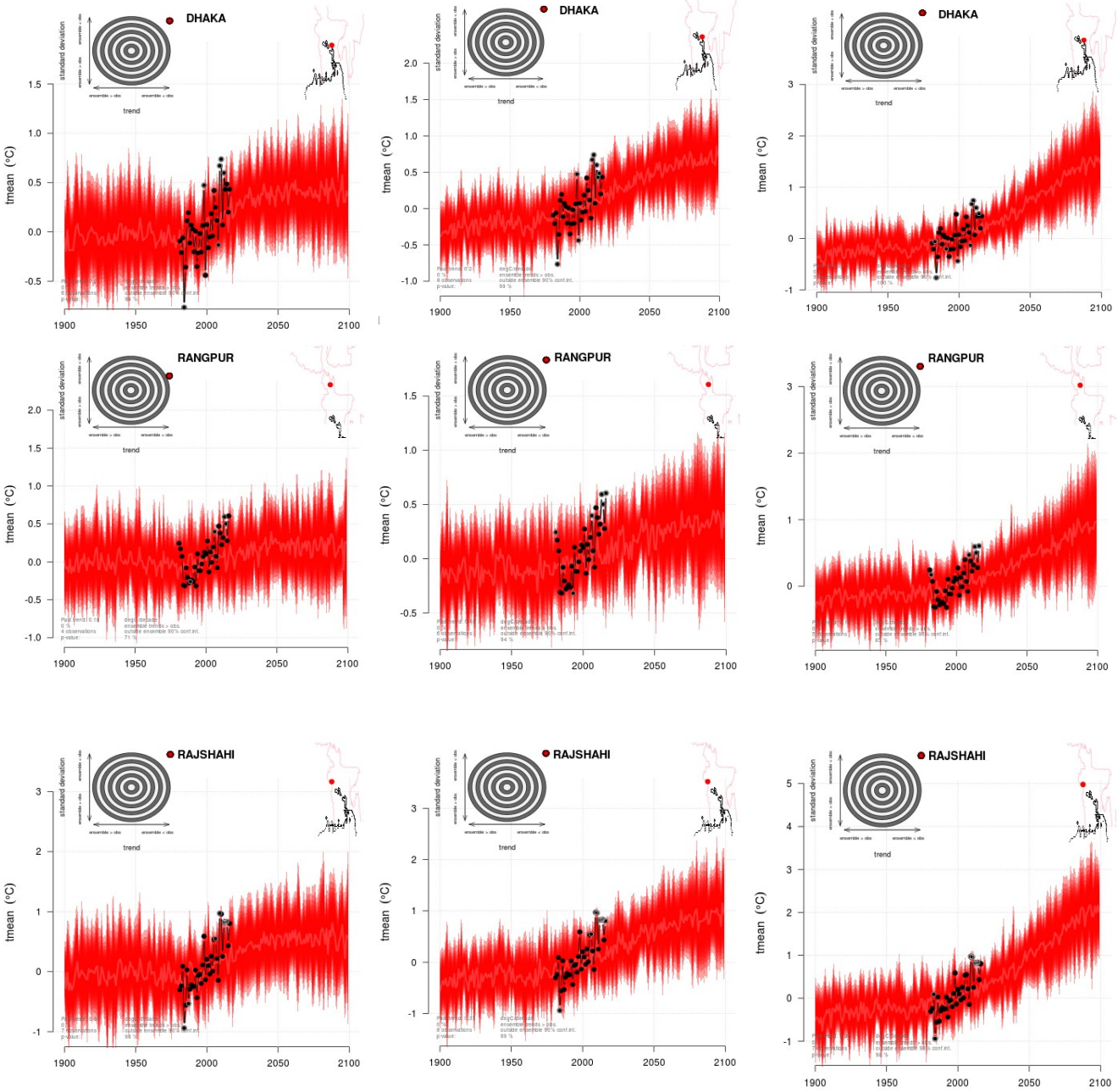

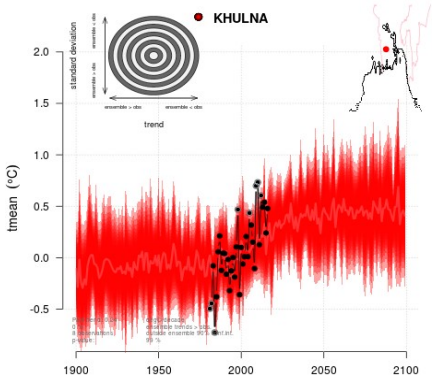
KHULNA
standard deviation
trend
tmean (°C)
2.0
1.5
1.0
0.5
0.0
-0.5
1900
1950
2000
2050
2100

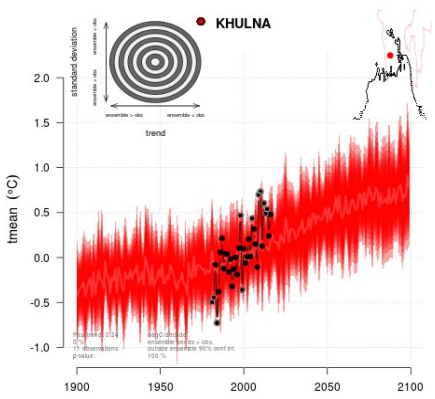
KHULNA
standard deviation
trend
tmean (°C)
2.0
1.5
1.0
0.5
0.0
-0.5
-1.0
1900
1950
2000
2050
2100

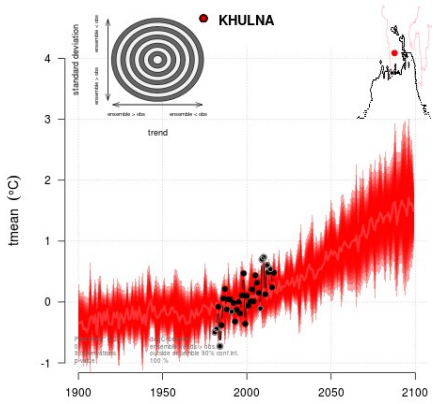
KHULNA
standard deviation
trend
tmean (°C)
4
3
2
1
0
-1
1900
1950
2000
2050
2100

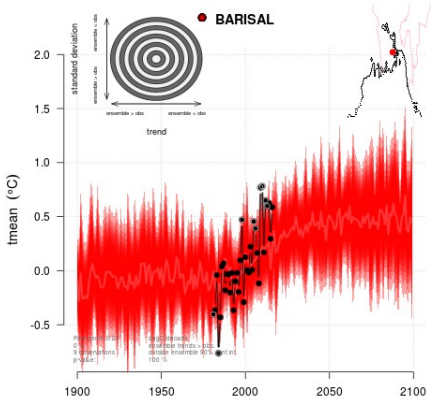
BARISAL
standard deviation
trend
tmean (°C)
2.0
1.5
1.0
0.5
0.0
-0.5
1900
1950
2000
2050
2100

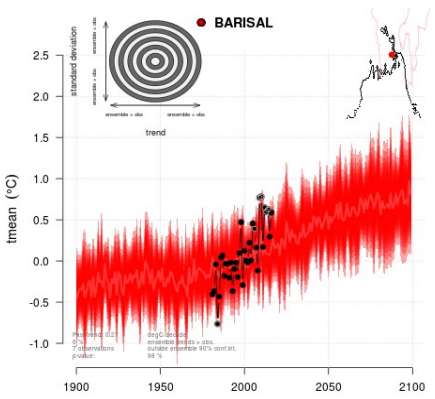
BARISAL
standard deviation
trend
tmean (°C)
2.5
2.0
1.5
1.0
0.5
0.0
-0.5
-1.0
1900
1950
2000
2050
2100

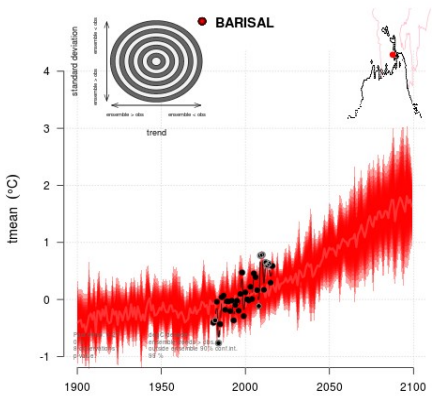
BARISAL
standard deviation
trend
tmean (°C)
4
3
2
1
0
-1
1900
1950
2000
2050
2100

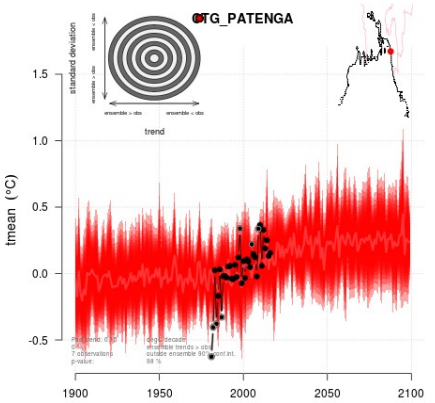
CTG_PATENGA
standard deviation
trend
tmean (°C)
1.5
1.0
0.5
0.0
-0.5
1900
1950
2000
2050
2100

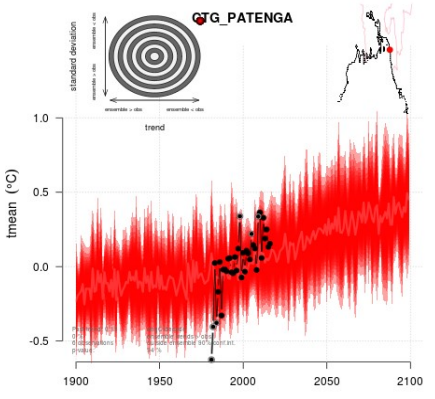
CTG_PATENGA
standard deviation
trend
tmean (°C)
1.0
0.5
0.0
-0.5
1900
1950
2000
2050
2100

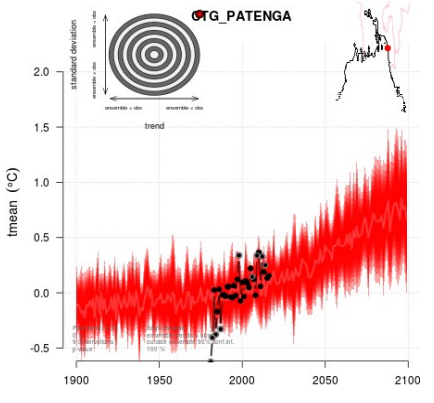
CTG_PATENGA
standard deviation
trend
tmean (°C)
2.0
1.5
1.0
0.5
0.0
-0.5
1900
1950
2000
2050
2100

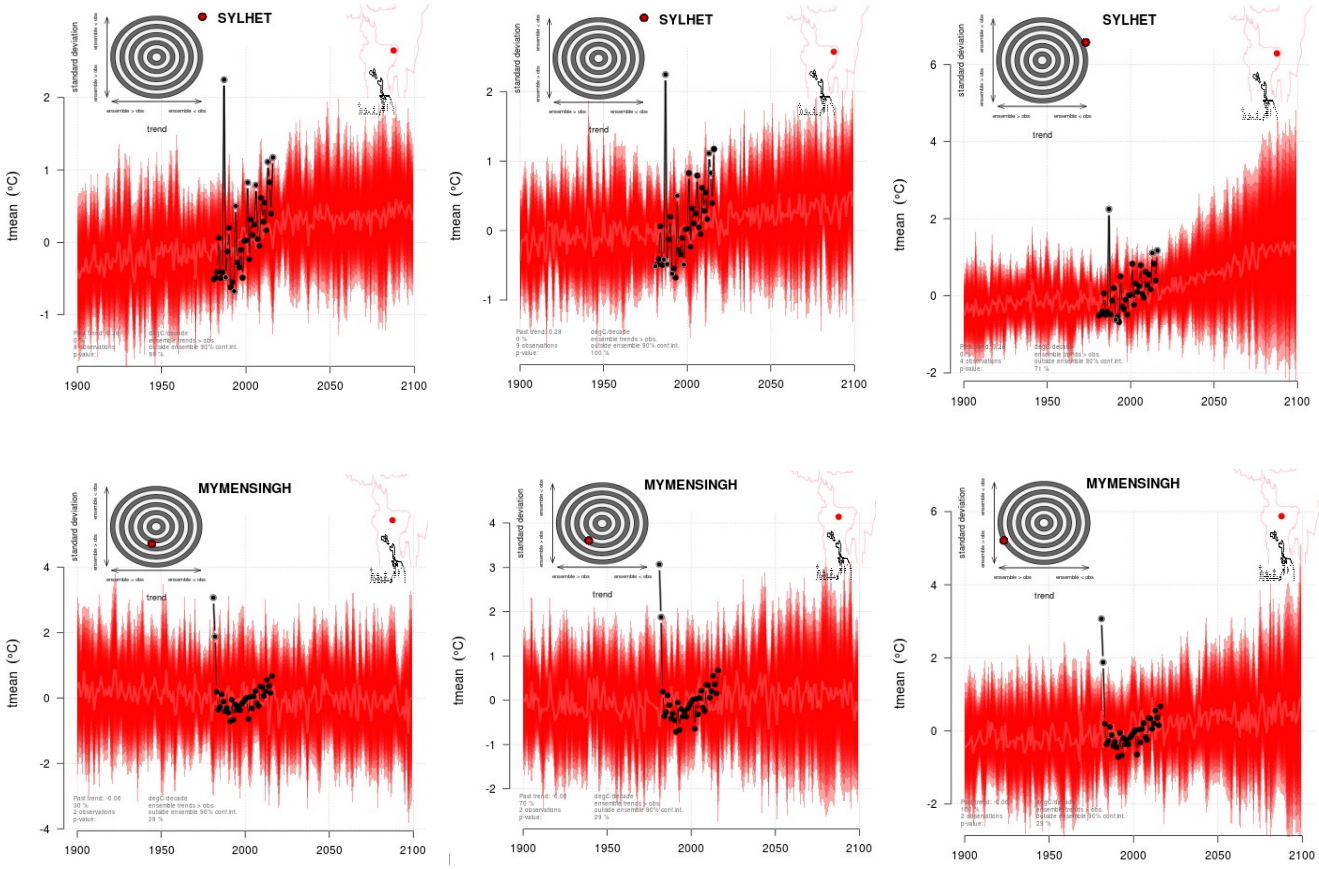

Fig.6.3.4: Mean temperature of monsoon season over divisional points change for different RCP scenarios run by CMIP5 experiments, respectively, relative to the period 1981-2010. The light central line is one standard deviation from the mean based on the included GCM simulations for each experiment and the gray-dashed lines mark the 90% confidence region. At the same times, wheel graph shows the probability of finding the observed number of values outside of the downscaled ensemble 90% Confidence Interval (CI), which is taken as a degree of how well fit the ensemble denotes the Interannual Variability (IAV). Values towards the top (bottom) recommend that the downscaled ensemble underestimates (overestimates) the IAV.

Fig. 6.3.4 shows downscaled climate projections of mean temperature in monsoon season at divisional places of Bangladesh for different RCPs (RCP2.6, RCP4.5 and RCP8.5) and wheel graphs show the probability of finding the observed number of values outside of the downscaled ensemble at 90% CI, which is taken as a measure of how well the ensemble represents the IAV at each station location. Projections of all station are underestimated the interannual variability for all RCPs except Mymensingh. The results are given in Table 6.3.1, which includes the average change in the mean temperature of the monsoon season relative to 1981-2010 for two periods of (a) the near future (2021-2050) and (b) the far future (2071-2100). The projection results indicate an increase in the monsoon mean temperature at Dhaka by 0.24°C in the near future and 0.3°C in the far future with RCP2.6. For RCP4.5, the near future warming is estimated to be 0.17°C, and

far future, it will be 0.5°C. The scenario of RCP8.5 suggests an increase of monsoon temperature by 0.36°C and 1.29°C for the near and far future, respectively. The mean projected change in monsoon temperature for Bangladesh, assuming for RCP2.6, is 0.25°C for the near future, and it is 0.33°C for the far future. Again, for RCP4.5, it is 0.13°C for the near future and 0.45°C for the far future. For the high emission scenario of RCP8.5, the near future estimated warming is about 0.37°C, and the far future warming is considerably higher at 1.27°C. The highest projected warming for RCP2.6 is 0.38°C at Sitakunda in the near future, and it will be 0.52°C at Maijdi Court (Noakhali) in the far future. For RCP4.5, the magnitude is 0.36°C (at Mymensingh) for the near future and 0.69°C (at Sitakunda) for the far future. For the worst emission scenario of RCP8.5, the projected warming is 0.61°C (at Madaripur) for the near future, and it is 1.93°C (at Sitakunda) for the far future.

Table 6.3.1: Projected anomaly of mean temperature of monsoon season compared to 1981-2010

Division	Station Location	Emission scenario					
		RCP2.6		RCP4.5		RCP8.5	
		Near Future	Far Future	Near Future	Far Future	Near Future	Far Future
Dhaka	Dhaka	0.24	0.3	0.17	0.5	0.36	1.29
	Tangail	0.26	0.35	0.13	0.48	0.35	1.29
	Faridpur	0.31	0.39	0.2	0.57	0.43	1.52
	Madaripur	0.22	0.26	0	0.29	0.61	1.5
Mymensingh	Mymensingh	0.11	0.02	0.36	0.33	0.02	0.25
Chattogram	Chattogram	0.11	0.17	0.05	0.25	0.16	0.64
	Cox'Bazar	0.28	0.39	0.11	0.52	0.42	1.49
	Chandpur	0.3	0.39	0.21	0.64	0.43	1.59
	Cumilla	0.25	0.33	0.09	0.38	0.36	1.2
	Feni	0.2	0.26	0.12	0.37	0.27	0.98
	Hatiya	0.22	0.28	0.15	0.47	0.37	1.26
	Kutubdia	0.28	0.38	0.12	0.52	0.42	1.48
	M_Court	0.38	0.52	0.16	0.67	0.54	1.92
	Rangamati	0.24	0.31	0.14	0.43	0.33	1.17
	Sandwip	0.23	0.3	0.13	0.39	0.3	1.08
	Sitakunda	0.38	0.5	0.2	0.69	0.55	1.93
	Teknaf	0.19	0.27	0.06	0.33	0.27	0.97
Khulna	Khulna	0.26	0.34	0.14	0.49	0.4	1.37
	Jashore	0.28	0.36	0.19	0.57	0.38	1.43
	Satkhira	0.2	0.26	0.11	0.44	0.36	1.2
Barishal	Barishal	0.28	0.37	0.16	0.53	0.41	1.45
	Patuakhali	0.28	0.37	0.14	0.52	0.43	1.49
	Bhola	0.2	0.25	0.12	0.39	0.32	1.07
	Khepupara	0.26	0.35	0.12	0.5	0.39	1.39
Rajshahi	Rajshahi	0.34	0.45	0.24	0.68	0.44	1.69
	Bogura	0.26	0.34	0.17	0.49	0.31	1.21
	Ishurdi	0.29	0.38	0.19	0.56	0.38	1.43
Rangpur	Rangpur	0.18	0.22	0.13	0.28	0.2	0.73
	Dinajpur	0.31	0.48	0	0.41	0.43	1.48
Sylhet	Sylhet	0.34	0.42	-0.03	0.11	0.6	1.38
	Srimangal	0.15	0.18	0.09	0.21	0.18	0.62
Country		0.25	0.33	0.13	0.45	0.37	1.27

[Projection range indication: (i) Light green color: -0.5 to 0.49°C; (ii) Red text: 0.5 to 1.0°C; (iii) Light Red fill: 1.1 to 2.0°C]

6.4 Temperature of Post-monsoon Season

An evaluation of the common EOFs from GCM and observed temperature are performed to measure the goodness of fit of the GCM output in respect of observation (local temperature). The residuals from the downscaled data are verified against adequacy. Screening of predictors has been conducted using the best ten (10) GCMs, which are used in the monsoon season also. The GCMs are ACCESS1.0.r1, BNU.ESM.r1, CanESM2.r2, CCSM4.r3, CMCC.CM.r1, CNRM.CM5.r1, EC.EARTH.r9, EC.EARTH.r12, FIO.ESM.r1, and FIO.ESM.r2 (where r means model realization). Among various stations temperature, the best cross-validated correlation predictors and predictand are selected as shown in Fig. 6.4.1 to Fig. 6.4.3 for different RCPs. These figures indicate that the correlation between predictors and predictands of temperature are 0.82, 0.78 and 0.8 for RCP2.6, RCP4.5 and RCP8.5, respectively.

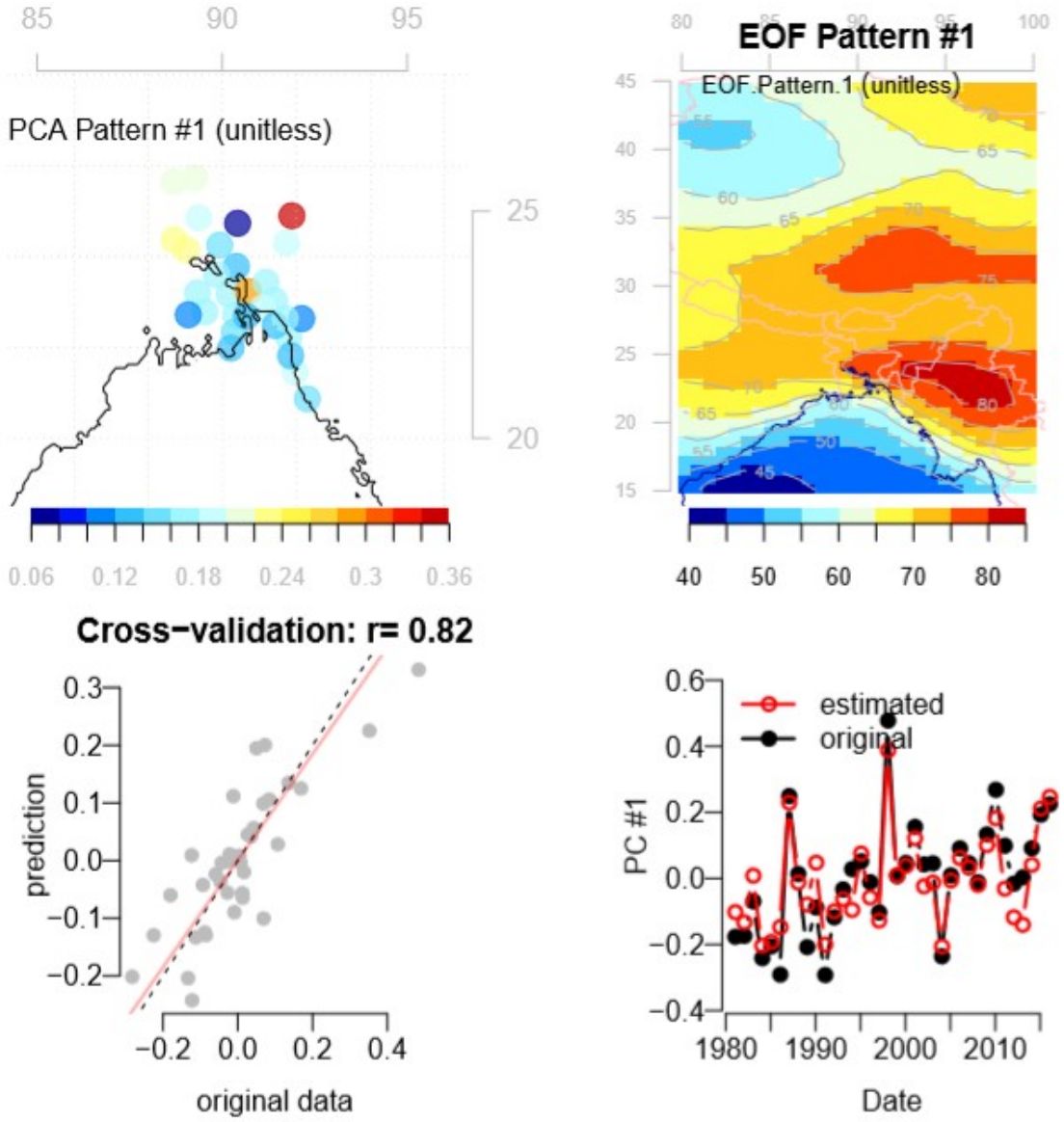

Fig. 6.4.1: Downscaled mean temperature of the post monsoon season based on the observed data and using PCA for downscaling a group of stations simultaneously for RCP2.6. The top-left panel shows the spatial pattern associated with the leading principal component (PC1) of the predictand. The top-right panel shows the leading spatial pattern of the predictor. The lower left panel indicates a cross-validation comparing the original PC1 of the predictand and the corresponding estimated values obtained by ESD. The lower-right panel shows time series of the estimated and original PC1 of the predictand.

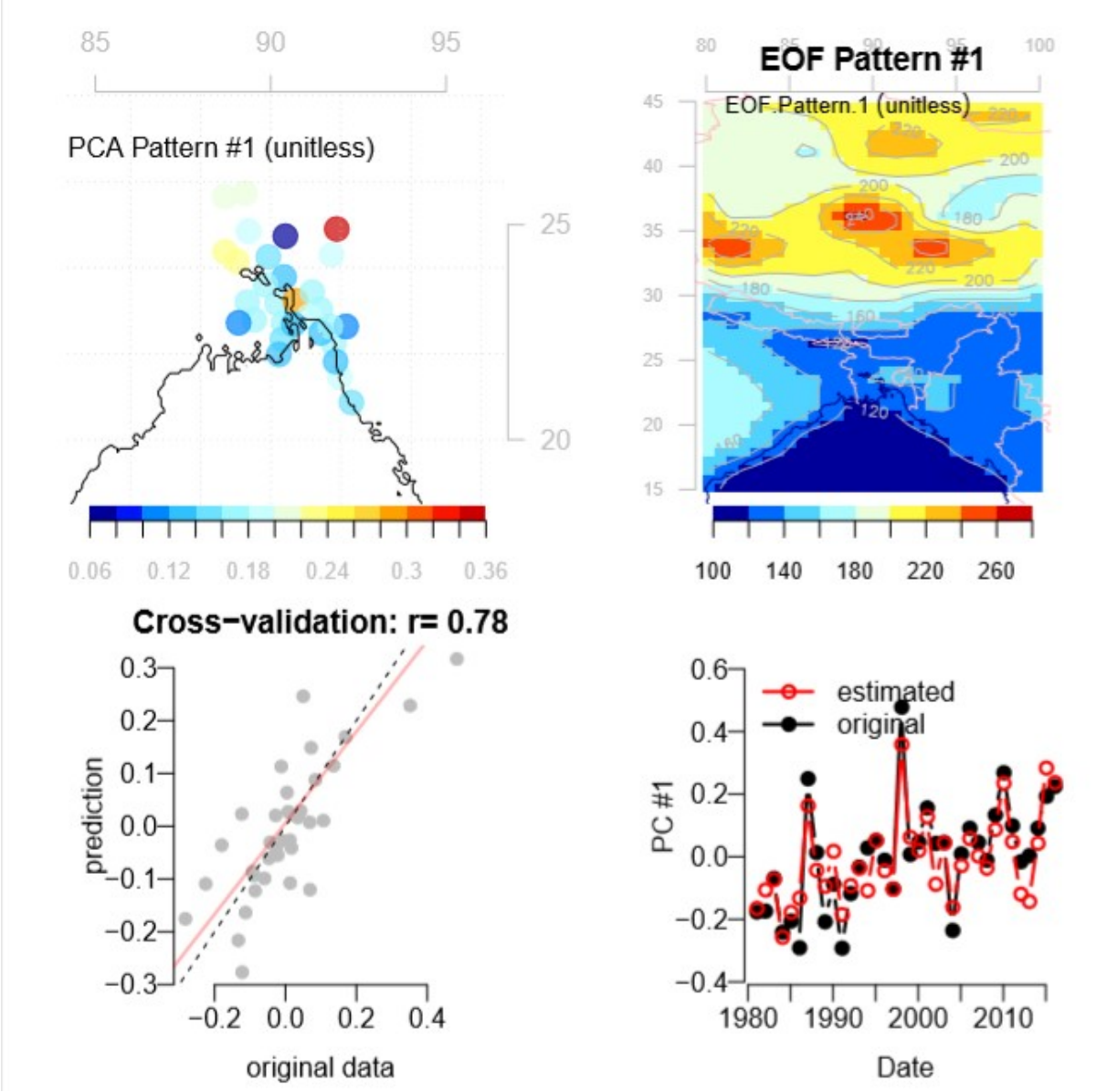

Fig.6.4.2: Downscaled mean temperature of the post monsoon season based on the observed data and using PCA for downscaling a group of stations simultaneously for RCP4.5. The top-left panel shows the spatial pattern associated with the leading principal component (PC1) of the predictand. The top-right panel shows the leading spatial pattern of the predictor. The lower left panel indicates a cross-validation comparing the original PC1 of the predictand and the corresponding estimated values obtained by ESD. The lower-right panel shows time series of the estimated and original PC1 of the predictand.

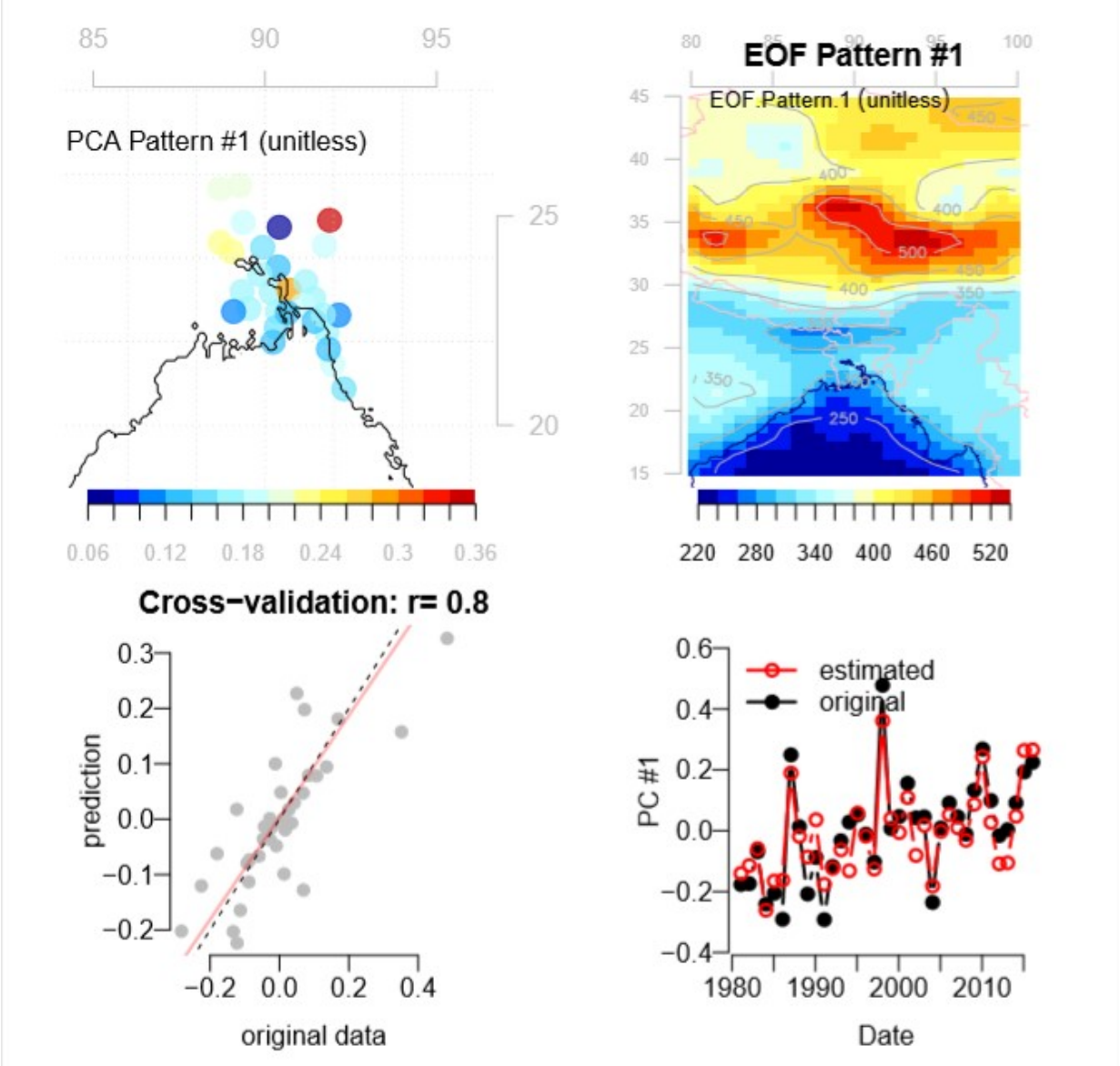

Fig. 6.4.3: Downscaled mean temperature of the post monsoon season based on the observed data and using PCA for downscaling a group of stations simultaneously for RCP8.5. The top-left panel shows the spatial pattern associated with the leading principal component (PC1) of the predictand. The top-right panel shows the leading spatial pattern of the predictor. The lower left panel indicates a cross-validation comparing the original PC1 of the predictand and the corresponding estimated values obtained by ESD. The lower-right panel shows time series of the estimated and original PC1 of the predictand.

RCP2.6 **RCP4.5** **RCP8.5**

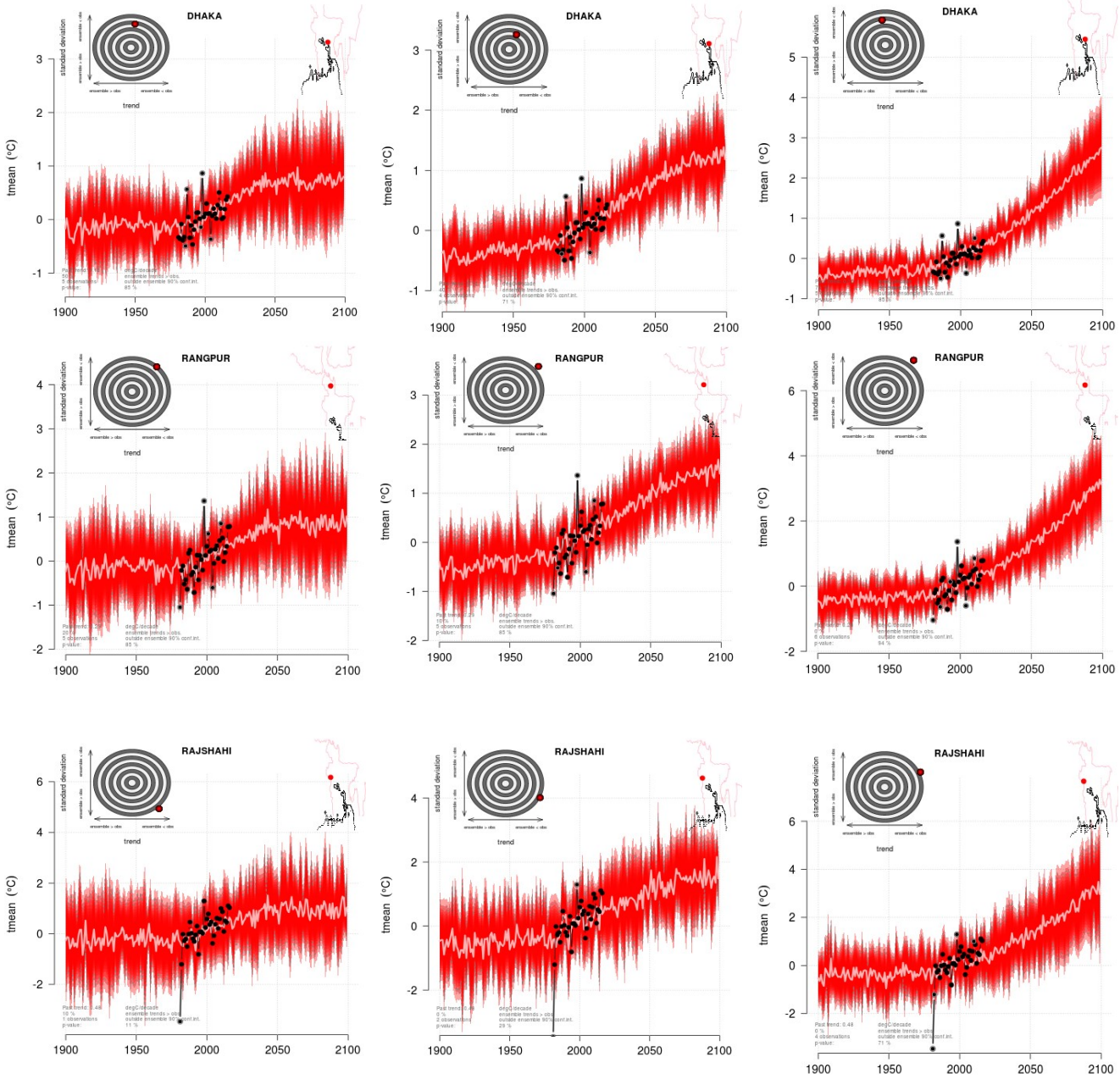

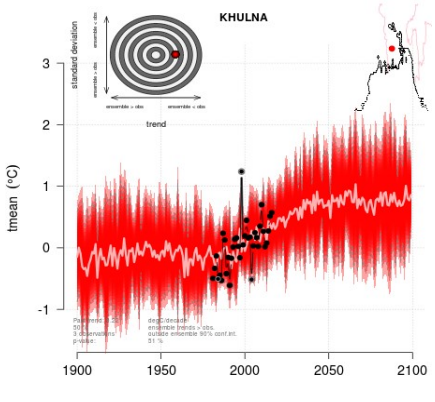
KHULNA
standard deviation
trend
tmean (°C)
1900
1950
2000
2050
2100

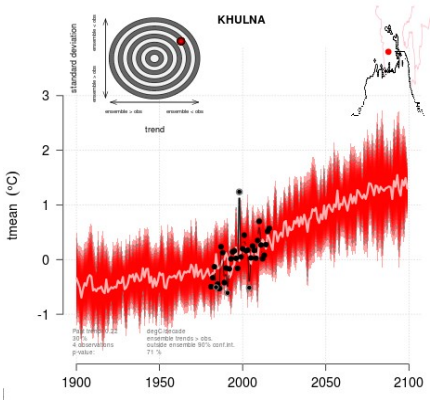
KHULNA
standard deviation
trend
tmean (°C)
1900
1950
2000
2050
2100

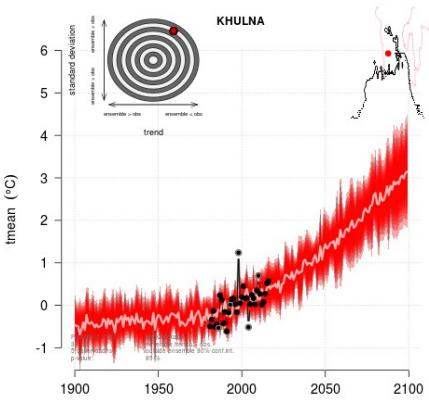
KHULNA
standard deviation
trend
tmean (°C)
1900
1950
2000
2050
2100

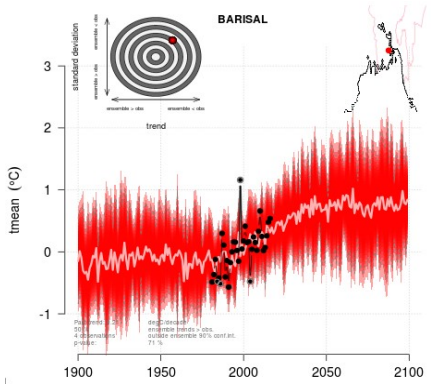
BARISAL
standard deviation
trend
tmean (°C)
1900
1950
2000
2050
2100

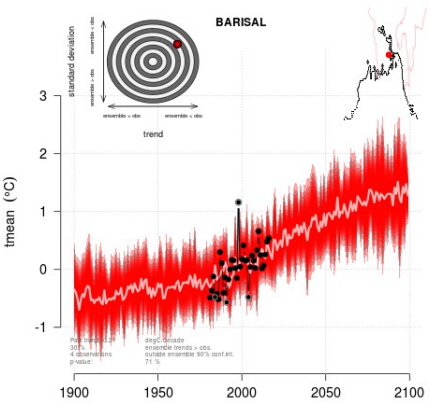
BARISAL
standard deviation
trend
tmean (°C)
1900
1950
2000
2050
2100

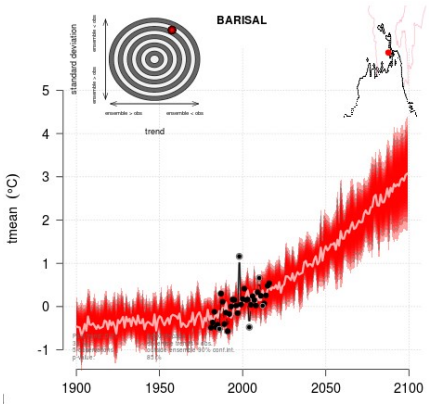
BARISAL
standard deviation
trend
tmean (°C)
1900
1950
2000
2050
2100

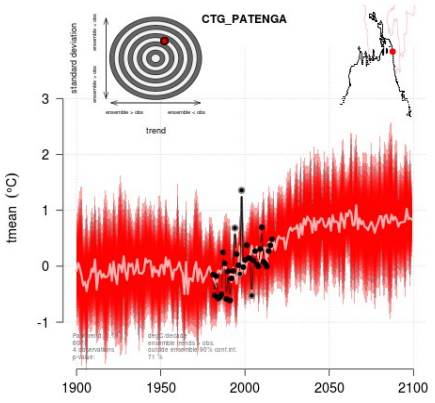
CTG_PATENGA
standard deviation
trend
tmean (°C)
1900
1950
2000
2050
2100

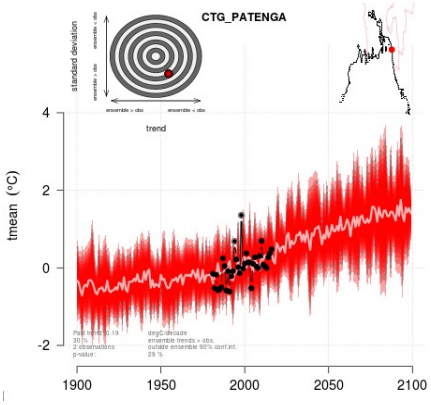
CTG_PATENGA
standard deviation
trend
tmean (°C)
1900
1950
2000
2050
2100

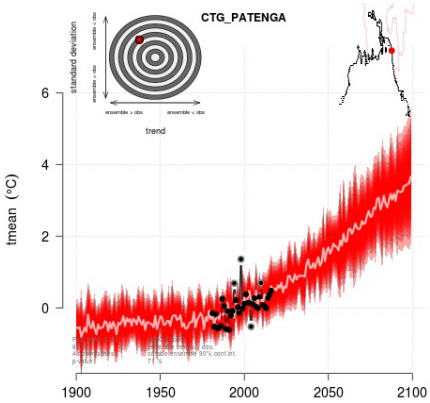
CTG_PATENGA
standard deviation
trend
tmean (°C)
1900
1950
2000
2050
2100

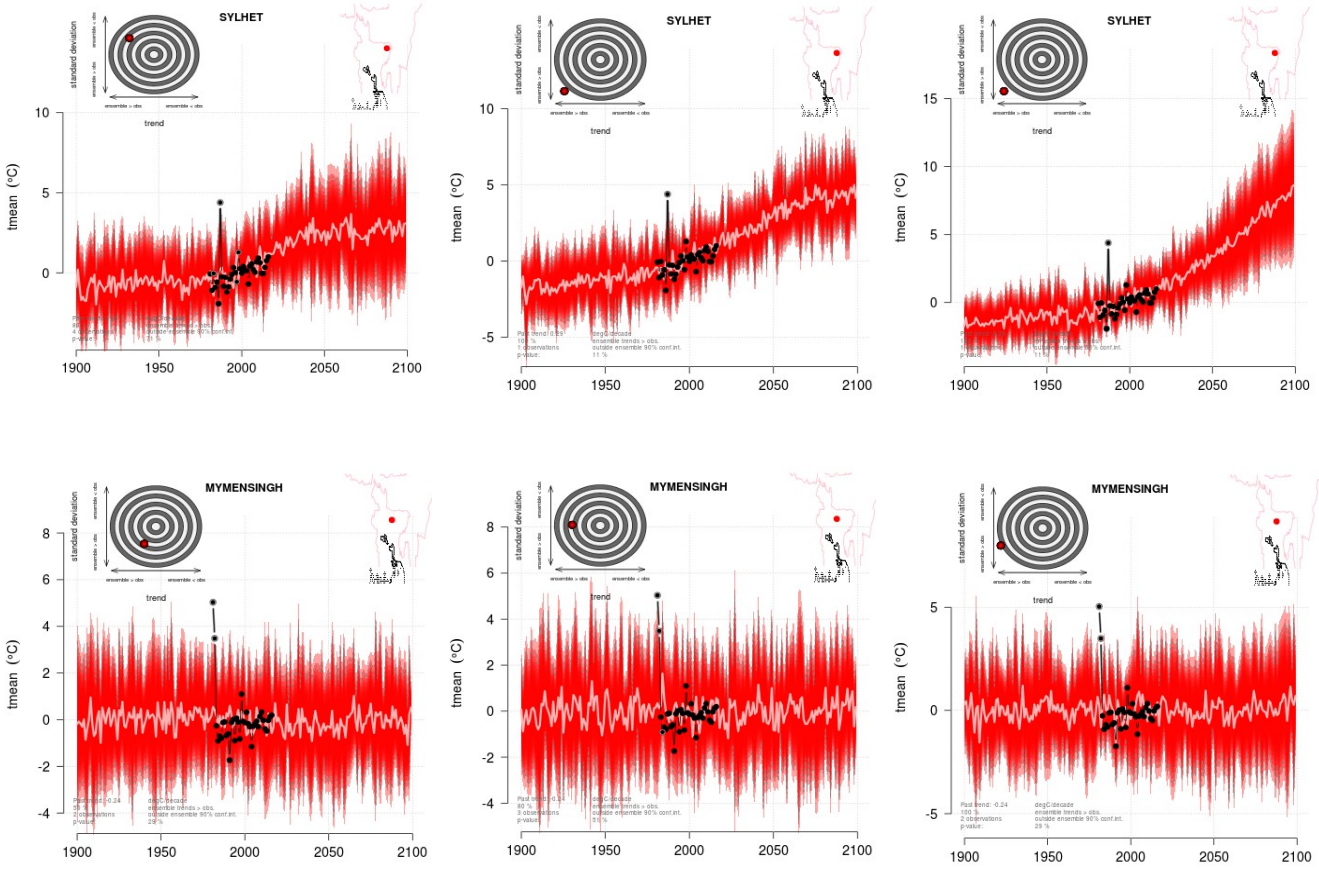

Fig.6.4.4: Mean temperature of post-monsoon season over divisional points change for different RCP scenarios run by CMIP5 experiments, respectively, relative to the period 1981-2010. The light central line is one standard deviation from the mean based on the included GCM simulations for each experiment and the gray-dashed lines mark the 90% confidence region. At the same times, wheel graph shows the probability of finding the observed number of values outside of the downscaled ensemble 90% Confidence Interval (CI), which is taken as a degree of how well fit the ensemble denotes the Interannual Variability (IAV). Values towards the top (bottom) recommend that the downscaled ensemble underestimates (overestimates) the IAV.

Fig. 6.4.4 shows downscaled climate projections of the mean temperature of the post-monsoon season at the divisional place in Bangladesh for different RCPs (RCP2.6, RCP4.5 and RCP8.5), and the wheel graph shows the probability of finding the observed number of values outside of the downscaled ensemble 90% CI, which is taken as a measure of how well the ensemble represents the IAV in each station. Projections at all stations are estimated the interannual variability well for all RCPs except at Rangpur and Sylhet. For RCP4.5 and RCP8.5, the interannual variabilities are underestimated at Rangpur and overestimated at Sylhet. The results are plotted in Table 6.4.1, which includes the average change in the mean temperature of the post-monsoon season relative to 1981-2010 for two periods of (a) the near future (2021-2050) and (b) the far future (2071-2100).

The projection results indicate an increase in the post-monsoon mean temperature at Dhaka by 0.52°C for the near future and 0.64°C for the far future for RCP2.6. For the scenario of RCP4.5, the increase of temperature by 0.61°C in the near future is warming, and 1.2°C in the far future. The scenario of RCP8.5 suggests an increase of post-monsoon temperature by 0.75°C and 2.28°C in the near and far future, respectively. The mean projected change in post-monsoon temperature 0verall Bangladesh for RCP2.6 is 0.6°C for the near future and 0.76°C for the far future. For RCP4.5, it is 0.72°C for the near future and 1.42°C for the far future. For the high emission scenario of RCP8.5, the estimated warming is 0.94°C in the near future, but in the far future, the warming is considerably higher at 2.81°C. The highest projected warming for RCP2.6 is 1.71°C in the near future, and it is 2.12°C in the far future. For RCP4.5, the projected warming of 1.99°C in the near future, and it is 4.21°C for the far future at Sylhet. For the most severe emission scenario of RCP8.5, the projected warming is 2.17°C for the near future and 6.89°C for the far future at the same place as Sylhet. So, it is clear that the mean anomaly of the average temperature of Sylhet is higher than that of all of the other BMD stations, which are also overestimated, as shown at Fig. 6.4.4.

Table 6.4.1: Projected anomaly of mean temperature of post-monsoon season compared to 1981-2010

Division	Station Location	Emission scenario					
		RCP2.6		RCP4.5		RCP8.5	
		Near Future	Far Future	Near Future	Far Future	Near Future	Far Future
Dhaka	Dhaka	0.52	0.64	0.61	1.2	0.75	2.28
	Tangail	0.33	0.49	0.43	0.96	0.71	2.11
	Faridpur	0.56	0.74	0.67	1.38	0.87	2.61
	Madaripur	0.98	1.28	1.12	2.45	1.12	3.66
Mymensingh	Mymensingh	-0.51	-0.28	-0.39	-0.2	0.06	0.34
Chattogram	Chattogram	0.64	0.75	0.78	1.41	1.01	2.99
	Cox'Bazar	0.72	0.85	0.87	1.58	1.12	3.31
	Chandpur	0.9	1.11	1.11	2.09	1.54	4.53
	Cumilla	0.56	0.71	0.67	1.33	0.89	2.66
	Feni	0.58	0.72	0.71	1.36	0.94	2.79
	Kutubdia	0.38	0.52	0.5	1.05	0.75	2.27
	M_Court	0.75	0.87	0.89	1.59	1.11	3.26
	Rangamati	0.22	0.31	0.3	0.62	0.51	1.5
	Sandwip	0.36	0.46	0.47	0.9	0.68	2.02
	Sitakunda	0.62	0.76	0.75	1.42	0.97	2.9
	Teknaf	0.84	0.81	1.06	1.56	1.26	3.72
Khulna	Khulna	0.57	0.7	0.68	1.3	0.9	2.65
	Jashore	0.52	0.66	0.62	1.23	0.82	2.45
	Satkhira	0.44	0.54	0.51	0.98	0.62	1.86
Barishal	Barishal	0.56	0.69	0.67	1.28	0.87	2.58
	Patuakhali	0.42	0.53	0.51	1	0.72	2.12
	Bhola	0.47	0.58	0.57	1.09	0.74	2.2
	Khepupara	0.47	0.58	0.57	1.07	0.75	2.21
Rajshahi	Rajshahi	0.8	0.96	0.85	1.59	1.01	2.84
	Bogura	0.61	0.78	0.72	1.43	0.97	2.85
	Ishurdi	0.98	1.29	1.13	2.43	1.26	3.98
Rangpur	Rangpur	0.59	0.77	0.69	1.39	0.94	2.74
	Dinajpur	0.58	0.77	0.69	1.42	0.96	2.83
Sylhet	Sylhet	1.71	2.21	1.99	4.21	2.17	6.89
	Srimangal	0.75	0.87	0.86	1.56	1.06	3.08
Country		0.6	0.76	0.72	1.42	0.94	2.81

[Projection range indication: (i) Light green color: -0.5 to 0.49°C; (ii) Red text: : 0.5 to 1.0°C; (iii) Light Red fill: 1.1 to 2.0°C and (iv) Light red fill with red text: ≥ 2.1°C]

6.5 Temperature of Winter Season

Based on the screening of predictors, projections are conducted using the best ten (10) GCMs, which are also used in monsoon and post-monsoon seasons. These GCMs are- ACCESS1.0.r1, BNU.ESM.r1, CanESM2.r2, CCSM4.r3, CMCC.CM.r1, CNRM.CM5.r1, EC.EARTH.r9, EC.EARTH.r12, FIO.ESM.r1, FIO.ESM.r2 (where r means model realization). Among various stations' temperatures, the best cross-validated correlation predictors and predictand are selected and are shown in Figure 6.5.1 to Figure 6.5.3, respectively, for different RCPs. These figures indicate that the correlation between predictors and predictands of temperature is 0.66, 0.61 and 0.59°C for RCP2.6, RCP4.5 and RCP8.5, respectively.

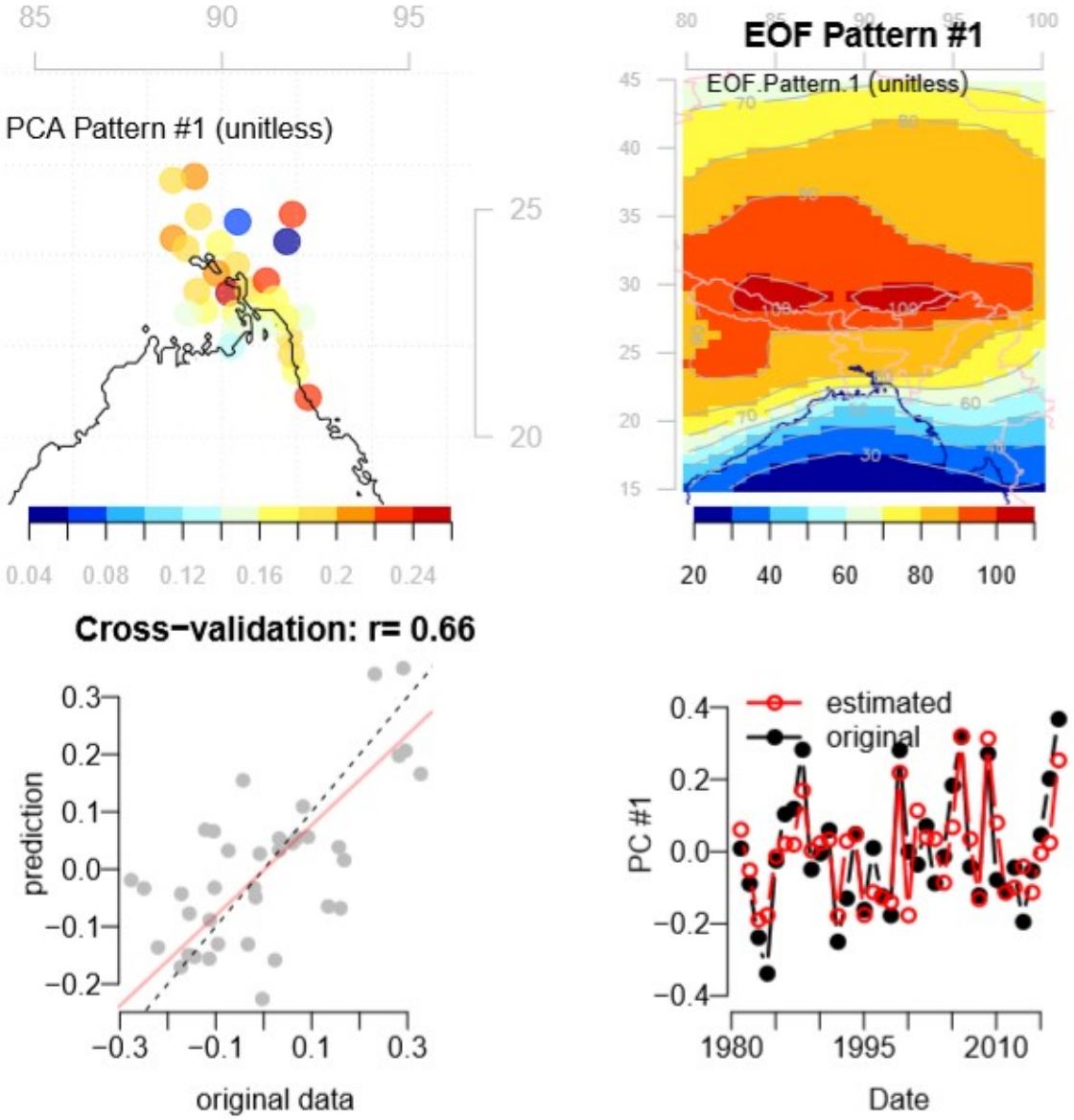

Fig. 6.5.1: Downscaled mean temperature of the winter season based on the observed data and using PCA for downscaling a group of stations simultaneously for RCP2.6. The top-left panel

shows the spatial pattern associated with the leading principal component (PC1) of the predictand. The top-right panel shows the leading spatial pattern of the predictor. The lower left panel indicates a cross-validation comparing the original PC1 of the predictand and the corresponding estimated values obtained by ESD. The lower-right panel shows time series of the estimated and original PC1 of the predictand.

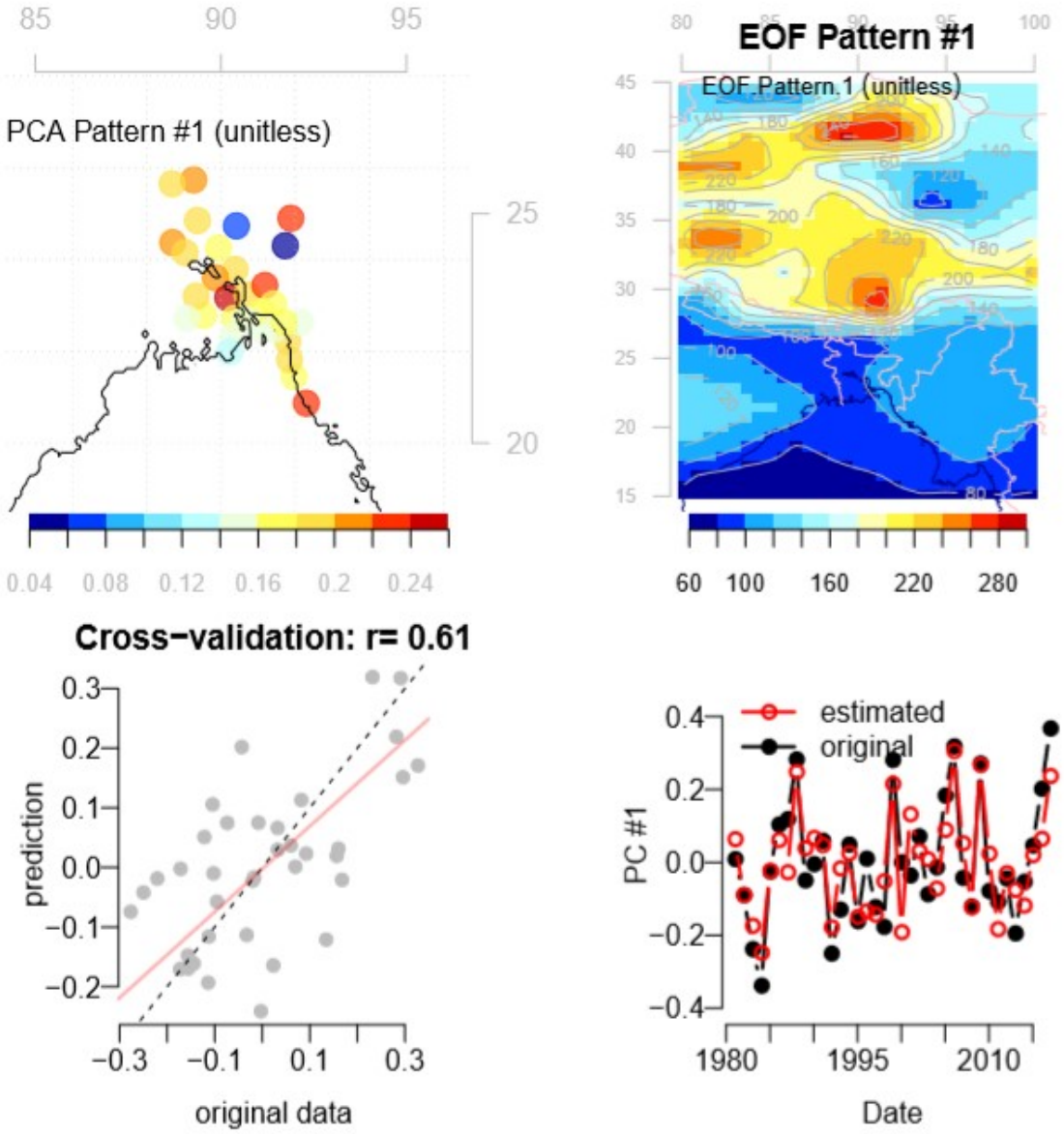

Fig. 6.5.2: Downscaled mean temperature of the winter season based on the observed data and using PCA for downscaling a group of stations simultaneously for RCP4.5. The top-left panel shows the spatial pattern associated with the leading principle component (PC1) of the predictand. The top-right panel shows the leading spatial pattern of the predictor. The lower left panel indicates a cross-validation comparing the original PC1 of the predictand and the

corresponding estimated values obtained by ESD. The lower-right panel shows time series of the estimated and original PC1 of the predictand.

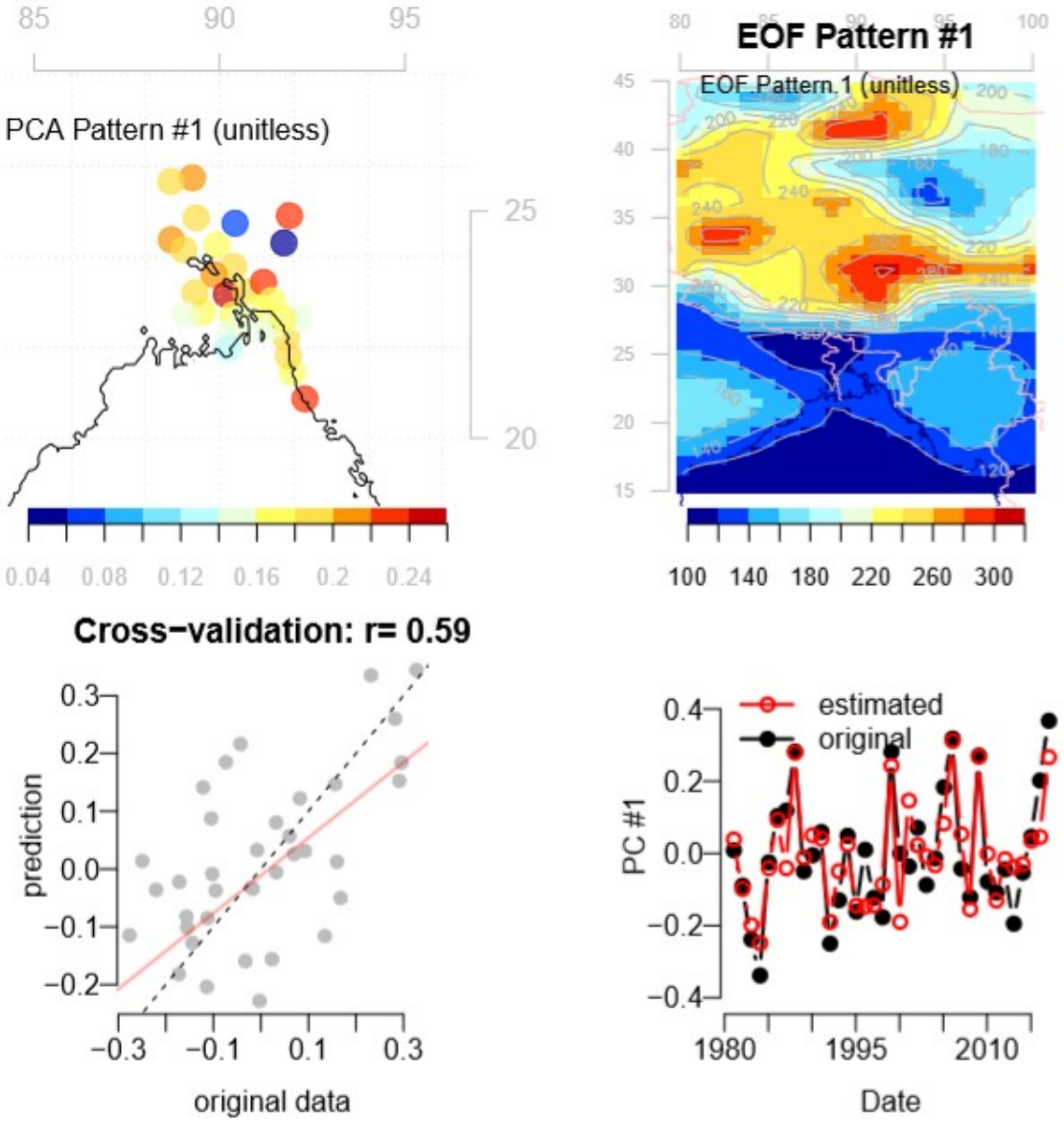

Fig. 6.5.3: Downscaled mean temperature of the winter season based on the observed data and using PCA for downscaling a group of stations simultaneously for RCP8.5. The top-left panel shows the spatial pattern associated with the leading principal component (PC1) of the predictand. The top-right panel shows the leading spatial pattern of the predictor. The lower left panel indicates a cross-validation comparing the original PC1 of the predictand and the corresponding estimated values obtained by ESD. The lower-right panel shows time series of the estimated and original PC1 of the predictand.

RCP2.6 **RCP4.5** **RCP8.5**

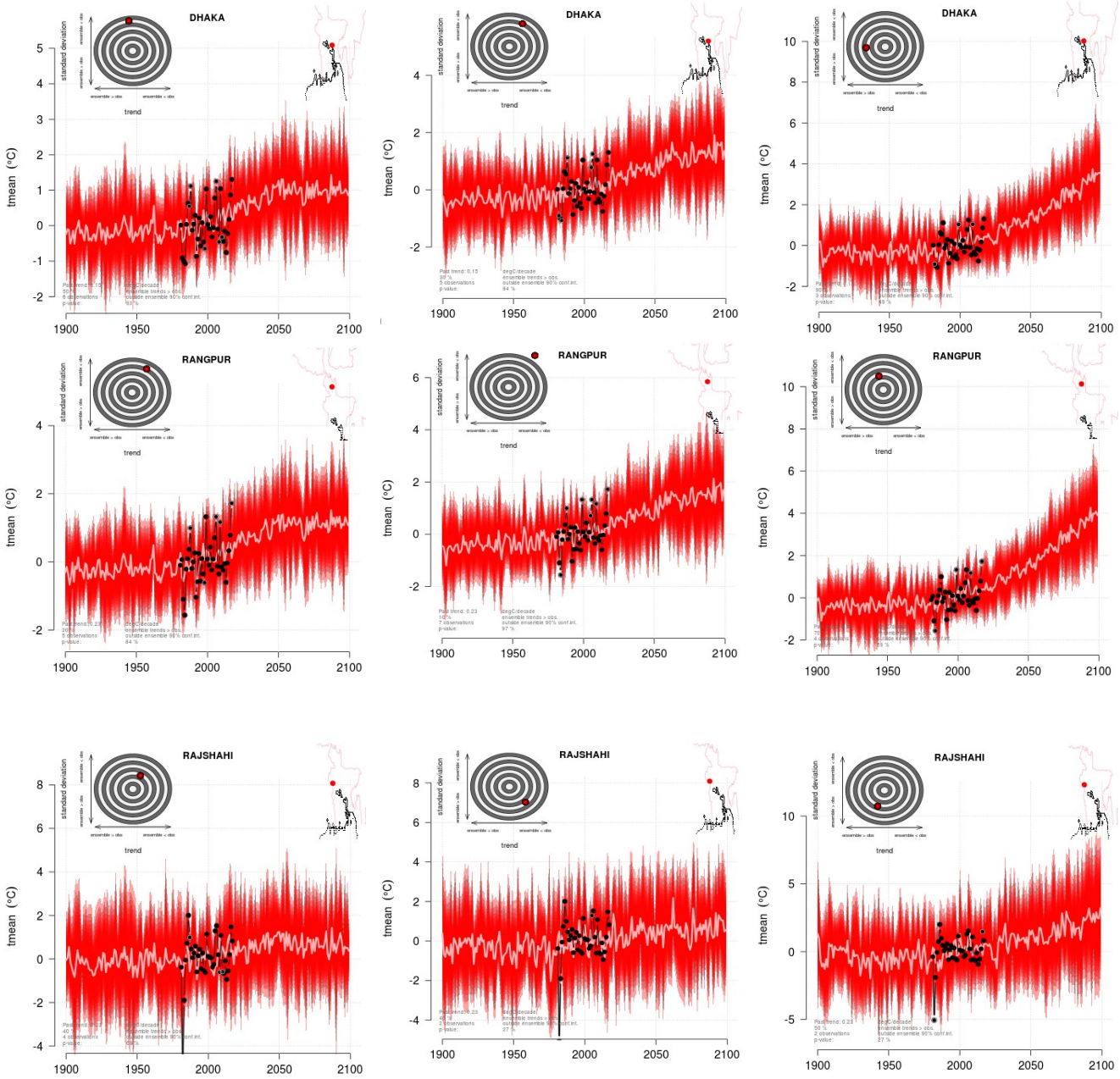

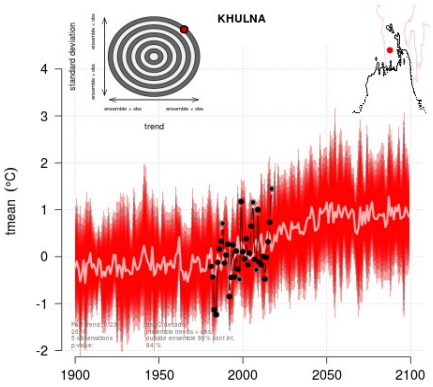
KHULNA
standard deviation
trend
tmean (°C)
1900
1950
2000
2050
2100

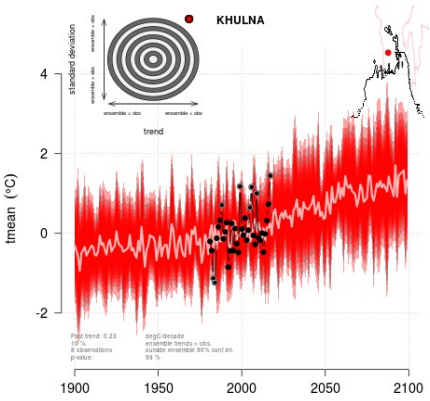
KHULNA
standard deviation
trend
tmean (°C)
1900
1950
2000
2050
2100

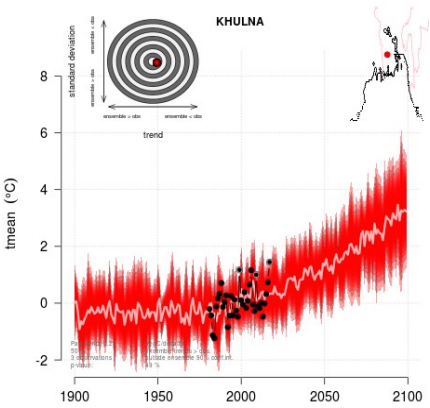
KHULNA
standard deviation
trend
tmean (°C)
1900
1950
2000
2050
2100

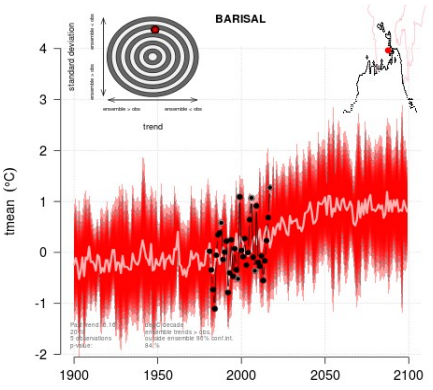
BARISAL
standard deviation
trend
tmean (°C)
1900
1950
2000
2050
2100

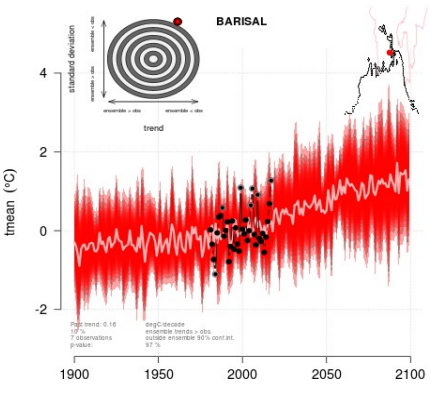
BARISAL
standard deviation
trend
tmean (°C)
1900
1950
2000
2050
2100

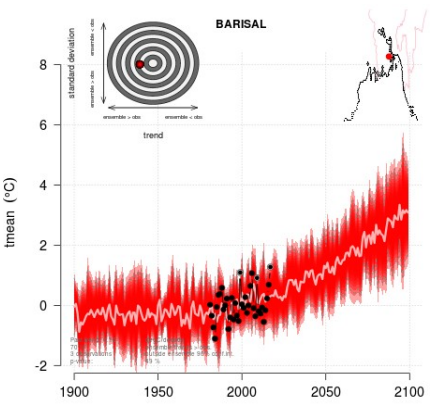
BARISAL
standard deviation
trend
tmean (°C)
1900
1950
2000
2050
2100

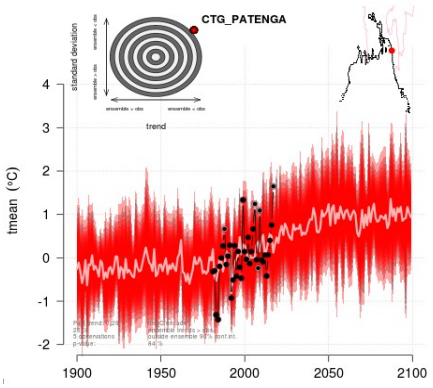
CTG_PATENGA
standard deviation
trend
tmean (°C)
1900
1950
2000
2050
2100

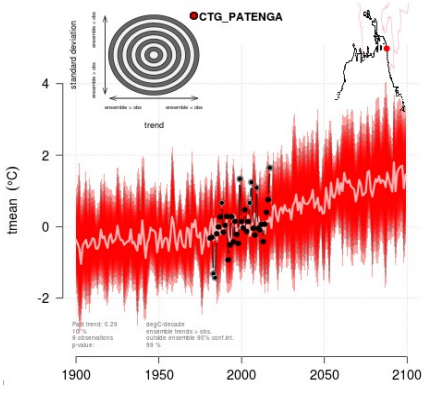
CTG_PATENGA
standard deviation
trend
tmean (°C)
1900
1950
2000
2050
2100

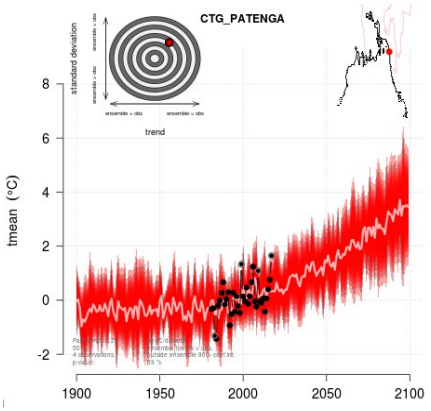
CTG_PATENGA
standard deviation
trend
tmean (°C)
1900
1950
2000
2050
2100

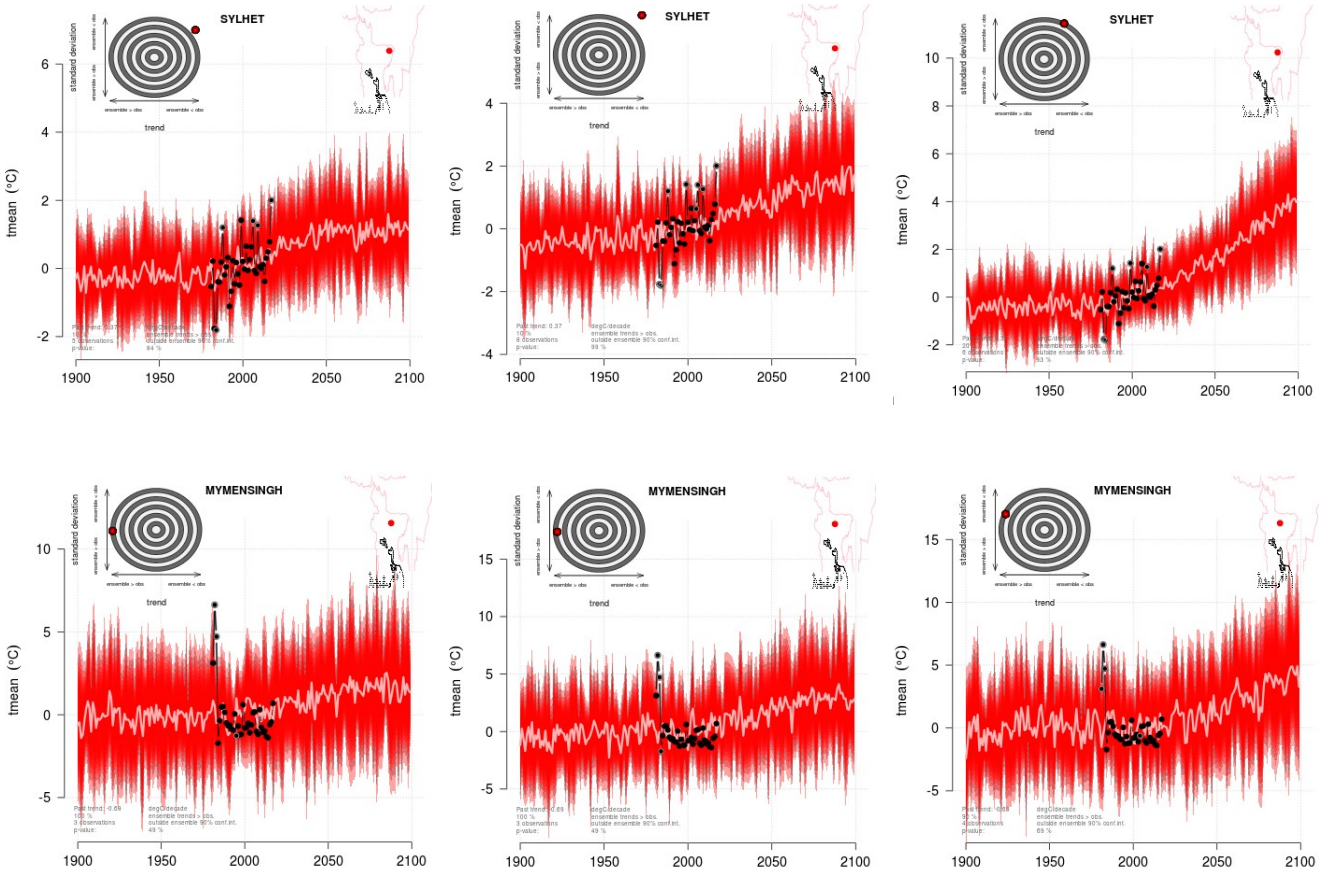

Fig.6.5.4: Mean temperature of winter season over divisional points change for different RCP scenarios run by CMIP5 experiments, respectively, relative to the period 1981-2010. The light central line is one standard deviation from the mean based on the included GCM simulations for each experiment and the gray-dashed lines mark the 90% confidence region. At the same times, wheel graph shows the probability of finding the observed number of values outside of the downscaled ensemble 90% confidence interval, which is taken as a measure of how well the ensemble represents the interannual variability. Values towards the top (bottom) suggest that the downscaled ensemble underestimates (overestimates) the interannual variability.

Fig. 6.5.4 shows downscaled climate projections of the mean temperature of the winter season at the divisional place of Bangladesh for different RCPs (RCP2.6, RCP4.5 and RCP8.5) and wheel graphs show the probability of finding the observed number of values outside of the downscaled ensemble at 90% confidence interval, which is taken as a measure of how well the ensemble represents the interannual variability at each station. Projections are well estimated for the interannual variability at almost all stations except Rangpur, Khulna, Chattogam and Sylhet stations for all RCPs. However, these four stations are underestimated the interannual variability for RCP4.5. The results are plotted in Table 6.5.1, which includes the average change in the mean

temperature of the winter season relative to 1981-2010 for two periods of (a) the near future (2021-2050) and (b) the far future (2071-2100). The projection results indicate an increase in the winter mean temperature at Dhaka by 0.48°C for the near future and 0.71°C for the far future with RCP2.6, but for RCP4.5, the near future warming is estimated to be about 0.41°C and far future it is 1.08°C. The scenario of RCP8.5 suggests an increase of winter temperature by 0.83°C and 2.86°C for the near and far future, respectively. The mean projected change in winter temperature overall country for RCP2.6 is 0.45°C for the near future and 0.71°C for the far future. For RCP4.5, it is 0.44°C for the near future and 1.16°C for the far future. For the high emission scenario of RCP8.5, the near future estimated warming is 0.86°C in the near future, and it is 2.83°C for the far future, which is considerably high. The highest projected warming for RCP2.6 is 0.58°C for the near future and 1.4°C for the far future. Similarly, for RCP4.5, the captured warming is 1.12°C for the near future and 2.8°C for the far future at Mymensingh. For the most severe emission scenario of RCP8.5, the projected warming is 1.97°C for the near future and 4.61°C for the far future at the same place as Mymensingh.

Table 6.5.1: Projected anomaly of mean temperature of winter season compared to 1981-2010

Division	Station Location	Emission scenario					
		RCP2.6		RCP4.5		RCP8.5	
		Near Future	Far Future	Near Future	Far Future	Near Future	Far Future
Dhaka	Dhaka	0.48	0.71	0.41	1.08	0.83	2.86
	Tangail	0.54	0.97	0.66	1.7	1.24	3.63
	Faridpur	0.5	0.79	0.47	1.26	0.94	3.15
	Madaripur	0.5	0.73	0.24	0.53	0.62	2.74
Mymensingh	Mymensingh	0.58	1.4	1.12	2.8	1.97	4.61
Chattogram	Chattogram	0.42	0.66	0.4	1.12	0.79	2.82
	Cox'Bazar	0.35	0.53	0.34	0.97	0.66	2.39
	Chandpur	0.47	0.73	0.46	1.28	0.9	3.08
	Cumilla	0.47	0.67	0.36	1.01	0.75	2.93
	Feni	0.42	0.67	0.41	1.11	0.81	2.65
	Hatiya	0.43	0.74	0.48	1.26	0.92	2.86
	Kutubdia	0.4	0.6	0.36	1.01	0.71	2.66
	M_Court	0.3	0.42	0.19	0.56	0.42	1.93
	Rangamati	0.47	0.83	0.58	1.52	1.08	3.17
	Sandwip	0.41	0.69	0.45	1.2	0.87	2.69
	Sitakunda	0.44	0.71	0.45	1.22	0.88	2.89
	Teknaf	0.57	0.98	0.67	1.83	1.26	4.05
Khulna	Khulna	0.41	0.63	0.38	1.04	0.75	2.64
	Jashore	0.57	0.86	0.51	1.28	1.03	3.11
	Satkhira	0.38	0.58	0.32	0.82	0.66	2.18
Barishal	Barishal	0.41	0.64	0.39	1.06	0.77	2.59
	Patuakhali	0.41	0.65	0.4	1.06	0.79	2.52
	Bhola	0.4	0.63	0.38	0.99	0.76	2.38
	Khepupara	0.35	0.54	0.32	0.86	0.64	2.13
Rajshahi	Rajshahi	0.48	0.47	0.15	0.42	0.44	1.95
	Bogura	0.5	0.77	0.46	1.22	0.92	3.03
	Ishurdi	0.49	0.76	0.46	1.23	0.92	2.98
Rangpur	Rangpur	0.5	0.8	0.5	1.34	0.97	3.29
	Dinajpur	0.44	0.7	0.42	1.13	0.82	2.9
Sylhet	Sylhet	0.46	0.74	0.45	1.26	0.88	3.24
	Srimangal	0.29	0.5	0.33	0.78	0.64	1.53
Country		0.45	0.71	0.44	1.16	0.86	2.83

[Projection range indication: (i) Light green color: -0.5 to 0.49°C; (ii) Red text: 0.5 to 1.0°C; (iii) Light Red fill: 1.1 to 2.0°C and (iv) Light red fill with red text: ≥ 2.1°C]

6.6 Summary

Analysis of the downscale result conducted using ESD depicts that the projections of mean temperatures in pre-monsoon season for the RCP2.6 emission scenario are positive both in the near future and far future, and it is with the ranges of 0.31 to 1.62°C and 0.12 to 2.03°C respectively. The projection of the highest warmings for both periods is found at Sitakunda, followed by Maijdi Court. No signature of cooling projection at the BMD station places is found under this scenario. For the RCP4.5 scenario, the projections of mean temperatures in pre-monsoon season are positive at all BMD station locations both in the near future and far future, except at Ishurdi, where it is likely to be negative. The highest magnitudes of projection of mean temperatures are 1.66°C (at Sitakunda) and 3.59°C (at Sitakunda) for the near future and far future, respectively, under this emission scenario. For the RCP8.5 scenario, the projections of mean temperatures in the pre-monsoon season are positive at all BMD station locations, with the range of 0.10 to 1.41°C in the near future. It is the highest at Sitakunda, followed by Maijdi Court. Under the same scenario, the projections of mean temperatures in the pre-monsoon season are positive at all BMD station locations. Its range is 0.10 to 5.74°C in the far future, with the maximum at Sitakunda followed by Maijdi Court. As a whole, the result depicts a dominant projection of warming in both the near and far future at the selected locations.

The projections of mean temperatures in monsoon season for the RCP2.6 emission scenario indicate a warmings scenario both in the near future and far future, and it is of 0.11 to 0.38°C and 0.02 to 0.52°C, respectively. The projection of the highest warmings situation for both of these periods is at Sitakunda. There is no evidence of a cooling phase in this scenario at the BMD station locations. For the RCP4.5 scenario, the projections of mean temperatures in the monsoon season are positive at all BMD station locations both in the near future and far future, except at Sylhet, where it is likely to be negative. The highest magnitudes of projection of mean temperatures are 0.36°C (at Mymensingh) and 0.69°C (at Sitakunda) for the near future and far future, respectively. For the RCP8.5 scenario, the projections of mean temperatures in the monsoon season are positive at all BMD station locations with the range of 0.02 to 0.61°C in the near future. It is the highest at Madaripur, followed by Sylhet. Under the same scenario, the projections of mean temperatures in the monsoon season are positive at all BMD station locations. Its range is 0.25 to 1.93°C in the far future, with the maximum at Sitakunda followed by Maijdi Court. As a whole, analysis depicts a dominant projection of warming in both the near and far future at the selected locations.

The projections of mean temperatures in post-monsoon season for the RCP2.6 emission scenario are -0.51 to 1.71°C and -0.28 to 2.21°C in the near future and far future, respectively. The projection of the highest warming for both of these periods is found at Sylhet. No signature of cooling projection at the BMD station places is found under this scenario except Mymensingh. For the RCP4.5 scenario, the projections of mean temperatures in post-monsoon season are positive at all BMD station locations both in the near and far future, except at Mymensingh. The highest magnitudes of projection of mean temperatures are 1.99°C and 4.21°C, both at Sylhet for the near

future and far future, respectively. For the RCP8.5 scenario, the projections of mean temperatures in post-monsoon season are positive at all BMD station locations, with the range of 0.06 to 2.17°C in the near future. It is the highest at Sylhet, followed by Chandpur station location. Under the same scenario, the projections of mean temperatures in post-monsoon season are positive at all BMD station locations. Its range is 0.34 to 6.89°C in the far future, with the maximum at Sylhet followed by Chandpur. As a whole, the result depicts a strong projection of warming in both the near and far future at the selected locations.

The projections of mean temperatures in the winter season for the RCP2.6 emission scenario are positive both in the near future and far future, with ranges of 0.29 to 0.58°C and 0.42 to 1.14°C, respectively. The projection of the highest warming for both of these periods is found at Mymensingh. No signature of cooling projection at the BMD station places is found under this scenario. For the RCP4.5 scenario, the projections of mean temperatures in the winter season are positive at all BMD station locations both in the near future and far future. The highest magnitudes of projection are 1.12°C and 2.8°C, both at Mymensingh for the near future and far future, respectively, under this emission scenario. For the RCP8.5 scenario, the projections of mean temperatures in the winter season are positive at all BMD station locations with the range of 0.42 to 1.97°C in the near future. It is the highest at Mymensingh and then in Teknaf. Under the same scenario, the projections of mean temperatures in the monsoon season are positive at all BMD station locations. Its range is 1.53 to 4.61°C in the far future, when the maximum projection is at Mymensingh, followed by Teknaf. As a whole, analysis depicts a dominant projection of warming in both the near and far future at the selected locations.

CHAPTER SEVEN: STATISTICAL DOWNSCALING OF RAINFALL

7.1 Rainfall of Pre-monsoon Season

An analysis of the common EOFs of the GCM simulations is performed to evaluate the goodness of fit of the GCMs output compared to observation-based data. The residuals from the downscaled data are verified against adequacy. Screening of predictors and predictor domains is conducted using corrected 05 (five) GCMs simulations and various rainfall stations, and the best-correlated predictors and predictand are selected. The selected GCMs are ACCESS1-0.r1i1p1, ACCESS1.3.r1i1p1, BCC-CSM1-1.r1i1p1, BNU-ESM.r1i1p1 and CanESM2.r1i1p (where r means model realization). The cross-validated correlation between the wet-day frequency's first principal component (PC1) and the corresponding PC1 estimated based on empirical-statistical downscaling is 0.8 in Fig. 7.1.1.

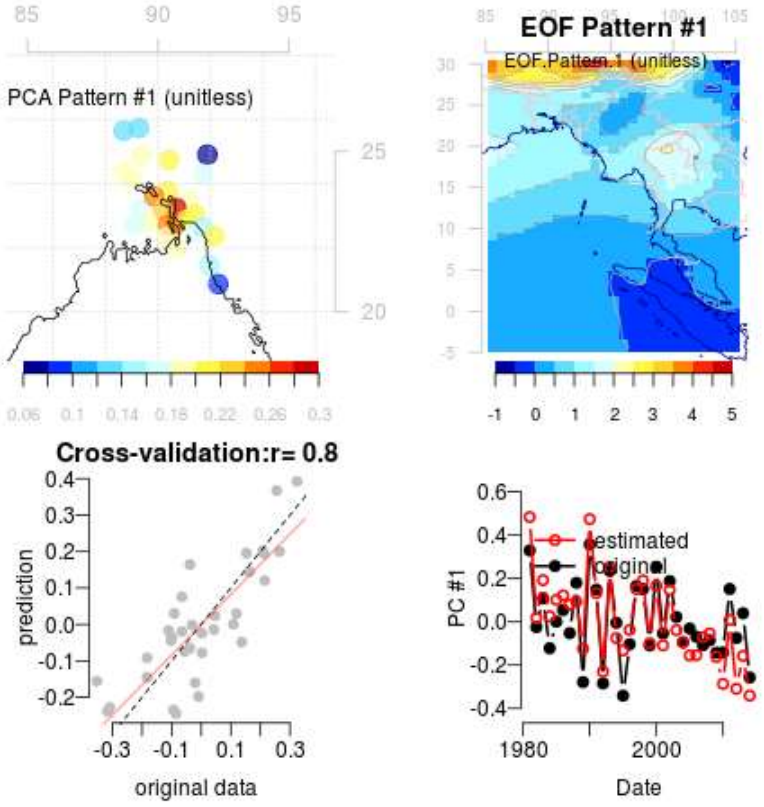

Fig. 7.1.1: Downscaled means the wet-day frequency of the pre-monsoon season based on the GCM and using PCA for downscaling a group of stations simultaneously. The top-left panel illustrates the spatial pattern connected with the leading principal component (PC1) of the predictand. The top-right panel express the leading spatial pattern of the predictor. The lower left panel indicates a cross-validation comparing the original PC1 of the predictand and the corresponding estimated values obtained by ESD. The lower-right panel indicates time series of the estimated and original PC1 of the predictand.

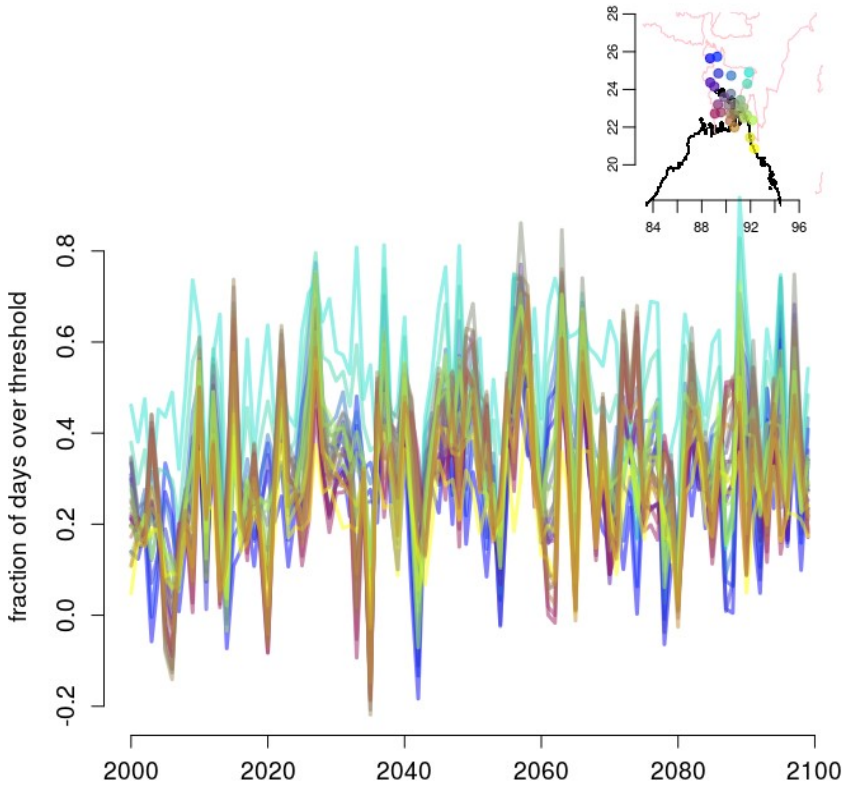

Fig. 7.1.2. Wet-day frequency of pre-monsoon season over station points change for RCP2.6 scenarios run by CMIP5 experiments, respectively, relative to the period 1981-2010.

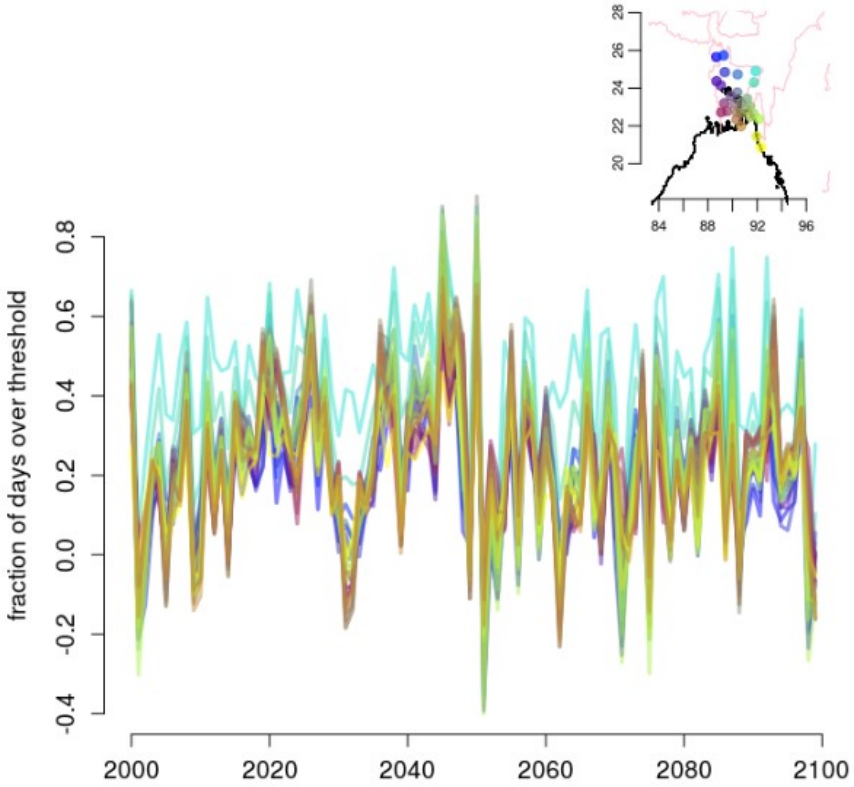

Fig. 7.1.3: Wet-day frequency of pre-monsoon season over station points change for RCP4.5 scenarios run by CMIP5 experiments, respectively, relative to the period 1981-2010

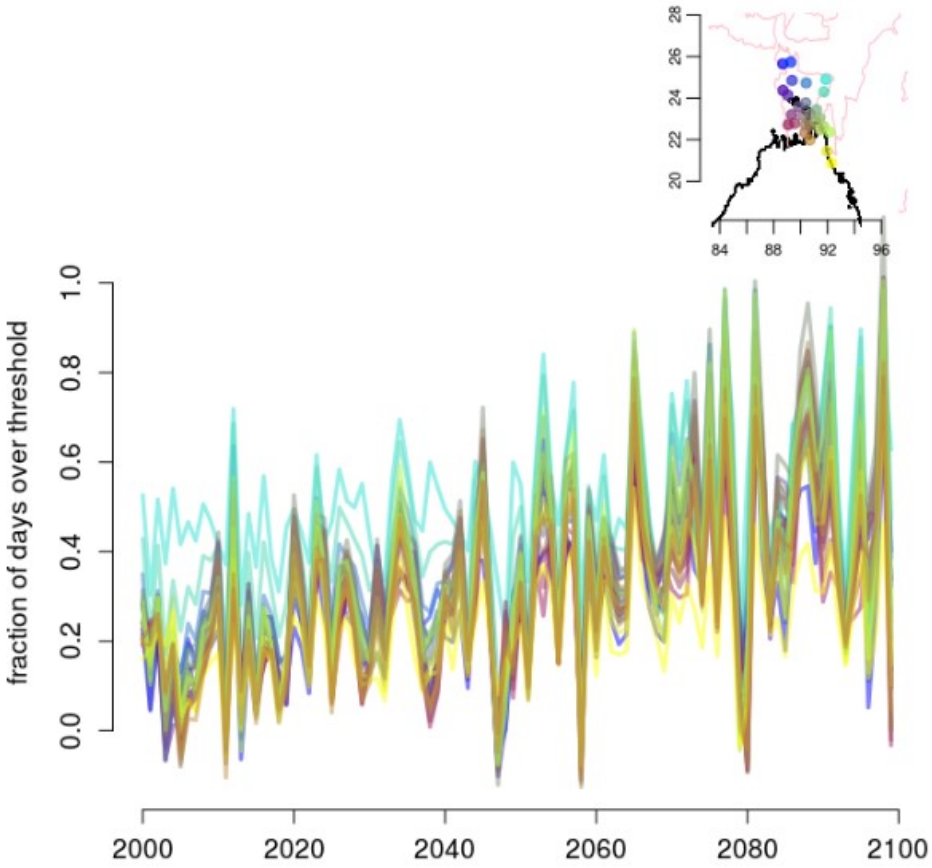

Fig.7.1.4: Wet-day frequency of pre-monsoon season over station points change for RCP8.5 scenarios run by CMIP5 experiments, respectively, relative to the period 1981-2010.

Figs. 7.1.2-7.1.4 shows downscaled wet-day frequency of pre-monsoon season at station points for different RCPs (RCP2.6, RCP4.5 and RCP8.5) in Bangladesh. The minimum amount of rainfall of one millimeter per day has been considered a wet-day, and deviation has been considered based on the average wet-day frequency recorded from 1981-2010. The magnitude of the wet-day frequency is higher over the northeastern part of the country and lower in the south and western parts of Bangladesh (Fig.7.1.2 and Fig.7.1.3). Analysis reveals that wet-day frequency is likely to increase over the country for RCP8.5 scenario (Fig.7.1.4). But the rate increment is higher in the northeastern part and comparatively lower in the south and western parts of county till 2050. After 2050, it is likely to increase at a higher rate till 2100 all over Bangladesh.

Fig. 7.1.5 to Fig. 7.1.8 shows downscaled climate projections of wet-day frequency of pre-monsoon season at divisional places of Bangladesh for different RCPs (RCP2.6, RCP4.5 and RCP8.5) and wheel graph shows the probability of finding the observed number of values outside of the downscaled ensemble at 90% CI, which is taken as a measure of how well the ensemble represents the IAV in each station location. Projections of all stations are well estimated for the interannual variability for all RCPs except Dhaka, Khulna, Rajshahi and Sylhet. Interannual variabilities are underestimated at Khulna and Sylhet for RCP8.5 and Dhaka and Rajshahi for RCP2.6.

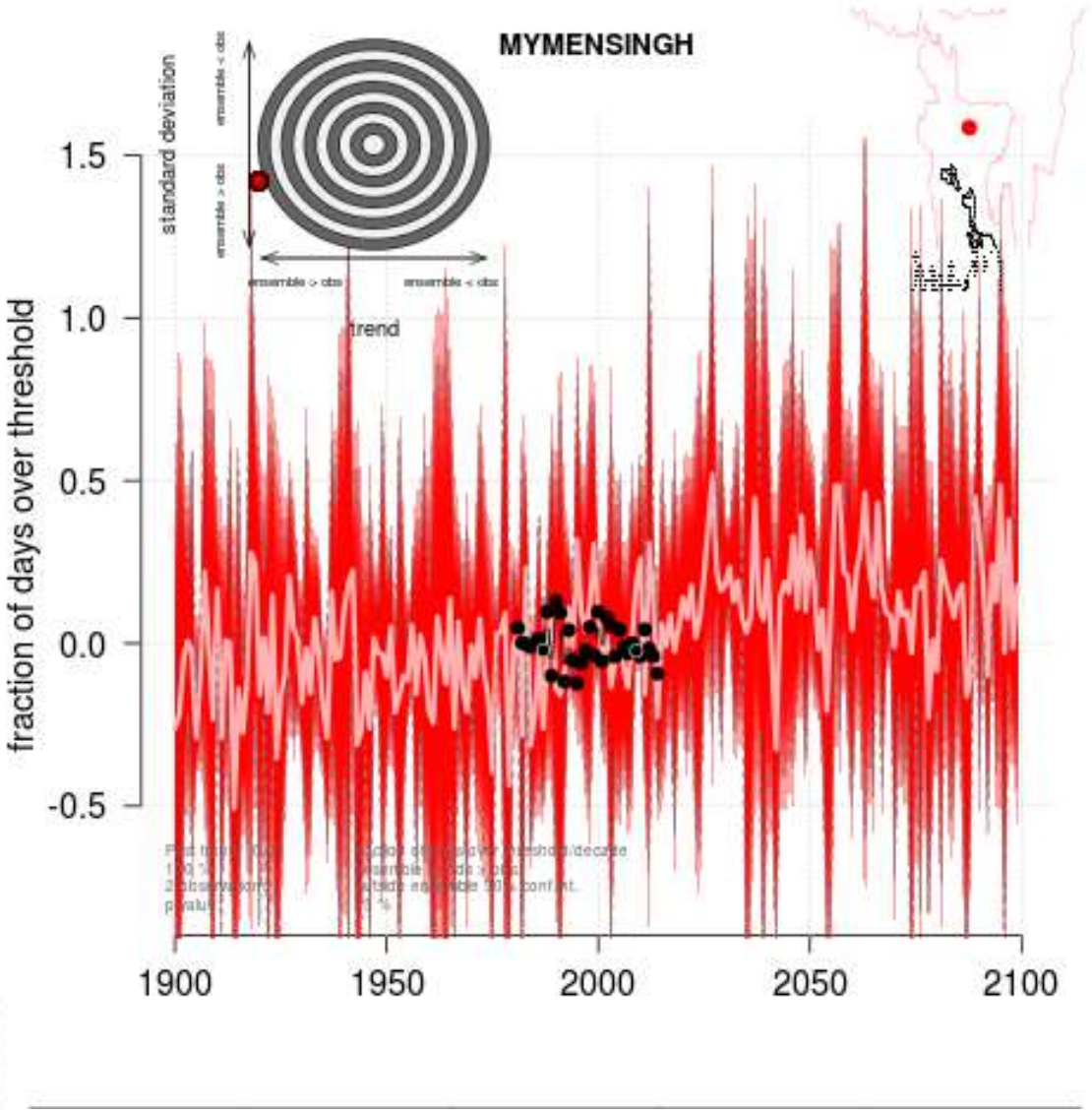

Fig.7.1.5: Wet-day frequency of pre-monsoon season over Mymensingh for different RCP2.6 scenarios run by CMIP5 experiments, respectively, relative to the period 1981-2010. The light central line is one standard deviation from the mean based on the included GCM simulations for each experiment and the gray-dashed lines mark the 90% confidence region. At the same times, wheel graph shows the probability of finding the observed number of values outside of the downscaled ensemble 90% Confidence Interval (IC), which is taken as a degree of how well fit the ensemble denotes the Interannual Variability (IAV). Values towards the top (bottom) recommend that the downscaled ensemble underestimates (overestimates) the IAV.

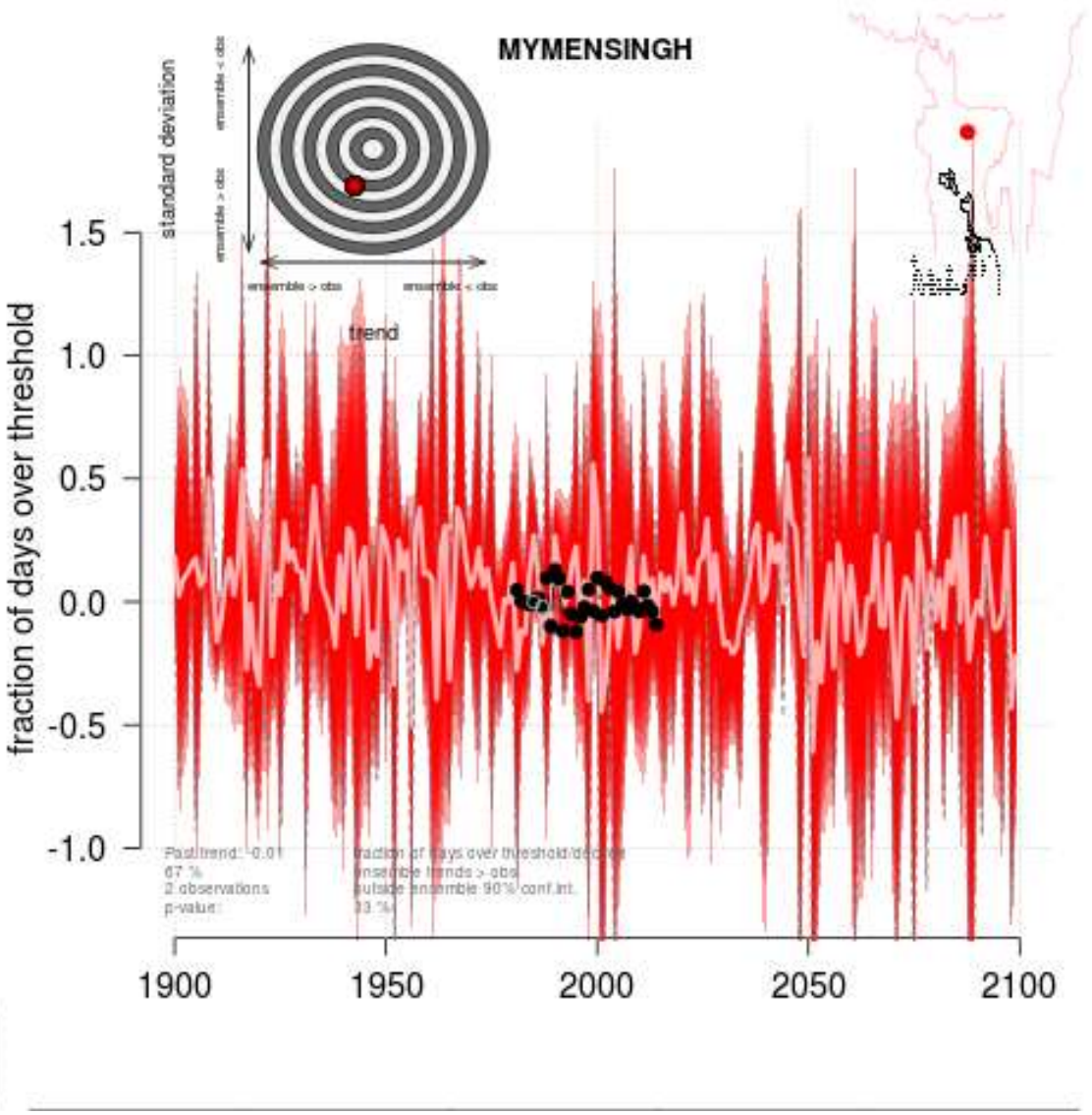

Fig.7.1.6: Wet-day frequency of pre-monsoon season over Mymensingh for different RCP4.5 scenarios run by CMIP5 experiments, respectively, relative to the period 1981-2010. The light central line is one standard deviation from the mean based on the included GCM simulations for each experiment and the gray-dashed lines mark the 90% confidence region. At the same times, wheel graph shows the probability of finding the observed number of values outside of the downscaled ensemble 90% Confidence Interval (CI), which is taken as a degree of how well fit the ensemble denotes the Interannual Variability (IAV). Values towards the top (bottom) recommend that the downscaled ensemble underestimates (overestimates) the IAV.

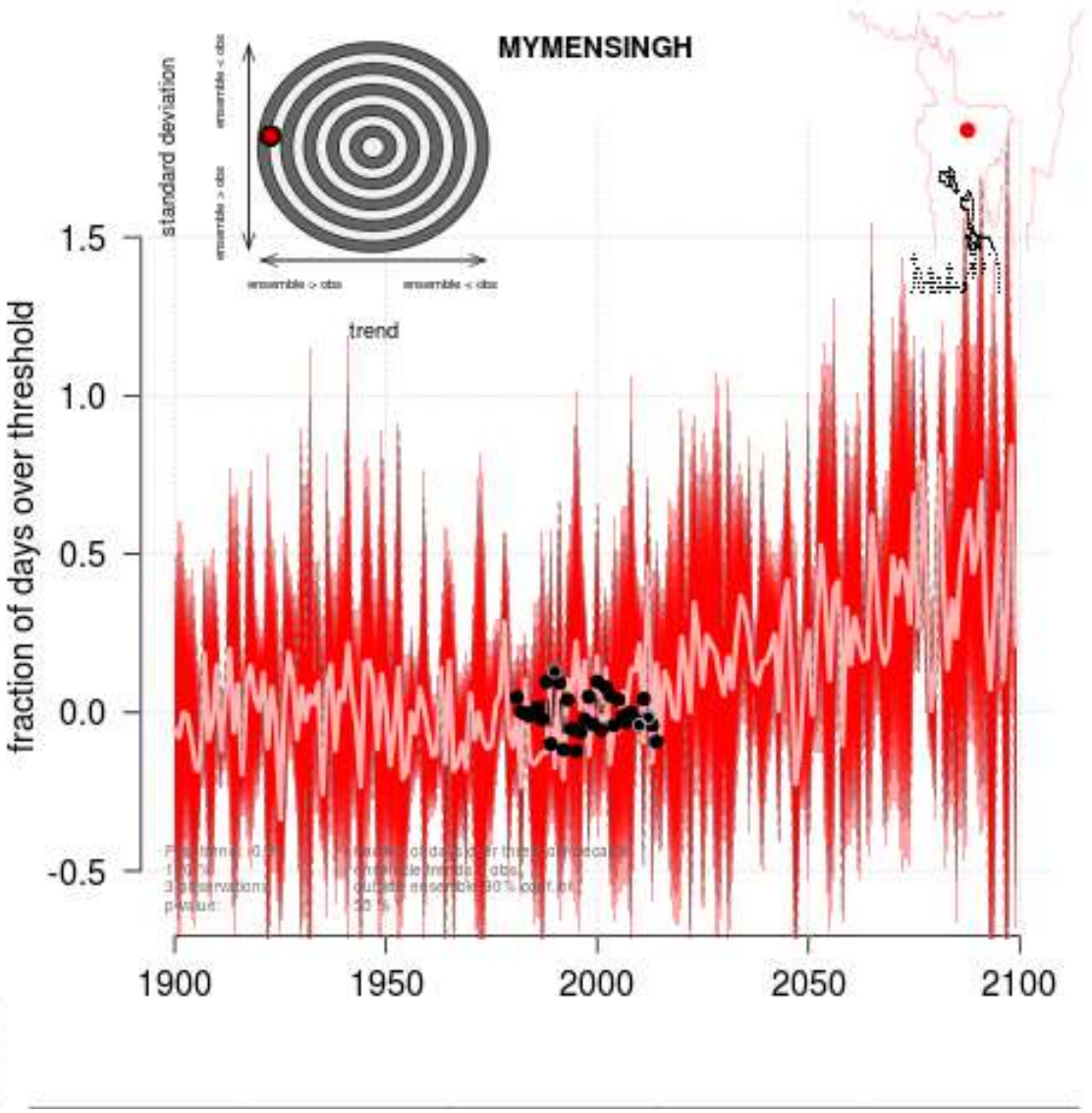

Fig.7.1.7: Wet-day frequency of pre-monsoon season over Mymensingh for different RCP8.5 scenarios run by CMIP5 experiments, respectively, relative to the period 1981-2010. The light central line is one standard deviation from the mean based on the included GCM simulations for each experiment and the gray-dashed lines mark the 90% confidence region. At the same times, wheel graph shows the probability of finding the observed number of values outside of the downscaled ensemble 90% Confidence Interval (CI), which is taken as a degree of how well fit the ensemble denotes the Interannual Variability (IAV). Values towards the top (bottom) recommend that the downscaled ensemble underestimates (overestimates) the IAV.

RCP2.6 **RCP4.5** **RCP8.5**

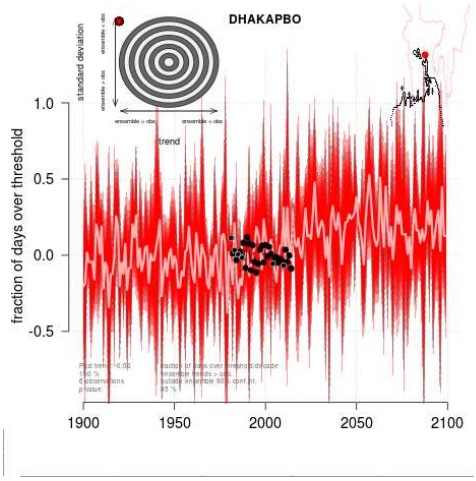

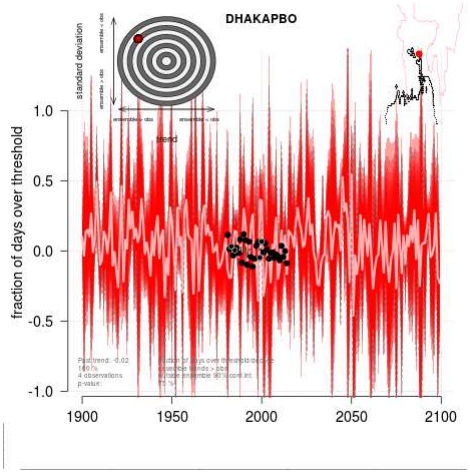

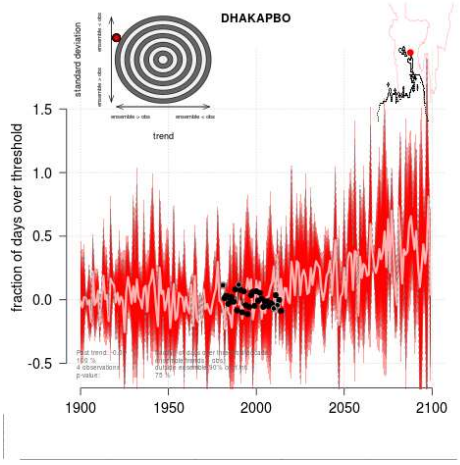

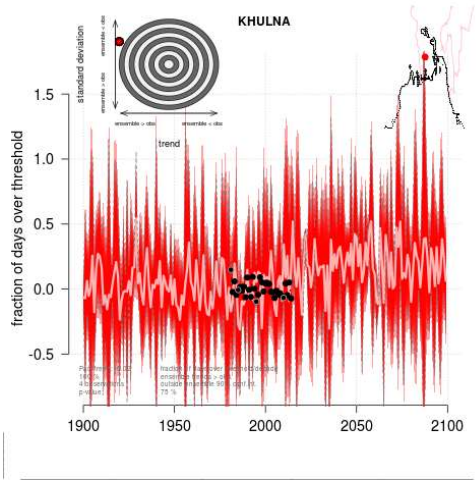

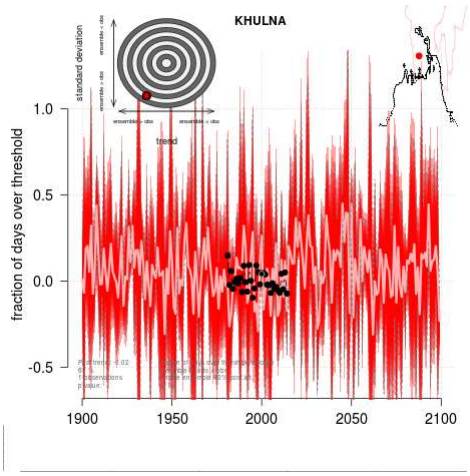

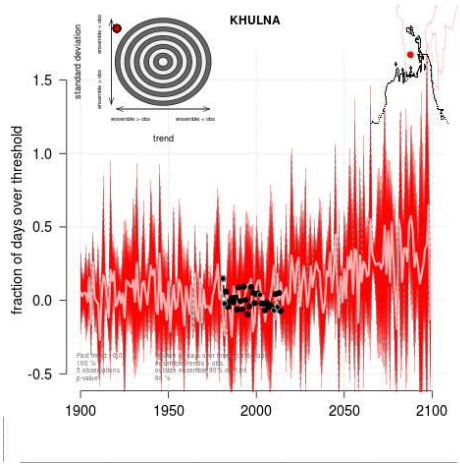

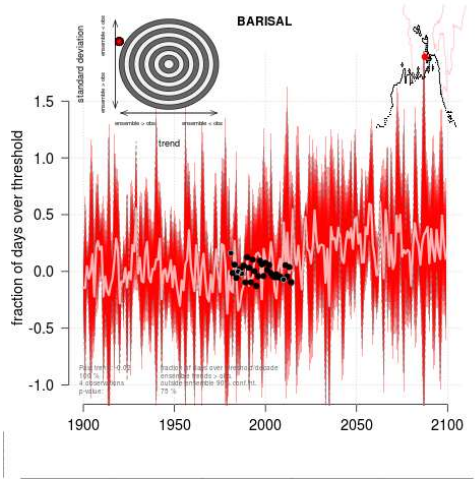

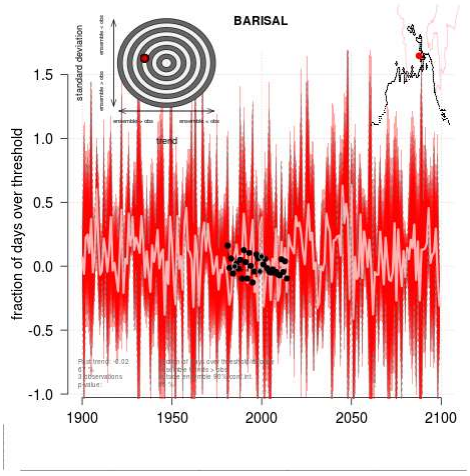

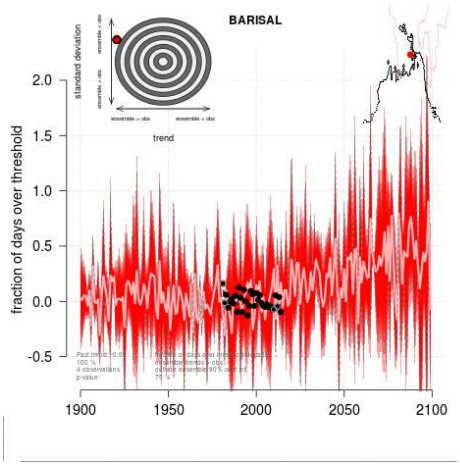

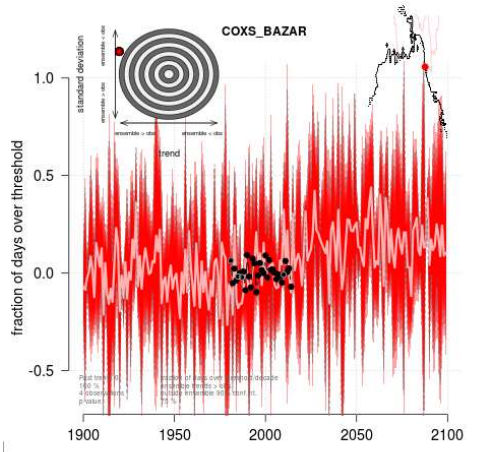
COXS_BAZAR
standard deviation
trend
fraction of days over threshold
1.0
0.5
0.0
-0.5
1900
1950
2000
2050
2100

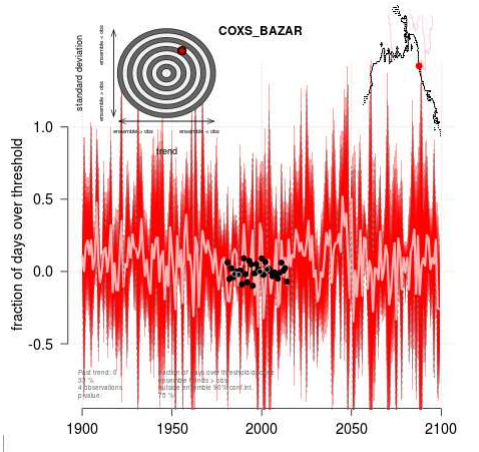
COXS_BAZAR
standard deviation
trend
fraction of days over threshold
1.0
0.5
0.0
-0.5
1900
1950
2000
2050
2100

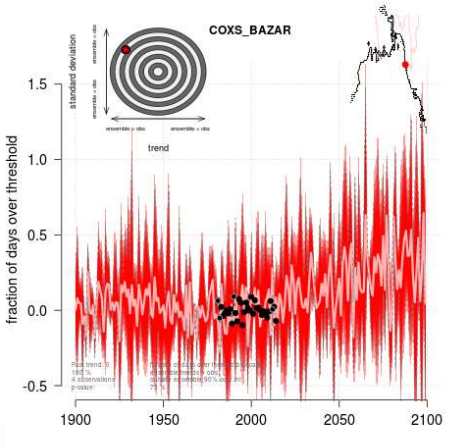
COXS_BAZAR
standard deviation
trend
fraction of days over threshold
1.5
1.0
0.5
0.0
-0.5
1900
1950
2000
2050
2100

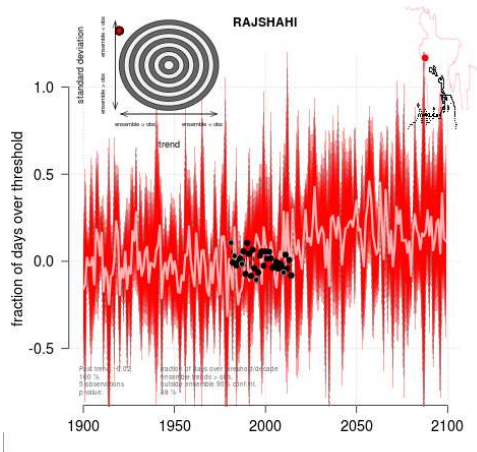
RAJSHAHI
standard deviation
trend
fraction of days over threshold
1.0
0.5
0.0
-0.5
1900
1950
2000
2050
2100

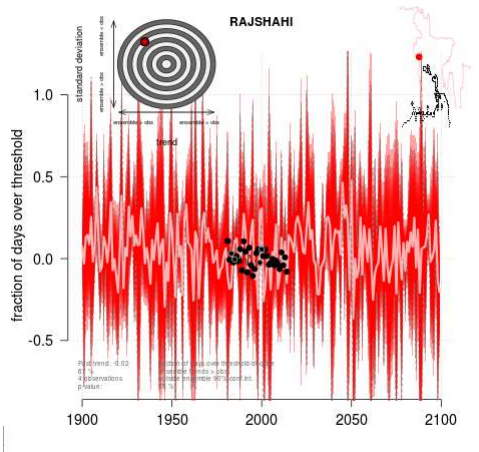
RAJSHAHI
standard deviation
trend
fraction of days over threshold
1.0
0.5
0.0
-0.5
1900
1950
2000
2050
2100

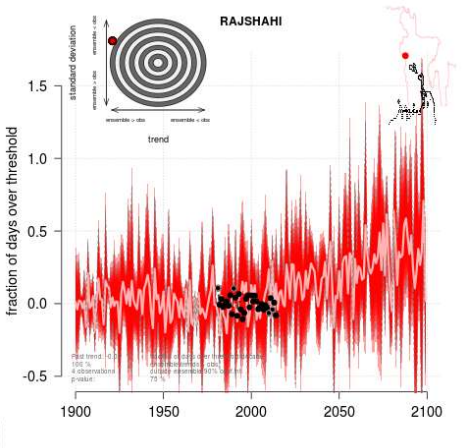
RAJSHAHI
standard deviation
trend
fraction of days over threshold
1.5
1.0
0.5
0.0
-0.5
1900
1950
2000
2050
2100

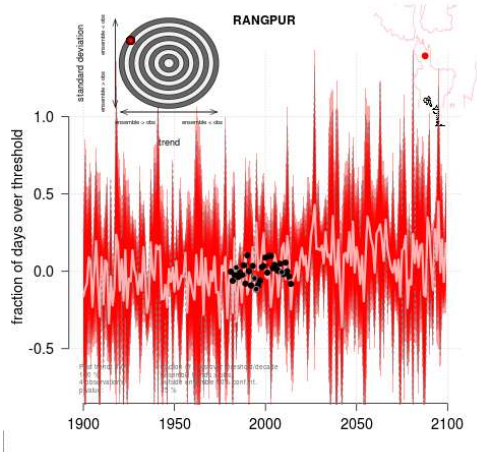
RANGPUR
standard deviation
trend
fraction of days over threshold
1.0
0.5
0.0
-0.5
1900
1950
2000
2050
2100

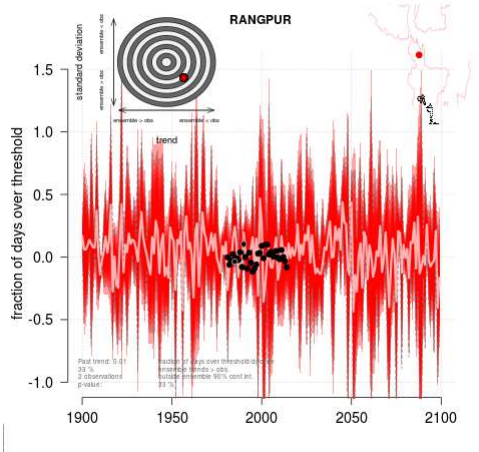
RANGPUR
standard deviation
trend
fraction of days over threshold
1.5
1.0
0.5
0.0
-0.5
-1.0
1900
1950
2000
2050
2100

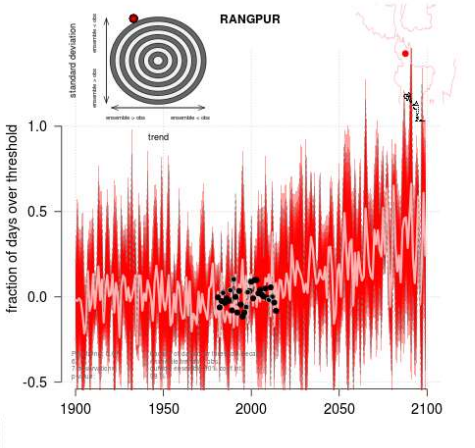
RANGPUR
standard deviation
trend
fraction of days over threshold
1.0
0.5
0.0
-0.5
1900
1950
2000
2050
2100

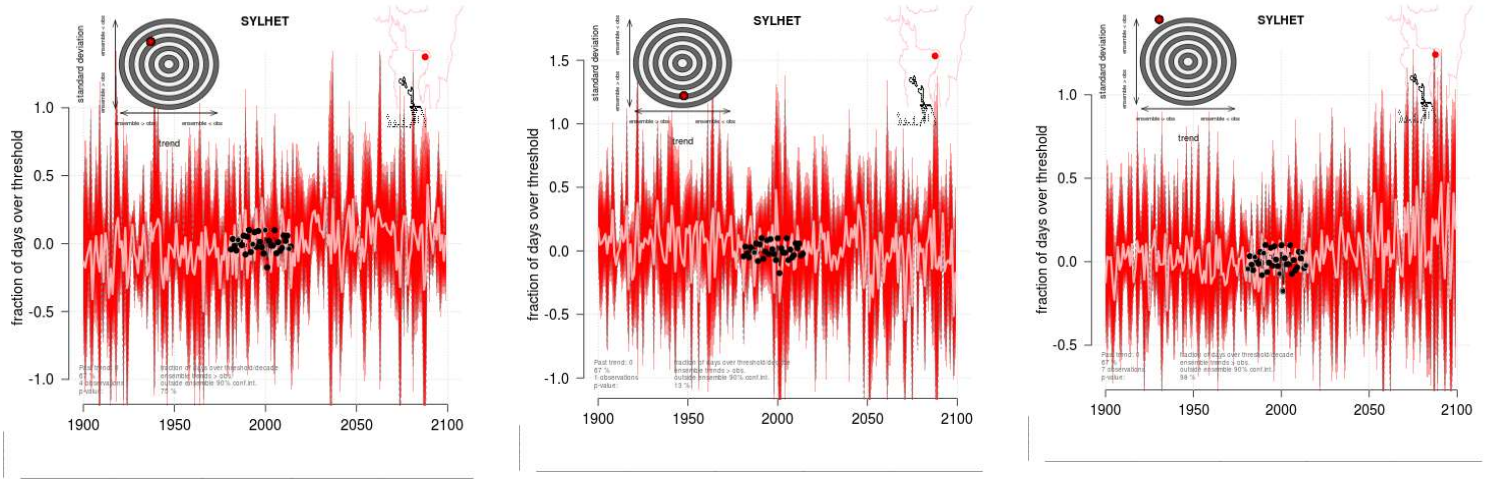

Fig.7.1.8: Wet-day frequency of pre-monsoon season over other division points change for different RCP scenarios run by CMIP5 experiments, respectively, relative to the period 1981-2010. The light central line is one standard deviation from the mean based on the included GCM simulations for each experiment and the gray-dashed lines mark the 90% confidence region. At the same times, wheel graph shows the probability of finding the observed number of values outside of the downscaled ensemble 90% Confidence Interval (CI), which is taken as a degree of how well fit the ensemble denotes the Interannual Variability (IAV). Values towards the top (bottom) recommend that the downscaled ensemble underestimates (overestimates) the IAV.

The projected anomaly of wet-day frequency of pre-monsoon season at BMD station locations relative to 1981-2010 for two periods of the near future (during 2021-2050) and the far future (during 2071-2100) are summarized in Table 7.1.1. The downscaled projections indicate a likely increase in the pre-monsoon wet-day frequency at Dhaka with a magnitude of 0.06 in the near future, and it is 0.05 in the far future for RCP2.6. For RCP4.5, the rate is 0.26 in the near future and 0.16 in the far future. The rate of wet-day frequency is positive with the magnitude of 0.07 and 0.29 in the near future and far future, respectively. For the case of the most severe scenario of RCP8.5, the likely increment of wet-days frequency is 0.07 and 0.29, respectively, in the near future and far future.

Similarly, the projected rate of wet-day frequency in the near future and far future is almost the same; it is 0.05 in the near future and 0.04 in the far future for RCP2.6 scenario. The projected rates are negative with the magnitudes of -0.04 and -0.09, respectively, in the near future and far future, respectively, at Sylhet. In this case, the highest magnitude is 0.1 in the near future at Madaripur, Barishal and Bhola, and 0.12 in the far future at Khulna and Satkhira locations. The mean projected change in pre-monsoon wet-day frequency in Bangladesh for RCP4.5 is 0.28 for the near future and 0.18 for the far future. For the severe emission scenario of RCP8.5, the near future projected frequency is not similar to the far future, and the far future frequency is 0.24, which is considerably higher in the near future (0.07). The lowest projected value for RCP8.5 is 0.04 at Bogura and Sylhet for the near future, and it is 0.14 at Sylhet for the far future and RCP4.5, the projection is 0.18 at Ishurdi & Satkira for the near future and 0.1 at Ishurdi for the far future. For RCP8.5, the highest projected value is 0.11 at Madaripur, Barishal, Bhola and Khepupara for the near future and 0.36 at Chandpur for the far future.

Table 7.1.1: Projected anomaly of wet-day frequency during pre-monsoon season compared to 1981-2010

Division	Station	Emission scenario					
	Location	RCP2.6		RCP4.5		RCP8.5	
		Near Future	Far Future	Near Future	Far Future	Near Future	Far Future
Dhaka	Dhaka	0.06	0.05	0.26	0.16	0.07	0.29
	Madaripur	0.1	0.11	0.33	0.21	0.11	0.31
	Faridpur	0.08	0.08	0.28	0.17	0.08	0.31
Mymensingh	Mymensingh	0.01	-0.03	0.3	0.18	0.06	0.3
Chattogram	Chattogram	0.04	0.02	-0.02	-0.03	-0.01	-0.13
	Cox'Bazar	0.04	0.03	0.36	0.24	0.09	0.26
	Chandpur	0.09	0.09	0.34	0.21	0.1	0.36
	Cumilla	0.03	0	0.31	0.2	0.07	0.27
	Feni	0.04	0.01	0.35	0.22	0.08	0.31
	Kutubdia	0.06	0.06	-0.03	-0.03	-0.01	-0.15
	M_Court	0.06	0.05	0.36	0.23	0.1	0.31
	Rangamati	0.03	-0.01	0.43	0.28	0.1	0.34
	Sandwip	0.04	0.04	0.29	0.19	0.08	0.24
	Sitakunda	0.02	0.01	0.39	0.26	0.1	0.27
	Teknaf	0.03	0.03	0.26	0.19	0.08	0.16
Khulna	Khulna	0.09	0.12	0.24	0.16	0.09	0.25
	Jashore	0.06	0.06	0.21	0.13	0.06	0.24
	Satkhira	0.09	0.12	0.18	0.12	0.08	0.22
Barishal	Barishal	0.1	0.1	0.34	0.22	0.11	0.34
	Patuakhali	0.08	0.1	0.31	0.21	0.1	0.27
	Bhola	0.1	0.11	0.35	0.23	0.11	0.34
	Khepupara	0.07	0.08	0.36	0.25	0.11	0.3
Rajshahi	Rajshahi	0.06	0.05	0.23	0.15	0.07	0.26
	Bogura	0.01	-0.03	0.25	0.14	0.04	0.27
	Ishurdi	0.06	0.05	0.18	0.1	0.05	0.26
Rangpur	Rangpur	-0.01	-0.05	0.28	0.18	0.05	0.24
	Dinajpur	-0.01	-0.05	0.27	0.17	0.05	0.23
Sylhet	Srimangal	0	-0.04	0.33	0.21	0.06	0.26
	Sylhet	-0.04	-0.09	0.28	0.17	0.04	0.14
Country		0.05	0.04	0.28	0.18	0.07	0.24

[Projection range indication: (i) Light red fill with red text: -0.6- to -0.2; (ii) Light red fill: -0.19 to 0; (iii) Light green: 0.001 to 0.5 and (iv) Green fill with dark green text: ≥ 0.51]

7.2 Rainfall of monsoon Season

An analysis of the common EOFs of the GCM simulations is performed to evaluate the goodness of fit of the GCM output with respect to observation-based data. The residuals from the downscaled data are verified against adequacy. Screening of predictors and predictor domains is conducted using corrected 03 (three) GCMs simulations and various rainfall stations, and the best-correlated predictors and predictand are selected. These are CanESM2.r1, CanESM2.r2, CanESM2.r3 (where r means model realization). The cross-validated correlation between the wet-day frequency's first principal component (PC1) and the corresponding PC1 estimated based on empirical-statistical downscaling is 0.56 in Fig. 7.2.1.

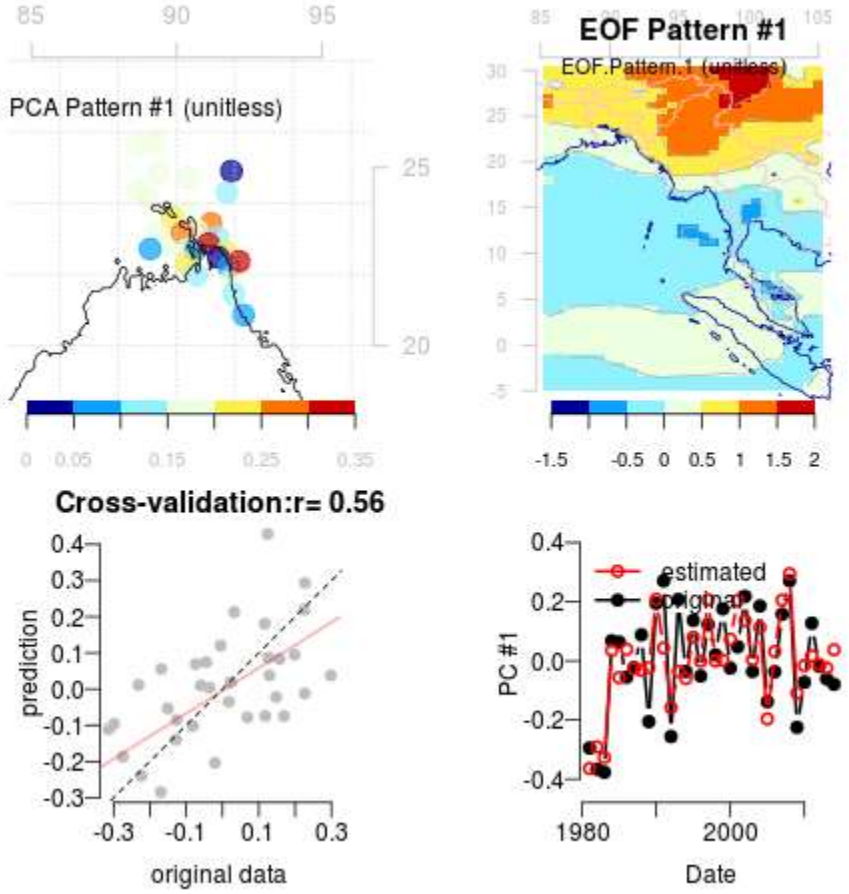

Fig.7.2.1: Downscaled means the wet-day frequency of the monsoon season based on the GCM and using PCA for downscaling a group of stations simultaneously. The top-left panel illustrates the spatial pattern connected with the leading principal component (PC1) of the predictand. The top-right panel express the leading spatial pattern of the predictor. The lower left panel indicates a cross-validation comparing the original PC1 of the predictand and the corresponding estimated values obtained by ESD. The lower-right panel indicates time series of the estimated and original PC1 of the predictand**.**

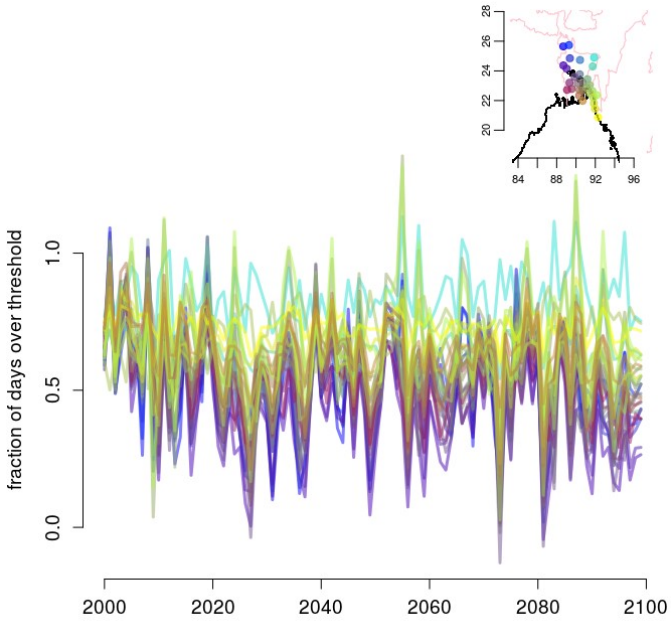

Fig. 7.2.2: Wet-day frequency of monsoon season over station points change for RCP2.6 scenarios run by CMIP5 experiments, respectively, relative to the period 1981-2010.

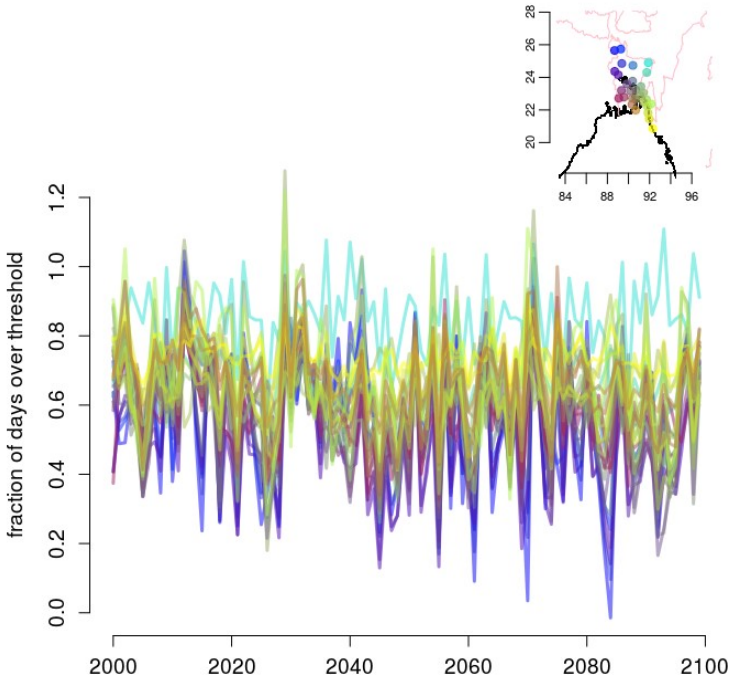

Fig.7.2.3: Wet-day frequency of monsoon season over station points change for RCP4.5 scenarios run by CMIP5 experiments, respectively, relative to the period 1981-2010.

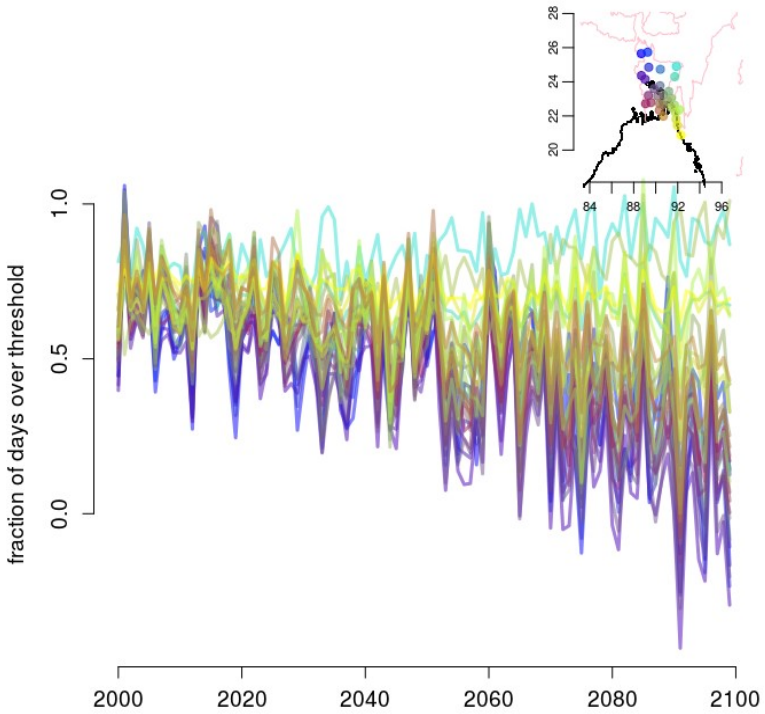

Fig.7.2.4: Wet-day frequency of monsoon season over station points change for RCP8.5 scenarios run by CMIP5 experiments, respectively, relative to the period 1981-2010.

Figs. 7.2.2-7.2.4 show downscaled wet-day frequency of monsoon season at station points for different RCPs (RCP2.6, RCP4.5 and RCP8.5) in Bangladesh. The threshold value is considered one millimeter of rain per day to define wet-day frequency. So, the fraction of days over this threshold estimates the wet-day frequency relative to the period of 1981-2010 for different RCPs. The magnitude of wet-day frequency is higher over the northeastern part of the country and lower over the northwestern part of Bangladesh for RCP2.6 and RCP4.5. However, there is no trend over the northeastern part of the country for RCP8.5 (Fig. 7.1.4). On the other hand, the wet-day frequency of the northwestern part of the country is sharply decreasing, and the area is likely to face less rainfall in far future.

Fig. 7.2.5 shows downscaled climate projections of wet-day frequency of monsoon season at the divisional place in Bangladesh for different RCPs (RCP2.6, RCP4.5 and RCP8.5). The wheel graph shows the probability of finding the observed number of values outside of the downscaled ensemble at 90% CI, which is taken as a degree of how the ensemble represents well the interannual variability in each station. Projections of all stations are well estimated the interannual variability for all RCPs except Barisal, Mymensingh and Chattogram for RCP2.6. Barisal, Mymensingh and Chattogram are underestimated interannual viabilities for RCP2.6, but it is underestimated at Sylhet for all RCPs.

RCP2.6 **RCP4.5** **RCP8.5**

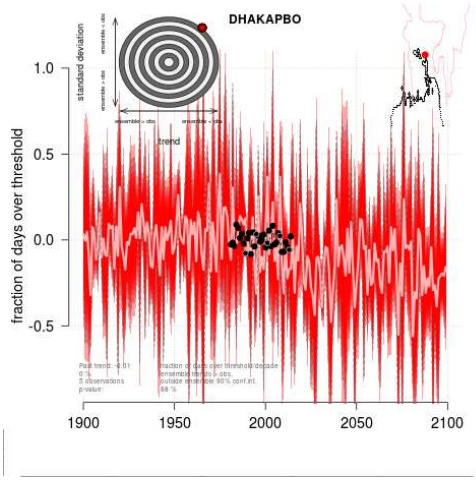

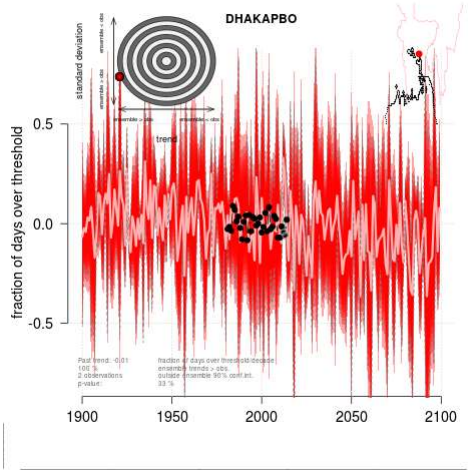

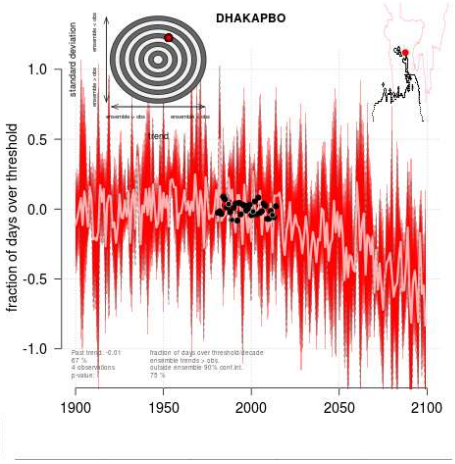

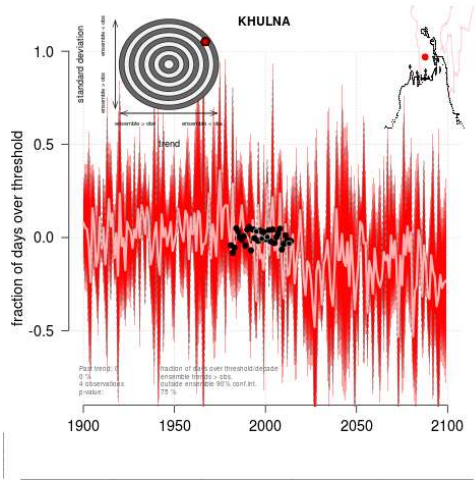

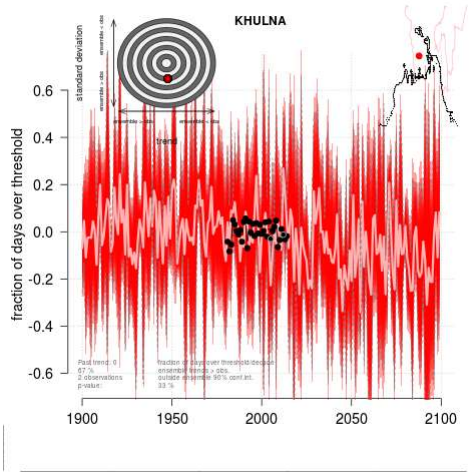

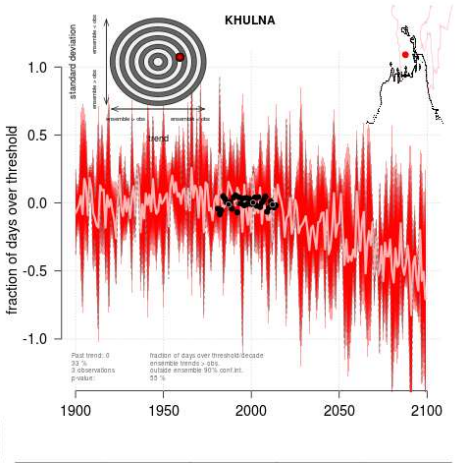

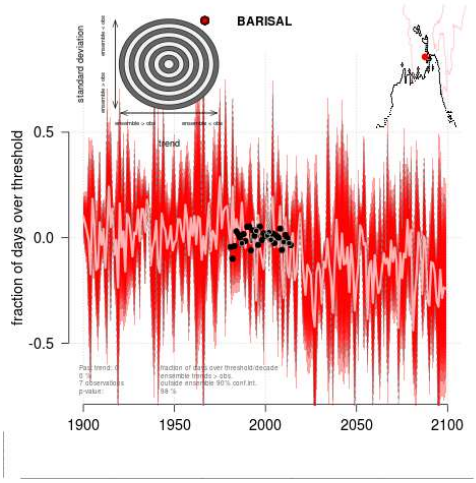

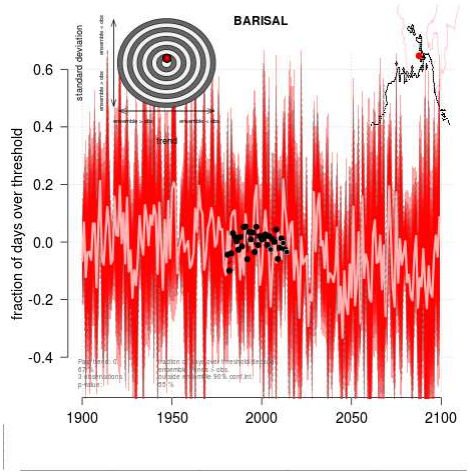

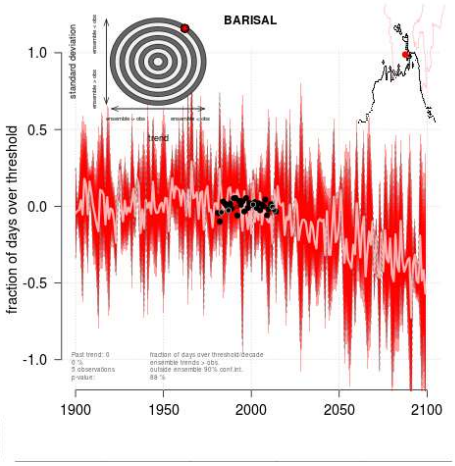

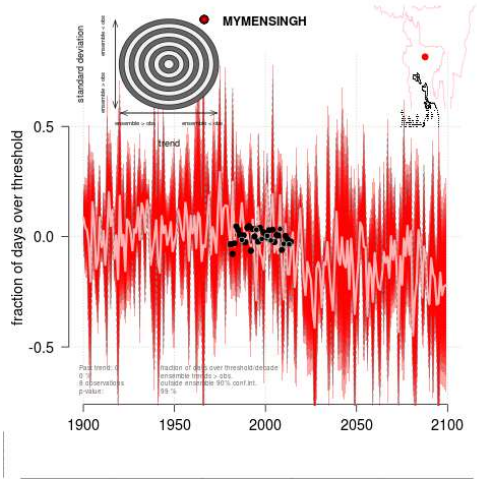
MYMENSINGH
standard deviation
trend
fraction of days over threshold
1900
1950
2000
2050
2100

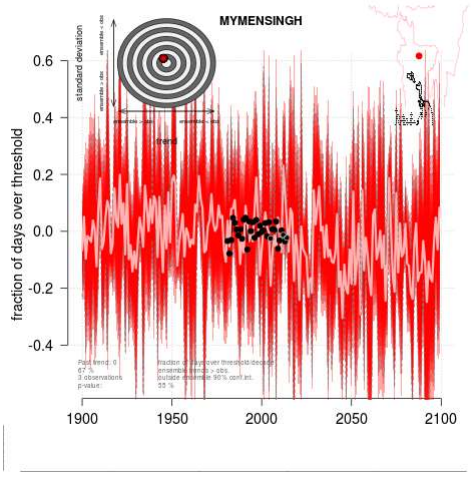
MYMENSINGH
standard deviation
trend
fraction of days over threshold
1900
1950
2000
2050
2100

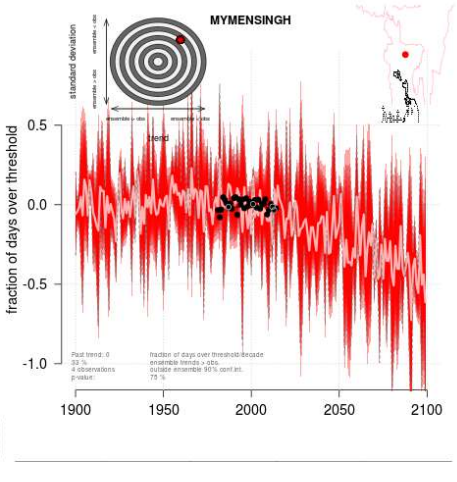
MYMENSINGH
standard deviation
trend
fraction of days over threshold
1900
1950
2000
2050
2100

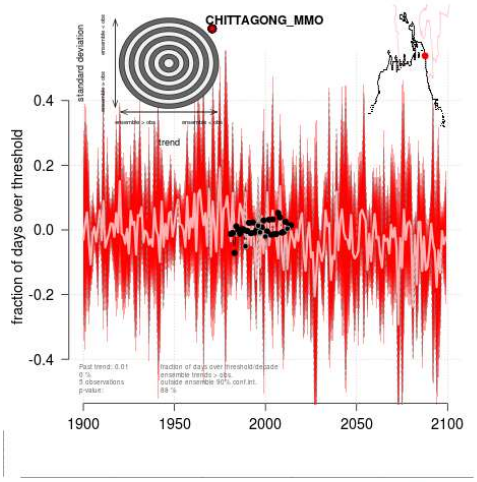
CHITTAGONG_MMO
standard deviation
trend
fraction of days over threshold
1900
1950
2000
2050
2100

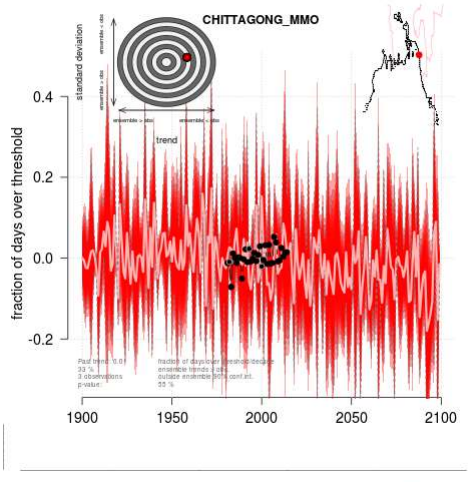
CHITTAGONG_MMO
standard deviation
trend
fraction of days over threshold
1900
1950
2000
2050
2100

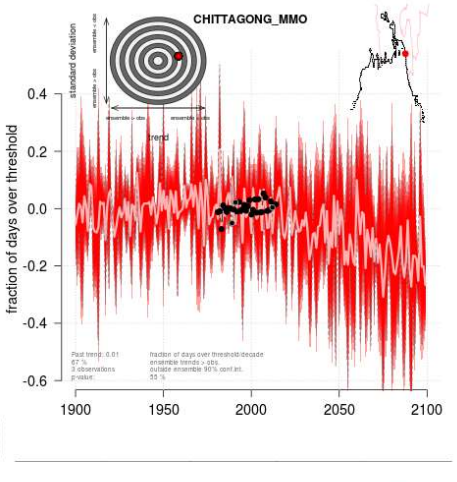
CHITTAGONG_MMO
standard deviation
trend
fraction of days over threshold
1900
1950
2000
2050
2100

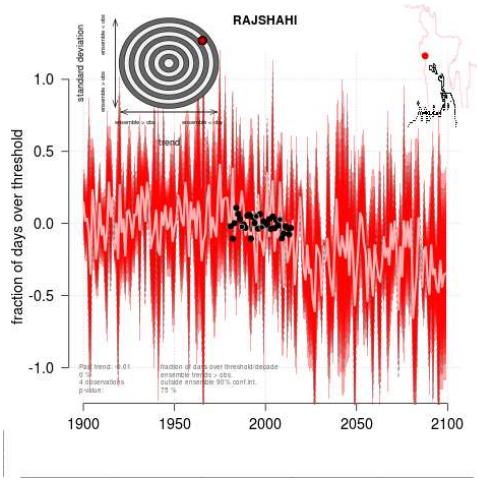
RAJSHAHI
standard deviation
trend
fraction of days over threshold
1900
1950
2000
2050
2100

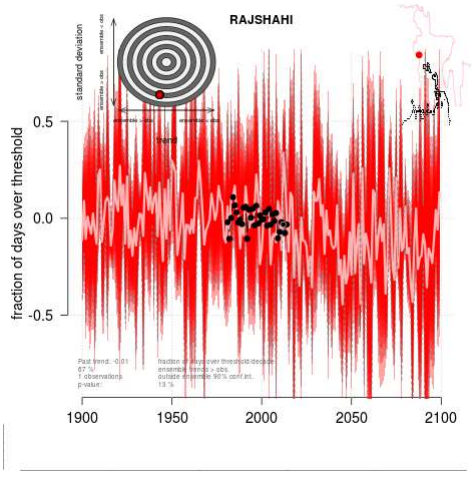
RAJSHAHI
standard deviation
trend
fraction of days over threshold
1900
1950
2000
2050
2100

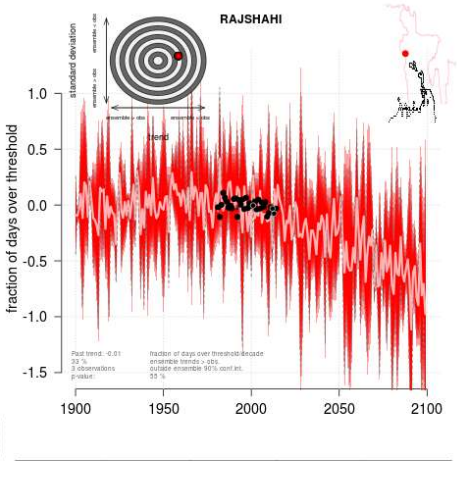
RAJSHAHI
standard deviation
trend
fraction of days over threshold
1900
1950
2000
2050
2100

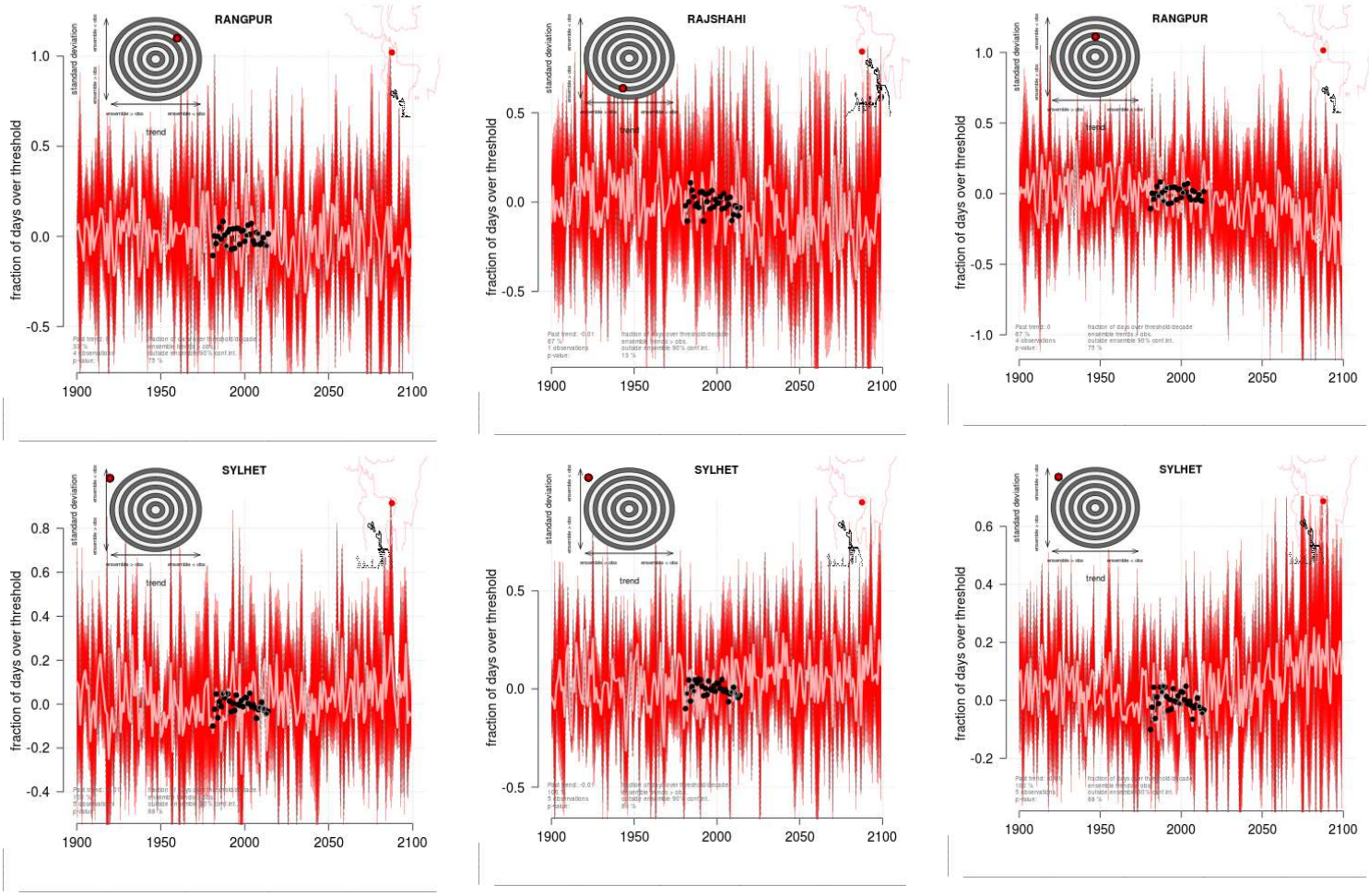

Fig.7.2.**5:** Wet-day frequency of monsoon season over some special points change for different RCP scenarios run by CMIP5 experiments, respectively, relative to the period 1981-2010. The light central line is one standard deviation from the mean based on the included GCM simulations for each experiment and the gray-dashed lines mark the 90% confidence region. At the same times, wheel graph shows the probability of finding the observed number of values outside of the downscaled ensemble 90% Confidence Interval (CI), which is taken as a degree of how well fit the ensemble denotes the Interannual Variability (IAV). Values towards the top (bottom) recommend that the downscaled ensemble underestimates (overestimates) the IAV.

The projected anomaly of the wet-day frequency of the monsoon season compared to the base period of 1981-2010 is summarized in Table 7.2.1, which includes the average change in the wet-day frequency of the monsoon season relative to 1981-2010 for two periods of the near future (2021-2050) and the far future (2071-2100). The downscaled projections indicate a likely decrease in the summer wet-day frequency at Dhaka of 0.05 for the near future, and it is 0.03 for the far future with RCP2.6. For RCP4.5, the likely rate is -0.03 in the near future and -0.07 in the far future. For the case of the most severe scenario of RCP8.5, it is likely -0.03 and -0.4 for the near and far future, respectively.

For RCP2.6, the projected wet-day frequency of the near future is the same as the far future, which is 0.03 over the country. In this case, the lowest magnitude is -0.06 at Satkhira in both the near and far future. The highest value of 0.13 is in the near future, and it is 0.18 in the far future, which are recognized both at Maijdi Court and Noakhali. The mean projected change in monsoon wet-day frequency for Bangladesh for RCP4.5 is -0.07 for the near and far future. For the high emission scenario of RCP8.5, the near future rate is -0;04, and for the far future is -0.24. The lowest projected value for RCP8.5 is -0.13, recognized at Rajshahi in the near future, and for the future, it is -0.54, which is identified at Faridpur in the far future. For the scenario of RCP4.5 recognized lowest value is -0.19 both at Jashore & Faridpur for the near future, and it will be the same at Faridpur in the far future. The highest value of 0.1 is captured at Rangpur, Dinajpur and Sylhet in the near future, and the same is at Sylhet in the far future. For RCP8.5, the highest projected value is 0.21 at Satkhira in the near future and 1.51 at Madaripur in the far future.

Table 7.2.1: Projected wet-day frequency anomaly of monsoon season compared to 1981-2010

Division	Station	Emission scenario					
	Location	RCP2.6		RCP4.5		RCP8.5	
		Near Future	Far Future	Near Future	Far Future	Near Future	Far Future
Dhaka	Dhaka	0.05	0.03	-0.03	-0.07	-0.03	-0.4
	Madaripur	0.03	0.01	-0.15	-0.14	-0.07	1.51
	Faridpur	0.02	-0.03	-0.19	-0.19	-0.11	-0.54
Mymensingh	Mymensingh	0.01	0	-0.1	-0.1	-0.07	-0.32
Chattogram	Chattogram	0.04	0.02	-0.02	-0.03	-0.01	-0.13
	Cox'Bazar	0.01	0.02	-0.06	-0.03	-0.01	-0.05
	Chandpur	0.04	-0.03	-0.13	-0.15	-0.08	-0.43
	Cumilla	0.06	0.07	-0.06	-0.05	-0.03	-0.22
	Feni	0	-0.03	-0.13	-0.12	-0.04	-0.02
	Kutubdia	0.06	0.06	-0.03	-0.03	-0.01	-0.15
	M_Court	0.13	0.18	0.05	0.05	0.03	-0.07
	Rangamati	0.11	0.15	0.01	0.04	0.05	0.06
	Sandwip	0.03	0.04	0.04	0.06	0.06	0.23
	Sitakunda	0.06	0.03	-0.1	-0.11	-0.05	-0.34
	Teknaf	0	0	-0.06	-0.04	-0.01	-0.06
Khulna	Khulna	0.02	0.01	-0.11	-0.11	-0.07	-0.36
	Jashore	-0.01	-0.05	-0.19	-0.18	-0.1	-0.42
	Satkhira	-0.06	-0.06	-0.17	-0.14	0.21	-0.43
Barishal	Barishal	0	0	-0.12	-0.1	-0.07	-0.3

Division	Station	Emission scenario					
	Location	RCP2.6		RCP4.5		RCP8.5	
		Near Future	Far Future	Near Future	Far Future	Near Future	Far Future
	Patuakhali	0.01	0	-0.18	-0.14	-0.07	-0.33
	Bhola	-0.01	-0.04	-0.1	-0.11	-0.07	-0.3
	Khepupara	0	0	-0.09	-0.08	-0.04	-0.19
Rajshahi	Rajshahi	-0.02	-0.03	-0.17	-0.16	-0.13	-0.53
	Bogura	0.05	0.05	-0.03	-0.06	-0.08	-0.43
	Ishurdi	0.01	0.01	-0.11	-0.1	-0.08	-0.37
Rangpur	Rangpur	0.09	0.12	0.1	0.06	0	-0.15
	Dinajpur	0.09	0.12	0.1	0.05	-0.04	-0.3
Sylhet	Srimangal	0.02	0.04	-0.02	-0.01	0.01	0.01
	Sylhet	0.02	0.08	0.1	0.1	0.03	0.12
Country		0.03	0.03	-0.07	-0.07	-0.04	-0.24

[Projection range indication: (i) Light red fill with red text: -0.6- to -0.2; (ii) Light red fill: -0.19 to 0; (iii) Light green: 0.001 to 0.5 and (iv) Green fill with dark green text: ≥ 0.51]

7.3 Rainfall of Post-monsoon Season

An analysis of the common EOFs of the GCM simulations is performed to evaluate the goodness of fit of the GCM output with respect to observation data. The residuals from the downscaled data are adequately verified. Screening of predictors and predictor domains is conducted using corrected 03 (three) GCMs simulations with rainfall data, and the best-correlated predictors and predictand are selected finally. This CanESM2.r2, CanESM2.r3, CanESM2.r4 (where r means model realization). The estimated cross-validated correlation between the first principal component (PC1) of the wet-day frequency and the corresponding PC1 based on empirical-statistical downscaling is 0.56 as in Fig. 7.3.1.

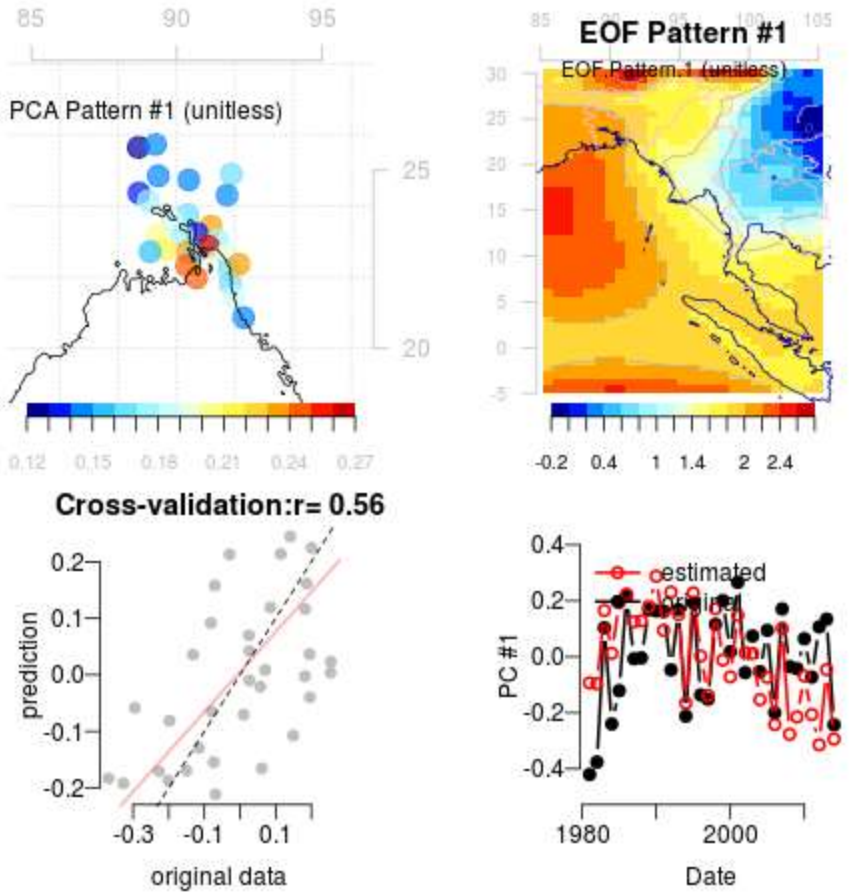

Fig.7.3.1: Downscaled means the wet-day frequency of the post-monsoon season based on the GCM and using PCA for downscaling a group of stations simultaneously. The top-left panel illustrates the spatial pattern connected with the leading principal component (PC1) of the predictand. The top-right panel express the leading spatial pattern of the predictor. The lower left panel indicates a cross-validation comparing the original PC1 of the predictand and the corresponding estimated values obtained by ESD. The lower-right panel indicates time series of the estimated and original PC1 of the predictand.

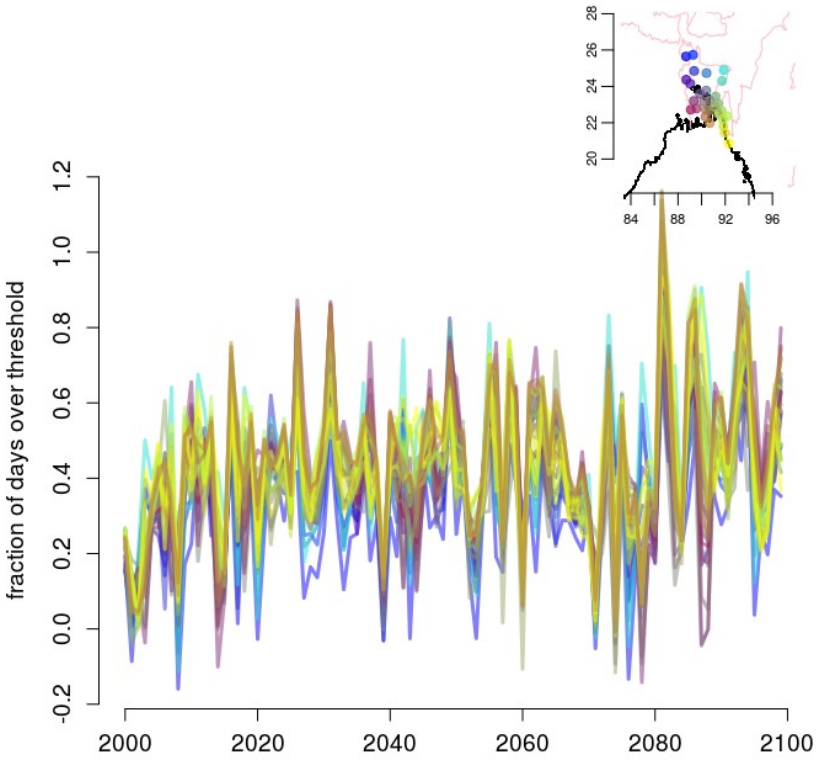

Fig. 7.3.2: Wet-day frequency of post-monsoon season over station points change for RCP2.6 scenarios run by CMIP5 experiments, respectively, relative to the period 1981-2010.

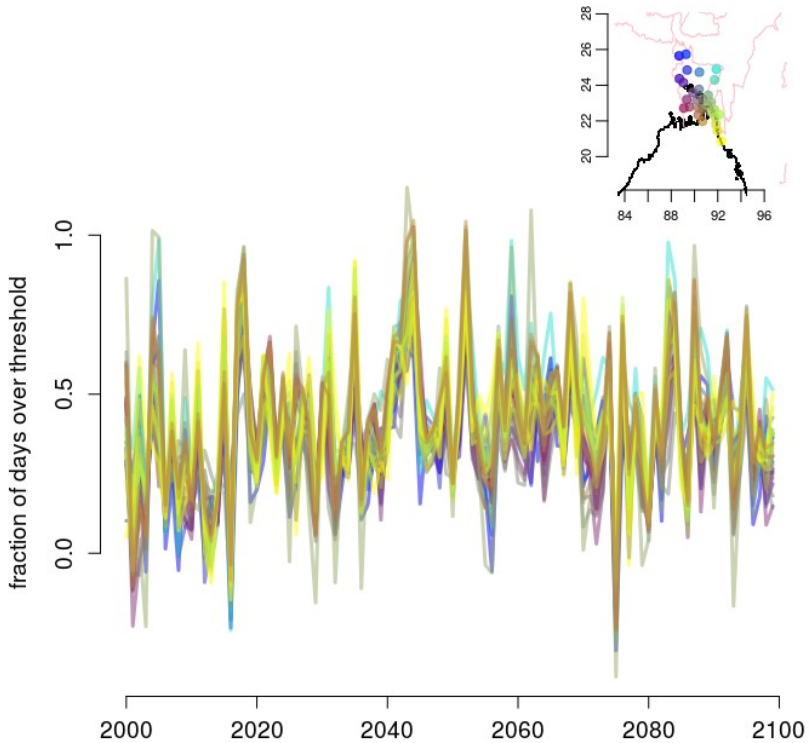

Fig.7.3.3: Wet-day frequency of post-monsoon season over station points change for RCP4.5 scenarios run by CMIP5 experiments, respectively, relative to the period 1981-2010.

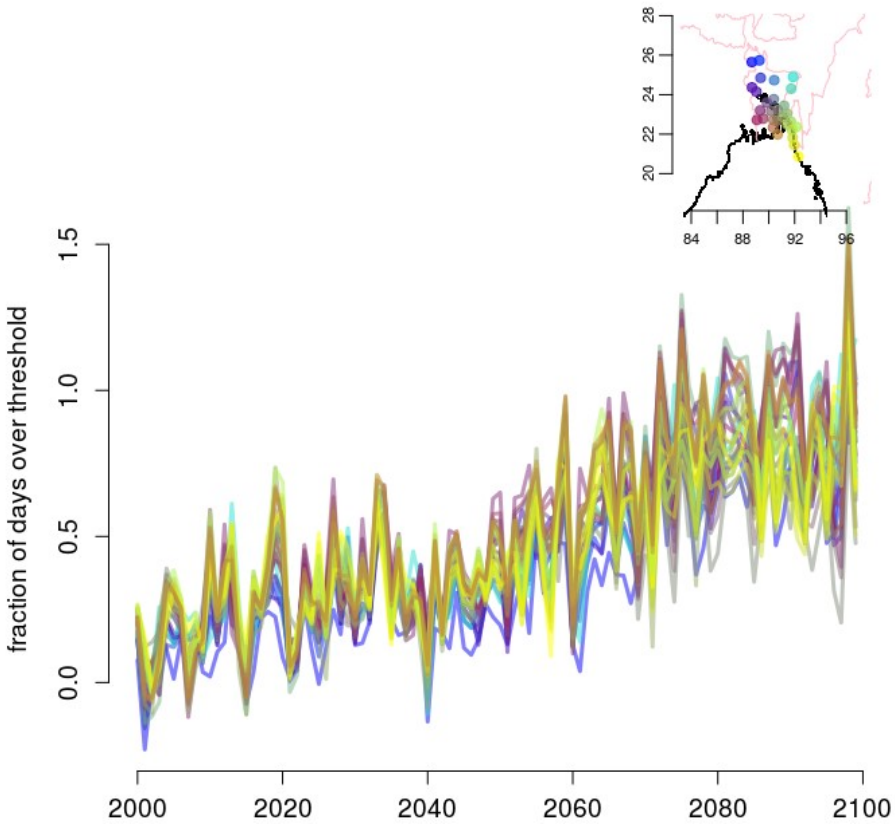

Fig.7.3.4: Wet-day frequency of post-monsoon season over station points change for RCP8.5 scenarios run by CMIP5 experiments, respectively, relative to the period 1981-2010.

Figs. 7.3.2-7.3.4 displays the downscaled wet-day frequency of post-monsoon season over station points for different RCPs (RCP2.6, RCP4.5 and RCP8.5) in Bangladesh. The threshold value is considered one millimeter of rain per day, called wet-day frequency. So, the fraction of days over the threshold express to estimate the wet-day frequency relative to the period 1981-2010 for different RCPs. This value of the southern part of the country is more prominent than in other parts of Bangladesh. There is no appreciable change based on periods (Fig.7.3.2 and Fig.7.3.3). But this value is gradually increased over the country up to 2100 for RCP8.5 (Fig.7.3.4), and the wet day frequency of the southern part is always higher than the rest part of the county.

Fig. 7.3.5 shows downscaled climate projections of wet-day frequency of post-monsoon season over the divisional place in Bangladesh for different RCPs (RCP2.6, RCP4.5 and RCP8.5), and the wheel graph shows the probability of finding the observed number of values outside of the downscaled ensemble at 90% confidence level, which is taken as a measure of how well the ensemble represents the interannual variability in each station. Projections of all stations are well estimated the interannual variability for all RCPs except some RCPs. But interannual variability is underestimated at Sylhet for RCP2.6, at Khulna and Chattogram for RCP4.5 and at Barisal and Rangpur for RCP8.5.

RCP2.6 **RCP4.5** **RCP8.5**

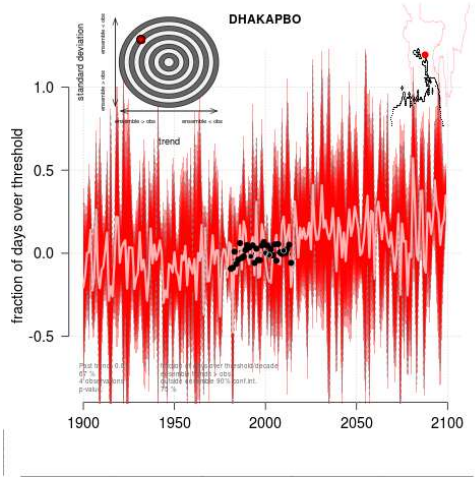

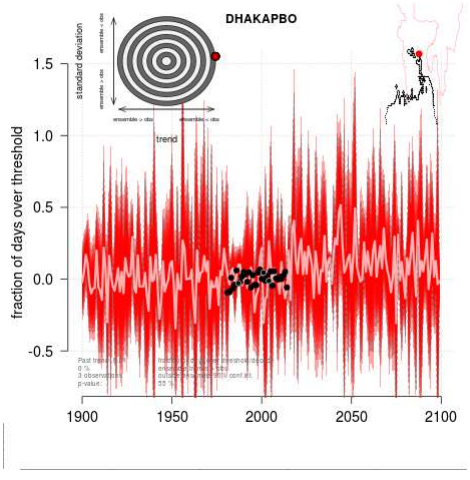

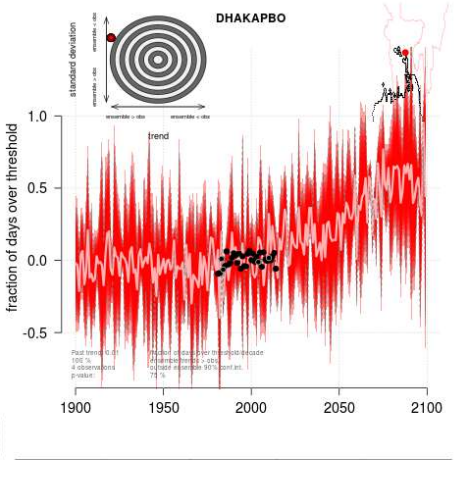

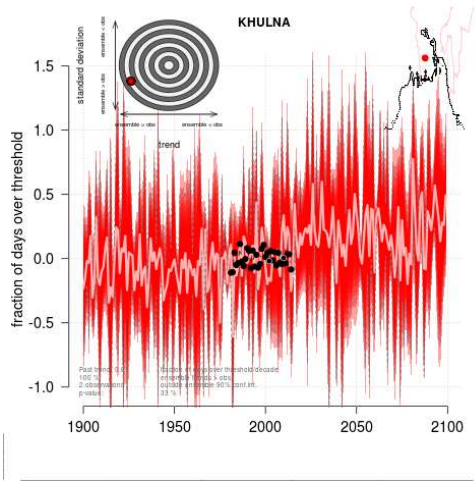

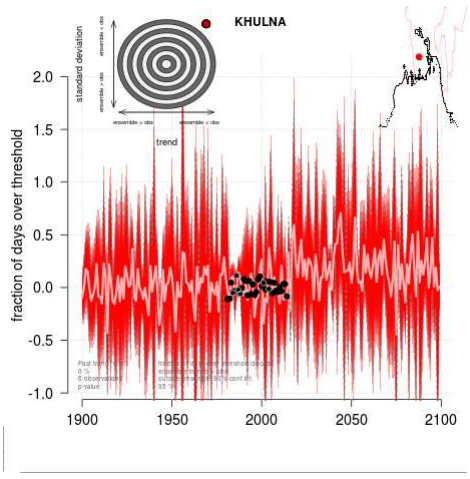

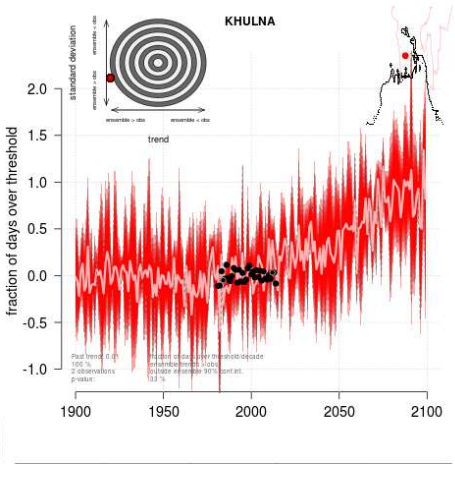

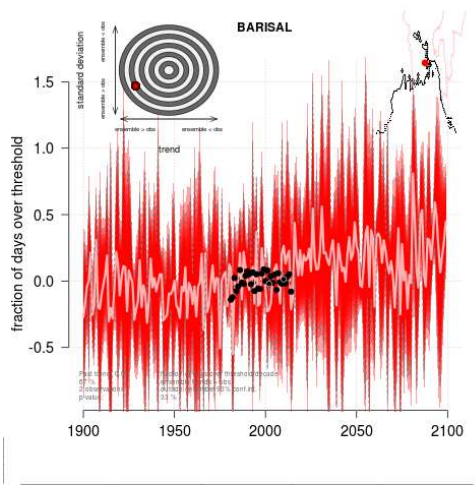

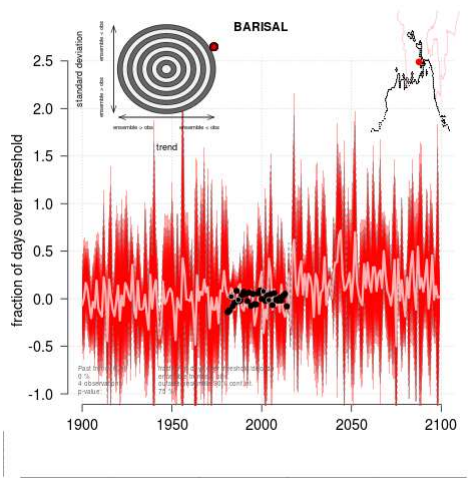

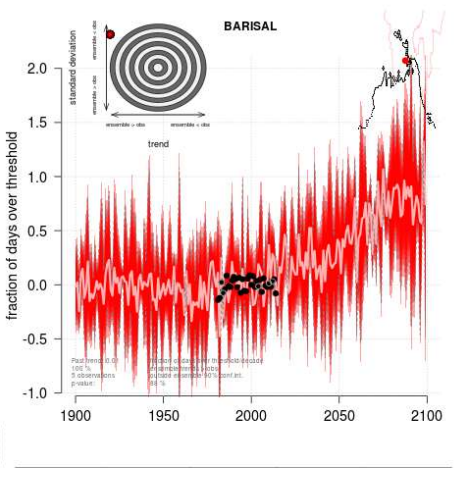

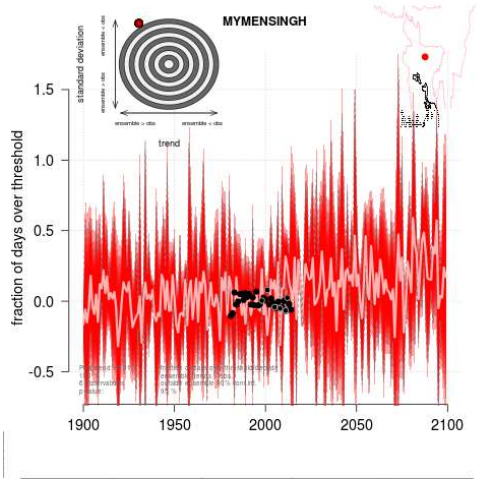
MYMENSINGH
standard deviation
trend
fraction of days over threshold
1900
1950
2000
2050
2100

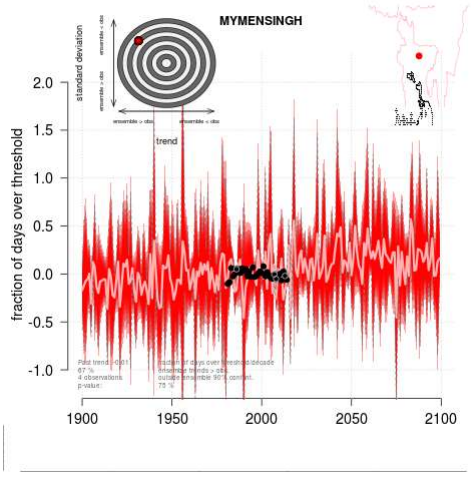
MYMENSINGH
standard deviation
trend
fraction of days over threshold
1900
1950
2000
2050
2100

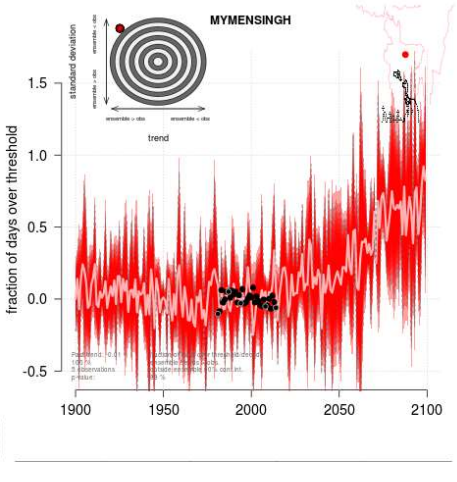
MYMENSINGH
standard deviation
trend
fraction of days over threshold
1900
1950
2000
2050
2100

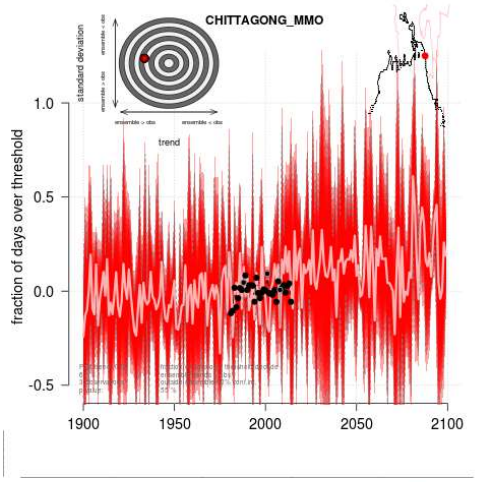
CHITTAGONG_MMO
standard deviation
trend
fraction of days over threshold
1900
1950
2000
2050
2100

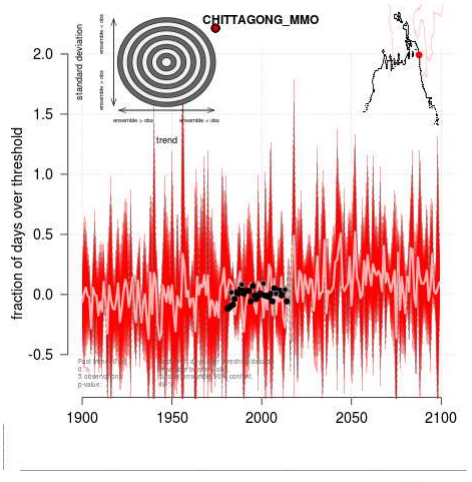
CHITTAGONG_MMO
standard deviation
trend
fraction of days over threshold
1900
1950
2000
2050
2100

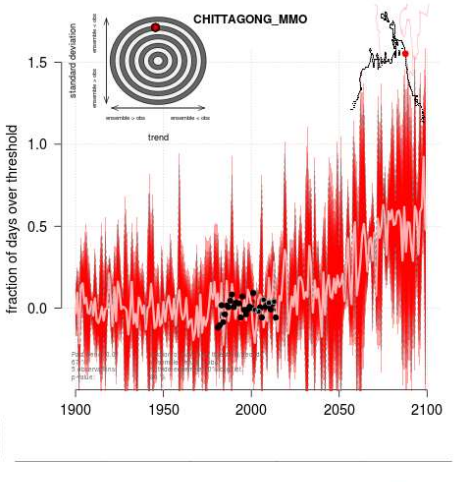
CHITTAGONG_MMO
standard deviation
trend
fraction of days over threshold
1900
1950
2000
2050
2100

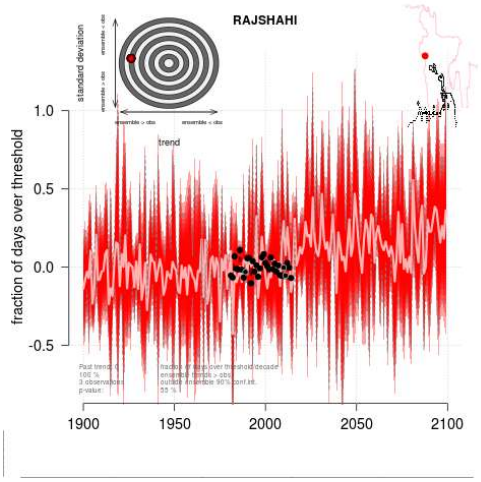
RAJSHAHI
standard deviation
trend
fraction of days over threshold
1900
1950
2000
2050
2100

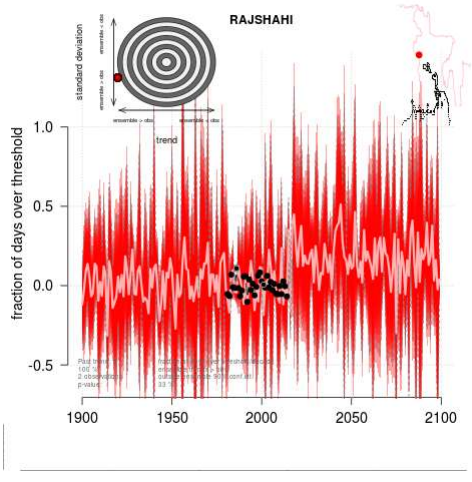
RAJSHAHI
standard deviation
trend
fraction of days over threshold
1900
1950
2000
2050
2100

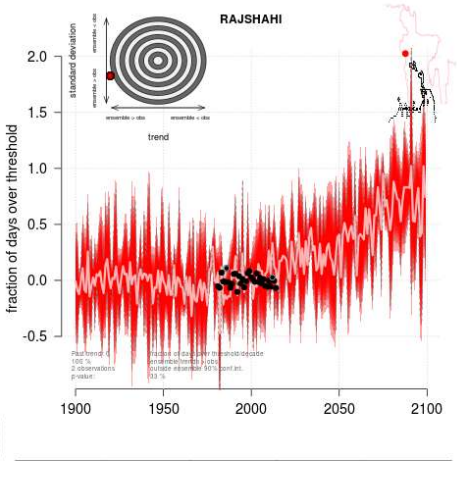
RAJSHAHI
standard deviation
trend
fraction of days over threshold
1900
1950
2000
2050
2100

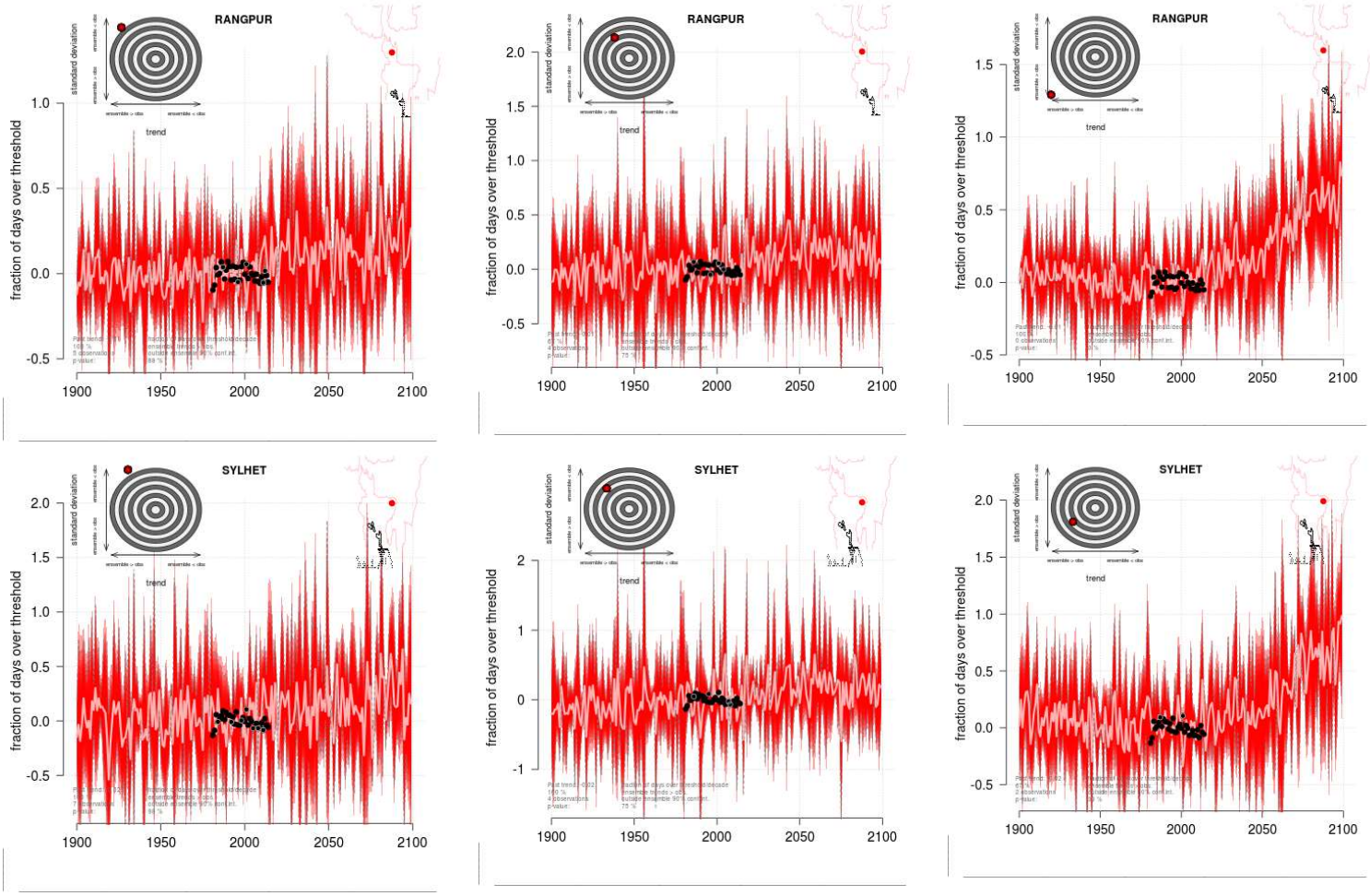

Fig.7.3.5: Wet-day frequency of post-monsoon season over divisional points change for different RCP scenarios run by CMIP5 experiments, respectively, relative to the period 1981-2010. The light central line is one standard deviation from the mean based on the included GCM simulations for each experiment and the gray-dashed lines mark the 90% confidence region. At the same times, wheel graph shows the probability of finding the observed number of values outside of the downscaled ensemble 90% Confidence Interval (CI), which is taken as a degree of how well fit the ensemble denotes the Interannual Variability (IAV). Values towards the top (bottom) recommend that the downscaled ensemble underestimates (overestimates) the IAV.

The projected anomaly of wet-day frequency of post-monsoon season compared to the base period of 1981-2010 is summarized in Table 7.3.1. Table 7.3.1 includes the average change in the wet-day frequency of the post-monsoon season relative to 1981-2010 for two periods of the near future (2021-2050) and far future (2071-2100). The downscaled projections indicate a decreasing trend in the post-monsoon wet-day frequency at Dhaka by 0.01 in the near future, and it is about zero in the far future with RCP2.6. For RCP4.5, the likely trends are 0.17 and 0.11 in the near future and far future, respectively. The most severe scenario of RCP8.5 is suggested the likely increasing trends of -0.03 and 0.34 in the near future and far future, respectively.

For RCP2.6, the likely trend of projected wet-day frequency in the near future is 0.02, and in the far future, it is 0.05 over the country, but the lowest value of it -0.03 is at Rajshahi, and the highest value of 0.08 is at Teknaf in the near future. For the same RCP, the lowest trend of projected wet-

day frequency is -0.06 at Chandpur, and the highest value of it is 0.14 at Teknaf. The mean projected trend of wet-day frequency in post-monsoon season for Bangladesh for RCP4.5 is 0.20 for the near future, and it is 0.16 for the far future. The lowest value of 0.09 is at Kutubdia, and the highest value of 0.32 is recognized at Faridpur, Bogura, and Cumilla in the near future. For the same RCP, the lowest value of 0.06 is at Maijdi Court (Noakhali), Kutubdia and Chandpur, and the highest value of 0.30 is at Bogura at the far future. For the high emission scenario of RCP8.5, the near future estimated frequency is not similar to the far future, and the far future likely frequency is 0.47, which is considerably higher than the near future of -0.01. The lowest projected value for RCP8.5 is -0.08 at Maijdi Court (Noakahali), and Rangamati and the highest projected wet-day frequency rate is 0.08 at Bogura in the near future. For RCP8.5, the highest projected value is 0.70, indicated at Bogura, but the lowest value of 0.19 is at Chandpur in the case of the far future.

Table.7.3.1: Projected wet-day frequency anomaly of post-monsoon season based on 1981-2010

Division	Station	Emission scenario					
	Location	RCP2.6		RCP4.5		RCP8.5	
		Near Future	Far Future	Near Future	Far Future	Near Future	Far Future
Dhaka	Dhaka	0.01	0	0.17	0.11	-0.03	0.34
	Madaripur	0	-0.02	0.14	0.07	-0.06	0.27
	Faridpur	-0.01	0	0.32	0.26	0.03	0.62
Mymensingh	Mymensingh	0.02	0.1	0.2	0.2	0.05	0.55
Chattogram	Chattogram	0.05	0.09	0.12	0.1	-0.04	0.37
	Cox'Bazar	0.07	0.12	0.13	0.11	-0.06	0.41
	Chandpur	-0.02	-0.06	0.13	0.06	-0.04	0.19
	Cumilla	0.02	0.05	0.32	0.26	0	0.69
	Feni	0.05	0.1	0.13	0.11	-0.03	0.4
	Kutubdia	0.05	0.07	0.09	0.06	-0.06	0.28
	M_Court	0.04	0.07	0.11	0.06	-0.08	0.39
	Rangamati	0.06	0.08	0.16	0.11	-0.08	0.43
	Sandwip	0.05	0.06	0.18	0.13	-0.06	0.43
	Sitakunda	0.06	0.08	0.12	0.09	-0.07	0.37
	Teknaf	0.08	0.14	0.12	0.12	-0.03	0.41
Khulna	Khulna	-0.01	-0.01	0.31	0.23	0.01	0.59
	Jashore	-0.02	-0.05	0.31	0.21	-0.01	0.52
	Satkhira	-0.01	0	0.22	0.17	0.01	0.44
Barishal	Barishal	0.01	0.02	0.25	0.18	-0.03	0.54
	Patuakhali	0.02	0.04	0.23	0.16	-0.04	0.52
	Bhola	0	0.01	0.15	0.11	-0.02	0.35
	Khepupara	0.03	0.06	0.22	0.17	-0.04	0.55
Rajshahi	Rajshahi	-0.03	-0.02	0.29	0.24	0.05	0.53
	Bogura	0	0.07	0.32	0.3	0.08	0.7
	Ishurdi	-0.01	0.03	0.28	0.24	0.04	0.6

Division	Station Location	Emission scenario					
		RCP2.6		RCP4.5		RCP8.5	
		Near Future	Far Future	Near Future	Far Future	Near Future	Far Future
Rangpur	Rangpur	-0.01	0.04	0.2	0.18	0.04	0.47
	Dinajpur	0	0.09	0.19	0.22	0.08	0.55
Sylhet	Srimangal	0.02	0.07	0.16	0.15	0.01	0.43
	Sylhet	0.03	0.13	0.2	0.22	0.06	0.61
Country		0.02	0.05	0.2	0.16	-0.01	0.47

[Projection range indication: (i) Light red fill with red text: -0.6- to -0.2; (ii) Light red fill: -0.19 to 0; (iii) Light green: 0.001 to 0.5 and (iv) Green fill with dark green text: ≥ 0.51]

7.4 Summary

Analysis of the downscaled result conducted using ESD shows that the projections of wet-day frequency anomalies in pre-monsoon season for the RCP2.6 emission scenario are positive both in the near future and far future. It is found to be very within the ranges of -0.04 to 0.1 and -0.09 to 0.12 per 30 years, respectively. The projections of the highest wet-day frequency for both periods are found at Madaripur, followed by Barishal and Bhola. In the case of the RCP4.5 scenario, the projections of wet-day frequency anomalies in the pre-monsoon season are positive at the maximum number of BMD station locations both in the near future and far future, and it is negative at very few stations. The highest magnitude of the projection of wet-day frequency for both the near future and far future is 4.3 and 2.8, and it is projected at Rangamati. Considering the RCP8.5 scenario, the projections of wet-day frequency in pre-monsoon season at BMD station locations are in the range of -0.01 to 0.11 in the near future. It is the highest at Madaripur, followed by Barishal, Bhola & Khepupara station locations. Under the same scenario, the projections of wet-day frequency in the pre-monsoon season are in the range of -0.15 to 0.36 in the far future, and it is the maximum at Chandpur, followed by Rangamati station. As a whole, the result depicts a considerable projection of the increasing wet-day frequency trend in the near and far future.

The projections of wet-day frequency anomalies in monsoon season selecting RCP2.6 emission scenario are positive both in the near future and far future, and it is found to lie with the ranges of -0.06 to 0.13 and -0.06 to 0.18, respectively. The projection of the highest wet-day frequency for both periods is found at Maijdi Court. In the case of the RCP4.5 scenario, the projections of wet-day frequency anomalies in the monsoon season are negative at the maximum number of BMD station locations both in the near future and far future, and a few numbers of stations are showing positive anomalies. The highest magnitude of the projection of wet-day frequency is 0.1 (Rangpur, Dinajpur & Sylhet) in the near future, and it is the same at Sylhet for the far future under this emission scenario. For the RCP8.5 scenario, the projections of wet-day frequency in the monsoon season are in the range of -0.13 to 0.21 in the near future. The projection is the highest at Satkhira. Under the same scenario, the projections of wet-day frequency at BMD station locations in the monsoon season are in the range of -0.54 to 1.51 in the far future, with the maximum at Madaripur.

As a whole, the result depicts a dominant projection of decreasing wet-day frequency in both the near and far future at the selected location positions.

Overall, the projections of wet-day frequency anomalies in post-monsoon season for the RCP2.6 emission scenario are positive both in the near future and far future, and it is with ranges of -0.03 to 0.08 and -0.06 to 0.14, respectively. The projection of the highest wet-day frequency is found at Teknaf for both of these periods. In the context of the RCP4.5 scenario, the projections of wet-day frequency anomalies in post-monsoon season are positive at all BMD station locations both in the near future and far future. The highest magnitude of the projection of wet-day frequency is 0.32 (at Faridpur) and 0.3 (at Bogura) for the near future and far future, respectively, under this emission scenario. For the RCP8.5 scenario, the projections of wet-day frequency in post-monsoon season are in the range of -0.08 to 0.08 in the near future. It is the highest at Bogura and Dinajpur station locations. Under the same scenario, the projections of wet-day frequency in post-monsoon season are in the range of 0.7 to 0.19 in the far future. The projection is the maximum at Bogura, followed by Cumilla. As a whole, the result depicts a dominant projection of decreasing wet-day frequency in the near future and increasing numbers in the far future at the selected locations.

CHAPTER EIGHT: FUTURE PROJECTION OF BANGLADESH

8.1 Future Climate Projections

The projections from the downscaled climate variables for different GCMs based on the emission scenarios RCP2.6, RCP4.5 and RCP8.5 are summarized in this chapter. The variables used in the projection are mean temperature and wet-day frequency for different seasons in Bangladesh. The best GCMs are also selected for different seasons based on their performance (Table 8.1)

Table: 8.1. Name of GCMs under my study

Variables	Seasons and number of GCMs	GCMs used under this study
Temperature	Pre-monsoon (10 GCMs)	ACCESS1-0-r1, ACCESS1.3-r1, BCC-CSM1-1-r1, BCC-CSM1-1-m-r1, BNU-ESM-r1, CanESM2-r1, CanESM2-r2, CanESM2-r4, CanESM2-r5, CCSM4-r1
	Monsoon (10 GCMs)	ACCESS1.0.r1, BNU.ESM.r1, CanESM2.r2, CCSM4.r3, CMCC.CM.r1, CNRM.CM5.r1, EC.EARTH.r9, EC.EARTH.r12, FIO.ESM.r1, FIO.ESM.r2
	Post-monsoon (10 GCMs)	ACCESS1.0.r1, BNU.ESM.r1, CanESM2.r2, CCSM4.r3, CMCC.CM.r1, CNRM.CM5.r1, EC.EARTH.r9, EC.EARTH.r12, FIO.ESM.r1, FIO.ESM.r2
	Winter (10 GCMs)	ACCESS1.0.r1, BNU.ESM.r1, CanESM2.r2, CCSM4.r3, CMCC.CM.r1, CNRM.CM5.r1, EC.EARTH.r9, EC.EARTH.r12, FIO.ESM.r1, FIO.ESM.r2
Rainfall	Pre-monsoon (05 GCMs)	ACCESS1-0.r1i1p1, ACCESS1.3.r1i1p1, BCC-CSM1-1.r1i1p1, BNU-ESM.r1i1p1, CanESM2.r1i1p1
	Monsoon (03 GCMs)	CanESM2.r1, CanESM2.r2, CanESM2.r3
	Post-monsoon (03 GCMs)	CanESM2.r2, CanESM2.r3, CanESM2.r4

**(Here, r = realization, i = initialization method and p = physics version)

The projection in this study based on three emission scenarios reflects an increase in the seasonal mean temperature in the future in different seasons in Bangladesh. As expressed here, all of the projection rates are for 30 years.

The high emission scenario of RCP8.5 with the radiative forcing of 8.5 Watts per metre square (W/m^2) in 2100 and the low-emission scenario of RCP2.6 describes a future in which CO2 emissions remain constant until the early 21st century and become constant by the end of the century. As a result, the radiative forcing reaches a value of around 3.1 W/m^2 by mid-century but returns to 2.6 W/m2 by 2100.

Based on this scenario, the results suggest that the average pre-monsoon mean temperature at meteorological sites in Bangladesh is likely to increase slightly in the near future by 0.62°C compared to 1981-2010. Similarly, it will be of 0.78°C in the far future. In the monsoon season, the mean temperature is projected to increase by 0.25°C and 0.33°C in the near future and far future. In the post-monsoon season, the near future and far future temperatures are likely to

increase by 0.6°C and 0.45°C, respectively. Again, in winter seasons, the near future and far future temperature projections are 0.45°C and 0.71°C, respectively. The annual projected increments in Bangladesh are +0.48°C and +0.65°C in the near and far future, respectively. The details are given in Fig. 8.1 and Table 8.2.

Table 8.2: Temperature Projection in Bangladesh for the different Emission Scenarios

Season/Annual	Emission scenario					
	RCP2.6		RCP4.5		RCP8.5	
	Near Future	Far Future	Near Future	Far Future	Near Future	Far Future
Pre-monsoon	0.62	0.78	0.5	1.19	0.54	2.04
Monsoon	0.25	0.33	0.13	0.45	0.37	1.27
Post-monsoon	0.6	0.76	0.72	1.42	0.94	2.81
Winter	0.45	0.71	0.44	1.16	0.86	2.83
Annual	0.48	0.65	0.45	1.06	0.68	2.23

Based on the scenario of RCP4.5, the results suggest that the pre-monsoon mean temperature in Bangladesh is likely to increase by 0.5°C in the near future. Then in the far future, the country's average temperature is projected to increase by 1.19°C. In the monsoon season, the country's mean temperature will likely increase by 0.13°C and 0.45°C in the near and far future. In post-monsoon season, the average temperature is projected to increase by 0.72°C, which will be 1.42°C in the future. Similarly, the projected increments are 0.44°C and 1.16°C in the near and far future at winter season, respectively.

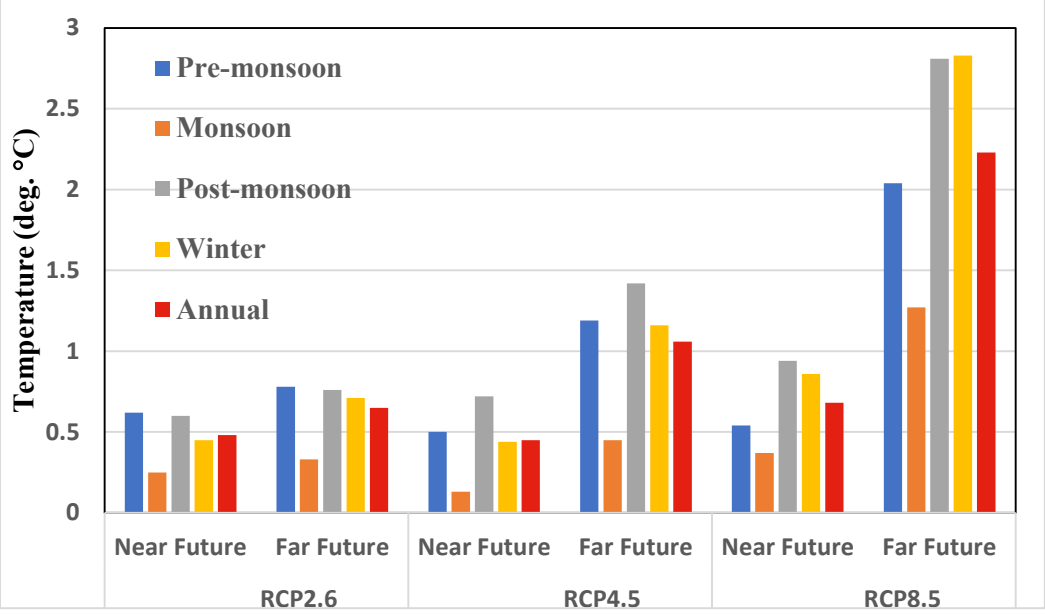

Fig.8.1: Temperature Projection for the different Emission Scenarios

The very high-emission scenario of RCP8.5 reveals that the pre-monsoon mean temperature in Bangladesh is likely to increase by 0.54°C in the near future. The projection suggests a rapid

increase in temperature, and the projected value is 2.04°C in the far future. In the monsoon season, the mean temperature projections are 0.37°C and 1.27°C in the near and far future, accordingly. In the post-monsoon and winter, near-future temperature projections in the near future are 0.94°C and 0.86°C, and for the far future, the projected magnitudes are 2.81°C and 2.83°C respectively. Following the scenarios of RCP4.5 and RCP8.5, the projection also indicates a warming situation in Bangladesh in the near future and far future. The warming is considerably higher, with magnitudes of about +1.06°C and +2.23°C for RCP4.5 and RCP8.5, respectively.

Table 8.3: Wet-day Frequency Projection in Bangladesh for the different Emission Scenarios

Season/Annual	Emission scenario					
	RCP2.6		RCP4.5		RCP8.5	
	Near Future	Far Future	Near Future	Far Future	Near Future	Far Future
Pre-monsoon	0.05	0.04	0.28	0.18	0.07	0.24
Monsoon	0.03	0.03	-0.07	-0.07	-0.04	-0.24
Post-monsoon	0.02	0.05	0.2	0.16	-0.01	0.47
Annual	0.03	0.04	0.14	0.09	0.01	0.16

Based on the scenario of RCP2.6, the average change of wet-day frequency during pre-monsoon season relative to 1981-2010 is shown in Table 8.3 and Fig.8.2. The analysis results suggest that the average pre-monsoon wet-day frequency over Bangladesh is likely to increase slightly with the magnitude of 0.05 in the near future. It shows a slight decreasing trend of 0.04 in the far future. In the monsoon season, wet day frequency is likely to increase by 0.03 in the near future. In post-monsoon, the near future wet day frequency is projected to increase by 0.02, and it is by 0.05 in the far future.

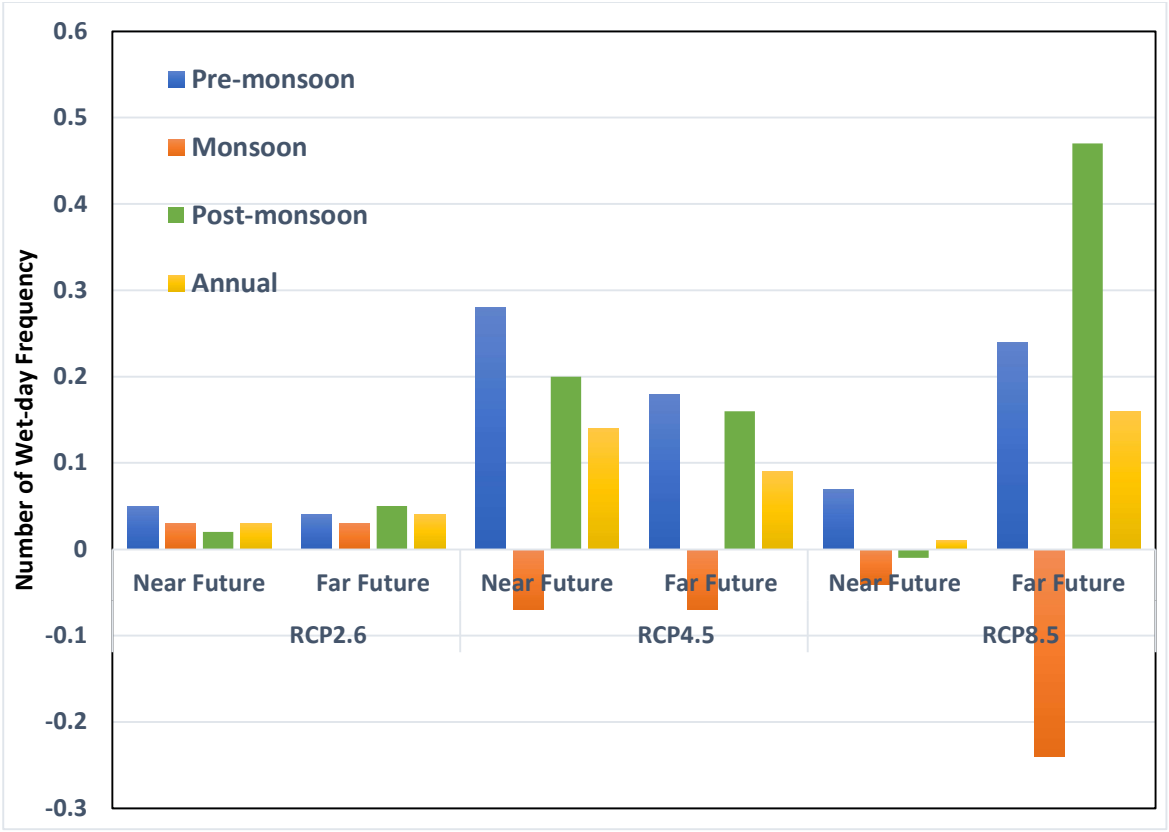

Fig.8.2: Wet-day Frequency Projection for the different Emission Scenarios

For the case of the scenario of RCP4.5, the average pre-monsoon wet-day frequency in Bangladesh is likely to increase by 0.28 in the near future, and it recognizes projected to increase further by 0.18 in the far future. In the monsoon season, wet-day frequency is projected to decrease by 0.07 both in the near and far future. Post-monsoon wet-day frequency is projected to increase by 0.2 and 0.16 both in the near and far future, respectively.

The study reveals that the average pre-monsoon wet-day frequency in Bangladesh is likely to increase by 0.07 in the near future and then rapidly increase to 0.24 in the far future, as per the case of the very high-emission scenario of RCP8.5. In the monsoon season, mean wet-day frequency is projected to decrease at the rate of -0.04 in the near future and then further decrease at the higher rate of -0.24 in the far future. Post-monsoon wet-day frequency is likely to decrease at the rate of -0.01 in the near future, but it shows an increase with the rate of 0.47 in the far future. Finally, for the low-to-moderate emission scenario of RCP4.5, the average projected wet-day frequency change in Bangladesh in the near future has an increasing trend of 0.14 in the near future, and it is of 0.09 in the far future. For the high-emission scenario of RCP8.5, the wet-day frequency is projected to change in Bangladesh in the near future with a rate of 0.01 in the near future and it is 0.16 in the far future.

8.2 Comparison of simulated projection with IPCC and Other Sources

All nations participated in the twenty-first Conference of Parties (COP21, held in Paris) jointly agreed to limit global warming to 2°C compared to pre-industrial levels and its subsequent efforts to limit the increment of temperature to 1.5°C under the Paris Agreement 2015. As a follow-up activity, the IPCC circulated a Special Report in October 2018 on the comparative impacts of global warming levels of 1.5°C and 2°C.

Chapters 6 and 7 of this study have evaluated the observed and future changes in temperature at micro and macro levels in Bangladesh. The study also calculates the projection of seasonal and country levels of temperature projection in Bangladesh (Table 8.2). In the case of the high emissions scenario of RCP8.5, the country's mean temperature is projected to increase by 2.23°C at the end of the 21st century. Similarly, for the low-to-moderate emission scenario of RCP4.5, the projection is the likely increase of temperature by 1.06°C at the end of the 21st century, which almost matches the IPCC Special Report published in October 2018.

Krishnan *et al*. (2020) opined that all-India annual, as well as summer monsoon, mean rainfall declined by around 6% during 1951-2015. It includes the area of the Indo-Gangetic Plains and the Western Ghats of the Indian subcontinent. However, this study reveals that the wet-day frequency is likely to increase slightly, and the wet-day frequency over the summer monsoon season is projected to decrease. It depicts that the mean monsoon rainfall is likely to decrease for RCP4.5 and RCP8.5 in Bangladesh (Table 8.3).

According to the findings of the IPCC, the continuous emissions of greenhouse gases (GHGs) will cause further warming in Bangladesh (IPCC, 2014). Mean temperatures in Bangladesh are expected to increase 1.4°C by 2050 and 2.4°C by 2100 (Mahmud *et al*., 2021, World Bank Report). The projection is noticeable for winter (December to February) and annual rainfall, when rainfall is projected to increase by 74 millimetres by 2040 to 2059. The assumption pointed out in the Work Bank Report almost complied with the information given in Tables 8.2 and 8.3.

CHAPTER NINE: CONCLUSION

9.1 Summary of research findings

The objective of this study is to prepare a future climate scenario for Bangladesh. The projection of future climate has been generated based on the simulations of future climate scenarios derived by the GCMs. Through this process, different GCMs are selected under the CMIP5 scenario and are then evaluated for their performance in Bangladesh region. GCMs outputs are analyzed in seasons wise, and their performances are found to vary among the seasons. It is found that the pre-monsoon temperature of 10 GCMs, namely ACCESS1-0-r1, ACCESS1.3-r1, BCC-CSM1-1-r1, BCC-CSM1-1-m-r1, NU-ESM-r1, CanESM2-r1, CanESM2-r2, CanESM2-r4, CanESM2-r5, and CCSM4-r1; for monsoon, post-monsoon and winter temperatures 10 GCMs namely ACCESS1.0.r1, BNU.ESM.r1, CanESM2.r2, CCSM4.r3, CMCC.CM.r1, CNRM.CM5.r1, EC.EARTH.r9, EC.EARTH.r12, FIO.ESM.r1, and FIO.ESM.r2 are finally selected. For rainfall analysis during pre-monsoon season 05 GCMs, namely ACCESS1-0.r1i1p1, ACCESS1.3.r1i1p1, BCC-CSM1-1.r1i1p1, BNU-ESM.r1i1p1 and CanESM2.r1i1p1; for monsoon season 03 GCMs namely CanESM2.r1, CanESM2.r2 and CanESM2.r3 and for post-monsoon 03 GCMs like CanESM2.r2, CanESM2.r3 and CanESM2.r4 finally selected.

Several statistical downscaling methods are used to understand and remove the gap between significant and local-scale climate variables. These models have the best skill to capture the climate of Bangladesh region, and therefore they are selected for use in this study to project the future climate of Bangladesh. The projections based on all of these GCMs are agreed that mean temperature is projected to increase for CMIP5 scenarios. On the other hand, the projection of wet-day frequency also shows a slight increase in Bangladesh at the end of this century.

Hence, the following conclusions can be drawn based on this study:

i. The three emission scenarios of RCP2.6, RCP4.5 and RCP8.5 reflects an increase in seasonal mean temperature in the future in Bangladesh. The low emission scenario of RCP2.6 explains that CO_2 emissions will remain fixed until the early 21st century and becomes negative by 2100. As a result, the rate of radiative forcing is expected to be about 3.1 W/m2 by mid-century, but it is expected to be lowered to 2.6 W/m2 by the end of this century. Based on this situation, analysis indicates that the average temperature in Bangladesh is likely to increase in the near future and then increase slightly further till the end of the 21st century.

ii. Following the low-to-medium emission scenario of RCP4.5, the mean projected warming of Bangladesh in the near future is lower than that of RCP2.6, but it is higher than that in the far future. Both near-future and far-future warmings for RCP4.5 are lower than that for the high-emission scenario of RCP8.5 in each season and for annual value. The annual warming levels in near and far futures for RCP4.5 are +0.45°C and +1.06°C. Similar to the low-emission scenario of RCP2.6, the middle emission scenario of RCP4.5 specifies a peak

in the beginning period with a maximum near the year 2050. Then a declining scenario of emissions of greenhouse gases can reduce the temperature noticeably after 2050, which is expected to lead to a stabilization condition of radiative forcing toward the end of the 21st century.

iii. The projected increase in mean temperature in winter, pre-monsoon and post-monsoon seasons indicates the likely increase in the frequency of warm nights in the winter season and the intensity of heat waves in pre-monsoon and post-monsoon seasons in Bangladesh. The temperatures over the southwest and northwest regions of Bangladesh are already very high (Table 6.1.1-6.4.1 and Table 8.2), and severe heat waves occur regularly. This situation could be worsened and could have a negative impact on the life and health of the people living in these areas due to the upcoming warming enhancement.

iv. For RCP2.6, the mean wet-day frequency over Bangladesh is likely to increase slightly in the near future, and a very slight decrease is projected in the far future (Table 8.3). For the low-to-moderate emission scenario of RCP4.5, the mean projected wet-day frequency in Bangladesh in the near future is likely to increase by 0.14 and 0.09 in the near future and far future. In the high-emission scenario of RCP8.5, the wet-day frequency change in Bangladesh in the near future is projected to increase by 0.01 in the near future and 0.16 in the far future.

v. It suggests rainfall is likely to decrease during the end of this century. The mean wet-day frequency is projected to decrease to -0.04 in the near future, and it is likely to decrease rapidly at the rate of -0.24 in a 30 years period in the far future. As more than 71% of the total annual rainfall occurs in Bangladesh in the monsoon season, this rainfall deficit may significantly impact the economic sectors in Bangladesh.

vi. CO2 emissions are expected to have severe consequences in the winter season in Bangladesh in terms of significant warming. Accordingly, all emission scenarios show an increase in mean temperature in Bangladesh, but RCP2.6 shows the temperature is likely to upsurge in the mid-century. The average temperature is projected to increase two times higher in the far future compared to the near future for RCP4.5. It is also supposed to increase four times higher for RCP8.5. Finally, as warming cannot be avoided, this research demonstrates an urgent requirement to set initiatives limiting the severity of climate change in the future.

9.2 Implications of this study

i. The rapid changes in climate projection by GCMs will place increasing stress on the country's natural environments, agricultural output, and freshwater resources while also triggering escalating infrastructure damage. These indicate that there is likely severe significance for the country's biodiversity, food and energy security, and community health. In the absence of quick adaptation measures, the influences of climate change are

likely to pose thoughtful challenges to supporting the country's fast economic growth and reaching the sustainable development goals (SDGs) permitted by United Nations (UN) Member States in 2015.

ii. The high probability of future reductions in carbon dioxide emissions from America, Europe, and Asia, will likely affect monsoon precipitation and its variability over the whole of Bangladesh. The effect of climate change on the accessibility of groundwater is a critical area of anxiety for the northwestern part of Bangladesh. The rising tendency for floods and drought conditions is because of changing precipitation patterns caused by climate change, which would harm freshwater recharge, posing threats to the country's water crisis. Similarly, the nation's food security may be placed under gradually more burden due to increasing year-to-year precipitation and extreme rainfall variability and rising droughts, floods, and temperatures that can interrupt rain-fed agricultural production and badly affect crop harvest. Rising temperatures will likely escalate energy demand for space cooling and other activities. Climate change could influence the consistency of the national energy setup and supply chain. The hazards posed by climate change can be noticeably exaggerated when a cascade of climate-related risks overlay or monitor one another. A county may experience an unusually long or extreme summer heat wave followed by intense floods that alternate with the shortening of wet-day spells.

iii. Low-lying shoreline areas, especially the southern part of Bangladesh coast, maybe witness the rising sea levels' destructive properties and increasing surface water salinity. Such sequences of events will become progressively more numbers if climate change continues unconstrained. According to the new IPCC Special Report 2018 on the various impacts between 1.5°C versus 2°C warming, the combined effect of these effects is that tropical countries such as Bangladesh are expected to gather knowledge of the most significant impacts on economic progress because of climate change.

iv. All of these impacts can be estimated in confidence utilizing the results summarized in this study.

9.3 Limitations of this study

To further improve this study, the following gaps would need to be addressed in the near future:

i. The uneven spatial distribution of BMD's observation stations over Bangladesh may lead to errors in assessing present-day temperature and precipitation changes, particularly over the hilly regions of the country, where there is a very scarce observational network.

ii. Confidence in the assessed long-term meteorological variables, such as temperature and precipitation trends, may be constrained by the data inhomogeneity due to changes in observation station positions.

iii. There has been an increase in extreme temperature events (e.g., heat waves) across the pre-monsoon season in Bangladesh (Rashid *et al*., 2021b). Therefore, substantial research studies are required on event attribution that assesses the probability or intensity of extreme temperature events.

iv. Assessment of combined projections of many variables over Bangladesh is required to understand. For example, expected changes in the combination of temperature and rainfall; soil moisture, rainfall and temperature mean and variability; combining temperature and humidity, etc.

v. Since water vapour is the most critical contributor to the natural greenhouse effect, more investigation is needed to recognize whether the amplified water vapour under local warming conditions leads to a significant optimistic response to human-intervention climate change.

vi. More realistic bio-geophysical processes-based land surface models are needed to assess the impact of land-use/land-cover change on the monsoon. The contemporary models need to sufficiently simulate our region's intra-seasonal summer monsoon variability.

vii. It is a great challenge to predict the attitude of climate forcing. There is limited information about significant influences of internal variability, for example, the Pacific Decadal Oscillation (PDO), Inter-decadal Pacific Oscillation (IPO) and other modes of variability. In recent decades, a weak relation between observed and ENSO monsoon rainfall. So, CMIP5 models do not capture the ENSO behaviour in the future and how ENSO–monsoon connection may develop.

9.4 future work

With the following IPCC report becoming available in the near future and with the next generation of GCMs (CMIP6) already available, it is desired that the methods applied in this study can be used to project the future climate of Bangladesh using the CMIP6's GCMs. It will be convenient to compare projections given by CMIP6 GCMs with the existing projection. The CMIP5 GCMs have limitations and often overestimate the extremely high temperature in this area. It would be remarkable to test the ability of CMIP6 GCMs and see if any development is linked to CMIP5 GCMs.

The frequency of events of extreme climate factors such as extreme precipitation, heat waves, cold waves and severe floods are expected to increase under a warmer climate, and it is very significant to project the frequency of these extreme events under future climate scenarios with suitable downscaling approaches and an assessment of statistical downscaling methods would be useful. The statistical downscaling methods used in this study are mainly regression types, for example, a stepwise multiple linear regression method. Although the performance of the GCMs models in this study is reasonably accurate for most climate variables, it is important to try other downscaling methods such as dynamical downscaling, weather typing and weather generation methods.

This study uses the downscaled climate variables to evaluate wet-day frequency in future scenarios, which is one of the potential applications. Still, many further applications can use these climate variables. For example, temperature projection to measure heat stress in the urban environment and energy consumption in power sectors are all possible uses of the information of this study.

REFERENCES

Ahmed. R. and Karmakar. S. (1993), "Arrival and withdrawal dates of the summer monsoon in Bangladesh." *International Journal of Climatology* 13(7):727 – 740, DOI : 10.1002 / joc.3370130703.

Akaike, H. (1974), "A new look at the statistical model identification." *IEEE Transactions on Automatic Control,* 19 (6), 716–723. https://doi.org/ 10.1109/TAC.1974.1100705.

Bangladesh Meteorological Department, Climatological Data. (1984), WMO/UNDP/BGD/79/013 TECH. NOTE NO.8.

Bangladesh Meteorological Department, Climatological Data. (1986), WMO/UNDP/BGD/79/013 TECH. NOTE NO. 9.

Bardossy, A. and Plate, E. (1992), "Space-time model for daily rainfall using atmospheric circulation patterns." *Water Resources Research*, 28(5): 1247-1259.

Benestad, R. E. (2001), "A Comparison between Two Empirical Downscaling Strategies." International *Journal of Climatology*, 21(13), 1645–68. https://doi.org/10.1002/joc.703.

Benestad, R. E. (2016), "Downscaling Climate Information," *Oxford Research Encyclopedia*, https://doi.org/10.1093/acrefore/9780190228620.013.27.

Benestad, R. E., Mezghani, A. and Parding, K. M. (2015), "The Empirical-Statistical Downscaling Tool & Its Visualisation Capabilities." *Met Report* 11/2015. Norwegian Meteorological Institute.

Benestad, R. E., Parding, K. M., Isaksen, K. and Mezghani, A. (2016), "Climate Change and Projections for the Barents Region: What Is Expected to Change and What Will Stay the Same?" *Environmental Research Letters*, 11(5), 054017.

Cess, R.D., *et al*., (1989), "Interpretation of cloud-climate feedback as produced by 14 atmospheric general circulation models." *Science,* 245, 513–516.

Cheung, C. C. (2014), "Using statistical downscaling to project the future climate of Hong Kong. (Thesis)." *University of Hong Kong, Pokfulam, Hong Kong SAR*. Retrieved from http : // dx.doi.org / 10.5353 / th_b5194728.

Collins, W.D., *et al*. (2006), "The Community Climate System Model: CCSM3." *J. Clim.,* 19, 2122–2143

Confalonieri, U., Menne, B., Akhtar, R., Ebi, K. L., Hauengue, M., Kovats, R. S., Revich, B., & Woodward, A. (2007), "Human health. Climate Change 2007: Impacts, Adaptation and Vulnerability. Contribution of Working Group II to the Fourth Assessment Report of the Intergovernmental Panel on Climate Change." *Cambridge University Press,* Cambridge, UK., 391-431.

Delworth, T., *et al*. (2006), "GFDL's CM2 global coupled climate models Part 1: Formulation and simulation characteristics." *J. Clim*., 19, 643– 674.

Dickinson, R.E., Errico, R.M., Giorgi, F. and Bates, G.T. (1989), "A regional climate model for the western Unites States." *Climate Change*, 15(3): 383-422.

Fahad, M.G., Islam, A.S**.**, Nazari, R., Hasan, M.A., Islam, G.M.T., Bala, S.K. (2017), "Regional changes of precipitation and temperature over Bangladesh using bias corrected multi-

model ensemble projections considering high emission pathways." *International Journal of Climatology*, 38(4), 1634-1648. doi:10.1002/joc.5284.

Fuentes, U. and Heimann, D. (2000), "An improved statistical-dynamical downscaling scheme and its application to the alpine precipitation climatology." Theoretical and Applied Climatology, 65, 119-135.

Giorgi, F., Hewitson, B. C., Christensen, J., Hulme, M., Von Storch, H., Whetton, P., Jones, R., Mearns, L., and Fu, C. (2001), "Regional Climate Information - Evaluation and Projections. In: Climate Change 2001: The Scientific Basis. Contribution of Working Group I to the Third Assessment Report of the Intergovernmental Panel on Climate Change." *Cambridge University Press: Cambridge.*

Guyennon, N., Romano, E., Portoghese, I., Salerno, F., Calmanti, S., Perangeli, A.B., Tartari, G., and Copetti, D. (2013), "Benefits from using combined dynamical-statistical downscaling approaches – lessons from a case study in the Mediterranean region." Hydrology and Earth System Sciences 17(2), 705-720.

Hayhoe, K., Edmonds, J., Kopp, R.E., Le Grande, A.N., Sanderson, B.M., Wehner, M.F., and Wuebbles, D.J. (2017), "Climate models, scenarios, and projections. In: Climate Science Special Report: Fourth." *National Climate Assessment*, Volume I.

Hostetler, S.W., Bartlein, P.J., and Alder, J.R. (2018), "Atmospheric and surface climate associated with 1986–2013 wildfires in North America." *Journal of Geophysical Research. Bio-geosciences*, v. 123, no. 5, p. 1588–1609, https://doi.org/10.1029/2017JG004195.

IPCC. (2001), "Climate Change 2001: The scientific basis: Contribution of Working Group I to the Third Assessment Report of the Intergovernmental Panel on Climate Change." *Cambridge University Press, Cambridge.*

IPCC. (2014), "Climate Change 2014: Synthesis Report. A Contribution of Working Groups I, II and III to the Fifth Assessment Report of the Intergovernmental Panel on Climate Change." Edited by the Core Writing Team, R.K. Pachauri, and L.A. Meyer. Geneva: IPCC.

IPCC, (2018), "Summary for Policymakers. In: Global Warming of 1.5°C. An IPCC Special Report on the impacts of global warming of 1.5°C above pre-industrial levels and related global greenhouse gas emission pathways, in the context of strengthening the global response to the threat of climate change, sustainable development, and efforts to eradicate poverty."

IPCC-TGICA. (2007), "General Guidelines on the Use of Scenario Data for Climate Impact and Adaptation Assessment." Version 2. Prepared by T.R. Carter on behalf of the Intergovernmental Panel on Climate Change, Task Group on Data and Scenario Support for Impact and Climate Assessment, 66.

Kajsa M. P, Andreas D., Carol F. M., Oskar A. L., Rasmus B., Helene B. E., Abdelkader M., Hilppa G., Olle R., Elisabeth V., Juliane E. Z., Ole B. C., Harilaos L. (2020), "GCMeval – An interactive tool for evaluation and selection of climate model ensembles." *Climate Services*, Volume 18, 100167, ISSN 2405-8807, https : // doi.org / 10.1016 / j.cliser. 2020. 100167.

Keeling, C. D. (1993), "A Brief History of Atmospheric Carbon Dioxide Measurements and Their Impact on Thoughts about Environmental Change." Paper presented at the Blue Planet

Prize 1993, Academic Award Commemorative Lecture, The Asahi Glass Foundation, Tokyo, Japan.

Khan, J.U., Islam, A.K.M.S., Das, M.K., Mohammed, K., Bala, S.Bala, Sujit K. and Islam, G. M.T. (2020), "Future changes in meteorological drought characteristics over Bangladesh projected by the CMIP5 multi-model ensemble." *Climatic Change* 162, 667–685. https://doi.org/10.1007/s10584-020-02832-0.

Khatun, Mossammat Ayesha., Rashid, Md. Bazlur and Hygen, Olav. Hans, (2016), "Climate of Bangladesh", *MET report*, no. 08/2016, ISSN 2387-4201, Climate, Norwegian Meteorological Institute. http://www.bmd.gov.bd/p/Climate-Report/.

Knutti, R., G.A. Meehl, M.R. Allen and D.A. Stainforth. (2006), "Constraining climate sensitivity from the seasonal cycle in surface temperature." *J. Clim*., 19, 4224–4233.

Krishnan R., Sanjay J., Mujumdar M., Ashwini Kulkarni A. and Supriyo C. (2020), "Assessment of Climate Change over the Indian Region." A Report of the Ministry of Earth Sciences (MoES), Government of India, *Springer Nature,* Singapore, pp. 73-92. https://doi.org/10.1007/978-981-15-4327-2

Lupo, A., and Kininmonth, W. (2013), "Global climate models and their limitations." *In Climate Change Reconsidered II: Physical Science*; NIPCC: Tempe, AZ, USA, pp. 9–148.

Mahmud, Iffat; Raza, Wameq A. and Hossain, Md Rafi. (2021), "Climate Afflictions. International Development in Focus.", Washington, DC: World Bank. © World Bank. https://openknowledge.worldbank.org/handle/10986/36333 License: CC BY 3.0 IGO.

Manabe, S., and Wetherald, R. T. (1967a), "Thermal Equilibrium of the Atmosphere with a Given Distribution of Relative Humidity." *Journal of the Atmospheric Sciences*, 24(3), 241- 259.

Manabe, S., and Wetherald, R. T. (1975b), "The Effects of Doubling the CO2 Concentration on the climate of a General Circulation Model." *Journal of the Atmospheric Sciences*, 32(1), 3-15.

Manabe, S and Bryan, K. (1969), "Climate calculations with a combined ocean-atmosphere model." *Journal of Atmospheric Sciences*, 26(4): 786–789. DOI: https://doi. org/10.1175/1520-0469(1969)0262.0.CO;2.

Maraun, D., and Widmann, M. (2018), "Statistical Downscaling and Bias Correction for Climate Research." *Cambridge: Cambridge University Press*. https://doi.org/10.1017/9781107588783.

Maraun, D. (2013), "Bias Correction, Quantile Mapping, and Downscaling." Revisiting the Inflation Issue, *J. Climate*, 26, 2137–2143, https://doi.org/10.1175/JCLI-D-12-00821.1.

Maraun, D. *et al*. (2010), "Precipitation downscaling under climate change: Recent developments to bridge the gap between dynamical models and the end user." *Reviews of Geophysics*, 48(3), RG3003 pp.1-34.

McGuffie, K. (2007), "A climate modelling primer (3rd ed. ed.)." *Chichester: Wiley*.

Mezghani, A., Dobler, A., Benestead, R. E., Haugen, J. E. and Parding, K. M. (2019), "Subsampling Impact on the Climate Change Signal over Poland Based on Simulations

from Statistical and Dynamical Downscaling." *Journal of Applied Meteorology and Climatology*, 58, 1061-1078.

Mohammed Khaled, Islam A. K. M. Saiful, Islam G. M. Tarekul, Alfieri Lorenzo, Khan Md. Jamal Uddin, Bala Sujit Kumar and Das Mohan Kumar. (2018), "Future Floods in Bangladesh under 1.5°C, 2°C, and 4°C Global Warming Scenarios." *J. Hydrol. Eng*., 23(12), DOI: 10.1061/(ASCE)HE.1943-5584.0001705.

Mukherjee, N., Khan, M. F. A., Hossain, B. M. T. A., Islam, A. K. M. S. Aktar, N. and Rahman, S., (2011), "3rd International Conference on Water & Flood Management" (3-5 July, Dhaka, Bangladesh) pp. 45-56.

Murphy, J.M., *et al*. (2004), "Quantification of modelling uncertainties in a large ensemble of climate change simulations." *Nature,* 430, 768–772.

Nakicenovic, N., Alcamo, J., Davis, G., de Vries, B., Fenhann, J., Gaffin, S., Gregory, K., Grübler, A., Jung, T., Kram, T., La Rovere, E., Michaelis, L., Mori, S., Morita, T., Pepper, W., Pitcher, H., Price, L., Riahi, K., Roehrl, A., Rogner, H.-H., Sankovski, A., Schlesinger, M., Shukla, P., Smith, S., Swart, R., van Rooijen, S., Victor, N., & Dadi, Z. (2000), "IPCC Special Report on Emissions Scenarios: Cambridge University Press."

National Strategy for Advancing Climate Modeling (2012), "Chapter: 7 Climate Model Development Workforce."

Nury, A. H., and Alam, J. B. (2013), "Performance Study of Global Circulation Model HADCM3 Using SDSM for Temperature and Rainfall in North-Eastern Bangladesh." *Journal of Scientific Research*, 6(1), 87–96. https://doi.org/10.3329/jsr.v6i1.16511

Paul N. Edwards. (2011), "History of climate modeling." *Clim Change*, 2, 128–139, DOI: 10.1002/wcc.95.

Peter Lynch, (2007), "The Origins of Computer Weather Prediction and Climate Modeling." *J. Comput. Phys,* doi:10.1016/j.jcp.2007.02.034

Piani, C., D.J. Frame, D.A. Stainforth, and M.R., Allen. (2005), "Constraints on climate change from a multi-thousand-member ensemble of simulations*." Geophys. Res. Lett.,* 32, L23825, doi:10.1029/2005GL024452.

Pour, S. H., Shahid, S., Chung, E.-S., Wang, X.-J. (2018), "Model output statistics downscaling using support vector machine for the projection of spatial and temporal changes in rainfall of Bangladesh." *Atmospheric Research,* 213, 149-162. https://doi.org/ 10.1016/j.atmosres.2018.06.006.

Rahaman, A. Z., Khan, M. F. A., Aktar, N., Al Hossain, B. T., Akand, K. and Noor, F. (2015), "Climate Change Scenarios of Bangladesh Using Statistical Downscaling Model (SDSM)." In 5th International Conference on Water & Flood Management.

Rahman, M. M., and Mcbean, E. A. (2011), "Proceedings of the Global Conference on Global Warming" (11-14 July, Lisbon, Portugal), pp. 1-6.

Randall, D.A., *et al*. (2003), "Confronting models with data: The GEWEX Cloud Systems Study." *Bull. Am. Meteorol. Soc.*, 84, 455–469.

Rashid, M. B., & Hossain, S. S. (2018), "Statistical Downscaling of Global Climate Model (GCM) Outputs for Climate Change Impact Assessment of Mean Temperature of the Winter Season over Bangladesh." *The Journal of NOAMI*, 35(1-2): 45-58.

Rashid, M. B., & Hossain, S. S. (2019), "Projections for Temperature of Monsoon Season over Bangladesh using Statistical Downscaling of Global Climate Model (GCM)." *The Atmosphere ,* 08(1):60-67.

Rashid, M. B., & Hossain, S. S. (2020), "Future Projection of Mean Temperature of Post-Monsoon Season Over Bangladesh Using Statistical Downscaling of Global Climate Models." *Journal of Engineering Science*, *11*(2), 27-35. https://doi.org/10.3329/jes.v11i2.50895.

Rashid, M. B., & Hossain, S. S. (2021a), "Bias Correction of Global Climate Model (GCM) Outputs and Its Statistical Downscaling of Pre-Monsoon's Wet-Day Frequency in Bangladesh." *Dew-Drop* ,07(1): 59-69.

Rashid, M. B., Hossain, S. S., Mannan, M.A., Parding, K.M., Hygen, H.O., Benestad, R.E. & Mezghani, A.K, (2021b), "Climate change projections of maximum temperature in the pre-monsoon season in Bangladesh using statistical downscaling of global climate models", *Adv. Sci. Res*., 1, 1–16, https://doi.org/10.5194/asr-18-99-2021.

Seaby, L. P., Refsgaard, J. C., Sonnenborg, T. O., Stisen, S., Christensen, J. H., & Jensen, K.H. (2013), "Assessment of robustness and significance of climate change signals for an ensemble of distribution-based scaled climate projections." Journal of Hydrology, 486(0), 479-493.

Shukla, J., *et al*. (2006), "Climate model fidelity and projections of climate change*." Geophys. Res. Lett*., 33, L07702, doi:10.1029/2005GL025579.

Spelman, M.J., and S. Manabe. (1984), "Influence of oceanic heat transport upon the sensitivity of a model climate." *J. Geophys.* Res., 89, 571–586.

Stocker, T., Qin, D., Plattner, G., Tignor, M., Allen, S., Boschung, J. (2013), "Climate change 2013: the physical science basis. Working Group 1 (WG1) contribution to the Intergovernmental Panel on Climate Change (IPCC) 5th Assessment Report (AR5)." *Cambridge*, UK and New York, NY.

Sultana, S., Mannan, M. A., Khan, M. A., Khandaker, R., & Md Kamrujjaman. (2020), "Pre-Existing Weather Phenomena for Spreading Dengue Fever Over Dhaka in 2019." *Journal of Engineering Science*, *11*(2), 99-106. https://doi.org/10.3329/jes.v11i2.50901.

Takayabu, I., H. Kanamaru, K. Dairaku, R. Benestad, H. von Storch, and J. H. Christensen. (2015), "Reconsidering the quality and utility of downscaling." *Journal of the Meteorological Society of Japan*, Vol. 94A, 31−45, https://doi.org/10.2151/jmsj.2015-042

Van Vuuren, D. P., Edmonds, J., Kainuma, M., Riahi, K., Thomson, A., Hibbard, K., Hurtt, G. C., Kram, T., Krey, V., Lamarque, J. F., Masui, T., Meinshausen, M., Nakicenovic, N., Smith, S. J., & Rose, S. K. (2011), "The representative concentration pathways: an overview." *Climatic Change*, 109(1-2), 5-31.

Wilby, R. L., Charles, S. P., Zorita, E., Timbal, B., Whetton, P., and Mearns, L. O. (2004), "Guidelines for Use of Climate Scenarios Developed from Statistical Downscaling

Methods." IPCC Task Group on Data and Scenario Support for Impacts and Climate Analysis (TGICA), 27pp.

Wilby, R. L., & Wigley, T. M. L. (1997), "Downscaling general circulation model output: a review of methods and limitations." *Progress in Physical Geography*, 21(4), 530-548.

Wilks, D. S., (2011), "Statistical Methods in the Atmospheric Sciences", Academic Press, Kidlington, Oxford, UK; Amsterdam, the Netherlands; Waltham, MA, USA; San Diego, California, USA.

Zorita, E. & von Storch, H., (1999), "The analog method as a simple statistical downscaling technique: comparison with more complicated methods." Journal of Climate 12(8), 2474-2489.

Appendices

Appendix 1: PUBLICATIONS FROM THIS THESIS

Published in Journal: 05 (five)

i. Rashid, M. B., & Hossain, S. (2018), "Statistical Downscaling of Global Climate Model (GCM) Outputs for Climate Change Impact Assessment of Mean Temperature of the Winter Season over Bangladesh." The Journal of NOAMI, 35(1-2): 45-58, NOAMI, Dhaka, Bangladesh

ii. Rashid, M. B., & Hossain, S. (2019), "Projections for Temperature of Monsoon Season over Bangladesh using Statistical Downscaling of Global Climate Model (GCM)." The Atmosphere , 08(1):60-67, BMD, Dhaka, Bangladesh

iii. Rashid, M. B., & Hossain, S. (2020), "Future Projection of Mean Temperature of Post-Monsoon Season Over Bangladesh Using Statistical Downscaling of Global Climate Models." Journal of Engineering Science, 11(2), 27-35, https://doi.org/10.3329/jes.v11i2.50895

iv. Rashid, M. B., & Hossain, S. (2021a), "Bias Correction of Global Climate Model (GCM) Outputs and Its Statistical Downscaling of Pre-Monsoon's Wet-Day Frequency in Bangladesh." Dew-Drop ,07(1): 65-75, BMD, Dhaka, Bangladesh

v. Rashid, M. B., Hossain, S., Mannan, M.A., Parding, K.M., Hygen, H.O., Benestad, R.E.,Mezghani, A.K, (2021b), "Climate change projections of Meanimum temperature in the pre-monsoon season in Bangladesh using statistical downscaling of global climate models", Adv, Sci. Res. Adv. Sci. Res., 1, 1–16, https://doi.org/10.5194/asr-18-99-2021.

Conference Publications/Proceedings: 02 (two)

i. Rashid, M. B., Hossain, S., "Evaluation of Empirical Statistical Downscaling Models' Skill in Predicting Mean Temperature of Post-monsoon Season of Bangladesh and Generate Future Downscaled Scenarios", International Conferences on Contemporary Research and Applications of Meteorology, 07 December, 2019, Venue: Bangladesh Meteorological Department (BMD), Agrargoan, Dhaka, jointly organized by DU, JU, KUET & BMD.

ii. Rashid, M. B., Hossain, S., "Statistical Downscaling of Wet-Day Frequency During Monsoon Season in Bangladesh", International Conference on Physics-2020, 5-7 March 2020, Venue: The Atomic Energy Center, Dhaka (AECD), Organized by Bangladesh Physical Society.

Appendix 2: R PROGRAMMING SCRIPTS

1. Programming script for fill up missing data

```
Rearrange <- function (St=11111,
                StRef1=10609,StRef2=11505,StRef3=41926,
                StartYear=1951,EndYear=2010){
                                        BMDdata <- read.fwf("Meanimum",c(5,9,7,7,9))
                                        colnames(BMDdata)<-c("St","Y","M","D","Mean")
                                        BMDdata$Mean[BMDdata$Mean<0]<-NA
                                        BMDdata <- cbind(BMDdata,(BMDdata$Mean))
                                        colnames(BMDdata)<-c("St","Y","M","D","Mean")
                                        D1 <- BMDdata[BMDdata[,1]==St,]
                                        D2 <- BMDdata[BMDdata[,1]==StRef1,]
                                        D3 <- BMDdata[BMDdata[,1]==StRef2,]
                                        D4 <- BMDdata[BMDdata[,1]==StRef3,]
                                NewData <- c()
                        Dates <- c(31,28,31,30,31,30,31,31,30,31,30,31)
                for (Year in StartYear:EndYear){
        for (Month in 1:12){
          for (Day in 1:Dates[Month]){
            d1 <- D1[D1$Y==Year & D1$M==Month & D1$D==Day,6]
            if (length(d1)==0) {d1 <- NA}
            d2 <- D2[D2$Y==Year & D2$M==Month & D2$D==Day,6]
            if (length(d2)==0) {d2 <- NA}
            d3 <- D3[D3$Y==Year & D3$M==Month & D3$D==Day,6]
            if (length(d3)==0) {d3 <- NA}
            d4 <- D4[D4$Y==Year & D4$M==Month & D4$D==Day,6]
            if (length(d4)==0) {d4 <- NA}
            NewData <- rbind(NewData,
                        c(Year,Month,Day,d1,d2,d3,d4))
        }
```

```
  }
 }
 NewData
}

Interpolator <- function(St=11111,
                         StRef1=10609,StRef2=11505,StRef3=41926,
                         StartYear=1951,EndYear=2018){
 Data <-
Rearrange(St=St,StRef1=StRef1,StRef2=StRef2,StRef3=StRef3,StartYear=StartYear,EndYear=EndYear)
 Cor1 <- cor(Data[,4],Data[,5], use="complete.obs")
 Cor2 <- cor(Data[,4],Data[,6], use="complete.obs")
 Cor3 <- cor(Data[,4],Data[,7], use="complete.obs")
 print(c(St,StRef1,Cor1))
 print(c(St,StRef2,Cor2))
 print(c(St,StRef3,Cor3))
 CorMat <- cbind(c(Cor1,Cor2,Cor3),c(5,6,7))
 CorMat <- CorMat[order(CorMat[,1],decreasing=TRUE),]
 Data <- Data[,c(1,2,3,4,CorMat[,2])]
 ModellAll <- lm(Data[,4]~Data[,5]+Data[,6]+Data[,7])
 Modell12 <- lm(Data[,4]~Data[,5]+Data[,6])
 Modell13 <- lm(Data[,4]~Data[,5]+Data[,7])
 Modell23 <- lm(Data[,4]~Data[,6]+Data[,7])
 Modell1 <- lm(Data[,4]~Data[,5])
 Modell2 <- lm(Data[,4]~Data[,6])
 Modell3 <- lm(Data[,4]~Data[,7])

 PredictAll <-
ModellAll$coeff[1]+ModellAll$coeff[2]*Data[,5]+ModellAll$coeff[3]*Data[,6]+ModellAll$coeff[4]*Da
ta[,7]
 Predict12 <- Modell12$coeff[1]+Modell12$coeff[2]*Data[,5]+Modell12$coeff[3]*Data[,6]
 Predict13 <- Modell13$coeff[1]+Modell13$coeff[2]*Data[,5]+Modell13$coeff[3]*Data[,7]
```

```
 Predict23 <- Modell23$coeff[1]+Modell23$coeff[2]*Data[,6]+Modell23$coeff[3]*Data[,7]
 Predict1 <- Modell1$coeff[1]+Modell1$coeff[2]*Data[,5]
 Predict2 <- Modell2$coeff[1]+Modell2$coeff[2]*Data[,6]
 Predict3 <- Modell3$coeff[1]+Modell3$coeff[2]*Data[,7]
 Data <- cbind(Data,PredictAll,Predict12,Predict13,Predict23,Predict1,Predict2,Predict3)
 NewData <- Data[,4]
 NewData[is.na(NewData)] <- Data[is.na(NewData),8]
 NewData[is.na(NewData)] <- Data[is.na(NewData),9]
 NewData[is.na(NewData)] <- Data[is.na(NewData),10]
 NewData[is.na(NewData)] <- Data[is.na(NewData),11]
 NewData[is.na(NewData)] <- Data[is.na(NewData),12]
 NewData[is.na(NewData)] <- Data[is.na(NewData),13]
 NewData[is.na(NewData)] <- Data[is.na(NewData),14]
 NewData <- cbind(Data,NewData)
 plot(c(1:length(NewData[,15])),NewData[,15])
 points(c(1:length(NewData[,4])),NewData[,4],col="green")
 NewData
}
```

2. Programming script for calculation of Correlation

```
require(RgoogleMaps)
BMD.Cor.St.Plot.Year.Temp <- function(St1=10609,MeanMin=1,StYear=1981,EndYear=2010){
  StList <- BMD.Reader.Station()
  Kart <- GetMap(center=c(23.5,90), zoom=7, destfile = "kart.png")
  StPos <- StList[StList[,10]==St1,5:6]
            tmp <- PlotOnStaticMap(Kart, lat = as.numeric(StPos[1]), lon = as.numeric(StPos[2]), destfile =
          "Kart1.png",    cex=1.5,pch=20, add=FALSE)
  StId <- StList[,10]
  StId<- StId[StId!=St1]
  CorMat <- c()
  for(St2 in StId){
       StCorRes <- c(St1,St2,NA)
   try(StCorRes <-BMD.Cor.St2.Year.Temp(St1,St2,MeanMin=MeanMin,StYear = StYear, EndYear =
EndYear),silent=TRUE)
   print(StCorRes)
   CorMat<-rbind(CorMat,
                StCorRes)
   if(!is.na(StCorRes[3])){
     StPos2 <- StList[StList[,10]==St2,5:6]
     Latitudes <- c(as.numeric(StPos[1]),as.numeric(StPos2[1]))
     Longitudes <- c(as.numeric(StPos[2]),as.numeric(StPos2[2]))
     LCol="Purple"
     LWD=1
     if(StCorRes[3]>=0.4){LCol="Darkred";LWD=2}
     if(StCorRes[3]>=0.5){LCol="black";LWD=2}
     if(StCorRes[3]>=0.6){LCol="Orange";LWD=2}
     if(StCorRes[3]>=0.7){LCol="Red";LWD=3}
     if(StCorRes[3]>=0.8){LCol="Green";LWD=3}
     if(StCorRes[3]>=0.9){LCol="Darkgreen";LWD=3}
     PlotOnStaticMap(Kart, lat = Latitudes, lon = Longitudes, destfile = "Kart1.png", FUN=lines,
lwd=LWD, col=LCol, add=TRUE)
```

```
  }
 }
 CorMat
}
BMD.Cor.St2.Year.Temp <- function(St1=11111,St2=10609,MeanMin=1,StYear=1981,EndYear=2010){
 Data <-
BMD.Data.Matcher.Temp(St1=St1,St2=St2,MeanMin=MeanMin,StYear=StYear,EndYear=EndYear,Mo
nth=TRUE,Day=FALSE,Norm=TRUE)
 Result <- c(St1,St2,
          cor(Data[,3],Data[,4],use="pairwise.complete.obs"))
 Result
}
BMD.Reader.Temp <- function(StNr=NA){#StNr is the local ID from BMD
 Data <- read.table("temp_2015.csv",header=TRUE,sep=",")
 if (!is.na(StNr)){Data<-Data[Data[,1]==StNr,]}
 Data
}

BMD.Reader.Station <- function(StNr=NA){
 Data <- read.csv("StList.csv",sep=";",dec=",")
 if (!is.na(StNr)){Data<-Data[Data[,10]==StNr,]}
 Data
}
BMD.Data.Matcher.Temp <-
function(St1=11111,St2=10609,MeanMin=1,StYear=1981,EndYear=2010,Month=FALSE,Day=TRUE,N
orm=FALSE){
 Cols <- c(1:4,(4+MeanMin))
 D1 <- BMD.Reader.Temp(StNr=St1)[,Cols]
 D2 <- BMD.Reader.Temp(StNr=St2)[,Cols]
 if (Month){
  Data <- BMD.Data.Matcher.Temp.Month(D1,D2,StYear=StYear,EndYear=EndYear,Norm=Norm)
 }
```

```
  if(Day){
    Data <- BMD.Data.Matcher.Temp.Day(D1,D2,StYear=StYear,EndYear=EndYear)
  }
  Data
}
BMD.Data.Matcher.Temp.Day <- function(D1,D2,StYear,EndYear){
  DaysInMonth <- c(31,28,31,30,31,30,31,31,30,31,30,31)
  Result <- c()
  for(Year in StYear:EndYear){
    for (m in 1:12){
      for (d in 1:DaysInMonth[m]){
        d1 <- NA
        d2 <- NA
        try(d1 <- D1[D1[,2]==Year & D1[,3]==m & D1[,4]==d,5],silent=T)
        try(d2 <- D2[D2[,2]==Year & D2[,3]==m & D2[,4]==d,5],silent=T)
        Result <- rbind(Result,
                        c(Year,m,d,d1,d2))
      }
    }
  }
  Result
}
BMD.Data.Matcher.Temp.Month <- function(D1,D2,StYear,EndYear,Norm=FALSE){
  DaysInMonth <- c(31,28,31,30,31,30,31,31,30,31,30,31)
  Result <- c()
  for(Year in StYear:EndYear){
    for (m in 1:12){
        d1 <- NA
        d2 <- NA
        try(d1 <- mean(D1[D1[,2]==Year & D1[,3]==m,5],na.rm=TRUE),silent=T)
        try(d2 <- mean(D2[D2[,2]==Year & D2[,3]==m,5],na.rm=TRUE),silent=T)
```

```
      Result <- rbind(Result,
                      c(Year,m,d1,d2))
    }
  }
  if (Norm){
    Result <- BMD.Data.Normilasation.Temp.Month(Result)
  }
  Result
}

BMD.Data.Normilasation.Temp.Month <- function(D,StNorm=1981,EndNorm=2010){
  D2 <- D[D[,1]>=StNorm & D[,2]<=EndNorm,]
    Norms <- c()
    for(m in 1:12){
      Norms <- rbind(Norms,
                     colMeans(D2[D2[,2]==m,],na.rm = TRUE))
      for (Kol in 3:4){
        D[D[,2]==m,Kol] <- D[D[,2]==m,Kol]-Norms[m,Kol]}
    }
  D
}
```

3. Programming script for Temp projection

```
library(esd)
path <- "Mean_pre_monsoon_temp"
source(file.path(path,'DS.R'))
source(file.path(path,'DSensemble.R'))
source(file.path(path,'map.R'))
source(file.path(path,'map.station.R'))
source(file.path(path,'plot.R'))
path.era <- file.path(path,'ERAINT')
filename.temp <- file.path(path,"Mean.rda")
if(file.exists(filename.temp)) {
  load(filename.temp)
} else {
  X <- read.table(file.path(path,"Mean_2017.csv"),header=TRUE,sep=",")
  meta <- read.table(file.path(path,"Stations_local_id.csv"),
                     header=TRUE,sep=",")
  for (id in 1:nrow(meta)) {
    lid <- meta$Local_ID[id]
    Y <- X[X$INDEX==lid,]
    Y[Y <= -999] <- NA
    t <- paste(Y[,2],Y[,3],Y[,4],sep='-')
    z <- zoo(Y[,5],order.by=as.Date(t))
    y <-
as.station(z,loc=as.character(meta$Station[id]),lon=meta$Longitude.E.[id],lat=meta$Latitude.N.[id],alt=
meta$Elavation.m.[id],param='t2m',unit='degC',src='BMD',stid=lid)
    if (id == 1) t2m <- y else t2m <- combine.stations(t2m,y)
  }
  attr(t2m,"variable") <- "tMean"
  save(file=filename.temp, t2m, meta)
}
it.season <- c('Mar','Apr','May')
```

```
t2m.4s <- as.4seasons(t2m)
T2M <- subset(t2m.4s, it="mam") #march, april, May
z <- coredata(T2M)
z[z < 3] <- NA
z -> coredata(T2M)
T2M <- subset(T2M, it=c(1981,2010))
nv <- apply(coredata(T2M),2,'nv')
ok <- nv>=30
T2M <- subset(T2M, is=ok)
T2M <- pcafill(T2M)
dev.new()
map(T2M, FUN='Mean',add.text = T, xlim=c(88, 93), ylim=c(20, 27))
dev.new()
map(T2M, FUN='trend',add.text = T)
t2m.era <- retrieve(file.path(path.era,'erai_tMean.nc'),
                    lon=c(0,180),lat=c(-50,50))
is.predictor <- list(lon=c(80,100),lat=c(15,45))
T2M.predictor <- subset(t2m.era, is=is.predictor)
T2M.4s <- as.4seasons(T2M.predictor)
T2M.predictor <- subset(T2M.4s, it='mam')
## EOF analysis:
graphics.off()
gc(reset=TRUE)
print(loc(T2M))
T2M.predictor <- as.annual(T2M.predictor)
T2M <- as.annual(T2M)
gcm <- retrieve(file.path(path,'CMIP5/rcp26','tasMean_Amon_ens_rcp26_000.nc'),lon=c(0,180),lat=c(-
50,50))
gcm.4s <- as.4seasons(gcm)
GCM <- as.annual(subset(gcm.4s,it = 'mam'))
comb <- combine(T2M.predictor,as.annual(GCM))
```

```
ds.pca <- DS.pca(PCA(T2M),EOF(comb),verbose = FALSE, plot=TRUE)

plot(ds.pca)

dev.copy2pdf(file = file.path(path,paste("ds_tMean_evaluate_rcp26_",paste(it.season,collapse="-
"),"_v3.pdf",sep="") ))

gcm <- retrieve(file.path(path,'CMIP5/rcp45','tasMean_Amon_ens_rcp45_000.nc'),lon=c(0,180),lat=c(-
50,50))

gcm.4s <- as.4seasons(gcm)

GCM <- as.annual(subset(gcm.4s,it = 'mam'))

dev.copy2pdf(file = file.path(path,paste("ds_tMean_evaluate_",paste(it.season,collapse="-
"),"_v3.pdf",sep="") ))

comb <- combine(T2M.predictor,as.annual(GCM))

#browser()

ds.pca <- DS.pca(PCA(T2M),EOF(comb),verbose = FALSE, plot=TRUE)

plot(ds.pca)

dev.copy2pdf(file = file.path(path,paste("ds_tMean_evaluate_rcp45_",paste(it.season,collapse="-
"),"_v3.pdf",sep="") ))

gcm <- retrieve(file.path(path,'CMIP5/rcp85','tasMean_Amon_ens_rcp85_000.nc'),lon=c(0,180),lat=c(-
50,50))

gcm.4s <- as.4seasons(gcm)

GCM <- as.annual(subset(gcm.4s,it = 'mam'))

comb <- combine(T2M.predictor,as.annual(GCM))

ds.pca <- DS.pca(PCA(T2M),EOF(comb),verbose = FALSE, plot=TRUE)

plot(ds.pca)

dev.copy2pdf(file = file.path(path,paste("ds_tMean_evaluate_rcp85_",paste(it.season,collapse="-
"),"_v3.pdf",sep="") ))

## Loop across the three rcps

for(rcp in c("rcp45","rcp85","rcp26")) {

  filename.dse <- file.path(path,

                    paste("dsensemble.tMean.",rcp,".",paste(it.season,collapse=""),"v3.rda",sep="") )

  if(file.exists(filename.dse)) {

    load(filename.dse)

  } else {

    dse.pca <- DSensemble.pca(PCA(T2M),predictor=T2M.predictor,
```

```
                    path=file.path(path,"CMIP5"),biascorrect=TRUE,
                    it=it.season, select = c(54:63),
                    rcp=rcp, pattern="tasMean_Amon_ens_", verbose=FALSE,
                    rel.cord=FALSE, lon=is.predictor$lon,
                    lat=is.predictor$lat,plot=TRUE)
  print('Done !')
  dse <- as.station(dse.pca)
  save(file=filename.dse,dse)
    rm("dse.rcp")
  gc(reset=TRUE)
 }
}
```

1. Programming script for fill up missing data

```
## Visualize scripts:#################
library(esd)
files.dse <- list.files(path,pattern="dsensemble.tMean",full.names=TRUE)
print(files.dse)
filename.dse <- files.dse[[1]] # 1= Dhaka.rda,    ### 2=Khunla.rda, ### 3=Satkhira
load(filename.dse)
it.season <- attr(dse.all,"it")
ylim <- c(10,25)  #winter min range
rcp <- "rcp85"
dse <- dse.all[[rcp]]
## Produce and save figure:
filename.fig <- file.path(path.fig,
                  paste("dsensemble.tMean.",loc(attr(dse,"station")),
                    ".",paste(it.season,collapse=""),
                    ".",rcp,".png",sep="") )
#pdf(file=filename.fig, width=8, height=6)
dev.new()
plot(dse,ylim=ylim,
```

```
    target.show=FALSE,map.show=FALSE,new=FALSE,legend.show=FALSE)
title(paste("Pre-monsoon min temperature "," (",rcp,")\n",
          loc(attr(dse,"station")),sep=""))
dev.print(png,filename.fig, width=500, height=450)
dev.off()
```

4. Programming script for Rainfall projection

```
library(esd)
path <- "~/ESD_oslo_2018_premonsoon_pr"
source(file.path(path,'DS.R'))
source(file.path(path,'DSensemble.R'))
source(file.path(path,'map.R'))
source(file.path(path,'map.station.R'))
source(file.path(path,'plot.R'))
path.era <- file.path(path,'ERAINT')
filename.pr <- file.path(path,"pr.rda")
if(file.exists(filename.pr)) {
  load(filename.pr)
} else {
  X <- read.table(file.path(path,"RAIN_2017.csv"),header=TRUE,sep=",")
  meta <- read.table(file.path(path,"Stations_local_id.csv"),
                     header=TRUE,sep=",")
  for (id in 1:nrow(meta)) {
    lid <- meta$Local_ID[id]
    Y <- X[X$INDEX==lid,]
    Y[Y <= -999] <- NA
    t <- paste(Y[,2],Y[,3],Y[,4],sep='-')
    z <- zoo(Y[,5],order.by=as.Date(t))
    y <-
as.station(z,loc=as.character(meta$Station[id]),lon=meta$Longitude.E.[id],lat=meta$Latitude.N.[id],alt=
meta$Elavation.m.[id],param='pr',unit='mm',src='BMD',stid=lid)
    if (id == -1) pr <- y else pr <- combine.stations(pr,y)
  }
   attr(pr,"variable") <- "pr"
  save(file=filename.pr, pr, meta)
}
## load bmd.rda
```

```
load('bmd.rda')
pr <- pr.bmd
it.season <- c('Mar','Apr','May')
## wetfreq=Estimate the wet-day frequency fw . Default threshold is 1mm/day.
pr.ann <- as.annual(subset(pr,it=it.season), FUN='wetfreq', threshold=1, nmin=80)
attr(pr.ann, "variable") <- "Wet-day frequency"
attr(pr.ann, "unit") <- "fraction of days over threshold"
X <- coredata(pr.ann)
PR <- pr.ann # annual(pr.it, nmin=4)
z <- coredata(PR)
z[z < 0] <- NA
z -> coredata(PR)
## Subset in time:
PR <- subset(PR, it=c(1981,2010))
plot(PR)
nv <- apply(coredata(PR),2,'nv')
ok <- nv>=30
PR <- subset(PR, is=ok)
pca <- pcafill(PR)
dev.new()
map(pca)
map(pca, FUN='mean',add.text = T, colbar = list(rev = TRUE))
dev.new()
map(PR, FUN='trend',add.text = T)
pr.era <- retrieve(file.path(path.era,'ERAINT_slp_mon.nc'),
                   lon=c(85,105),lat=c(-5,30))
pr.era.ann <- as.annual(subset(pr.era,it = it.season),nmin=3)
is.predictor <- list(lon=c(85,105),lat=c(0,30))
PR.predictor <- subset(pr.era, is=is.predictor)
PR.predictor <- pr.era.ann #subset(PR.4s, it='jjas')
era <- subset(pr.era.ann,it = c(1981,2010))
```

```
eof <- EOF(era)
plot(eof,ip =1)
plot(eof,ip = 2)
plot(eof,ip = 3) # ip is the ith principal component
corfield.field.station(subset(PR,is=20),era) # for frequency
corfield.field.station(subset(pr,is=20),era) # for the mean amount
map(eof)
pca <- subset(pca,it= c(1981,2010))
map(pca,FUN='mean',colbar = list(col=rainbow(n=10), rev =TRUE))
map(pca,FUN='mean',colbar = list(rev =TRUE),add.text = TRUE)
index(pca) <- as.Date(paste(index(pca),'-01-01',sep=''))
index(eof) <- as.Date(paste(index(eof),'-01-01',sep=''))
ds <- DS.pca(PCA(pca),eof)
png(filename = 'ds1_freq_BMD.png')
plot(ds)
dev.off()
)
class(sta)
cor(subset(sta,is = loc(sta) == 'DhakaPBO'),subset(subset(PR,is= loc(PR) == 'DhakaPBO'),it =
c(1981,2010)))
plot.zoo(subset(sta,is = loc(sta) == 'DhakaPBO'),
        subset(subset(PR,is= loc(PR) == 'DhakaPBO'),it = c(1981,2010)),
        ylim = c(0.5,0.8),xlim = c(.5,.8))
cor(subset(sta,is = loc(sta) == 'Chittagong_MMO'),
    subset(subset(PR,is= loc(PR) == 'Chittagong_MMO'),it = c(1981,2010)),use = 'complete.obs')
plot.zoo(subset(sta,is = loc(sta) == 'Chittagong_MMO'),
        subset(subset(PR,is= loc(PR) == 'Chittagong_MMO'),it = c(1981,2010)),
        ylim = c(0.5,0.8),xlim = c(.5,.8))
cor(subset(sta,is = 1),
    subset(subset(PR,is= 1),it = c(1981,2010)),use = 'complete.obs')
plot.zoo(subset(sta,is = loc(sta) == "Coxs_Bazar"),
```

```
        subset(subset(PR,is= loc(PR) == "Coxs_Bazar"),it = c(1981,2010)),
        ylim = c(0.5,1),xlim = c(.5,1))
sapply(1:29,function(i) cor(subset(sta,is = i),subset(subset(PR,is= i),it = c(1981,2010)),use =
'complete.obs'))
graphics.off()
cbind(loc(sta),
     as.numeric(round(sapply(1:29,function(i) cor(subset(sta,is = i),subset(subset(PR,is= i),it =
c(1981,2010)),use = 'complete.obs')),digits = 2)))
PR.predictor <- as.annual(PR.predictor)
PR <- as.annual(PR)
plot(PR)
gcm <- retrieve(file.path(path,'CMIP5/rcp85','pr_Amon_ens_rcp85_000.nc'),
              lon=c(85,105),lat=c(-5,30))
it.season <- c('Mar','Apr','May')
GCM <- as.annual(subset(gcm,it=it.season),nmin=3)
comb <- combine(era,GCM)
index(comb) <- as.Date(paste(index(comb),'-01-01',sep=''))
index(c) <-  as.Date(paste(index(attr(comb, "appendix.1")),'-01-01',sep=''))
ds.comb <- DSensemble.pca(PCA(pca),path = file.path(path,'CMIP5'),
                        rcp = 'rcp85',predictor = file.path(path.era,'ERAINT_slp_mon.nc'),
                        verbose = TRUE,pattern = 'pr_',select = c(5:7),plot = TRUE
plot(ds.comb)
```

5. Programming script for Product generation

```
library(esd)
cc.bmd <- function(loc='dhaka', rcp='rcp26', ref=c(1981,2010)){
  cat('Experiment',loc,rcp,ref)
  load(paste('monsoon_mean_temp/dsensemble.tmean.', rcp,'.JunJulAugv3.rda', sep=''))
  id <- grep(pattern = loc, x= loc.nms, ignore.case = T)
  x <- dse[[id]]
  x.anomaly <- as.anomaly(x = x, ref = ref)
    cc.nf <- mean(subset(x.anomaly, it = c(2021,2050)), na.rm=T)
  cc.ff <- mean(subset(x.anomaly, it = c(2071,2100)), na.rm=T)
  df <- data.frame(cc.nf = cc.nf, cc.ff =cc.ff)
  cat(' ', round(cc.nf, digits=2), round(cc.ff, digits = 2), '\n')
  invisible(df)
}
load (paste('monsoon_mean_temp/dsensemble.tmean.rcp26.JunJulAugv3.rda', sep=''))
loc.nms <- names(dse)
out <-matrix(NA, length(loc.nms), 6)
colnames(out) <- c('rcp26.nf', 'rcp45.nf', 'rcp85.nf',
                   'rcp26.ff', 'rcp45.ff', 'rcp85.ff')
rownames(out) <-loc.nms
i <- 1
for (loc in loc.nms){
  out[i,1] <- as.numeric(cc.bmd(loc, rcp='rcp26')$cc.nf)
  out[i,2] <- as.numeric(cc.bmd(loc, rcp='rcp45')$cc.nf)
  out[i,3] <- as.numeric(cc.bmd(loc, rcp='rcp85')$cc.nf)
  out[i,4] <- as.numeric(cc.bmd(loc, rcp='rcp26')$cc.ff)
  out[i,5] <- as.numeric(cc.bmd(loc, rcp='rcp45')$cc.ff)
  out[i,6] <- as.numeric(cc.bmd(loc, rcp='rcp85')$cc.ff)
  i <- i+1
}
write.csv(round(out,digits = 2), file='cc_bmd_tmean.csv', quote=FALSE)
```

6. Programming script for plotting

```
plot.station <- function(x,plot.type="single",new=TRUE,
                         lwd=3,type='l',pch=0,main=NULL,col=NULL,
                         xlim=NULL,ylim=NULL,xlab="",ylab=NULL,
                         errorbar=TRUE,legend.show=FALSE,
                         map.show=TRUE,map.type=NULL,map.insert=TRUE,
                         usegooglemap=TRUE,zoom=NULL,
                         cex.axis=1.2,cex.lab=1.2,cex.main=1.2,
                         mar=c(4.5,4.5,0.75,0.5),fig=NULL,
                         alpha=0.5,alpha.map=0.7,
                         verbose=FALSE,...) {
 if (verbose) print('plot.station')
 par(las=1)
 if (!is.numeric(lon(x)) | !is.numeric(lat(x))) {
  map.show <- FALSE
 }
 if(map.show) {
  if (verbose) print('show map')
  if (is.null(map.type)) {
   if( inherits(x,"field") | length(lon(x))!=length(lat(x)) |
       (length(lon(x))==2 & length(lat(x))==2) ) {
     map.type <- "rectangle"
   } else {
     map.type <- "points"
   }
  }
  if (verbose) print(map.type)
 }
  if(is.null(fig) & new) {
   fig <- c(0,1,0,0.95)
   if (map.show & map.insert) fig[4] <- 0.8
```

```
}
if (legend.show) fig[3] <- 0.05
if (is.null(xlim))
  xlim <- range(index(x))
if (verbose) {print(xlim); print(ylim)}
 if (plot.type=="single") {
  if (is.null(ylab)) {
    ylab <- esd::ylab(x) # ggplot2 ylab can interfere with esd
  }
  if (inherits(ylab,"try-error")) ylab <- attr(x,'unit')
} else {
  if (is.null(ylab)) {
    if ((length(levels(factor(stid(x))))>1) & (length(levels(factor(varid(x))))<=1)) {
      ylab <- stid(x)
    } else
      ylab <- varid(x)
  } else {
    if (is.null(main)) {
      if ((length(levels(factor(stid(x))))>1) & (length(levels(factor(varid(x))))<=1)) {
        main <- levels(factor((attr(x,'longname'))))[1]
      } else {
        main <- levels(factor(loc(x)))[1]
      }
    }
  }
  if (is.null(col)) {
  if (is.null(dim(x))) {
    col <- "blue"
  } else if (!is.null(lon(x)) & !is.null(lat(x)) &
             length(lon(x))==dim(x)[2] &
             length(lat(x))==dim(x)[2]) {
```

```
    nx <- (lon(x)-min(lon(x)))/diff(range(lon(x)))
    ny <- (lat(x)-min(lat(x)))/diff(range(lat(x)))
    if ( all(is.finite(nx) & is.finite(ny)) ) {
      col <- rgb(1-ny,nx,ny,1)
    } else {
      col <- rainbow(dim(x)[2])
    }
  } else {
    col <- rainbow(length(x[1,]))
  }
}
if(is.null(alpha.map)) alpha.map <- alpha
col.map <- adjustcolor(col,alpha.f=alpha.map)
col <- adjustcolor(col,alpha.f=alpha)
ns <- length(stid(x))
errorbar <- errorbar & !is.null(err(x))
if(map.show & !map.insert) {
  vis.map(x,col.map,map.type,add.text=FALSE,map.insert=map.insert,
          cex.axis=cex.axis,cex=1.8,usegooglemap=usegooglemap,
          zoom=zoom,verbose=verbose)
  new <- TRUE
}
cls <- class(x)
if("seasonalcycle" %in% cls) xaxt <- "n" else  xaxt <- NULL
class(x) <- "zoo"
if(new) dev.new()
if(!is.null(fig)) par(cex.axis=1,fig=fig,mar=mar)
par(bty="n",xaxt="s",yaxt="s",xpd=FALSE)
plot.zoo(x,plot.type=plot.type,xlab=xlab,ylab=ylab,
         col=col,xlim=xlim,ylim=ylim,lwd=lwd,type=type,pch=pch,
         cex.axis=cex.axis,cex.lab=cex.lab,cex.main=cex.main,
```

```
        xaxt=xaxt,main=main,...)
 if("seasonalcycle" %in% cls) {
  axis(1,at=seq(1,12),labels=month.abb,cex.axis=cex.axis,las=2)
 }
 par0 <- par()
 if (plot.type=="single") {
  if (errorbar) {
   segments(index(x),x-err(x),index(x),x+err(x),
          lwd=3,col=rgb(0.5,0.5,0.5,0.25))
  }
    par(fig=c(0,1,0,0.1),new=TRUE, mar=c(0,0,0,0),xaxt="s",yaxt="s",bty="n")
  plot(c(0,1),c(0,1),type="n",xlab="",ylab="")
  if(legend.show) {
   legend(0.01,0.95,paste(attr(x,'location'),": ",
                  #attr(x,'aspect'),
                  #attr(x,'longname')," - ",
                  round(attr(x,'longitude'),2),"E/",
                  round(attr(x,'latitude'),2),"N (",
                  attr(x,'altitude')," masl)",sep=""),
        bty="n",cex=0.6,ncol=3,text.col="grey40",lty=1,col=col)
  }
  if (map.show & map.insert) vis.map(x,col.map,map.type=map.type,cex=1,
                          cex.axis=0.65,add.text=FALSE,
                          map.insert=map.insert,usegooglemap=usegooglemap,
                          zoom=zoom,verbose=verbose)
  par(fig=par0$fig,mar=par0$mar,new=TRUE)
  plot.zoo(x,plot.type=plot.type,type="n",xlab="",ylab="",
        xaxt="n",yaxt="n",xlim=xlim,ylim=ylim,new=FALSE)

 }
}
```